NOTE TO USER

This reproduction is the best copy available.

UMI®

P

University of Alberta

Sedimentology, Ichnology, and High-resolution Allostratigraphy of the Falher "C" Member, Spirit River Formation, west-central Alberta, Canada

by

Ian Andrew Armitage ©

A thesis submitted to the Faculty of Graduate Studies and Research in partial fulfillment of the requirements for the degree of Master of Science

Department of Earth and Atmospheric Sciences

Edmonton, Alberta

Edmonton, Alberta
Spring, 2002

National Library
of Canada

Acquisitions and
Bibliographic Services

395 Wellington Street
Ottawa ON K1A 0N4
Canada

Bibliothèque nationale
du Canada

Acquisitions et
services bibliographiques

395, rue Wellington
Ottawa ON K1A 0N4
Canada

Your file Votre référence

Our file Notre référence

The author has granted a non-exclusive licence allowing the National Library of Canada to reproduce, loan, distribute or sell copies of this thesis in microform, paper or electronic formats.

The author retains ownership of the copyright in this thesis. Neither the thesis nor substantial extracts from it may be printed or otherwise reproduced without the author's permission.

L'auteur a accordé une licence non exclusive permettant à la Bibliothèque nationale du Canada de reproduire, prêter, distribuer ou vendre des copies de cette thèse sous la forme de microfiche/film, de reproduction sur papier ou sur format électronique.

L'auteur conserve la propriété du droit d'auteur qui protège cette thèse. Ni la thèse ni des extraits substantiels de celle-ci ne doivent être imprimés ou autrement reproduits sans son autorisation.

0-612-69679-0

Canadä

University of Alberta

Library Release Form

Name of Author: Ian Andrew Armitage

Title of Thesis: Sedimentology, Ichnology, and High-Resolution Allostratigraphy of the Falher "C" Member, Spirit River Formation, west-central Alberta, Canada

Degree: Master of Science

Year this Degree Granted: 2002

Permission is hereby granted to the University of Alberta Library to reproduce single copies of this thesis and to lend or sell such copies for private, scholarly, or scientific research purposes only.

The author reserves all other publication and other rights in association with the copyright in the thesis, and except as herein before provided, neither the thesis or any substantial portion thereof may be printed or otherwise reproduced in any material form whatever without the author's prior written permission.

Ian Armitage

Ian A. Armitage

2209 Carleton Street S.W.
Calgary, Alberta T2T 3K4
Canada

January 4, 2002

University of Alberta

Faculty of Graduate Studies and Research

The undersigned certify that they have read, and recommend to the Faculty of Graduate Studies and Research for acceptance, a thesis entitled **Sedimentology, Ichnology, and High-resolution Allostratigraphy of the Falher "C" Member, Spirit River Formation, west-central Alberta, Canada** submitted by **Ian Andrew Armitage** in partial fulfillment of the requirements for the degree of Master of Science

Dr. S. George Pemberton - Supervisor

Dr. Charles R. Stelck

B. S. Heming

Dr. Bruce S. Heming - External Examiner

Date November 22, 2001

We shall not cease from exploration
And the end of all our exploring
Will be to arrive where we started
And know the place for the first time.
-T. S. Elliot

Dedicated to my loving mother Judy,
whose creativity and inspiration have no bounds.

Abstract

Within the Deep Basin of west-central Alberta, the Spirit River Formation is comprised of eight major transgressive-regressive sequences that prograded into the Clearwater Sea during the Lower Cretaceous. The Falher "C" Member is one such transgressive-regressive sequence containing mixed coarse-grained sandstone and conglomerate reservoirs that are estimated to contain 3.5 bcf of recoverable gas and natural gas liquids. The Falher "C" Member is further sub-divided into units C1, C2, C3 and C4 through recognition of key allostratigraphic surfaces that bound five facies associations representative of fully and marginal marine environments. Two of the five facies associations, termed FA2 and FA3, contain facies successions of greatest reservoir potential. Facies that constitute FA2 are readily observed within the C2 unit, and were deposited in wave-dominated upper shoreface and foreshore settings during a forced regression. Facies comprising FA3 represent sequential infilling of tidal channels and lateral accretion of a barrier spit-platform during the ensuing transgression and deposition of the Falher C3 unit. Facies slice maps and net conglomerate isopach thickness maps show that the regressional C2 unit is confined to an east-west trend within the Wapiti Field. Mapping has also shown that the distribution of reservoir facies deposited during the C3 transgression was strongly influenced by antecedent topographic elements within the C2 interval. Delineation of the facies architecture of coarse-grained reservoirs within the Falher "C" Member and extrapolation of these trends using key bounding allostratigraphic surfaces has contributed toward a refined exploration strategy in the Deep Basin of west-central Alberta.

Acknowledgements

First and foremost, I would like to acknowledge the support and guidance of Dr. George Pemberton. Thank you Jedi for all the knowledge you have passed on to me, I'll be satisfied with only a small fraction of its expanse. Thank you also for your patience, and for laughing at my jokes. I shall miss our stories very much.

Another individual who has contributed endless amounts of wisdom to me over the years is Dr.. Murray Gingras. Murr nurtured my earliest interests in sedimentology and ichnology. He has always had great faith and confidence in my ability, and has always stuck by me as a mentor, and as a friend. I look forward to our future collaborations with great enthusiasm.

Special thanks to Demian Robbins and Tom Saunders who were instrumental in the final stages of thesis preparation and synthesis. Thanks also extended to Dr. Zonneveld who provided me with some of the drafting material incorporated into my thesis. I would also like to extend sincere thanks to other members of the Ichnology Research Group. In no particular order these people are: Susan Fleming, Jason Lavigne, Steve "Scoop" Hubbard, Eric "Crack" Hanson, Michelle Spila, Corriene Bagdan, Chad Harris, Jeff Reinprect, Carly Barnett, Gladys Fong, Errin Kimball, Arjun Keswani, Rozalia Pak, Glenn Schmidt and Cynthia "Hot Lips" Hagstrom.

Financial and logistical support for my thesis has been provided by NSERC and Anderson Exploration Ltd. (formerly Ulster Petroleum Ltd.). Many thanks to Dr. Tom Moslow, Peter O'Leary and Glenn Murdoch for their input into the project as well as for their assistance in locating and viewing many important cored intervals of the Falher "C" Member.

I would like to thank the members of my defence committee. Apart from the Jedi both committee members Dr. Bruce Heming and Dr. Charles Stelck provided me with insightful comments and suggestions for improvement on the contents of my thesis. It was a great honor to have one of the Giants in North American stratigraphy on my committee. Thank you Dr. Stelck.

Last, and by no means least, I would like to say thanks to my two good friends and field school partners Jason Frank and Paul Glombick. Who knows where the path would have lead had we not teamed-up...

Table of Contents

CHAPTER ONE: Introduction

1.1 Introductory remarks........1
1.2 Study area and well control........2
1.3 Regional stratigraphy and paleogeography........5
1.4 Historical overview........8
1.5 Objectives........12
1.6 Methodology........13

CHAPTER TWO: Facies associations and depositional environments of the Falher "C" Member

2.1 Introduction........14
2.2 Facies Association One (FA1): storm-dominated lower shoreface........17
  Sedimentology........17
  Ichnology........19
  Interpretation and Discussion........20
2.3 Facies Association Two (FA2): wave-dominated upper shoreface and foreshore........23
  Sedimentology........23
  Porosity and Permeability Development within Falher "C" Conglomerates (Facies F10)........25
  Interpretation and Discussion........26
2.4 Facies Association Three (FA3): tidal inlet........32
  Sedimentology........32
  Ichnology........33
  Interpretation and Discussion........33
2.5 Facies Association Four (FA4): brackish back-barrier........38
  Sedimentology........38
  Ichnology........39
  Interpretation and Discussion........40
2.6 Facies Association Five (FA5): coastal plain........46
  Sedimentology........46
  Interpretation and Discussion........47

CHAPTER THREE: Key Stratigraphic Surfaces and Stratal Architecture of the Falher "C" Member

3.1 Introduction..89

3.2 Significant Stratigraphic Surfaces and Sub-division of the Falher "C"

Dip-section A-A' and E-E'..90

Strike-section G-G'..92

3.3 MFS/TSE1: Contact between C1 and Uppermost Falher "D"

Description and Occurrence..95

Interpretation..95

3.4 RSE: Contact between C2 and C1

Description and Occurrence..96

Interpretation..96

3.5 MFS/TSE2/MxFS: Contact between C3 and C2

Description and Occurrence..97

Interpretation..98

3.6 First Coal: Contact between C4 and C3

Description and Occurrence..99

Interpretation..99

3.7 Stratal Architecture of the Falher "C" Member..100

Internal stratigraphic relationships observed within the C3 Unit..........102

CHAPTER FOUR: Four-stage Depositional Model of the Falher "C" Member

4.1 Introduction..110

Normal vs. Forced Regression..110

4.2 Stage I: Relative rise of sea level and initial transgression of the Falher "C" shoreline..113

4.3 Stage II: Increase in sediment supply following a forced regression.115

4.4 Stage III: Relative rise of sea level and subsequent transgression following lowstand..119

4.5 Stage IV: Normal regression with constant sediment supply..............122

CHAPTER FIVE: Conclusions

5.1 Conclusions..124

REFERENCES..125

APPENDIX I: Core Logs...135
APPENDIX II: Cross-sections...172
APPENDIX III: Maps...176

List of Tables

CHAPTER ONE

Table 1: List of examined Falher "C" core..5
Table 2: Albian Boreal Biotic Provinces (Jeletzky, 1971)..9
Table 3: Foraminiferal zones of the western interior of Canada (Caldwell *et al.*, 1978)..............9

CHAPTER TWO

Table 4: Facies subdivision of the Falher "C" Member..15

List of Figures

CHAPTER ONE

Figure 1: Map of Canada showing extent of Boreal sea during the latest Early Albian (Williams & Stelck, 1975)....3
Figure 2: Detailed map of the study area....4
Figure 3: Correlation chart showing the stratigraphic subdivision of Lower Cretaceous sequences Alberta and British Columbia....7

CHAPTER TWO

Figure 4: Gamma-ray log and calibrated core interval for well 7-24-67-10W6M....18
Figure 5: Idealized HCS sequence (Dott & Bourgeois, 1982)....21
Figure 6: Gamma-ray log and calibrated core interval for well 11-8-67-10W6M....29
Figure 7: Gamma-ray log and calibrated core interval for well 7-15-67-10W6M....35
Figure 8: Tripartite subdivision of wave-dominated barred estuarine depositional system (Dalrymple *et al.*, 1992)....41
Figure 9: Gamma-ray log and calibrated core interval for well 10-30-67-11W6M....43
Figure 10: Gamma-ray log and calibrated core interval for well 11-30-68-8W6M....45
Figure 11: Gamma-ray log and calibrated core interval for well 10-1-68-9W6M....48

CHAPTER THREE

Figure 12: Dip-oriented stratigraphic cross-sections: A-A' and F-F'....91
Figure 13: Strike-oriented stratigraphic cross-section: G-G'....93
Figure 14: 3-D fence diagram or the Falher "C" Member....101
Figure 15: Stratigraphic and paleogeographic context of 7-15-67-10W6M and 6-13-67-11W6M within the C3Unit....103

CHAPTER FOUR

Figure 16: Normal vs. forced regressions (Posamentier *et al.*, 1992)....111
Figure 17: Stage I: initial transgression of the Falher shoreline following a rise of RSL....114
Figure 18: Stage II: increase in sediment supply following a forced regression....118
Figure 19: Diagramatic cross-section of the shoreface and nearshore system (Hunter *et al.* 1979)....116
Figure 20: Stage III: Rise of RSL and subsequent transgression following lowstand....121
Figure 21: Stage IV: Normal regression accompanying progradation....123

List of Plates

CHAPTER TWO

Plate 1: Facies Association One (FA1), and Facies Association Two (FA2)....49
Plate 2: Facies Association Three (FA3), Facies Association Four (FA4), and Facies Association Five (FA5)....50
Plate 3: Plane parallel and sub-parallel laminated very fine-grained sandstone (facies F5)....52
Plate 4: Non-bioturbated and bioturbated amalgamated storm sandstone (facies F5)....54
Plate 5: Coarse-grained storm bedding and scoured contacts....56
Plate 6: Intensely bioturbated siltstone (facies F4), and very fine-grained sandstone (facies F5)....58
Plate 7: Commonly occuring solitary ichnogenera within very fine-grained sandstone (facies F5)....60
Plate 8: Composite *Diplocraterion* Burrows....62
Plate 9: Vertically oriented Ichnogenera....64
Plate 10: Normal and reverse graded bedding....66
Plate 11: Unimodal conglomerate (facies F10 A)....68
Plate 12: Interbedded coarse-grained sand (facies F9) and chert conglomerate (facies F10 A, B, C, and D....70
Plate 13: Bedding plane views of several coarse-grained facies within 10-9-67-10W6M....72
Plate 14: Variation in matrix composition within polymodal chert conglomerate interval (facies F10 D)....74
Plate 15: Trough cross-stratification and planar cross-stratification (facies F6 and F7)....76
Plate 16: Cryptically bioturbated sandstone (Facies F5 and F6), produced by interstitial meiofauna....78
Plate 17: *Macaronichnus* assemblage....80
Plate 18: Physically and biologically churned fine-grained facies (facies F2-F4)....82
Plate 19: Low diversity brackish water trace fossil assemblages....84
Plate 20: Soft sediment deformation structures and rooted bedding....86
Plate 21: Organic-rich mudstone and coal facies (facies F1 and F11)....88

CHAPTER THREE

Plate 22: Varying expression of basal transgressive surface of erosion (TSE1) separating the Falher “C” from the underlying Falher “D” Member in core....105
Plate 23: Sharp, regressive surface of erosion (RSE)....107
Plate 24: Second transgressive surface of erosion (TSE2)....109

CHAPTER ONE: Introduction

1.1 Introductory Remarks

This subsurface study focuses on the integration of ichnology with sedimentology and allostratigraphy as an aid in delineating the facies architecture of coarse-grained conglomeratic shorelines and their associated environments of deposition. Cores employed in this study were recovered from the Lower Cretaceous Albian-age Falher "C" Member of the Spirit River Formation, west-central Alberta. The Falher "C" Member is one of eight major northward prograding shoreface sequences within the Spirit River Formation. Each of these shoreface sequences is punctuated by episodic shoreline regressions and subsequent transgressions as revealed by well log response and core analysis. Close examination of cored intervals of the Falher "C" reveals a complex hierarchy of sequence stratigraphic surfaces that bound genetically related packages of sediment. Examination of the external geometry and internal heterogeneity of these packages of sediment is adressed in this study incorporating ichnology with process sedimentology and allostratigraphy. When used synergistically with conventional methods of process sedimentology and sequence stratigraphy, ichnology proves an effective tool that enhances sub-surface basin analysis.

Ichnological analysis of Falher "C" core provided data essential to proper understanding of the relative influence of fluvial, tidal and marine controls on deposition of facies associations. Ichnology provides a means of reconstructing the paleoenvironmental conditions believed responsible for the distribution of facies within the study area. Environmental constraints on the behavior of organisms are often reflected in the adaptive burrowing strategy an organism employs to deal with the imposed stress. Recognition of the ethological significance of trace fossils found in core is what sets ichnology apart from other standard methods of sedimentological analysis. Environmental factors such as salinity, temperature, turbidity, available oxygen, food supply, sedimentation rate, hydrodynamic energy and substrate consistency are responsible for the observed variations in trace fossil morphology. These important parameters are not detectable utilizing conventional process sedimentology. When these environmental factors are combined with data generated from separate lines of sedimentologic investigation such as facies and log analysis, a more accurate and sound gological interpretation can be made. Furthermore, sedimentology, and ichnology contribute to stratigraphic analyses through comparison of trace fossil assemblages and their location within the stratigraphic framework. Such observations are viewed as an effective means of determining the relative timing of depositional and erosional episodes associated with relative changes in sea level, sediment supply, and regional subsidence.

Application of these concepts through subsurface mapping provides a predictive tool that can be used in petroleum exploration and exploitation.

The results of this study serve industrial and academic interests alike. From the perspective of the oil and gas industry in Canada, the results have contributed toward a refined exploration strategy in the Deep Basin of Alberta. This study contributes toward the existing knowledge-base of reservoir geologists and engineers, through description and interpretation of facies and trace fossil assemblages and the stratigraphic context in which they are found within the Falher "C" Member. Mapping of economic and non-economic trends provides a visual means of demonstrating lateral and successive heterogeneity of the stratigraphic framework manifested by the Falher "C" Member. The scale, distribution, and three dimensional predictability of reservoir and non-reservoir units portrayed in maps constructed for this study provide workers with a means of comparing or contrasting other play types in the Deep Basin. Similar play types in separate hydrocarbon pools regardless of geologic age may be compared and contrasted with the models found in this study.

Academic interests are served by this study through a continued effort at the University of Alberta toward understanding the distribution and ichnological disparity between Mesozoic sequences in Alberta and British Columbia. Research results of this study will contribute valuable data to the Ichnology Research Group. A primary goal of the Ichnology Research Group is regional correlation of all Lower Cretaceous intervals in Alberta and Saskatchewan.

1.2 Study Area, and Well Control

The study area lies within the deep basin of western Canada (figure 1), and covers 1958 km^2 of land area encompassed by townships 66-68, ranges 7-13 west of the sixth meridian (figure 2). Included within the study area are portions of the Elmworth and Wapiti gas fields. The Wapiti River demarcates the boundary between the two. The Elmworth field lies north of the river, and the Wapiti field lies to the south (figure 2).

184 wells penetrate the Falher "C" Member within the study area. Of this total, 33 wells include conventional core recovered from the Falher "C" Member (table 1). The majority of these cored well locations coincide with producing hydrocarbon pools located within township 67, ranges 7 to 13 west of the sixth meridian. Core lengths vary between 5 and 22 meters. In total, approximately 550 m of core were incorporated into this study.

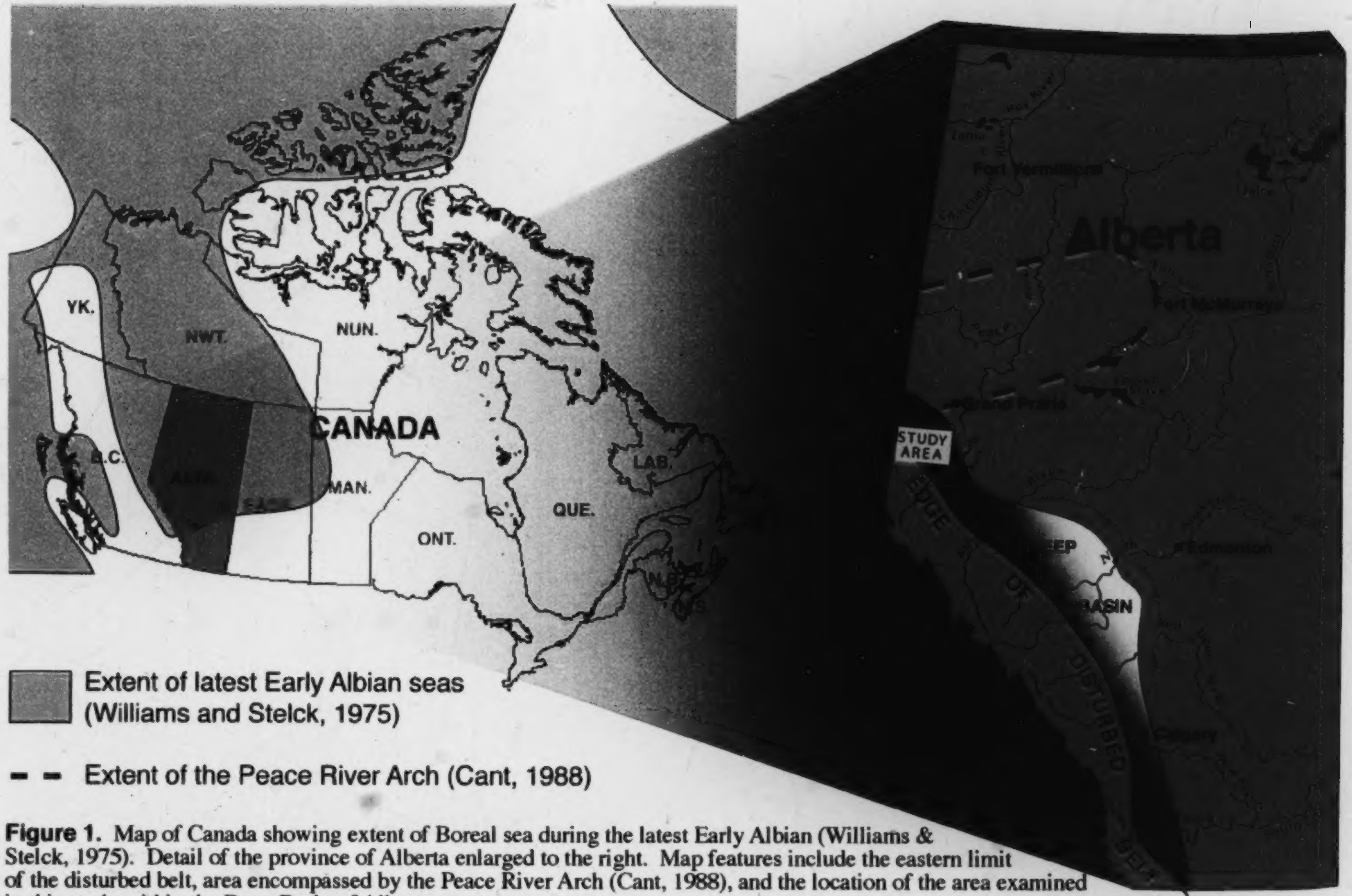

Figure 1. Map of Canada showing extent of Boreal sea during the latest Early Albian (Williams & Stelck, 1975). Detail of the province of Alberta enlarged to the right. Map features include the eastern limit of the disturbed belt, area encompassed by the Peace River Arch (Cant, 1988), and the location of the area examined in this study within the Deep Basin of Alberta.

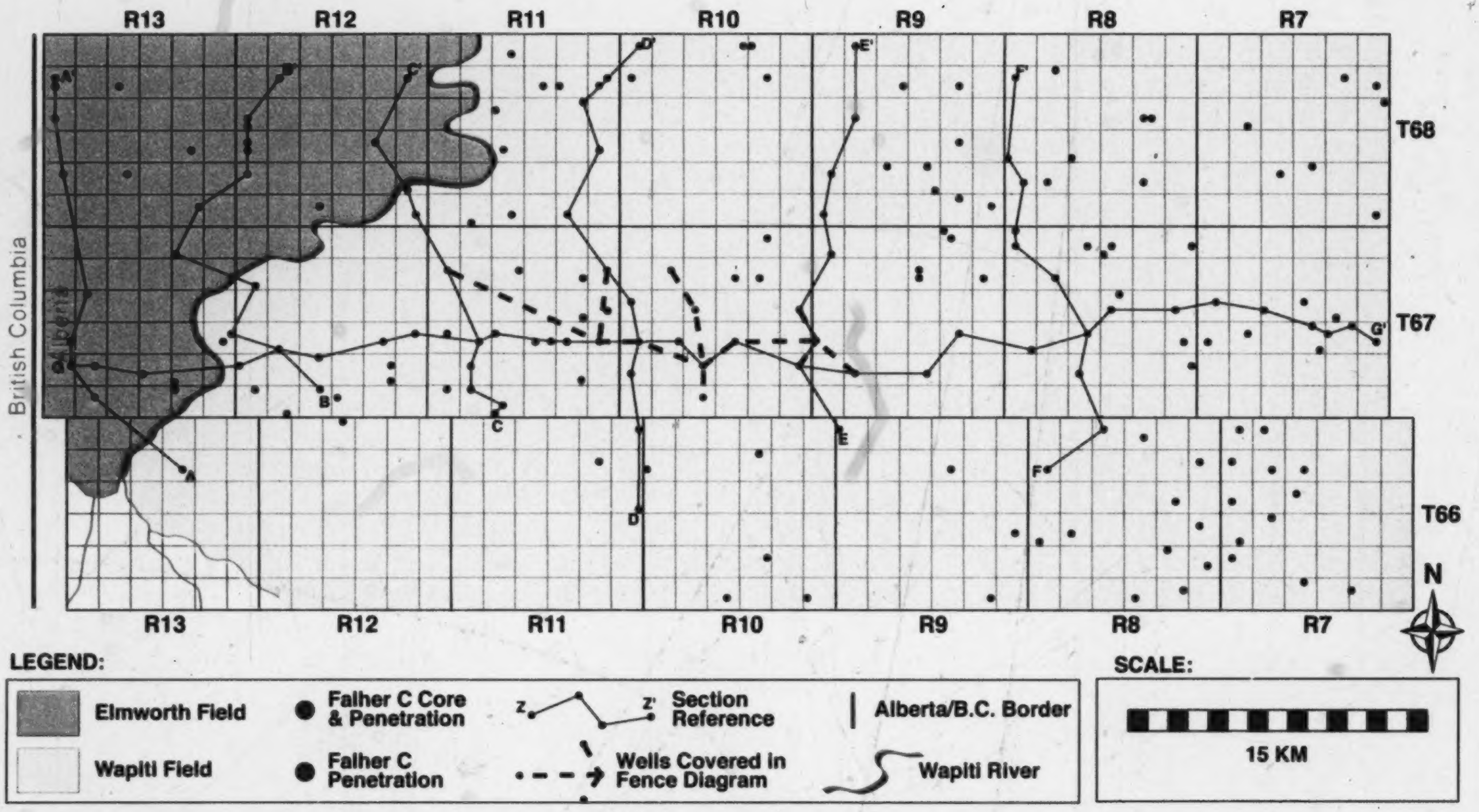

Figure 2. Map of the study area including portions of the Elmworth (purple shade) and Wapiti (tan shade) gas fields. The provincial border between Alberta and British Columbia (shown in green) lies on the western margin of the study area. The location of the 184 wells that have penetrated the Falher "C" Member either contain core (red dot), or have only recovered downhole wireline log data. The coverage of seven stratigraphic cross-section lines (solid black line), and a fence diagram (thick black dashed line) is also shown.

Table 1. List of cored Falher "C" intervals within the study area including: calibrated top and bottom of core interval (m), total length (m), and cross-section reference code.

Well Location				Core interval (m)			
l.s.d.	Section	Township	Range (W6)	Top	Bottom	Total Length (m)	Cross-Section Reference
11	7	68	12	2473	2490.25	17.25	B-B'
6	25		11	2112.25	2187	14.75	D-D'
6	16			2253.5	2268.25	14.75	
6	16			2277.25	2294.75	17.5	
10	1		9	2198.25	2217.25	18.5	
11	30		8	2001	2019.75	18.75	F-F'
10	5	67	13	2958.25	2967	8.75	
10	5			2792.25	2805.25	13	A-A'
3	17		12	2728.5	2736.25	7.75	B-B'/G-G'
9	11			2549	2555.25	6.25	
1	11			2548	2568	20	
12	7			2746.25	2755.25	9	G-G'
14	4			2681	2695.75	14.75	B-B'
12	3			2613	2621.5	8.5	
10	30		11	2421	2438.75	17.75	C-C', F.D.
10	25			2406	2420	14	D-D', F.D.
6	13			2437.75	2450.25	12.5	G-G', F.D.
11	8			2500	2519.25	19.25	C-C'
10	29		10	2386	2400	22	F.D.
7	24			2317.75	2337.5	19.75	E-E'
6	21			2453	2473	20	F.D.
7	18			2438.75	2455.75	17	D-D'/G-G', F.D.
7	15			2516	2534.75	18.75	G-G', F.D.
10	12			2475	2485	10	E-E'/G-G', F.D.
10	9			2351.25	2361.25	10	G-G', F.D.
10	4			2477	2489.25	12.25	F.D.
5	18		9	2368	2331	13	E-E', F.D.
10	14			2295	2304	9	G-G'
6	8			2385.25	2399.75	14.5	G-G', F.D.
10	16		8	2250.75	2269.25	18.5	G-G'
11	22		7	2083.75	2103	19.25	
10	17			2160.25	2174	13.75	
1	15			2121.75	2135	13.25	
16	14			2499.5	2504.5	5	G-G'
12	14			2102.25	2115	12.75	G-G'

1.3 Regional Stratigraphy and Paleogeography

The Falher Member of the Spirit River Formation is superposed on the Wilrich Member, and lies stratigraphically below the Notikewin Member (figure 3). Distinction between the three Members within the subsurface is made on a lithological basis through the use of down-hole petrophysical well logs that have been calibrated to cored intervals (figure 3). Further subdivision of the Falher Member is based primarily on thickness and pattern correlation between wells. Thickly bedded coarse-grained clastic units typically produce bell or funnel-shaped gamma-ray responses. In contrast, shaly intervals deflect the gamma-ray curve right and major coal horizons appear as "spikes" on the sonic log. Similar methods employed in other studies (*e.g.* Cant, 1984; Arnott, 1993; Rouble & Walker, 1997; Casas & Wlaker, 1997), show that the Falher Member can be subdivided into A, B, C, D, and E units in order of increasing stratigraphic age. Within the study area, the Falher C is recognized as a coarsening upward coarse-grained clastic unit, capped by carbonaceous shales and thickly bedded coals (figure 3).

The Lower Cretaceous Fort Saint John Group includes sedimentary sequences in the Northeastern B.C. Foothills and the Peace River Plains that were deposited during the Early Albian inundation of the western interior of Canada by the Clearwater Sea (McLearn, 1944). Prior to the Early Albian transgression, the Aptian seas were restricted to a narrow strip of the Arctic Plain between the Mackenzie Delta and Darnley Bay area (Jeletzky, 1971). As a result, the Aptian Bullhead Group is comprised of sedimentary sequences deposited in piedmont-alluvial, floodplain, and coal-forming environments (Stott, 1984). Further demonstration of regional non-marine conditions during the Aptian is the stratigraphic equivalence of the uppermost Formation of the Bullhead Group, the Gething Formation, with the Ostracod Zone or Calcareous Member in the central Alberta plains and foothills (figure 3). These latter units contain calcareous shale and limestone with a fresh water fauna (Stott, 1984).

Marine encroachment into the western interior began in the Early Albian as the Clearwater Sea transgressed southward via the Mackenzie River Basin (Stelck *et al.*, 1956). The Sea's southernmost shores are interpreted to have trended west/east at about the latitude of Calgary, Alberta (figure 1). The massive marine shale sequence of the Moosebar Formation was deposited within the Clearwater Sea, and crops out in the northeastern B.C. and central Alberta foothills. Within the west-central Alberta and oil sands regions of Alberta, these fully marine shales comprise the Wilrich and Clearwater Formations respectively (figure 3). By late Early Albian-time, nearshore, shoreface and marginal marine conditions had stabilized regionally between Twp. 64-78, depositing thick sequences of coarse clastic, carbonaceous shales and abundant coals within northeastern B.C. and west-central Alberta (Cant, 1984). Only the upper portion of these thick sequences of conglomerate, sandstone, shale and coal are represented by the marine Gates Formation in northeastern B.C. along the Peace River in the type section, and are laterally equivalent with the Falher and Notikewin Members of the Spirit River Formation in west-central Alberta (figure 3). Maximum stratigraphic thickness of the Moosebar-Gates interval occurs between Bullmoose Mountain and the town of Peace River and is thought to parallel structural trends related to the Peace River Arch (Stott, 1968). The Gates Formation and Falher-Notikewin Members of the Spirit River Formation are laterally conformable with the Upper Mannville and Grand Rapids Formations of central Alberta and oil sands regions (figure 3).

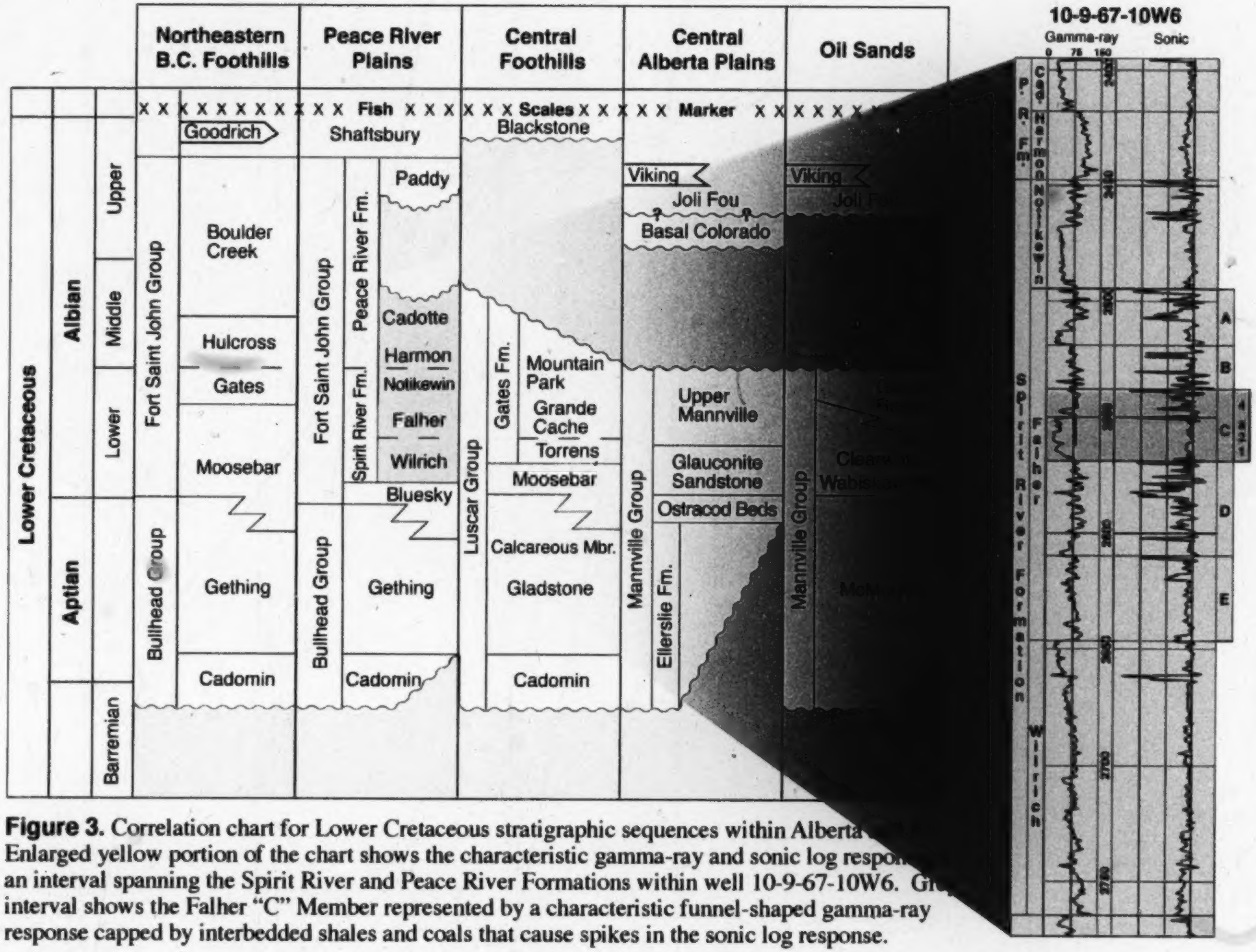

Figure 3. Correlation chart for Lower Cretaceous stratigraphic sequences within Alberta
Enlarged yellow portion of the chart shows the characteristic gamma-ray and sonic log respon
an interval spanning the Spirit River and Peace River Formations within well 10-9-67-10W6. Gr
interval shows the Falher "C" Member represented by a characteristic funnel-shaped gamma-ray response capped by interbedded shales and coals that cause spikes in the sonic log response.

A second regionally significant transgressive pulse of the Clearwater Sea reestablished primarily shale deposition within the northeastern B.C. and central Alberta regions. Within the subsurface of Alberta a uniformly thick shale succession comprises the basal portion of the Peace River Formation and is termed the Harmon Member. The Hulcross Formation crops out in northeastern B.C., and is laterally equivalent with the Harmon Member (figure 3). Nearshore coarse-clastic deposition accompanied northward retreat of the Clearwater Sea toward the end of the Middle Albian as indicated by the deposition of the coarsening upward sandstone Cadotte Member of the Peace River Formation (figure 3). Little is known of the extent of late Middle Albian deposition in the central and oil sands regions of Alberta. Regionally, the uppermost contacts of the Mannville and Luscar Groups are accepted as disconformable, as is the upper contact of the Cadotte Member (figure 3). The interpreted lacuna that variably spans the Mid- and Upper Albian in eastern and central Alberta, lessens westward into a conformable succession in northeastern B.C. termed the Boulder Creek Formation.

A large proportion of what is known about the paleogeographic distribution of the Lower Cretaceous Albian Clearwater Sea within the western interior of Canada is attributed to biostratigraphic zonations of molluscan and foraminiferal specimens. Jeletzky (1964), recognized that the North American Boreal Biotic Province was characterized by its ammonite, belemnite, *Buchia*, and *Aucellina* faunas. A general lack of diversity within the invertebrate faunas of the Boreal Province is viewed as a result of relative coolness of the Clearwater Sea, compared with the more southerly and westerly marine realms of North America during the Lower Cretaceous (Jeletzky, 1971). Table 2 demonstrates Jeletzky's (1971) zonation of the Boreal Biotic Province. Of chief importance to the stratigraphy of the Spirit River Formation is *Arcthoplites irenense* and *Arcthoplites macconnelli* Subzones of the ammonite Zone of *Beudanticeras affine*. These subzones confirm flooding of the Peace River region by the late Lower Albian (Jeletzky, 1971). Age equivalent foraminiferal zones of the western interior of Canada are examined by Caldwell *et al.* (1978). Table 3 highlights the *Marginulinopsis collinsi-Verneuilinoides cummingensis* Subzone within the *Gaudryina nanushukensis* Zone. Two foraminiferal biofacies exist within the subzone. The calcareous *M. collinsi* biofacies is an expression of the offshore fully marine conditions of the Clearwater Sea, while agglutinated *V. cummingensis* is representative of more restricted marginal marine (brackish-water), conditions (Caldwell *et al.*, 1978).

1.4 Historical Overview

The first geological investigations highlighting Lower Cretaceous Albian-aged rocks were those reported by Alfred R. C. Selwyn in 1875- a momentous year that also recorded the death of Sir William Logan, founder and constant benefactor of the Geological Survey of Canada. In

Table 2. Fossil zones of the boreal biotic province (modified from Jeletzky, 1971)

	STAGE		ZONES	SUBZONES
LOWER CRETACEOUS	ALBIAN	Upper	*Neogastroplites*	*Neogastroplites mclearni*
				Neogastroplites americanus
				Neogastroplites muelleri
				Neogastroplites cornutus
				Neogastroplites haasi
				UNKNOWN
		Middle	*Gastroplites*	*Gastroplites ? liardense*
				Gastroplites canadensis
				Pseudopulchellia pattoni
				UNNAMED ZONE
		Lower	*Beudanticeras affine*	*Arcthoplites mcconnelli*
				Arcthoplites irenense
				"Lemuroceras c.f. indicum"
				Cleoniceras c.f. subbaylei
				Sonneratia c.f. kitchini

Table 3. Foraminiferal zones of the interior plains of Canada (Caldwell *et al.*, 1978)

	STAGE		ZONES	SUBZONES
LOWER CRETACEOUS	ALBIAN	Upper	*Miliammina manitobensis*	*Haplophragmium swareni*
				Haplophragmoides postis goodrichi
				Verneuilina canadensis
			Haplophragmoides gigas	
		Middle	*Gaudryina nanushukensis*	*Ammobaculites wenonahae*
				Ammobaculites sp.
				Haplophragmoides multiplum
		Lower		*Marginulopsis collinsi- Verneuilinoides cummingensis*
				Trochammina mcmurrayensis
				Rectobolivina sp.

a *Report on Exploration in British Columbia* (1877), Selwyn described shales outcropping along the Peace River five miles downstream of Hudson Hope as Mesozoic shales belonging to Division II. These same shales appear again in a subsequent Survey Report of Progress by George M. Dawson entitled; *Report on an Exploration from Port Simpson on the Pacific Coast to Edmonton on the Saskatchewan, Embracing a Portion of the Northern part of British Columbia and the Peace River Country* (1881). In this report Dawson incorporated Selwyn's description of the Lower Shales, and named them the Fort St. John Shales after a river exposure about a mile downstream of Fort St. John, British Columbia.

In 1917 McLearn continued exploration westward of Hudson Hope and described sandstones exposed along the walls of the canyon of the Peace River as belonging to the "Bull Head Mountain Formation", and recognized the Fort Saint John Shales as "…embraces all the strata lying between the Bull Head Mountain below and the Dunvegan sandstones above." McLearn (1918, 1923), further subdivided the sandstone and the underlying shale downstream of Hudson Hope as the Gates Formation and Moosebar Shales respectively.

Wickenden and Shaw (1943), investigated the Pine River area and made a five part subdivision of rocks belonging to the Fort St. John Group. From oldest to youngest, their stratigraphic succession included: Moosebar, Commotion, Hasler, Goodrich, and Cruiser Formations. Similar studies in separate regions of Northeastern B.C. and the District of MacKenzie encountered regional variations of facies successions, and led to unique stratigraphic terminology. It was not until 1950 that an attempt was made to compile a comprehensive summation of the work performed on the lower Cretaceous. McLearn & Kindle (1950), recognized "Because the lithological succession varies from place to place it is not possible to use one, uniform classification of the strata for all of northeastern British Columbia. Local classifications are required." Also included in McLearn & Kindle (1950), was a section detailing some of the paleogeographic aspects of the Lower Cretaceous that could be surmised from work completed up until that point, however detailed and accurate paleogeographic maps remained largely elusive. By the author's own admission, any attempt to produce accurate paleogeographic maps would prove "...useless to attempt [paleogeographic map generation] until some important problems of correlation are settled and more is known of the subsurface stratigraphy of the Lower Cretaceous of the interior regions of Canada..." (McLearn & Kindle, 1950).

The Alberta Study Group (1954), and Badgley (1952), were among the first investigators to extend the correlation of Lower Cretaceous rocks into the subsurface of the Peace River and west-central Alberta regions. Numerous wildcat wells had been drilled, and allowed for the interpretation and correlation of subsurface facies with the stratigraphic framework established within the foothills of northeastern British Columbia. Beneath the Peace River plains the Alberta Study Group (1954), subdivided the Fort St. John Group into the Spirit River Formation, the Peace River Formation, and the Shaftesbury Formation. The stratigraphically lowermost Formation, the Spirit River Formation, was further subdivided into Members termed the Wilrich, Falher and Notikewin Members from oldest to youngest respectively.

Paleontological investigations of Early Cretaceous rocks took place in conjunction with field studies beginning with Whiteaves (1885, 1893), who reported upon sample collections made by Selwyn, Dawson, and McConnell. Among the studies specific to specimens recovered from the Fort St. John Group are those reports made by McLearn (1944), McLearn & Kindle (1950), Stelck (1956), Jeletzky (1964, 1968, 1971), and Caldwell *et al.* (1978). These reports provide valuable discussion of the distribution, composition and zonation of Early Cretaceous mega- and microfauna.

It was recognized as early as 1881 (Dawson, 1881, p. 114 B), that the source of Early Cretaceous shoreline sediments was likely west of the Rocky Mountains. Petrographic studies on sandstone and conglomerate revealed an abundance of quartz mineralogy. An overall paucity of feldspar negated any claim of an igneous source for Early Cretaceous clastic accumulations. As it turns out, the sediment source was the only element of the Early Cretaceous sandstones that workers agreed upon. Regarding the paleogeographic orientation of coarse-grained formations, speculations range from northwest/southeast (McLearn, 1944; Jeletsky, 1971; McLean, 1979), to west-southwest/east-southeast as suggested by Stott (1968).

The discovery of hydrocarbon in the Deep Basin Elmworth gas field in 1976 lent impetus to the study of coarse-grained reservoir units in the subsurface of Alberta. As the focus on lithostratigraphic description and correlation began to subside, many workers began to investigate the sedimentological relationship between occurrences of reservoir quality sandstone and conglomerate in the Deep Basin of Alberta and adjacent foothills of northeastern B.C. McLean (1979), examined the influence of tectonics and sediment provenance on the updip limit of gas saturation. Leckie & Walker (1982), developed a depositional model based upon outcrop occurrences of the Gates Formation. They provided a basis for distinguishing fluvial from beach conglomerates, and suggested that the model could be used a predictive tool for stratigraphically equivalent reservoirs in the Deep Basin.

As drilling activities in the Deep Basin continued, the wealth of subsurface data in the form of core and petrophysical well logs grew. Petrographic studies of cored intervals in the Spirit River group attempted to shed light upon the controls of porosity/permeability distribution in sandstone and conglomerates (Cant, 1983; Cant & Ethier 1984; Rahmani, 1984). It was determined that the trapping mechanism within the Deep Basin was intimately related to a combination of both stratigraphic and diagenetic controls. Cant (1983) found that post-depositional diagenetic alteration of sandstones rendered them tight relative to stratigraphically down-dip porous conglomerate reservoirs. Cant then suggested that gas generated in down-dip coal beds would be trapped beneath tight sandstones within these porous conglomeratic reservoirs. Cant & Ethier (1984) recognized a disparity in the performance of conglomeratic reservoirs, and postulated that the success of a well was not solely dependant on the presence of conglomerate, but also the mode of conglomerate as determined by the original depositional environment.

Utilizing core analyses, Cant (1984) recognized eight major transgressive and regressive cycles within Spirit River Formation. In his study, major characteristics of coarsening upward sequences were attributed to high-energy wave dominated environments of deposition and proximity to the active orogenic belt. Leckie (1986), identified only seven transgressive/regressive cycles in northeastern British Columbia, and suggested that the cyclicity and lateral extent of the sequences were related to the tectonic thrusting and loading of the Peace River arch. Preliminary calculations of coastal retreat/progradation and the duration of each transgressive/regressive Falher cycle are also presented in Leckie (1986).

Over the last decade, much attention has been centered on the sedimentology and high-resolution allostratigraphy of individual cycles within both the Falher and Notikewin Members. Refined drilling practices have uncovered increasingly subtle trapping styles, and as such, have required detailed mapping and sedimentological models as a basis for further exploration. Arnott (1993) subdivided the Falher "D" pool into four sub-members (termed D1, D2, D3, D4), based upon observed changes in the genetically related successions of strata and their bounding surfaces identified in core. From this study it was found that not only was relative sea level important in controlling reservoir strata, but also temporal changes in the nature of sediment being supplied to the Falher shoreline. A similar study of the Falher "A" and "B" (Rouble & Walker, 1997), integrated detailed facies analysis and principles of allostratigraphy to divide the Falher A and B members into four distinct allomembers, termed A1, A2, B1, and B2. Casas & Walker (1997), provide a detailed facies analysis and recount the depositional history of the Falher C and D. In Casas & Walker (1997), the Falher C consists of four sub-members that are termed C1, C2, C3, and C4. Regarding the Falher D, facies descriptions, and depositional geometries and environments differ sharply from Arnott (1993), however the four sub-members remain. Most recently, Caddel (2000), completed a thesis detailing the sedimentology and stratigraphy of the Falher "C" Member within the foothills of northeastern British Columbia. The study determined the predictive geometries and spatial relationships between reservoir and non-reservoir quality facies and extrapolated these trends into the subsurface via a sequence stratigraphic framework established primarily in outcrop exposures of the Falher "C" Member.

1.5 Objectives

Research on the Falher "C" Member was initiated with several objectives in mind:

1. Subdivision of cored intervals of the Falher "C" Member into sedimentary facies based upon characteristic lithology, lithological accessories, physical and biogenic sedimentary structures.
2. Grouping of facies into facies assemblages that represent architectural elements of larger depositional systems.
3. Genesis of a suite of subsurface maps including: structural top, net isopach thickness, net sand thickness, and facies slice maps.
4. Construction of a high-resolution allostratigraphic framework for the Falher "C" Member that incorporated interpretation of lateral variability in facies architecture and localized alllostratigraphic surfaces identified in core.
5. Synthesis of a multi-stage depositional model for the Falher "C" Member that illustrates the interrelationship between relative sea level fluctuation, local sediment supply and autocyclic depositional controls.

1.6 Methodology

Examination of thirty-five cored intervals recovered from Falher "C" Member wells took place at the Alberta Energy and Utilities Board (AEUB) Core Research Center in Calgary, Alberta. The majority of the cores examined in this study are open to public viewing, however several were confidential. Access to these cores is limited to employees and contractors of Anderson Exploration Limited, and joint venture companies.

This study employs a multidisciplinary approach to characterizing the geology of the Falher "C" Member incorporating principles of ichnology, process sedimentology, geophysical well log analysis, and allostratigraphy. Initial facies subdivision of Falher C core was based upon lithology, lithological accessories, grain-size, and physical/sedimentary structures. Several facies associations were synthesized from grouping of distinct successions of primary facies. Genetic linkage between facies comprising the same association is established through stacking order, thickness variation, contact relationships, sedimentological chacteristics, and ichnological characteristics.

Trace fossil assemblages constitute an important aspect of each facies association in that they represent a collective response to environmental stress imposed on a community of organisms inhabiting a depositional environment. Inherent elements used to differentiate and characterize each fossil assemblage include; trace fossil abundance, ichnogenus diversity, burrow size variation, and ethology.

Another important aspect of the observed facies associations is their bounding surfaces. Facies associations are commonly viewed as architectural elements of a depositional system, therefore the contacts between facies associations represent responses to allocyclic and autocyclic changes imparted on a depositional system. Allocyclic changes within a depositional system (eg. sea-level change and sediment supply) are of regional consequence, and are reflected in the character of contacts between facies associations. Examination and establishment of these bounding stratigraphic surfaces is imperative for generation of a valid stratigraphic framework.

All of the cored intervals examined in this study were calibrated to accompanying geophysical well log data. Among the available log data, the gamma-ray and sonic log profiles proved most useful for correlation of calibrated cored intervals with wells lacking core data. In this manner, well log profiles of facies associations and bounding sequence stratigraphic surfaces were extrapolated throughout the study area, and a high-resolution allostratigraphic framework was generated. Selected methods illustrating this stratigraphic framework include; stratigraphic cross-sections, paleogeographic facies slice maps, isopach thickness maps, a structural top map, and a three-dimensional fence diagram.

CHAPTER TWO: Facies Associations and Depositional Environments

2.1 Introduction

Division of the Falher "C" member into facies is based upon physical and biological characteristics observed in core (table 4). Among the defining features inherent to each of the facies are lithology, grain size, and physical and biogenic sedimentary structures. As a general rule, the eleven interpreted facies were organized in a coarsening-upward fashion beginning with facies F1 (organic-rich shale) and extending to facies F10 (chert conglomerate). The exception to the rule is facies F11, a mineralogical oddball designated as a sub-bitumenous coal. Further sub-division of the conglomerate facies F10 into sub-facies A, B, C, and D is based upon disparities in sorting and conglomerate type. Reasons for this sub-division are discussed in Section 2.3.

Facies associations are groupings of genetically related facies that have been deposited and modified by both sedimentary and biological processes active within an environment of deposition. Once deposited, sediments are subject to varying degrees of physical and biological reworking. The degree to which sediments become reworked following deposition is dependant upon a range of physical and biological processes that are inherent to the environment of deposition. Evidence of these processes in core is present as a distinctive succession of facies. Reconstruction of the depositional environment is accomplished by interpreting observed facies successions through analogy with similar successions in both ancient and modern examples.

In the Falher "C" Member, depositional environments encompassing the marine, marginal marine, and non-marine realm are characterized by five facies associations that exhibit a distinctive succession within core. These five facies associations are as follows: FA1: storm dominated lower shoreface to offshore transition; FA2: wave dominated upper shoreface and foreshore; FA3: tidal inlet; FA4: brackish back-barrier; FA5: fluvial distributay plain.

Table 4. Table of facies observed in the Falher "C" Member.

FACIES	GRAIN SIZE & LITHOLOGY	PHYSICAL SEDIMENTARY STRUCTURES	BIOGENIC SEDIMENTARY STRUCTURES	DEPOSITIONAL ENVIRONMENT
[redacted]	[redacted]	[redacted]	[redacted]	[redacted]
F2	Organic-rich Shale	Wavy carbonaceous laminae, horizontal lamination, assymmetrical lamination, inclined planar lamination	Rh, m; U.B., c-a	Lagoon, Lake
[redacted]	[redacted]	[redacted]	[redacted]	[redacted]
F4	Sand/Shale-rich Siltstone	Wavy heterogeneous laminae, lenticular bedding, convolute laminae, assymmetrical lamination, synaeresis cracks	Ch, r-c; Cy, m-c; Gy, r; Pa, m-c; Pl, m; Rh, c; Sk, m; Te, c-a	Distal Lwr. Shoreface, Interdistrbutary Bay, Intertidal Flat, Lagoon, Fluvial Distributary Plain
[redacted]	[redacted]	[redacted]	[redacted]	[redacted]
F6	Fine-grained Sandstone	Horizontal to steeply inclined cross-bedding, trough cross-bedding, H.C.S., symmetrical ripples, climbing ripples	Co, r; Fu, c; Ma, a; Op, r; Pa, m-c; Pl, m; Rh, c; Sk, r	Proximal Lwr. Shoreface, Distal & Proximal Upr. Shoreface, Foreshore, Backshore, Tidal Channel
[redacted]	[redacted]	[redacted]	[redacted]	[redacted]
F8	Very Coarse-grained Sandstone	Massive bedding, gently to steeply inclined bedding	-	Foreshore
[redacted]	[redacted]	[redacted]	[redacted]	[redacted]

Table 4 (*Cont.*). Table of facies observed in the Falher "C" Member.

FACIES		GRAIN SIZE & LITHOLOGY	PHYSICAL SEDIMENTARY STRUCTURES	BIOGENIC SEDIMENTARY STRUCTURES	DEPOSITIONAL ENVIRONMENT
F10	[redacted]	[redacted]	[redacted]	[redacted]	[redacted]
	B	Bimodal, Matrix-supprted Chert Conglomerate	Normal graded bedding, trough cross-bedding, steeply inclined bedding	-	Foreshore
	[redacted]	[redacted]	[redacted]	[redacted]	[redacted]
	D	Polymodal, Clast-Supported Chert Conglomerate	Normal graded bedding, reverse graded bedding, gently inclined bedding	-	Proximal Upr. Shoreface
[redacted]	[redacted]	[redacted]	[redacted]	[redacted]	[redacted]

***Key to abbreviated ichnogenera:** **Ar**: Arenicolites, **As**: Asterosoma, **Ch**: Chondrites, **Co**: Conichnus, **Cy**: Cylindrichnus, **Dl**: Diplocraterion, **Fu**: Fugichnia, **Gy**: Gyrolites, **Ma**: Macaronichnus, **Op**: Ophiomorpha, **Pa**: Paleophycus, **Pl**: Planolites, **Rh**: Rhizomes, **R**: Rhizocorallium, **Ro**: Rosellia, **Sk**: Skolithos, **Te**: Teichichnus, **Tr**: Terebellina, **Th**: Thalassinoides, **U.B.**: Unidentifiable Bioturbation.
Key to occurence: **r**: rare, **m**: moderate, **c**: common, **a**: abundant.

2.2 Facies Association One (FA1): storm-dominated lower shoreface.

Facies represented by FA1 are distributed throughout the Falher "C" Member within the study area. In some instances FA1 represents the whole volume of the marine-deposited succession in the Falher "C" (plate 1, A). However, FA1 most commonly occupies the basal portion of the Falher C, and lies directly upon non-marine deposits ascribed to the Falher D interval. FA1 is typically overlain by coarser-grained facies of FA2 (plate 1, B). In rare cases FA1 is missing from the sequence, replaced by the laterally equivalent FA4 succession. Facies common to FA1 are; F1, F4, F5, F8 and F10 C.

Sedimentology

The most abundant and thickly bedded facies in FA1 is facies F5 (figure 4). F5 is a very fine-grained sandstone displaying gently inclined parallel to sub-parallel lamination (plate 3). The grains are typically well sorted and comprise the very fine sand range between very fine lower and very fine upper (4.0-3.0 ϕ). Discrete pebble and granule stringers are aligned parallel to lamination. Continuous stratigraphic thickness varies between 0.5 m to as much as 8.0 m within this facies. Bedding contacts are typically sharp and erosive. Locally they are gradational where F5 is underlain by F4 and overlain by F6.

Internally F5 may be further subdivided based upon contacts between laminae, lamina sets, beds and bed sets. Contacts between laminations are distinguished based upon mineralogy and texture emphasized by color contrast between laminae (plate 3). Dark laminations are composed of micaceous flakes and organic detritus. Lighter laminations are composed of quartz, silt and diagenetic clay minerals. Lamina sets are commonly comprised of laminae that are sub-parallel and are dipping along the same plane. Grading within lamina sets is common, expressed as an upward transition from light laminae at the base to dark at the top of individual laminae (plate 3). Contacts between beds within F5 occur across planes that exhibit an observable change in the net orientation of laminae sets. The inclination of this bedding contact plane typically does not exceed 10° from the horizontal (plate 3). Series of stacked beds comprised of parallel to sub-parallel lamine are commonly capped by oscillation and combined flow ripples. Bedset contacts are interpreted where rippled beds are truncated at low angle (<10°), by parallel to sub-parallel laminae. Placement of bed set contacts is difficult within thickly-bedded intervals of similar dipping bed sets of parallel to sub-parallel laminae. Locally, truncated vertically subtending burrows commonly demarcate hidden bedding junctions, facilitating identification of such surfaces (plate 4).

Vertical successions of F5 are commonly interrupted by discrete beds of facies F8 or

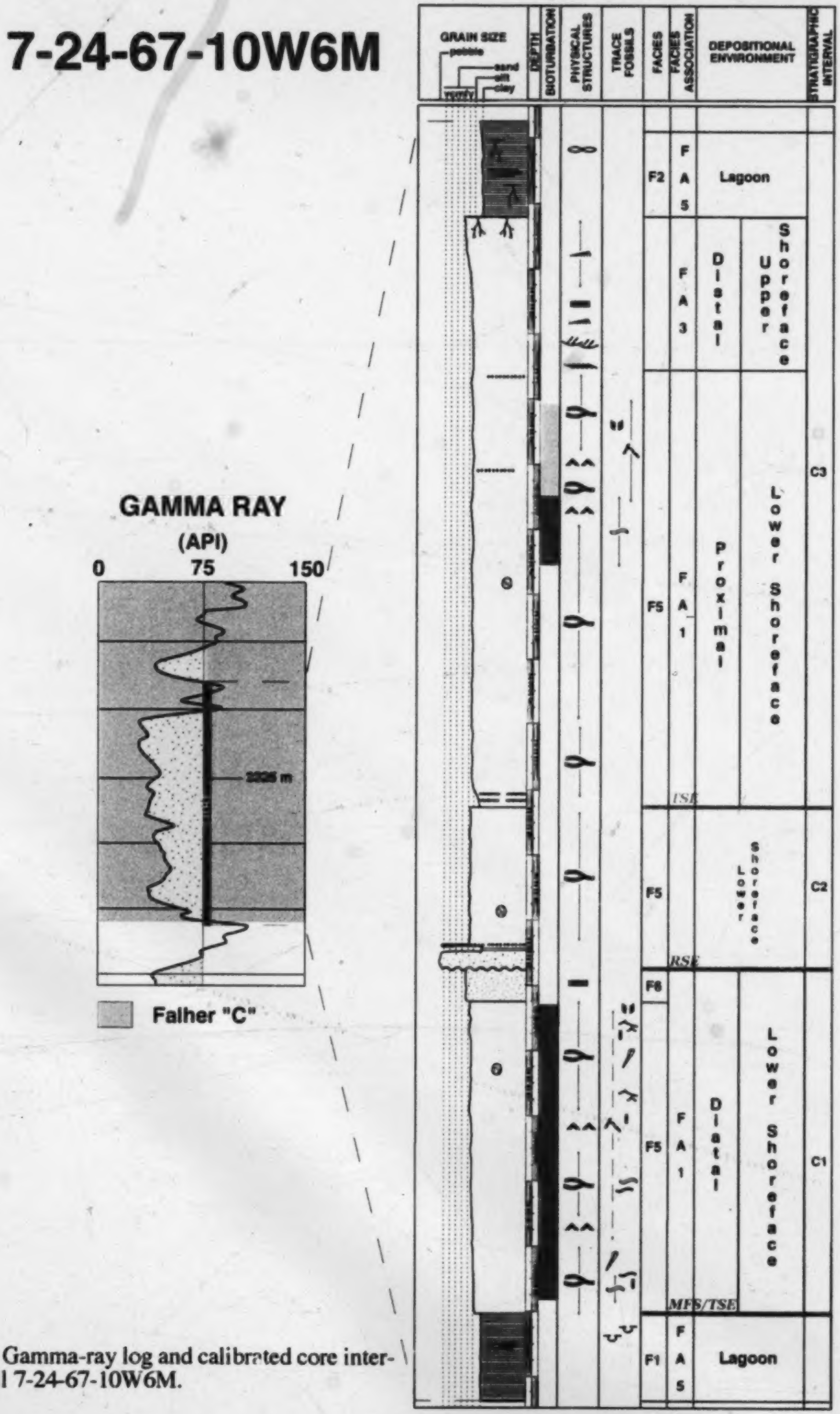

Figure 4. Gamma-ray log and calibrated core interval for well 7-24-67-10W6M.

F10C (plate 5). Facies F8 is a poorly sorted, very coarse-grained quartz sandstone (1.0-2.0 ϕ), while facies F10C a bimodal clast supported quartz conglomerate. Physical structures are typically absent in both facies. Where these facies are present, lower bedding contacts are sharp and scoured while the overlying contact is typically sharp and reworked (plate 5, C). Bedding thickness of these facies rarely exceeds 0.25 m. Local examples range up to 0.35 m thick.

In cored intervals where facies F5 does not directly overlie organic-rich mudstone of the Falher "D" Member, the basal portion of FA1 is represented by facies F4, a bioturbated sandy shaly siltstone. This facies is heavily mottled by bioturbation to the extent where no recognizable features of primary bedding are present with the exception of rare discontinuous wavy carbonaceous laminations. Siderite is common within this facies, expressed as nodular concentrations along discrete bedding horizons, and as partially sideritized portions of trace fossil burrow linings (*e.g. Rosellia* bulbs). Upper and lower bedding contacts of facies F4 are sharp, and locally bioturbated. Total thickness of this facies ranges from 0.30 m to 2.30 m.

Ichnology

Two trace fossil assemblages are present within FA1. The first assemblage is dominantly composed of horizontally-oriented burrows, produced primarily by deposit feeding organisms. It is comprised of the following ichnogenera: *Palaeophycus* (c), *Planolites* (m-c), *Rhizocorrallium* (r), *Chondrites* (c), *Rosselia* (c), *Terebellina* (m), *Asterosoma* (r), and *Cylindrichnus* (r). These biogenic structures are characteristic of the *Cruziana* ichnofacies. In general, occurrence of this trace fossil suite is restricted to the basal intervals of FA1 where primary bedding has been strongly overprinted or destroyed by bioturbation (Plate 6).

The second trace fossil assemblage comprises: *Skolithos* (m-c), *Arenicolites* (r-m), *Diplocraterion* (m), *Palaeophycus* (c-a), *Teichichnus* (m-c), *Ophiomorpha* (r-c), and abundant escape structures. The majority of the biogenic structures within this assemblage show both suspension and deposit feeding behavior and represent elements of the *Skolithos* and *Cruziana* ichnofacies respectively. Typical occurrences of this assemblage include: (i) the uppermost bed within a laminated bedset that is moderately to completely bioturbated by primarily horizontally oriented ichnogenera such as *Palaeophycus* (Plate 6, C and D), and *Teichichnus* (Plate 7, A), (ii) vertically subtending ichnogenera such as *Skolithos* (Plate 9, A and D), *Arenicolites* (Plate 9, C), and *Diplocraterion* (Plate 8) that cross-cut primary bedding within underlying bed sets (Plate 4, C). Alternatively the uppermost bioturbated bed within laminated bed sets is missing, and only vertically subtending trace fossils remain. In such instances, concealed bed junctions are revealed where the upper portions of these ichnogenera have been erosionally planed-off during deposition of the overlying bedset (plate 4).

Within FA1, solitary forms of several ichnogenera are interspersed within the facies succession. Ichnogenera such as *Teichichnus* (Plate 7, A), *Ophiomorpha* (Plate 7, D), *Rosellia* and numerous escape traces (Plate 7, B and C), commonly occur at discrete intervals throughout FA1. Generally little disruption of the primary depositional fabric is exhibited.

Interpretation and Discussion

The facies succession within FA1 is interpreted to represent a shoaling upward sequence deposited by storm sedimentation within the lower shoreface. FA1, and in particular facies F5, contain amalgamated stacked bed sets of low angle sub-parallel planar lamination interpreted as hummocky cross-stratification (HCS). HCS has generated much debate regarding its origin and the exact nature of the process controlling its formation (Duke *et al.*, 1991). One hypothesis suggests that HCS lamination results from the fallout and subsequent remoulding of hummocks and swales by elevated wave orbital motions (*e.g.* Harms *et al.*, 1975, Dott & Bourgeois, 1982; and Duke, 1985). Others have proposed that the development of HCS bedding is strongly dependant upon combined flows generated by strong geostrophic current superimposed upon oscillatory wave motions (*e.g.* Nottvedt & Kreisa, 1977; Swift *et al.*, 1983; Hunter & Clifton, 1982). Regardless of the exact nature of the depositional processes involved in HCS formation, there is consensus among sedimentologists that HCS bedding is formed below fairweather wave base during intense storms.

Periodic disruption of the fine-grained vertical succession of facies F5 by interdigitated occurrences of coarser-grained facies F8 and F10C is interpreted as storm deposition of sediments carried into the lower shoreface by rip-currents during peak storm activity. Rapid deposition and 'freezing' of a suspended sediment cloud is the process that has been invoked to explain the absence of sedimentary structure within these storm beds (Hunter & Clifton, 1982). Locally developed plane parallel bedding within storm bedding is probably due to deposition by tractive sheet-flow. This is likely on the basinward end of storm driven currents (Swift *et al.*, 1983). All occurrences of coarse-grained storm bedding were characterized by a sharp erosive lower contact, where initial flows scoured into the underlying beds. The contact between coarse-grained storm beds is predominately gradational, probably due to waning storm currents that reworked the uppermost portions of storm deposited bedding.

Figure 5 shows an idealized hummocky sequence as conceptualized by Dott & Bourgeois (1982). Peak storm wave oscillation and reworking is represented by amalgamated beds of laminae sets within the lower portion of the sequence. The lower portion is then overlain by wave-ripple laminae sets representing the waning stages of the storm. The time scale within which amalgamated HCS bed sets and capping bed sets of wave ripple sets is shown in figure

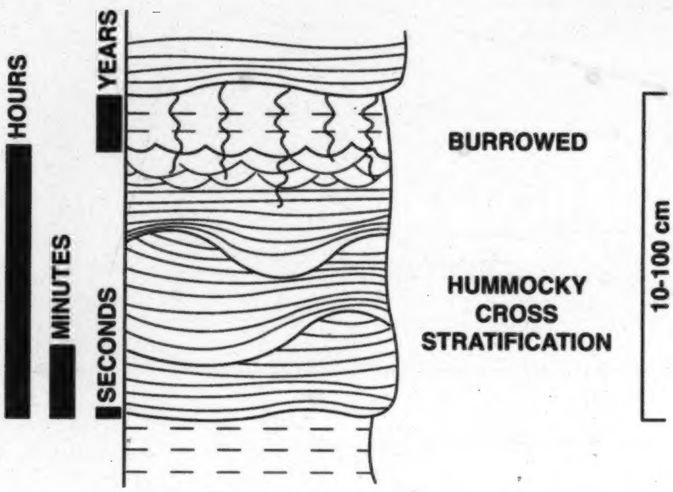

Figure 5. Idealized HCS sequence as conceptualized by Dott &Bourgeois (1982). Basal storm amalgamated lamina sets are overlain by wave ripple lamina sets that become bioturbated by opportunistic species during periods of relative quiescence. Relative time frame represented by each element of the succession is denoted to the left of the sequence. Total thickness range of the succession is shown to the right.

5. Beds deposited above the lower sequence become bioturbated by opportunistic species during periods of relative quiescence following storm activity. Over a time scale of weeks, months or even years of storm inactivity, the uppermost succession may become completely bioturbated by a stable benthic community within which populations are at or near equilibrium conditions (Pemberton *et al.*, 1992; Pemberton & MacEachern, 1997).

Close examination of the distribution of trace fossil assemblages within FA1 further supports a storm origin for the depositional succession. The two assemblages found within FA1 are interpreted as a pre- and post-storm assemblages. The pre-storm or fair-weather assemblage comprises trace fossil morphologies consistent with deposit feeding behavior characteristic of the *Cruziana* ichnofacies. The degree of bioturbation in facies containing the fair-weather assemblage is typically high to extreme, reflecting complete bioturbation of the substrate by a stable benthic community during low rates of deposition within the transitional offshore to distal lower shoreface. In contrast, the post-storm assemblage is primarily comprised of vertically-oriented ichnogenera that are representative of the *Skolithos* ichnofacies, in which suspension feeding behavior is most prevalent. Facies containing the post-storm assemblage are interspersed throughout the uppermost portions of the FA1 succession. These facies are moderately bioturbated and record the initial flourishing of opportunistic species within defaunated substrates following intense storm scouring and deposition within the lower to middle shoreface. Similar occurrences of pre- and post-storm assemblages within storm-deposited Cretaceous sequences have been reported from the Cardium Formation, Alberta, (Pemberton & Frey, 1984; Vossler & Pemberton, 1989) and the Spring Canyon Member of the Blackhawk Formation, Utah, (Kamola, 1984; Frey, 1990; Pemberton *et al.* 1992).

Sedimentologic and ichnological characteristics at variance with the idealized sequence of HCS bedding lend valuable insight into the proximity of sedimentation within the lower shoreface (Dott, 1983). Figure 4 shows a core log from 7-24-67-10W6M within the study area. The interval of core extending from 2336.00 m to 2331.25 m contains a succession of FA1 that includes cyclical bedding of amalgamated HCS capped by laminae sets of wave ripple lamination. A mixed *Skolithos-Cruziana* ichnofacies is also present within this interval. An overlying interval of FA1 within 7-24-67-10W6M (2328.25 m-2321.50 m), contains a thicker interval of amalgamated HCS, a paucity of wave rippled laminae sets and a much less diverse storm assemblage of trace fossils dominated by *Ophiomorpha*. Although both intervals are interpreted to have been deposited within the lower shoreface, the upper interval was probably deposited in shallower regions of the lower shoreface. Only storms of the greatest intensity and duration are likely to rework sediments deposited within the offshore transition to distal settings of the lower shoreface. This is reflected in a greater record of fair-weather deposition (*i.e.* beds reworked by post-storm assemblages) preserved between successive HCS sequences within the lower interval of 7-24-67-10W6M (figure 4). Sediments at shallower depths are subject to more frequent scouring and reworking by storms of lower intensity than those influencing sediments in distal settings. Facies deposited during fair-weather deposition are removed in proximal settings by subsequent scouring at wave-base during peak storm activity. This is reflected by the abundance of amalgamated bed sets of HCS and lack of trace fossils indicative of deposit feeding within the upper interval of 7-24-67-10W6 (figure 4). An ichnologic consequence of the greater depths to which storms scour away facies is the preferential preservation of only the more deeply tiered trace fossils (ie. *Ophiomorpha*), and removal of shallow tiered traces (Frey & Goldring, 1992; Pemberton & MacEachern, 1997).

2.3 Facies Association Two (FA2): wave-dominated upper shoreface and foreshore

FA2 comprises fine to coarse-grained sandstone and conglomerate facies that constitute the greatest reservoir potential within the Falher "C" Member. FA2 is composed of facies F6, F7, F9 and F10. These facies typically lie disconformably above and below very fine-grained silty facies of FA1 (Plate 1, B). Vertical and lateral variability of grain size and facies bedding thickness within FA2 is greater than any of the other facies associations observed in this study. There is a marked absence of biogenic sedimentary structures in FA2. Consequently, interpretation of depositional contexts for FA2 facies is highly dependent on process sedimentology. The impact of this on reservoir sedimentology cannot be overstated because the vertical and lateral variability of grain size, sorting, and conglomerate type, are intimately tied to porosity and permeability.

Sedimentology

The most fine-grained facies of FA2 is a trough cross-bedded, arenaceous sandstone designated as facies F6 (3.00-2.25 ϕ). These fine-grained sands are sub-rounded, and are moderately sorted. Steeply inclined tangential laminae terminate along sharp, erosive lower contacts that dip as much as 30° relative to a horizontal plane. Bedding contacts between lamina sets are commonly curvilinear and concave upward. Locally, laminations are internally graded. Similar to facies F5, a color change from light to dark grey marks a transition from quartz-rich mineralogy to predominately organic and micaceous flakes in the upper potions of laminae. Commonly, pebble-granule size stringers are developed parallel to bedding contacts ranging from horizontal to moderate (~20°) inclination (plate 3,B). Bedding thickness varies between 0.20 m to 0.15 m thick. Combined bed set thickness within facies F6 varies between 0.20 m to 2.40 m. Both gradational and sharp erosive contacts are observed separating facies F6 from a moderately sorted, medium-grained sandstone (2.00-2.25 ϕ), termed facies F7.

Facies F7 commonly forms a coarsening upward succession within FA2. In some examples it replaces facies F6 within the basal portions of FA2. In general, the sedimentary structures are comparible to those in facies F6. However, bedding plane contact angles are not as severe as compared with those in facies F6. 1-2 cm thick horizontal planar beds are occasionally graded in a normal fashion (plate 10, A). Contacts between bed sets remain sharp and erosive, but are more planar than those in facies F6. Bedding thickness varies between 0.10 m and 0.25 m while bed set thickness ranges between 0.45 m to 1.25 m.

Within FA2, an interbedded facies designated as F9 is commonly present. This facies is present beneath the thickly bedded conglomerate termed facies F10. Facies F9 is composed of poorly sorted fine- to coarse-grained sandstone and clast-supported chert pebble conglomerate.

Bedding contacts between these two lithologies are sharp and scoured. Physical structures include horizontal to gently inclined planar tabular cross-stratification that is crudely graded. Bedset thickness of the poorly sorted sandstone varies between about 0.05 m to 0.25 m. Conglomerate bed set thickness tends to be greater than that of the poorly sorted sandstone and ranges up to 0.25 m. Total bed set thickness of facies F9 range between 0.50 m to 3.25 m.

Facies F10 is a conglomerate facies that is further subdivided into four sub-facies termed A, B, C, and D. Differences in modality and the degree of matrix support are the basis for the subdivision. The first of the four sub-facies, F10 A, is a unimodal chert granule conglomerate, lacking a sandstone matrix (plate 11, A). The high degree of sorting and lack of contrasting grain sizes makes differentiation of sedimentary structure a tenuous proposition. However, isolated 1 cm thick beds of fine or medium-grained sandstone suggest that the facies is horizontal planar bedded (plate 11). In addition to these fine- and medium-grained sandstone interbeds, well sorted very coarse-grained sandstone beds are also common, and range in thickness from less than 0.05 m to 0.15 m thick. Larger pebble-sized chert clasts are interspersed within facies F10 A (plate 11, C and D), but do not appear to be preferentially concentrated along bedding contacts as stringers. Bedding thickness of F10 A ranges from 0.20-0.70 m, and contacts are generally sharp and erosive.

Facies F10 B and F10 C are both bimodal chert pebble conglomerates. Differences between the two facies arise in the degree of matrix or clast support. Bimodal matrix supported chert conglomerate (facies F10 B), occurs less frequently within FA2 than does the clast supported chert conglomerate (facies F10 C). It also tends to be more thinly bedded, ranging from less than 0.10 m to 0.50 m. Sedimentary structures include normal graded bedding, trough cross-stratification and gently inclined planar bedding. Beds of F10 B typically represent transitional horizons between clast supported conglomerate facies (F10 C and D), and finer-grained facies (plate 12, A). When facies F10 B is interbedded with relatively finer-grained facies (*e.g.* F7, F8), the matrix texture and composition closely resembles that of the adjacent finer-grained facies. Consequently, bedding contacts tend to be more poorly defined and gradational within facies F10 B.

In contrast to subfacies F10 B, subfaices F10 C comprises a thicker and more continuous succession within FA2. These clast supported bimodal chert pebble conglomerates contain well sorted fine to medium-grained quartz-rich sandstone matricies. Clast size ranges from granules to pebbles with rare cobble-sized clasts. Isolated development of patchy diagenetic clay within the matrix is commonly observed on bedding planes (plate 12). Bedding thickness can be as great as 1.00 m, but generally ranges between 0.10 m and 0.60 m. Bedding structure includes gently to steeply inclined cross-stratification, as well as trough cross-stratification. Both normal and reverse grading are observed within facies F10 C (Plate 10, B,C, and D).

The final conglomerate subfaices recognized in FA2 is termed facies F10 D. This conglomerate is a polymodal (comprising three clast sizes), clast-supported chert conglomerate. Clast sizes range from granules to cobbles with higher, yet equal proportions of granules and pebbles sized clasts. Individual clasts are typically equant and well rounded, clast surfaces commonly pitted and pock-marked (plate 13). Rare clasts that are disproportionately elongated along one axis display no preferential orientation (*i.e.* imbrication) at core scale. Bedding contacts are most commonly gradational and reworked. Physical structures are difficult to observe owing to limitations of core scale and the coarseness of grain sizes, however, periodic interdigitated medium to coarse-grained sandstone beds suggest flat to gently inclined plane parallel bedding. Bedding thickness in F10 D ranges from 0.04 to 0.75 m. Where matrix is present, matrix compositions within facies F10 D are more variable than those in F10 B and C, and include sideritized mud, well-sorted medium-grained sandstone, and very coarse-grained sand (Plate 14). Matrix composition has a profound effect on post-burial alteration of the petrophysical characteristics of facies F10 D, the most apparent of which is on porosity and permeability further discussed below.

Porosity and Permeablity Development Within Falher "C" Conglomerates (Facies F10).

When visually evaluating conglomerate intervals within the Falher "C", variation in sorting and conglomerate type is of paramount importance. Within the context of this study, subdivision of conglomerate facies F10 into unimodal (A), bimodal matrix and clast supported (B and C respectively) and polymodal (D), subfacies recognizes this importance. Unimodal and polymodal chert conglomerates (facies F10A), lacking a quartz sand matrix, represent facies of greatest reservoir potential because of a high degree of interconnectivity between large open pore spaces. Development of porosity and permeability within conglomerate facies containing sand matricies (ie. facies F10B, F10C, F10D) is dependant upon the proportion of matrix and clasts present in a given volume of core.

An interesting relationship between porosity and permeability develops in clast supported conglomerates that have a sand matrix; as porosity is reduced by an increase in the proportion of relatively voluminous non-porous areas (clasts), permeability increases because fluids can migrate through channels created at the clast/matrix boundary (Cant & Ethier, 1984). Furthermore, it is probable that permeabilities exhibited by clast supported conglomerates (facies F10 C, and D), would be higher than those shown by matrix supported conglomerates (facies F10 B), owing to the fact that contacts between clasts would interlink the channels between matrix sand and chert clasts.

Much of the reduction or enhancement of porosity and permeability within conglomeratic facies has taken place following deposition as a consequence of lithology-dependent diagenetic control (Cant, 1983; Cant & Ethier, 1984). Reduction of porosity within tight fine-grained sandstone intervals that typify FA1 has been attributed to such factors as the formation of quartz overgrowths, cementation by carbonates and clays, and crushing of sedimentary fragments (Cant, 1983). Bimodal conglomerate facies F10 B and C, as well as polymodal F10 D facies, are also susceptible to these same factors because of matrix composition. Cant & Ethier (1984), have observed quartz overgrowths and patchy carbonate and kaolinite cementation of sandy quartz-rich matricies present within bimodal conglomerates. Particularly dramatic examples of compactional suturing and stylolitization of polymodal conglomerate are observed within Falher "C" core (Plate 14, C), and discussed further by Cant (1983). The subdivision of facies F10 is largely based upon sorting and conglomerate type (ie. modality, and degree of matrix support), however it is also important to recognize the predominance of matrix lithology in the control of porosity reduction.

Interpretation and Discussion

FA2 is interpreted to have been deposited within wave-dominated upper shoreface and foreshore settings during long-term progradation of the Falher "C" shoreline. The lowermost contact between FA2 and FA1 formed by scouring of the underlying FA1 succession in association with longshore migration of rip-channels. Subsequent deposition of the basal facies F6 and F7 of FA2 is presumed to have occurred within longshore troughs located landward of oblique, shoreline-attached bars. In some cored examples these two comparatively fine-grained facies are missing, and interbedding of fine-grained sandstone and conglomerate is observed above the basal contact. Interbedding of sand and conglomerate facies at the base of the FA2 succession is interpreted to represent deposition within the distal upper shoreface. The interbedded nature of facies at the base of FA2 is likely reflects cyclic fluctuation of the depth to wave base over time. Onshore-directed currents beneath wavebase, laden with sediment derived from the lower shoreface, deposited the sand-sized fraction of F9. The coarser-sized fraction of F9 was deposited during relative deepening of wavebase during storm activity. Offshore-directed rip-currents deposited coarser grained material within distal regions of the upper shoreface and seaward.

Alternatively, it is possible the interbedding of F9 has an origin similar to facies F6 and F7. In this case, facies F9 was deposited within longshore troughs located landward of oblique, shoreline-attached bars. Relatively fine-grained sediments were derived from the lower shoreface. During periods of relative quiescence, landward directed currents associated with wave swell drove these sediments up the basinward-dipping flank and overtop the crest of bars, depositing them within the longshore trough. The conglomeratic fraction of facies F9 was derived from proximal settings within the upper shoreface and foreshore during storm activity. Seaward-directed rip-currents would have carried this material basinward following wave scouring of the proximal upper shoreface and foreshore.

Conglomeratic facies F10 is interpreted to have been deposited within the proximal upper shoreface where combined wind and wave generated geostrophic currents associated with peak storm activity were greatest. Clast supported F10 facies (C and D) were deposited at the toe of the foreshore where intense winnowing of the finer-grained matrix took place in concert with maximum swell activity. Matrix-supported conglomerates were deposited in comparatively low-energy settings within sea-ward facing portions of the longshore trough. Facies capping the FA2 succession reflect accretion of the foreshore during progradation of the shoreline. F10A is the most commonly preserved facies in the uppermost divisions of FA2. The high degree of sorting and horizontal orientation of suggest processes associated with swash-backwash flow were the most important controls on composition of very coarse-grianed sandstones (F8), and unimodal conglomerate (F10A).

Facies successions similar to those described and interpreted for FA2 have been amply recognized in separate examples from both the modern and the ancient sedimentary record (Vos & Hobday, 1977; Hunter *et al.*, 1979; Hunter, 1980; Leithold & Bourgeois, 1984; Greenwood & Mittler, 1985; Bourgeois & Leithhold, 1984; Bergman & Walker, 1987; Massari & Parea, 1988; Hart & Plint, 1989). Several observations and interpretations regarding coarse-grained upper shoreface and foreshore deposits proposed in these studies parallel those proposed in this study. It seems worthwhile to highlight some common features of such deposits. These include: (i) the inferred existence of shoreline attached oblique bar and rip channel morphology at the time of deposition, (ii) the implied concomitance between shoreface deposition and fluvial supply in order to account for the disparities in grain size and sorting, (iii) vertical zonation of sediment grain size, with the coarsest fraction concentrated within intervals deposited at the base of the foreshore or beachface, and (iv) a marked absence of bioturbation produced by invertebrate organisms.

The variability of grain-size distribution, sedimentary structure, bedding thickness and contact relationships between facies within FA2 attests to the dynamic and complex nature of nearshore systems. A continuum exists within nearshore systems, ranging from a purely reflective state and one that is purely dissipative (Short, 1984; Wright & Short, 1984). At any given stage between the two end-members, the nearshore system may be characterized by the relative development of a longshore bar-trough morphology (Wright & Short, 1984). The hydrodynamic regime within nearshore systems that exhibit a bar-trough morphology has been examined in detail by observing the distribution and orientation of sedimentary structures within modern coastal settings (Davidson-Arnott & Greenwood, 1974; Hunter *et al.*, 1979; Greenwood & Mittler, 1985). It has been recognized that nearshore systems characterized by a bar-trough morphology could be effectively divided into several sub-environments based upon identification of structural facies that reflect the predominant hydrodynamic regime active within each sub-environment (Hunter *et al.*, 1979; Greenwood & Mittler, 1985). Common to both studies are the following sub-environments (from basinward to landward respectively); (i) inner offshore/seaward slope, (ii) bar crest/bar, (iii) longshore trough, (iv) inner longshore trough/seaward slope of inner bar (Hunter *et al.*, 1979; Greenwood & Mittler, 1985). An additional sub-environment termed the rip-channel facies is defined in Hunter *et al.* (1979). Of direct importance to this study is the vertical sequence produced by long-term progradation of the five sub-environments. In both of the studies outlined above, the low preservation potential of the longshore bar under continued progradation is recognized. Hunter *et al.* (1979) suggested that the "erosion of the bar should result in a distinct, lateral surface below the rip-channel facies." This erosive surface is equated with the base of the FA2 succession in this study. Core observed from well 11-8-67-10W6M (figure 6) shows a typical succession of facies characterizing FA2 within the study area. The upward succession of facies within FA2 mimics the succession proposed in Hunter *et al.* (1979), and supports the predicted vertical succession of facies that are preserved following progradation of barred shorefaces.

Fluvial sediment supply contemporaneous with shoreface sedimentation has been invoked to account for the compositional disparity within many conglomeratic shoreface and foreshore sequences (Wescott & Ethridge, 1980; Bourgeois & Liethhold, 1984; Leithold & Bourgeois, 1984; Numec & Steel, 1984). Because there exists a disparity in the grain size and sorting characteristics, and hence reservoir properties, between fluvial and marine-deposited conglomerate, distinguishing between the two deposits becomes essential for reservoir characterization. Clifton (1973) noted an important distinction between wave-worked and alluvial conglomerates. Wave-worked conglomerates are well-segregated into discrete and laterally regular beds. Whereas their alluvial counterparts are less well segregated. Furthermore, progradational sandstone and conglomerate sequences deposited in wave-dominated shoreface settings generally coarsen upward whereas fluvially deposited sequences generally fine-upward reflecting waning flood stages and gradual abandonment of fluvial tracts (Numec & Steel, 1984). As shown by Wescott & Ethridge (1980), alluvial and marine deposited conglomeratic sequences may be genetically interlinked through fan-delta sedimentation. The authors identify a transition zone as the most significant feature of fan-delta sedimentation, wherein fluvial deposits are subsequently modified by marine processes. The resulting sequence deposited within the transition zone exhibits interfingering of both alluvial and marine sediments. Interpretation of the relative influence of fluvial and marine processes responsible for deposition of the facies within FA2 is best approached from a paleogeographic perspective and is covered in detail in Chapter 4, Section 4.3.

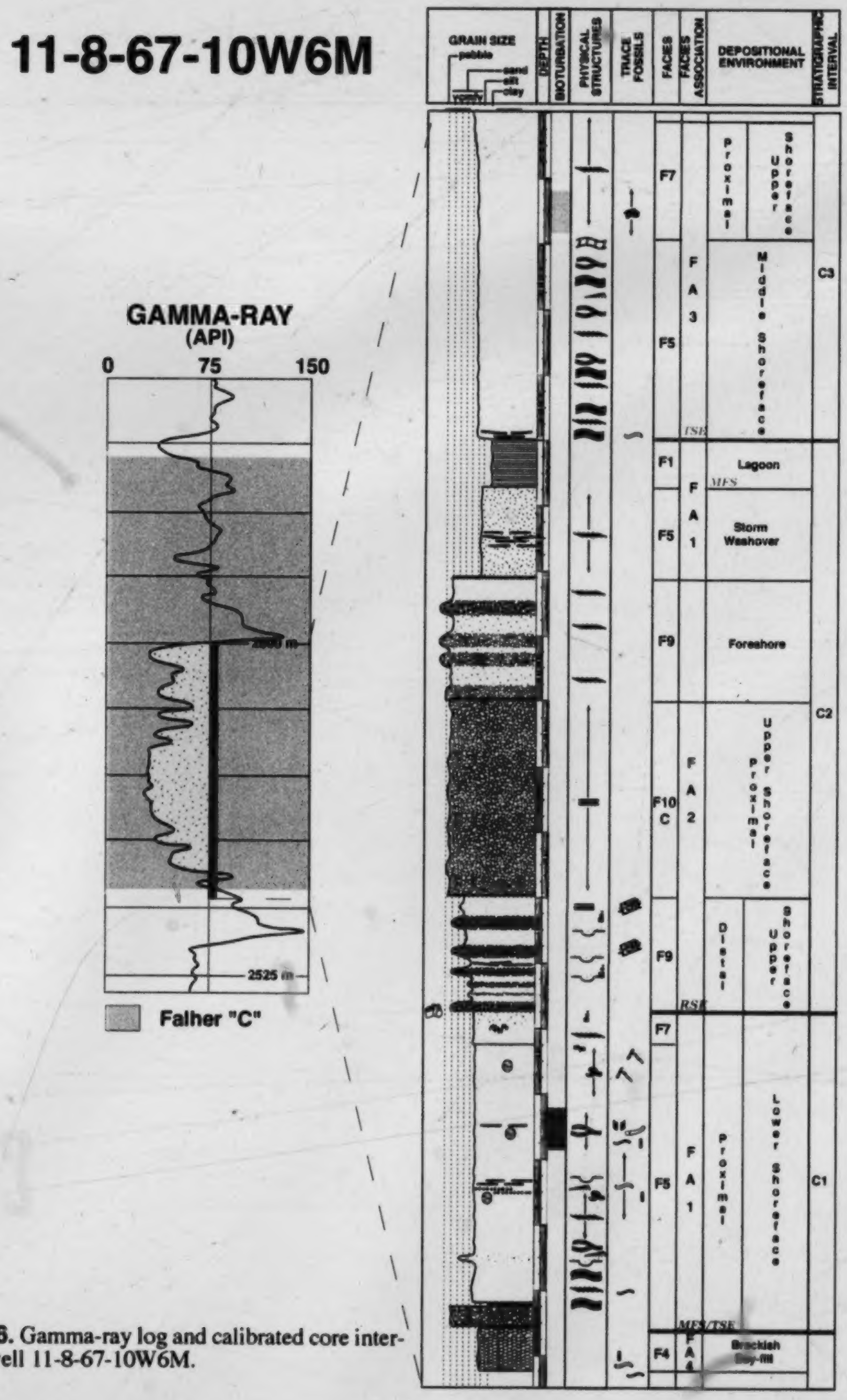

Figure 6. Gamma-ray log and calibrated core interval for well 11-8-67-10W6M.

Observations of grain size distributions and sorting characteristics on modern beaches (*e.g.* Bluck, 1967, 1969; Kirk, 1980; Orford & Carter, 1982) have been adopted by workers to account for the distribution in grain size and sorting in ancient sequences. Bourgeois & Leithold (1984), and Massari & Parea (1988) noted that the coarsest-grained fraction of a vertical beach succession was concentrated at the base of the foreshore. Stratigraphic positioning of these deposits below relatively finer-grained facies interpreted as foreshore deposits is well demonstrated within this study from several cores. Well 11-8-67-10W6M contains a typical interval of FA2 in which facies F10C stratigraphically underlies foreshore deposits of facies F8 and F10A (Figure 6). The relative position of these coarse-grained deposits within the depositional succession is in agreement with Bluck's (1967) downbeach distribution of particle size in response to variation in wave energy across the shoreface profile. Bluck (1967) proposed that the coarsest-grained fraction of sediments would be concentrated within the lower portion of the foreshore. A subsequent study performed by Orford (1975) confirmed those findings and attributed the degree of pebble zonation to the manner in which energy is expended in terms of wave phase and breaker type. Orford (1975) also found that the zone of maximum pebble accumulation was a product of swell wave action and appears to be greatest at the toe of the foreshore.

Within the foreshore, the dominant sedimentary processes are swash and backwash flow. Initial surging of water up the beachface carries sediments as both suspended and bedload. As water percolates and dissipates energy into the underlying substrate, it loses its competency and deposits progressively finer-grained sediment up the foreshore. Any water that has not overtopped the berm or percolated into the foreshore is returned seaward via backwash flow. The diminished velocity and competency of the backwash current transports sediment as sheetflow. Under the processes of swash-backwash action, fine-grained deposits within the foreshore become well sorted and plane parallel laminated (Figure 6). The angle of inclination of bedding within the foreshore is indirectly related to grain-size in that the greater the amount of percolation during swash flow, the greater the asymmetry between swash and backwash flow. Greater asymmetry between swash and backwash flow leads to a steeper angle of the foreshore (Bourgeois & Leithold, 1984).

The absence of bioturbation in the FA2 succession and in similar ancient deposits is interpreted to reflect the control of several environmental factors that limited activity by organisms. Outpouring of sediment laden fresh water from rivers into the fully marine nearshore would have imposed a turbidity stress, and at the same time, altered the chemistry of marine waters thereby discouraging bioturbation. One major assumption made is that the coarse nature of grain sizes associated with FA2 have not masked the life activity of potential trace making organisms. As noted by Bromley (1995), the greatest proportion of the biomass within the upper shoreface and foreshore is represented by interstitial meiofauna. Evidence of the interstitial life activity of these organisms is termed cryptic bioturbation, and within this study is commonly discernible in sediments of grain size up to and including fine sand (This Chapter, Section 2.5). Within conglomeratic facies containing a mean grain size of -6 - -4 ϕ, any trace of bioturbation by organisms of comparable size would be impossible to detect. An interesting point is that the physical size of an invertebrate required to produce even cryptically bioturbated textures within conglomeratic facies, would more than suffice to produce almost all of the observable ichnogenera within relatively finer-grained facies! For this reason, in instances where conglomerates have undergone observable bioturbation, it is interpreted to have been formed by unusually large macrofauna (Clifton, 1981; Bourgeois & Leithold, 1984; Leithold & Bourgeois, 1984).

2.4 Facies Association Three (FA3): tidal inlet.

FA3 stratigraphically overlies FA1 and represents a grouping of facies that were deposited during a distinct episode of sediment supply and relative change of sea-level. Deposition of FA3 was closely related to, and certainly influenced by, processes active within FA2. As a result, the FA3 facies succession contains many of the facies that are included within FA2. FA3 is characterized by a fining upward succession that is overlain by organic-rich, shaly fine-grained facies associations FA4/FA5 (Plate 2, A). The upper contact of FA3 is often deeply rooted, indicating a period of subaerial exposure prior to deposition of FA5. Facies included within FA3 are as follows; F6, F7, F8, and F9.

Sedimentology

The three most common and thickly bedded facies present in FA3, in order of increasing grain size, are facies F6, F7, F8 and F9 (table 4). The basal portions of FA3 are characterized by a fining upward succession from facies F7 to F6. Overall upward fining of the facies is accompanied by a change in sedimentary structure from trough cross-stratification with intermittent combined-flow ripples to gently inclined planar tabular cross-stratification. Bedding thickness typically increases up-section and is not influenced by grain size. Within trough cross-stratified intervals, contacts between beds are sharp and bedding thickness varies between 0.55 m and 1.6 m. Total thickness of bed sets that fine upward can reach 5.00 m. Grain texture is subangular and sorting is moderate. Tangential foreset and bottom set lamina are internally graded. Lithologic accessories include angular to sub-angular mud rip-up clasts and pebble stringers. Coalified wood clasts are locally abundant and are commonly aligned parallel to bedding contacts.

The contact between trough cross-stratified facies and overlying sediments containing plane parallel laminated bed sets is sharp and erosive. Across this contact there is a dramatic increase in sorting and bedding thickness. Grain sizes are typically either medium-grained (facies F7) or fine-grained (facies F6). However, interbeds with very coarse-grained sandstone (facies F8) are locally common. An interbedded sandstone and conglomerate (facies F9) was also observed in some intervals. Beds within these interbedded facies are horizontally planar laminated, normally graded, and exhibit local interbedding with assymetrical ripple laminated beds no greater than 0.25 m thick. Overall, the mineralogy becomes more quartzose upwards with a marked lack of organic detritus and micaceous flakes. Bedding thickness within the upper portion of FA3 ranges from 1.0 m to 1.85 m. Moderately to abundantly bioturbated intervals of *Macaronichnus* are present throughout this interval. Within the uppermost portions of the succession, fine-grained sandstones (facies F6) are characterized by horizontal planar-tabular bed sets that commonly exhibit rooting. FA3 typically is capped by a sharp, rooted contact overlain with coal beds. Root structures commonly penetrate 0.30 m or more into the uppermost beds of FA3. Locally FA3 is overlain by massive shale beds. Where this is the case no root traces have been observed.

Ichnology

The uppermost facies within FA3 have undergone extensive cryptobioturbation However the nature of the bioturbation is such that primary sedimentary structures are predominantly left intact, and in some cases even enhanced (plate 16). In contrast to the well-defined burrow walls and spreiten burrow structures produced by macrofauna, 'cryptic' bioturbation is subtle. It is characteristically expressed by the blurring of dark laminae (*i.e.* "fuzzy" lamination) that are otherwise sharp and distinct (plate 16).

Fine sandstone facies within FA3 contain an assemblage of *Macaronichnus segregatis* that has preserved the primary structural fabric (plate 17; A, B). In contrast with thickly bedded intervals of cryptobioturbation that reach a thickness of 1.5 m, the *Macaronichnus segregatis* intervals range in thickness from approximately 0.50 m to 1.00 m. The degree to which the beds are bioturbated by *Macaronichnus segregatis* varies from abundant to complete. In instances where bedding has been completely churned by the tracemaker, laminae are preserved between linear concentrations of circular/tubular *Macaronichnus segregatis* burrows (plate 17; A). Laminae coincide with mica flakes and heavy mineral concentrations at the burrow periphery (plate 17; A). Rare linear tubes that are obliquely inclined to primary bedding have also been observed (plate 17; B).

Interpretation and Discussion

The fining upward vertical succession of facies represented by FA3 is interpreted to represent deposition within a laterally migrating tidal inlet channel and adjacent accretionary spit platform. The basal facies of the succession were deposited in the deepest portion of the tidal channel. The moderately sorted and mixed nature of sediment grains within the facies probably attests to the two primary sediment sources (back-barrier and fore-barrier) supplying the tidal channel. Although no paleocurrent data is available for the lowermost facies within FA3, it is interpreted that the sedimentary structures present (*i.e.* TCS) represent ebb-oriented bedforms that migrated seaward in response to ebb-tidal processes. The graded nature of tangential fore- and toe-set laminae attests to the waning of tidal current flow as it approached slack water. Mud rip-up and wood clasts were derived from back-barrier environments and incorporated into the channel deposits during ebb-flow. Evidence for flood-oriented tidal current deposition is present as intermittently developed assymetrical ripple lamination in the upper intervals of FA3. Ripple lamination is interpreted as evidence for flood-tidal deposition along the shallow margins of a given tidal channel.

A sharp contact overlying the lower interval of the FA3 succession likely represents successive progradation of spit platform facies deposited over the tidal channel margin of the tidal inlet following lateral migration. The contact emphasizes compositional differences as well as the contrasting sedimentary textures and structures between facies of the tidal channel and spit platform sub-environments. Above the contact there is a dramatic increase in sorting, quartz content, and a marked absence of mud rip-up and wood clasts. This compositional shift reflects sourcing of sediments up-drift of the inlet mouth, and subsequent accretion of the quartzose sands onto the spit platform. Sedimentary structures within the deposits of the inferred spit-platform sub-environment are indicative of hydrodynamic processes associated with flood tidal currents and wave swell activity. Between low and high tide, landward-directed wave surge would have worked in concert with flood oriented tidal currents through the inlet mouth. These combined flows are expressed as ripple laminated beds deposited within the top set portion of the spit platform. Horizontal planar laminae that are internally graded are interpreted to have been deposited at low tide, when the spit-platform was partially exposed to swash-backwash flow.

The uppermost facies of FA3 are composed of horizontal planar-tabular bed sets that were deposited during accretion of a subaerially exposed spit. Accretionary events interpreted to have been associated with spit berm development and washover sedimentation during storm enhanced tides. Rooting at the top of FA3 indicate that vertical accretion of the spit was sufficient to allow growth of land plants on depositional highs unaffected by inundating marine waters. Figure 7 shows a typical succession of facies preserved within FA3.

A paradox exists between the geomorphic extent of modern tidal inlets and the depositional record representing their lateral inlet migration within barrier island complexes. Kumar & Saunders (1974) recognized that although tidal inlets represent only a small portion of the aggregate length of barrier island complexes of Fire Island New York (as little as 2%), sedimentary sequences representing tidal inlet migration dominate the sedimentary record (85%) of the former barrier island complex. The high preservation potential of tidal inlet successions is due in part to their role as depositional sinks into which sediments from sources both landward and seaward of the barrier accumulated. A large percentage of inlet deposition occurs below mean low tide within tidal channels, and hence these types of deposits stand a good chance of being preserved (Kumar & Saunders, 1974). Another point of particular significance to this study is that the migration of tidal inlets can potentially deposit laterally extensive successions of reservoir quality facies. These are more likely to be cored than facies successions possessing a lower cross-

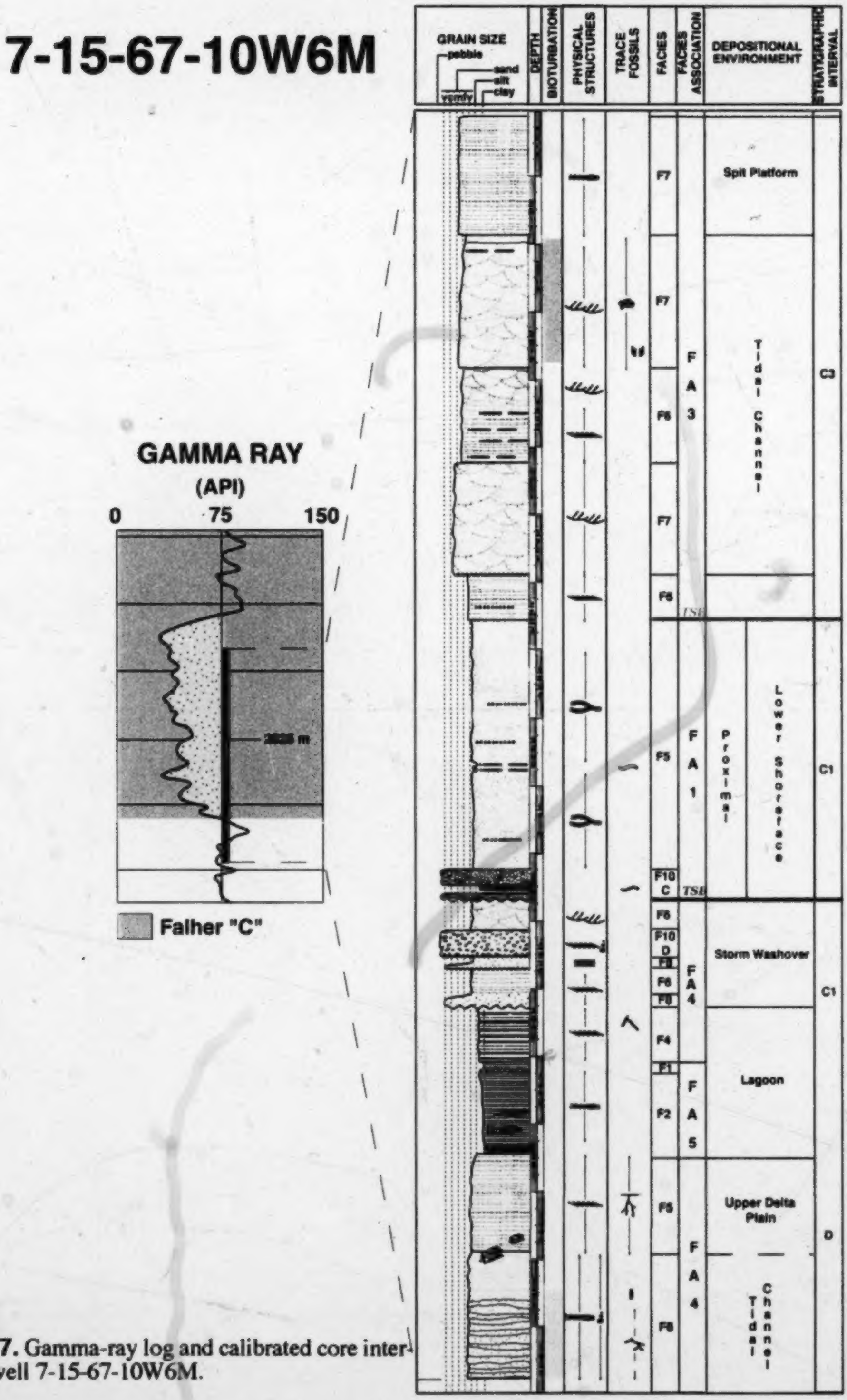

7-15-67-10W6M

Figure 7. Gamma-ray log and calibrated core interval for well 7-15-67-10W6M.

sectional area (eg. aggradational fluvial successions, or FA5). Consequently, a disproportionately high amount of core recovered from the Falher "C" Member incorporates tidal inlet successions (FA3) compared to fluvial successions (FA5).

Many modern studies have attempted to characterize a predictable facies succession produced by inlet migration (Kumar & Saunders, 1974; Moslow & Heron, 1978; Hayes, 1980; Heron *et al.*, 1984; Moslow & Tye, 1985). Although the successions described in the above studies vary considerably in facies thickness, texture, and composition, each shares a gross fining upward stratigraphic order of facies that contain similar physical structures and contact relationships. The up-section stacking order is as follows: (i) an erosional basal contact that is commonly overlain by a coarse-grained lag deposit, originally deposited at the base of a deep channel, (ii) steeply inclined trough cross-bedded facies interpreted as the main tidal channel facies, (iii) a shallow channel or spit platform margin facies consisting of inclined planar tabular cross-stratified beds with intermittent ripple laminated beds, and (iv), a capping succession of gently inclined to horizontally laminated beds indicative of deposition on the main spit-beach face (Kumar & Saunders, 1974; Moslow & Heron, 1978; Hayes, 1980; Heron *et al.*, 1984 and Moslow & Tye, 1985). Reddering (1983), has also observed and described a similar facies succession in an anomalous situation of updrift migration of the tidal inlet, against longshore current direction.

Cryptic bioturbation is believed to be indicative of the life activity of meiobenthic organisms that are present interstitially within the substrate penecontemporaneously with deposition (Howard & Frey, 1975). As the name suggests, cryptic bioturbation is of small scale, as are the tracemakers to which the bioturbation is attributed. Known tracemakers of cryptic bioturbation include; Nematodes, Harpacticoid Copepods, Haustoriid Amphipods, Taradigrads, Knorhynchids, and Ostracods (Pemberton *et al.*, 2001). Interstitial feeding by meiobenthic organisms is usually targeted at foodstuffs located between sedimentary grains and on the grain surfaces. Feeding and passive disruption of the primary sedimentary fabric of the substrate through the locomotive activity of meiofauna is believed to account for the fuzzy lamination that is characteristic of cryptically bioturbated substrates (Howard & Frey, 1975).

The trace fossil *Macaronichnus segregatis* was originally attributed to the deposit feeding behavior of the opheliid polychaete *Ophilidae limincina* (Clifton & Thompson, 1978), shown in plate 17, C. Other possible tracemakers include; *Euzonus mucronata*, and *Excirolana chiltoni* (Saunders, *pers. comm.*, 2001), shown in Plate 17, C (ii and iii respectively). It is not unreasonable to assume that all three of the organisms mentioned above could be responsible for producing *Macaronichnus segregatis* within the same environment of deposition. The principle food source for these organisms is the microbiota found on sedimentary grains. Sedimentary sand grains with a rough surface texture and greater surface area are selectively ingested because they contain a higher bacteria count than smooth surfaced dark micaceous flakes (Clifton & Thompson, 1978). Grain sorting in this manner accounts for the dark halos surrounding a lighter colored burrow core that are distinctive of *Macaronichnus spp*.

The presence of *Macaronichnus segregatis* within a sedimentary succession is indicative of deposit feeding within the upper shoreface and foreshore environments. This is because no other environments of deposition contain an "oxygenated window" that is maintained within the substrate as a permanent, hydrodynamically-sustained feature (Saunders *et al.*, 1994). McLachlan *et al.* (1985) have shown that circulation of oxygenated surface water several meters into a sand-rich substrate is accompanied by the filtering of voluminous quantities of dissolved and finely particulate organic matter, whereupon the mixture is mineralized at depth. Saunders *et al.* (1994) speculated that polychaete worms adapted to feeding within this endobenthic habitat containing an abundant, perpetually replenishing food supply during the Lower Cretaceous.

The deposit feeding behavior has passed into the depositional record because the feeding activity is carried out at depths below those portions of the upper shoreface and foreshore that are erosionally removed by wave and longshore hydrodynamic processes. Organisms that produce *Macaronichnus segregatis* are thought to be restricted to energetic, exposed wave-dominated environments (ie. upper shoreface and foreshore). However this is not to say that the trace fossil will not be found within seemingly unrelated deposits. In at least one cored interval, *Macaronichnus segregatis* overprinted facies that constitute the uppermost portions of the tidal channel (Figure 7). It is interpreted that the host substrate or habitat in which deposit feeding took place included sediments deposited within the tidal inlet channel, and the sedimentary structures (ie. trough cross-stratified sandstones), were subsequently overprinted by *Macaronichnus segregatis* possibly at low tide. Other evidence of the possible tidal control of the bioturbated *Macaronichnis segregatis* zone is the rare occurrence of vertical morphologies (plate 17, B). These forms are interpreted to be adjustment responses by the bioturbating organism in response to the rise or fall of tides that may control the depth to the nutrient-rich zone (Saunders, *pers. comm.*, 2001).

2.5 Facies Association Four (FA4): brackish back-barrier.

Within the Falher "C", FA4 is underlain by FA3 or FA2 and primarily comprises a relatively conformable succession of sand-rich and shale-rich, fine-grained facies (Plate 2, B). In some localities within the study area, FA4 represents the total record of Falher "C" deposition. A unique variety of hydrodynamic and biological processes was likely responsible for deposition of FA4 as indicated by a wide range of physical and biogenic sedimentary structures. In addition, many of the trace fossils present reflect behavioral response to environmental stresses that cannot be deciphered on a purely sedimentologic basis. FA4 is either overlain by FA5, or disconformably by FA1. Facies encountered within FA4 are as follows; F1, F2, F3, F4, F5 and F6.

Sedimentology

Within FA4, thickness and development of the fining upward bed sets of sandstone facies F5 and F6 varies with the relative proportion of shale-rich siltsone and mudstone facies (facies F4 to F1). Successions of FA4 with low proportions of shale-rich facies contain sucessions of facies F6 and F5 that range in thickness from 0.80 m to 5.50 m. Within one bed set, facies F5 gradationally overlies facies F6. Both facies display gently to moderately inclined planar tabular cross-stratification consisting of well sorted, sub-angular quartzose sandstone with spherulitic siderite. The lower contact is commonly sharp and erosive and incorporates mudstone rip-up clasts and pebble stringers. Coalified wood clasts and organic detritus are locally present along bedding contacts. The upper contact between facies F5 and overlying facies is either gradational or sharp. Fining continues above F5 beds with deposition of sandy shale-rich siltstone (facies F4). There is no apparent change in the structure of bedding within facies F4 where it overlies facies F5, however the capping beds within F4 may contain combined-flow ripples or simple flat parallel lamination. Alternatively, fining upward bed sets of facies F6 and F5 may be sharply overlain by strongly bioturbated and interbedded facies F3. Facies F3 contains interbedded fine-grained sandstone and silty mudstone. Lamination within facies F3 is internally graded from coarse to fine, producing a rhythmic appearance. Syneresis cracks are commonly present within the silty, mud-rich lamina. Overall facies F3 shows horizontal plane parallel cross-bedding with intermittently abundant mudstone rip-up clasts and organic detritus. Siderite is also present within both sand-rich and shale-rich beds.

The facies succession of FA4 is locally dominated by shale-rich facies F1, F3 and F4. Within these successions, thickly bedded intervals of facies F6 or F5 are partially to completely absent. When present, facies F5 is typically composed of well sorted, clean quartzose sandstone with minimal detrital clays and micaceous flakes. Bedding thickness of sand-rich facies in silt-dominated successions varies from less than 0.25 m up to 1.20 m. Of the other facies comprising FA4, the finest-grained is F1, a massively-bedded fissile shale containing siderite nodules and carbonaceous wood clasts. Bedding thickness ranges from 0.20 m to 3.40 m. Physical and biogenic sedimentary structures are typically absent. In contrast, facies F2 exhibits more features, possibly due to the slightly coarser sand and silt fraction. Physical structures observed in facies F2 include horizontal and convolute lamination, lenticular bedding, flaser bedding, and syneresis cracks. In some cases, primary bedding within facies F2 was destroyed and overprinted by a monospecific *Teichichnus* assemblage. Accumulations of facies F3 and F4 are comparable to those described for the sand-rich FA4 succession, but tend to be more heavily bioturbated and thickly bedded. Bedding thickness of facies F3 ranges from 0.75 m to as great as 2.00 m whereas beds of facies F4 vary between 0.50 m and 2.15 m thick.

Ichnology

Trace fossil assemblages within FA4 include four groupings of recurring ichnogenera. Several generalizations can be made regarding these assemblages including; (i) low diversity, (ii) low abundance, (ii) overall reduction in size and (iv) simplified burrow morphology compared with assemblages observed within FA1. The most dramatic example of the above characteristics is a monospecific assemblage of *Teichichnus* (c). This assemblage is typical of facies F4 and contains only one type of ichnogenera. Burrows do not exceed 1 cm in diameter, and much of the primary lamination remains preserved (plate 19,A).

A second trace fossil assemblage within FA4 contains; *Teichichnus* (m-c), *Ophiomorpha* (m), *Planolites* (m), and *Palaeophycus* (m). This assemblage is most commonly observed in conjunction with facies F3. Both *Planolites* and *Palaeophycus* are restricted to organic-rich shale laminae whereas extensive *Teichichnus* burrows cross-cut interbedded sand/shale graded beds over intervals of a few cemtimeters to as much as 0.20 m. Grain size trends of graded laminae are typically preserved within burrow spreite, displaced downward about half a burrow diameter (plate 19, B and D). *Ophiomorpha* burrows also cross-cut primary bedding and contrast sharply with *Teichichnus* in burrow composition, containing a structureless, shale-rich infill enveloped within a serrated silty burrow wall.

Sandstone facies F5 contains an assemblage of *Skolithos* (m), *Arenicolites* (c-a), *Teichichnus* (c-a), *Palaeophycus* (c), *Planolites* (m-c), and *Cylindrichnus* (r-m). The predominant form within this assemblage is diminutive *Arenicolites* (plate 19, C). These vertical U-shaped tubes are do not typically exceed 3 mm and the burrow walls are lined with organic matter that contrasts sharply with the surrouding quartzose matrix and burrow fill. Of the other forms present, *Cylindrichnus* burrows are steeply inclined (~40°) relative to horizontal lamination within beds of F5 (plate 19, C). Much of the primary carbonaceous laminae remain, only partially disturbed by bioturbation (plate 19, C).

The fourth and final trace fossil assemblage within FA4 is associated with organic-rich silty mudstone facies F2 (Plate 18, A and B). Ichnogenera included within this assemblage are; *Thalassinoides* (c), *Chondrites* (m-c), *Planolites* (c), and *Palaeophycus* (c-a). The ichnofabric within facies F2 shows pervasive to complete reworking of the primary depositional fabric. Locally, discontinuous organic-rich shale laminae remain. Associated with these shale laminae are diminutive *Chondrites* burrows that are no greater than 1 mm in tube diameter. Dominating the overall appearence of the ichnofabric are robust *Thalassinoides* burrows that can reach 2.5 cm diameter. These large burrows are commonly overprinted by *Planolites*, *Palaeophycus* and *Teichichnus* burrows with mean tube diameters of about half a centimeter.

Interpretation and Discussion

The proportions of sand-rich and shale-rich facies within FA4 vary according to the inferred back-barrier setting from which a core was recovered from the subsurface. Cored successions of FA4 containing abundant sand-rich facies (F5 and F6), were deposited within flood-tidal deltaic and storm washover fan environments. The bioturbated shale-rich facies (F1, F2, F3, and F4) encountered in FA4 represent deposition within more central locales such as embayed brackish settings. Textural and compositional disparity between the two successions that characterize FA4 is illustrated in figure 8. It is important to emphasize the tripartite distribution of: (A) total depositional energy, (B) estuarine sub-environments, and (C) facies heterogeneity within wave-dominated estuaries (Dalrymple *et al.* 1992; Reinson, 1992). Deposition of coarse-grained facies containing primarily quartzose grain compositions takes place within the marine dominated portion of the estuary where the total energy (calculated as the sum of energy generated by wave and tidal currents), is greatest. Moving progressively inland from the barrier complex, the total energy is reduced dramatically despite the additional influence of current energy related to river discharge (figure 8). The resulting facies succession of the central bay primarily comprises fine grained sediments of mixed marine/fluvial origin that are variably bioturbated by a distinctive brackish-water faunal suite. Fining upward, sand-rich facies successions containing abundant detrital organic grains are encountered landward of the central bay, within bay head delta and fluvial distributary channel environments (figure 8).

Facies associations representative of flood tidal deltas and washover fans have a high preservation potential because they are deposited within sheltered regions of the back-barrier, away from the eroding shoreface and migrating inlet channels. The volume of literature regarding the sedimentology and architectural interrelationship between flood-tidal delta and washover fan

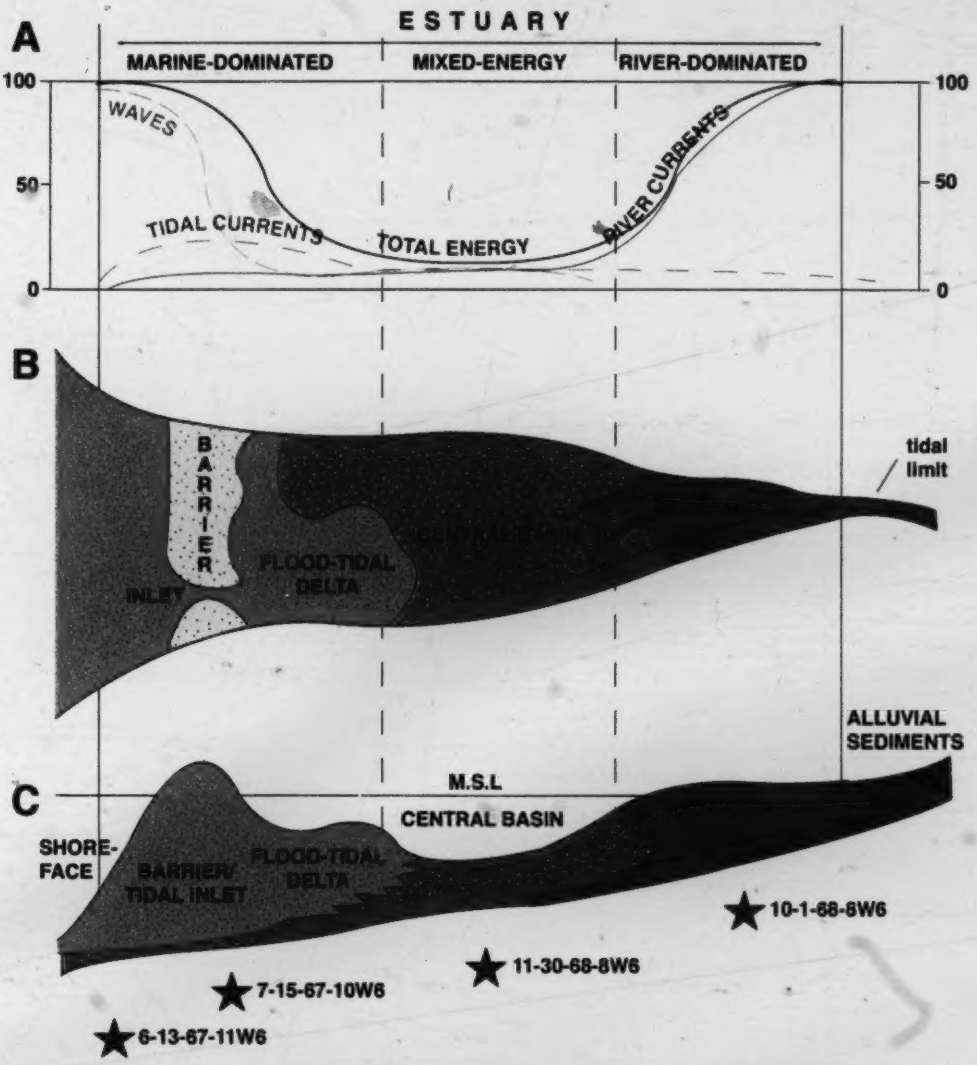

Figure 8. Tripartite distribution of (A) total energy, (B) depositional environments, and (C) facies associations, characteristic of wave-dominated embayed estuarine depositional systems (Dalrymple *et al.*, 1992). Starred locations showing the interpreted paleoenvironmental context of several of the cored intervals discussed in this chapter.

deposits attests to this fact (*e.g.* Kumar & Saunders, 1974; Kraft *et al.*, 1979; Hayes, 1980; Berelson & Heron, 1985; Boersma, 1991; Murakoshi & Masuda, 1991). Many of these studies are dedicated to outcrop exposures where the distinction between the two stratigraphically distinct sedimentary deposits can be made with a relatively high degree of precision (Berelson & Heron, 1985; Hennesy & Zarillo, 1987). It is more difficult when attempting to differentiate between the two deposit types in core. Analyses of core requires that environmental interpretation be based upon a succession of facies, rather than lateral correlation with adjacent deposits in outcrop.

Facies deposited during storm washover sedimentation within a back-barrier are distinguished from flood-tidal deltaic deposits based upon their stratigraphic relationship with other facies associations observed in core. In this study, facies characteristic of storm washover sedimentation erosively overlie horizontal planar laminated foreshore or spit-beachface facies characteristic of FA2 and FA3 respectively (Figure 6). Facies diagnostic of the washover sands are fine-grained to inclined planar laminated (F5 or F6) and contain interbedded sedimentary structures indicative of episodic rapid sedimentation (*i.e.* graded bedding and climbing ripples). The landward portion of the washover fan complex contains facies that have interfingered with finer-grained, thinly bedded lagoonal mudstones. Locally these exhibit evidence of soft sediment deformation developed in response to rapid loading of the overlying washover sands.

Figure 9 shows a typical succession of facies interpreted as flood tidal delta deposits. Inclined planar tabular cross-bedded fine-grained sandstone facies were deposited as large flood-tidal deltaic lobes prograded landward, toward the central basin of the embayment. These sandstone facies are composed of well sorted, clean quartzose sandstones indicative of a dominantly marine source seaward of the inlet. Overall fining upward of the facies (F6 and F7) resulted from inlet-migration/closure and consequent waning of sand supply.

Sand-rich facies interpreted as flood-tidal deltaic deposits are locally interdigitated with relatively finer-grained pro-delta and lagoonal mudstones (Figure 9). The graded interlaminated fine-grained sand and shale facies F3 is considered to be tidally deposited. The coarse-grained current ripple laminated fraction of the facies (4.0-3.0 ϕ) was deposited during peak tidal flow, while the finer-grained portion of the bedload remained suspended in the water column. Subsequent fallout of the suspended fines during slack water phase was responsible for deposition of the shale laminae. Synaeresis cracks are commonly observed within the shale laminae of facies F3, and are indicative of large fluctuations in salinity (Burst, 1965). In addition to synaeresis cracks, a brackish assemblage of trace fossils consisting of *Teichichnus*, *Ophiomorpha*, *Planolites* and *Palaeophycus* overprints the sedimentary structures. Of these ichnogenera, the most diagnostically significant for facies F3 are vertically extensive *Teichichnus* burrows that cross-cut interlaminated shale and sand beds. This style of *Teichichnus* burrowing is indicative of relatively continuous sedimentation. This is consistent with a pro-delta environment where the animal maintained equilibrium with the sediment-water interface, producing a spreiten burrow (Pemberton, *pers. comm.*, 2001).

Paleolandwardly, sand-rich flood-tidal delta and washover fan successions diminish in stratigraphic thickness and become laterally equivalent with shale-rich facies successions interpreted as central brackish basin-fill (Figure 8, C). The Falher "C" interval within well 11-30-68-8W6M is wholly comprised of a succession of facies that were deposited within the central brackish basin complex (Figure 10). The most striking aspect of the central brackish basin-fill

10-30-67-11W6M

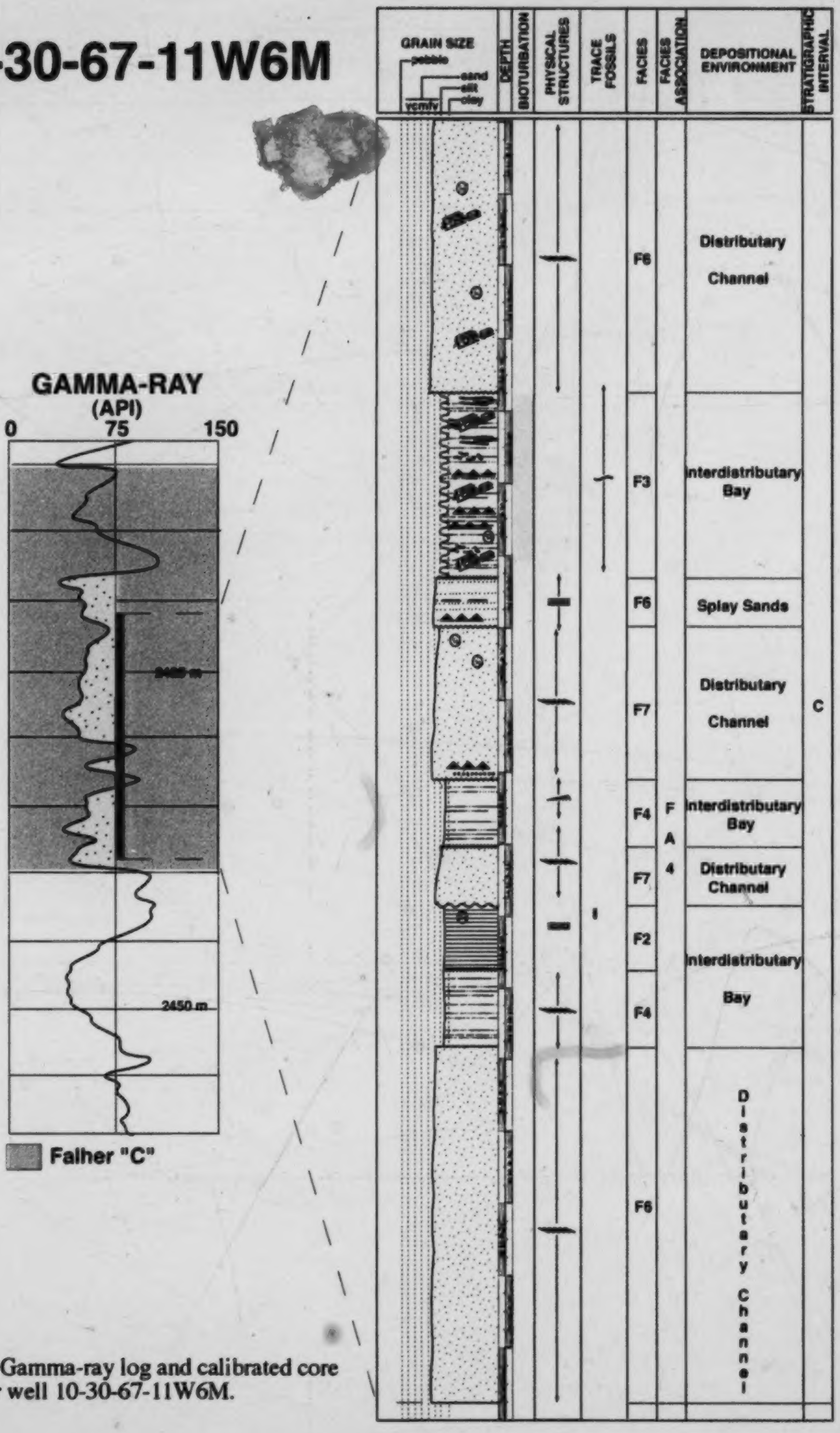

Figure 9. Gamma-ray log and calibrated core interval for well 10-30-67-11W6M.

sequence is the sedimentologic and ichnologic complexity of the facies succession (Figure 10). The central brackish basin constitutes a zone of depositional energy convergence between marine-generated tidal currents, and fluvial currents (Figure 10). The sedimentological complexity of the facies succession within well 11-30-68-8W6M is partially attributable to the fact that a degree of overlap likely exists between marine, tidal, and fluvial processes and deposits.

The interval within 11-8-68-8W6M is comprised of variable and sporadically occurring trace fossil assemblages that bear a strong resemblance to other estuarine Cretaceous successions described from Western Canada (*e.g.* Wightman *et al.*, 1987; Beynon *et al.* 1988; MacEachern *et al.*, 1992; Pemberton & Wightman, 1992; MacEachern & Pemberton, 1994). These similarities are consistent with what has become known as the brackish-water model, initially outlined in Pemberton *et al.* (1982), and most recently reviewed by Gingras *et al.* (1999). Ichnological patterns inherent to the brackish-water model include: (i) a low diversity of trace fossil forms and suites dominated by a single ichnogenus, (ii) predominance of diminutive traces, (iii) morphologically simple marine forms constructed by trophic generalists, (iv) vertical and horizontal traces common to the *Skolithos* and *Cruziana* ichnofacies, and (v) locally dense ichnofossil populations. A monospecific trace fossil assemblage that most closely exemplifies these patterns is a *Teichichnus* assemblage most readily observed within the central bay mudstones.

11-30-68-8W6M

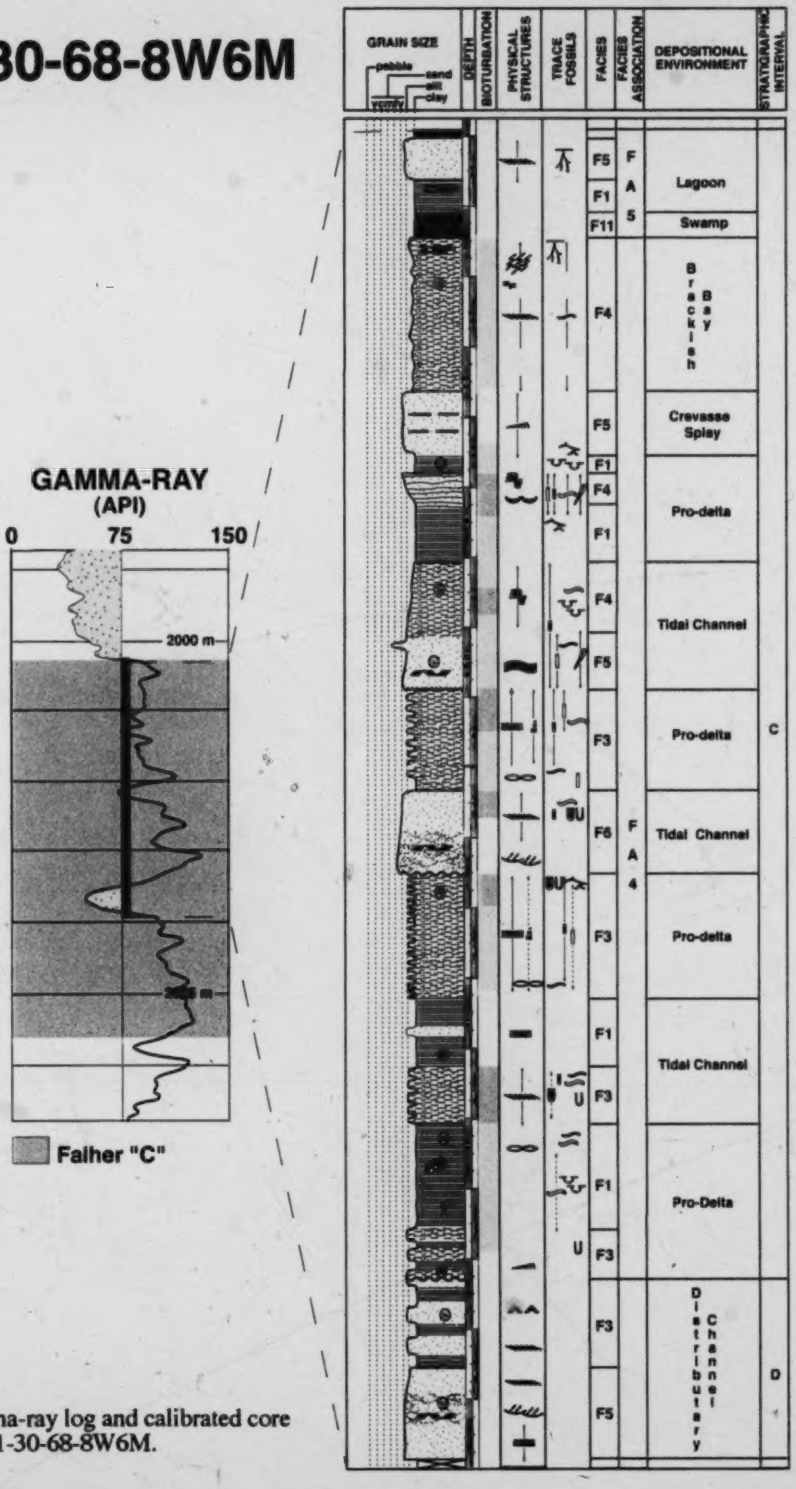

Figure 10. Gamma-ray log and calibrated core interval for well 11-30-68-8W6M.

2.6 Facies Association Five (FA5): fluvial channels and coastal plain.

Facies of FA5 are organic-rich and form a fining upward succession (Plate 2, C). Intervals of FA5 are restricted to the uppermost portion of the Falher "D", and Falher "C" Members. Both the lower and upper contacts of FA5 are disconformable. The lowermost being sharp and deeply rooted and the uppermost, sharp and reworked. A marked lack of trace fossils and the abundance of organic mudstone and coal facies testifies to a nonmarine origin of the facies succession within FA5. Facies contained within the FA5 succession are; F7, F6, F5, F4, F3, F1 and F11.

Sedimentology

The idealized succession of FA5 includes stacked, fining upward sandstone facies F7, F6, and F5 within the lower interval. The lower contact is sharp and erosive and immediately overlain by moderately sorted, subangular medium-grained or fine-grained sandstones (facies F7 and F6 respectively). Both facies are trough cross-bedded and contain variable abundance of mudstone rip-up and coalified wood clasts. Abundant organic detrital matter, siderite, and discontinuous wavy laminations are common. Bedding thickness ranges from 0.75 m to 2.3 m. Medium and fine-grained sandstone facies fine upward into a very fine-grained sandstone facies (F5), containing asymmetrical current ripples. Facies F5 fines in turn to a sandy shaly siltstone (facies F4), containing abundant coaly laminations interbedded with asymmetrical current ripples. Cyclical interbedding of fine-grained sandstone and silty mudstones characterizes facies F3. Discrete beds of facies F3 are often present separating fining upward successions within the lower interval of FA5. These beds are characterized by convolute lamination and extensional micro-faulting (plate 20), and are typically not thicker than 0.25 m. Facies F5 is commonly missing from the lower portion of the succession, where amalgamated beds of trough cross-stratified sandstones can reach thicknesses of 4.75 m.

The uppermost intervals are primarily composed of thickly bedded organic-rich shale and sub-bituminous coal (facies F1 and F11 respectively). The contact with the underlying succession is invariably sharp and deeply rooted. Root structures typically continue up-section as a penetrative feature within facies F1 and F11. They are locally absent in mottled fossiliferous fissile shale beds. The mottled appearance of beds of facies F1 is partially due to localized small-scale bioturbation. Pyrite is also locally present as disseminated grains, and nodular siderite is common. Fossils within the shale beds include carbon-film leaf and stem remains, disarticulated gastropods and bivalve shells, and ostracod tests. Bedding thickness in facies F1 ranges from 0.30 m up to 3.00 m. Contacts between shale-rich facies and coaly F11 are commonly gradational.

Discontinuous carbonaceous heterolithic laminae thicken into continuous beds of sub-bituminous coal varying in thickness from less than 0.10 m to 0.65 m. Total thickness of the upper succession within FA5 can reach 6.00 m, but more commonly ranges from 2.50 m and 5.00 m.

Interpretation and Discussion

FA5 contains a fining upward succession of facies that was deposited contemporaneous with lateral accretion of a fluvial point bar. The succession lies on a sharp erosional contact that was created as the main channel incised into the alluvial plain. Thickly bedded planar and trough cross-stratified facies present at the basal portions of the succession represent deposition within the main channel that formed the outer margin of the meander bend. Progressively finer-grained, and thinly bedded facies, comprised of ripple lamination, were superposed on the trough cross-stratified channel facies as the point-bar accreted laterally toward the outer portion of the meander. Evidence of point-bar instability is present in the form of soft sediment deformation and microfaulting within interbedded sand/shale facies (figure 11). Channel avulsion, and subsequent abandonment of the meander bend initiated ponding within the resultant oxbow lake. Extensive rooting and relatively thick coal beds attest to the ephemeral nature of lacustrine deposits preserved within the uppermost portions of the facies succession within FA5.

Other occurrences of FA5 show interbedding of organic-rich shaly facies with thickly bedded coal horizons that were deposited within the floodplain dissected by meandering fluvial environments described above. Kalkreuth & Leckie (1989) have postulated that the relatively low ash and sulphur content of coal seams formed on Cretaceous strandplains is attributable to the zone of peat accumulation being protected from fluvial flooding. In floodplain areas adjacent to active clastic fluvial environments subject to channel avulsion and crevassing, high-quality, low ash coals are unlikely to form (McCabe, 1984). Therefore, it is likely that peat generation took place within raised swamps that were sufficiently elevated above low lying areas subject to detrital input concomitant with flooding events.

Facies deposited within fluvial environments ideally show a complex three-dimensional arrangement that can be reconstructed in the same manner as paralic successions; utilizing architectural elements and their bounding discontinuities. However, in contrast to marine-deposited sequences, fluvial deposits are limited in lateral extent and therefore require a greater resolution than that afforded by core studies. Detailed facies analysis of fluvial sequences is limited primarily by the ambiguity of contact relationships between architectural elements interpreted from core.

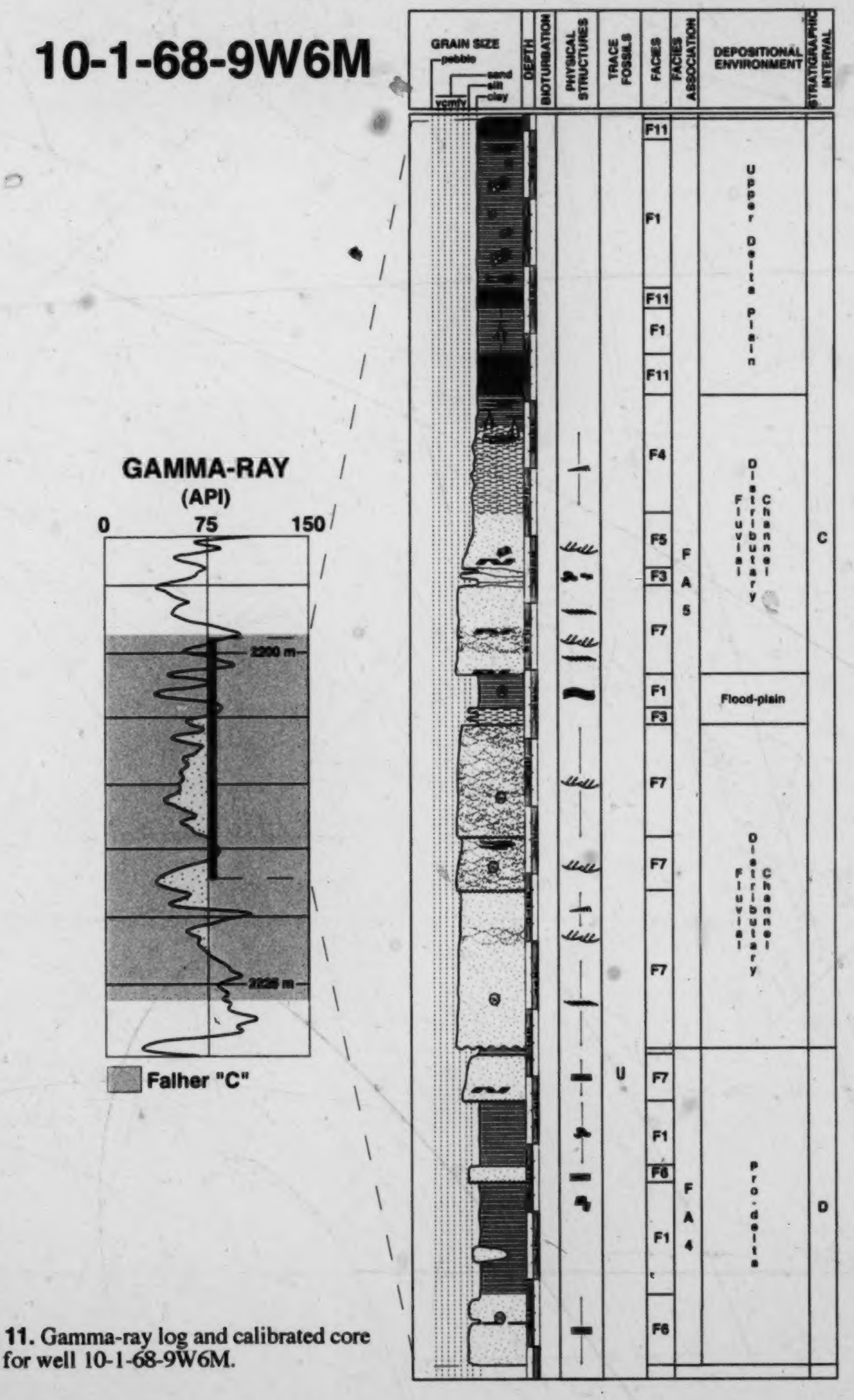

Figure 11. Gamma-ray log and calibrated core interval for well 10-1-68-9W6M.

Plate 1 [illegible] (FA1) and Facies Association Two (FA2). A: Within well location [illegible] present in Facies F5 consisting of well sorted very fine grained quartz arenite. Physical structures include gently inclined [illegible] confined to the base [illegible] and upper [illegible] is enveloped by FA1 within well [illegible]. The lower contact between FA2 and FA1 [illegible] grain size and sorting. Basal facies of FA2 are typically display [illegible] typically erosively overlain by [illegible] within FA2 are well [illegible] structures [illegible] planar tabular horizontal bedding. No trace fossils have been identified within FA2.

...m 7-24-67-10W6 (2356.00 m–2321.50 m). FA1 occupies the marine portion of Falher C [illegible] depression. The dominant facies ...y inclined parallel and sub-parallel lamination and discrete beds of oscillatory and combined flow ripples. Bioturbation is ... occurrence of [illegible] and pervasive occurrence of [illegible] B: FA2 ... FA1 ... sharp and erosive, and is interpreted as a regional discontinuity. Above this contact [illegible] marked change in mean ...ly sorted pebbly medium-grained sand [illegible] and bimodal matrix-supported chert conglomerate (facies F9). Basal facies are ... F10D and F10C respectively [illegible] development of planar tabular cross-stratification. The uppermost facies ...ble chert conglomerate (facies F10A). Bedding contacts between these two facies are sharp [illegible] and planar. Physical

A
B
C

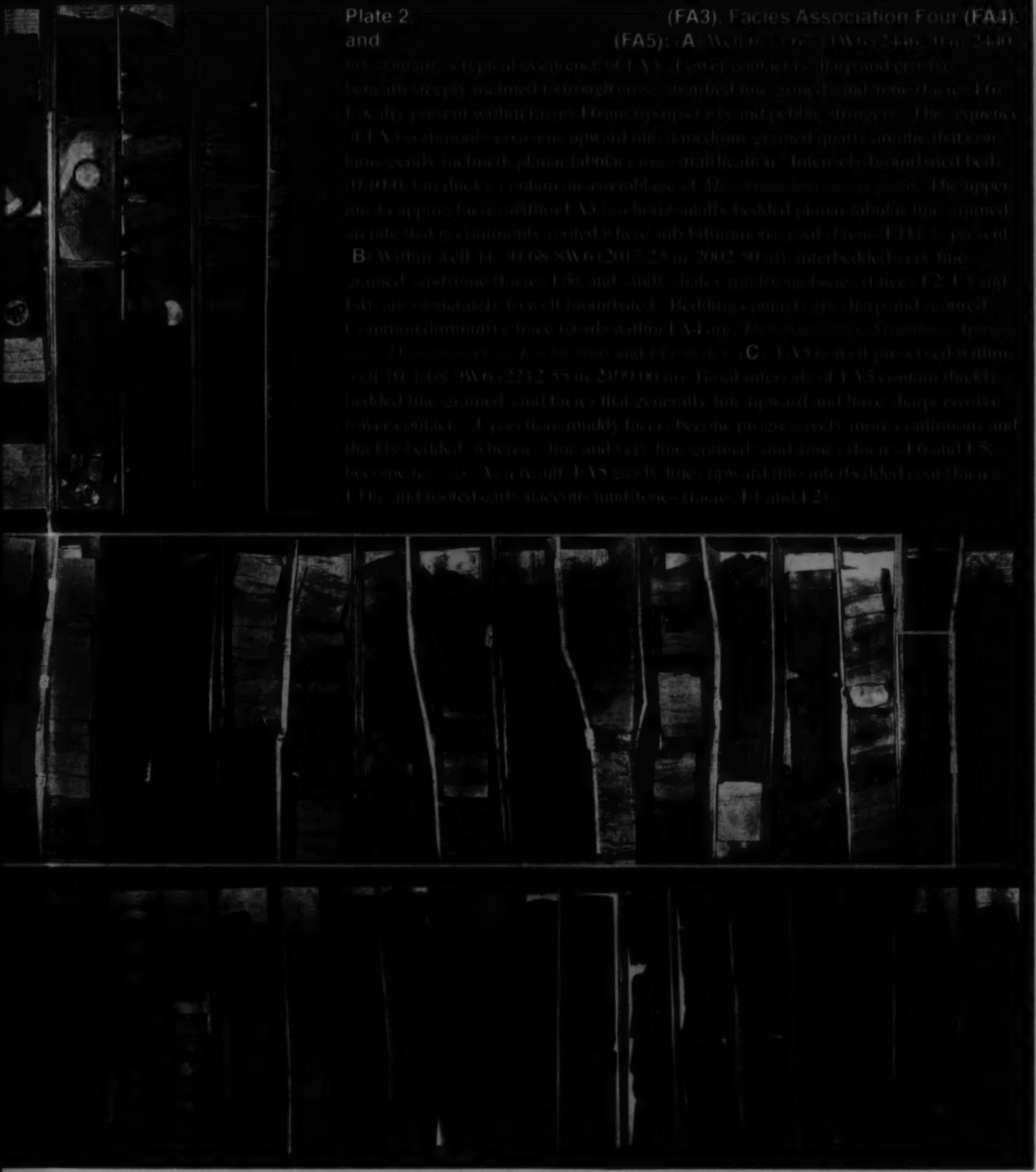

Plate 2. [illegible] (FA3), Facies Association Four (FA4), and [illegible] (FA5): A) Well 6-[illegible]-67-[illegible]W6 (2446.30 m-2440 m) contains a typical sequence of FA3. Lower contact is sharp and erosive beneath steeply inclined to trough cross-stratified fine-grained sandstone (facies F6). Locally present within facies F6 are rip-up clasts and pebble stringers. The sequence of FA3 commonly coarsens upward into a medium-grained quartz arenite that contains gently inclined, planar tabular cross-stratification. Intensely bioturbated beds (0.10-0.3 m thick) contain an assemblage of *Macaronichnus segregatis*. The upper most capping facies within FA3 is a horizontally bedded planar tabular fine-grained arenite that is commonly rooted where sub-bituminous coal (facies F11) is present. B) Within well 11-30-68-8W6 (2017.28 m-2002.80 m), interbedded very fine-grained sandstone (facies F5) and sandy shale / mudstone facies (facies F2, F3 and F4) are moderately to well bioturbated. Bedding contacts are sharp and scoured. Common diminutive trace fossils within FA4 are: *Thalassinoides*, *Skolithos*, *Arenicolites*, *Diplocraterion*, *Teichichnus* and *Planolites*. C) FA5 is well preserved within well 10-1-68-9W6 (2212.55 m-2199.00 m). Basal intervals of FA5 contain thickly bedded fine-grained sand facies that generally fine upward and have sharp erosive lower contacts. Upsection, muddy facies become progressively more continuous and thickly bedded, whereas fine and very fine-grained sandstones (facies F6 and F5) become less so. As a result, FA5 grossly fines upward into interbedded coal (facies F11) and rooted carbonaceous mudstones (facies F1 and F2).

Plate 3. Plane parallel and sub-parallel laminated very fine-grained sandstone (facies F5): (**A**) Gently inclined lamination within silty very fine-grained sandstone (1-11-67-12W6, 2557.86 m); (**B**) Pebble and granule stringers aligned parallel with inclined lamination within facies F5 (6-13-67-11W6, 2477.59 m); (**C**, **D**) Silty, parallel to sub-parallel laminated very fine-grained sandstone. Bedding contacts are less than ten degrees (11-30-68-8W6, 2017.75 m; 7-18-67-10W6, 2442.53 m).

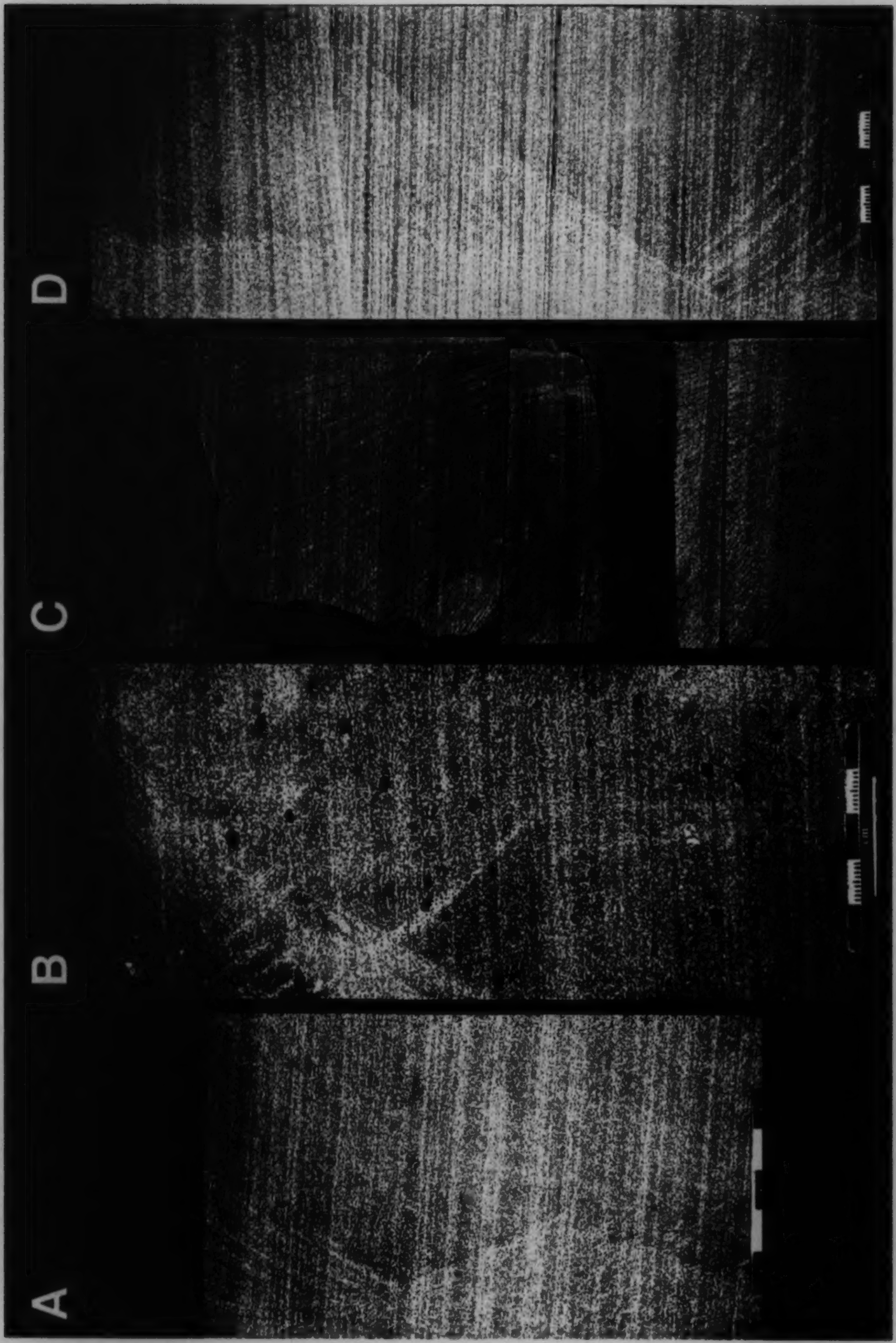
A
B
C
D

Plate 4. Non-bioturbated and bioturbated amalgamated storm sandstone (facies F5): (**A**) Parallel to sub-parallel laminae sets bounded by gently inclined (<10), bedding contacts. Discrete 3.5 cm-thick bed of wave ripple laminae caps lower amalgamated bed set (1-15-67-7W6, 2130.00 m); (**B**) Stratigraphically lower interval within the same well (2130.75-2131.00 m). Periodic appearence of *Skolithos* and *Palaeophycus* burrows likely represents the work of opportunists following storm abatement and relative fairweather quiescence; (**C**) *Teichichnus* and retrusive *Diplocraterion* burrows highlighted by dark colored fines ?stowed? at depth during interveining periods of fairweather deposition (1-11-67-12W6, 2550.75 m).

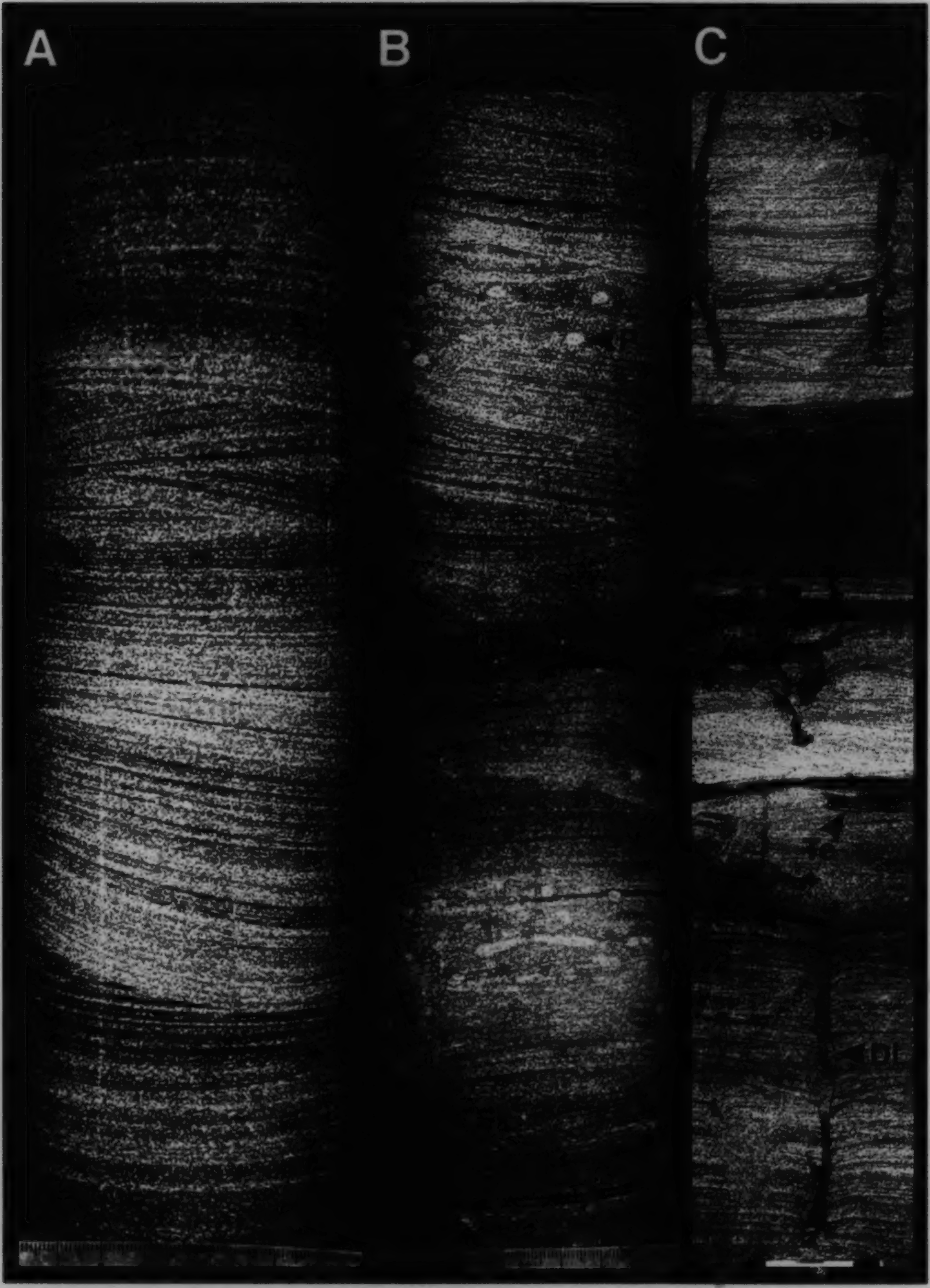
A
B
C
bl

Plate 5. Coarse-grained storm bedding and scoured contacts: (**A**) Scoured, erosive contact separating cross-stratified pebbly medium-grained storm sandstone bed from underlying parallel laminated very fine-grained sandstone (9-11-67-12W6, 2554.45 m); (**B**) Scour-and-fill structure (gutter cast), defining the contact between separate storm deposited sandstone beds (7-15-67-12W6, 2523.33 m); (**C**) Interbedded sandstone and clast-supported bimodal conglomerate. Storm generated currents likely responsible for temporary increase in current carrying capacity during which time pebble-sized clasts were transported (6-21-67-10W6, 2456.00 m); (**D**) Cobble- and pebble-sized clasts suspended in poorly sorted very coarse-grained sandstone. Deposition of the storm bed was rapid and likely took place as gravity flow (7-18-67-10W6, 2445.90 m).

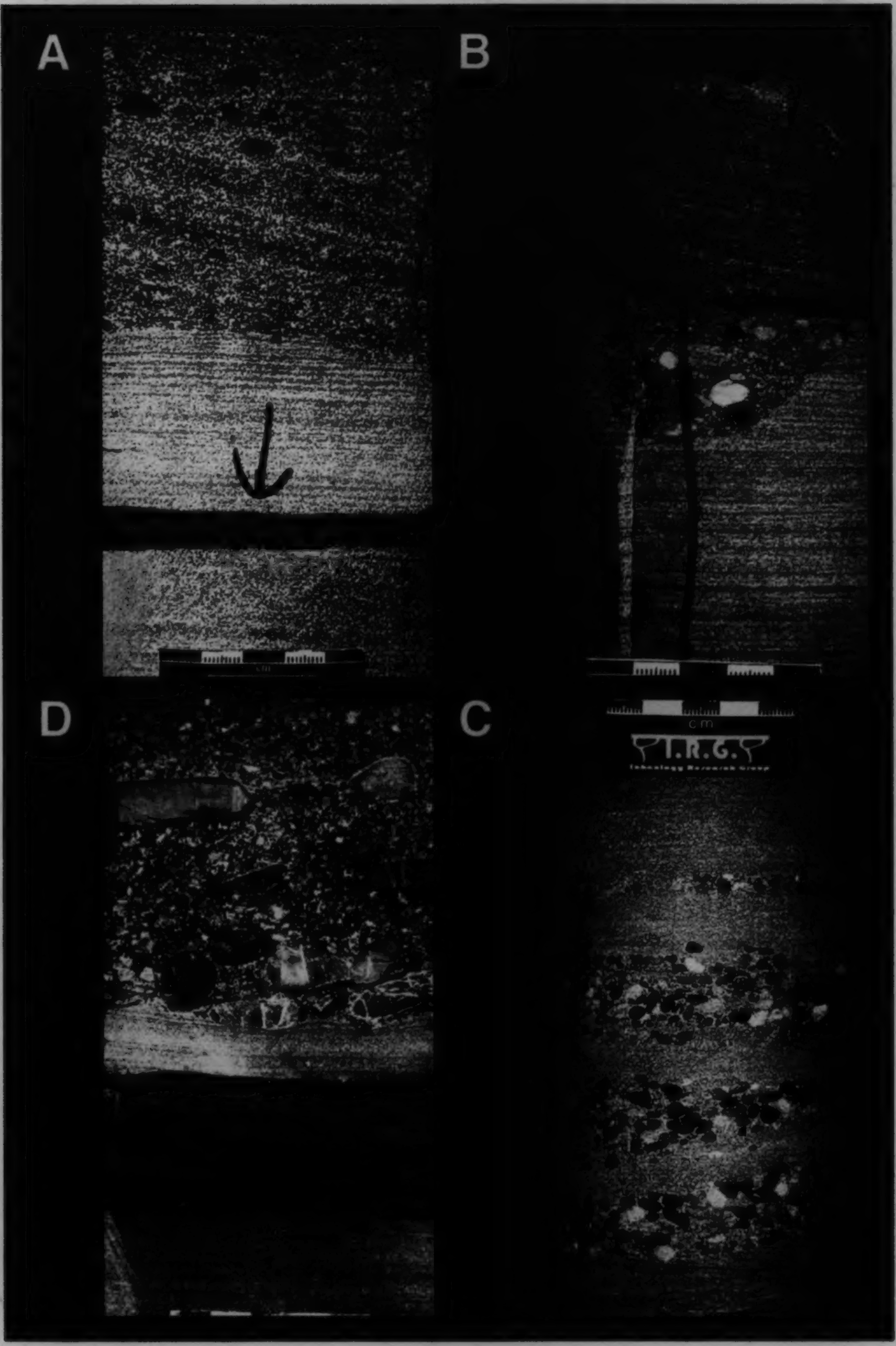
A
B
D
C
cm
cm
I.R.G.

Plate 6. Intensely bioturbated siltstone and very fine-grained sandstone: (**A**) Biologically churned interval of shaly, silty very fine-grained sandstone (facies F5). Among the dominant ichnogenera present are *Terebellina*, *Palaeophycus*, *Planolites*, and *Asterosoma* (1-11-67-12W6, 2562.60 m); (**B**) Close-up view of intensely bioturbated sandy, shaly siltstone (facies F4). Clearly visible are *Terebellina*, *Thalassinoides*, and *Planolites* (10-12-67-10W6, 2482.8 m); (**C**) *Palaeophycus* and *Paramacaronichnus* burrows in vertical section. Both ichnogenera are morphologic elements of the same composite burrow network (6-21-67-10W6, 2456.20 m); (**D**) Bedding-plane view of *Palaeophycus* and *Paramacaronichnus* mottled, very fine-grained sandstone (6-21-67-10W6, 2456.10 m).

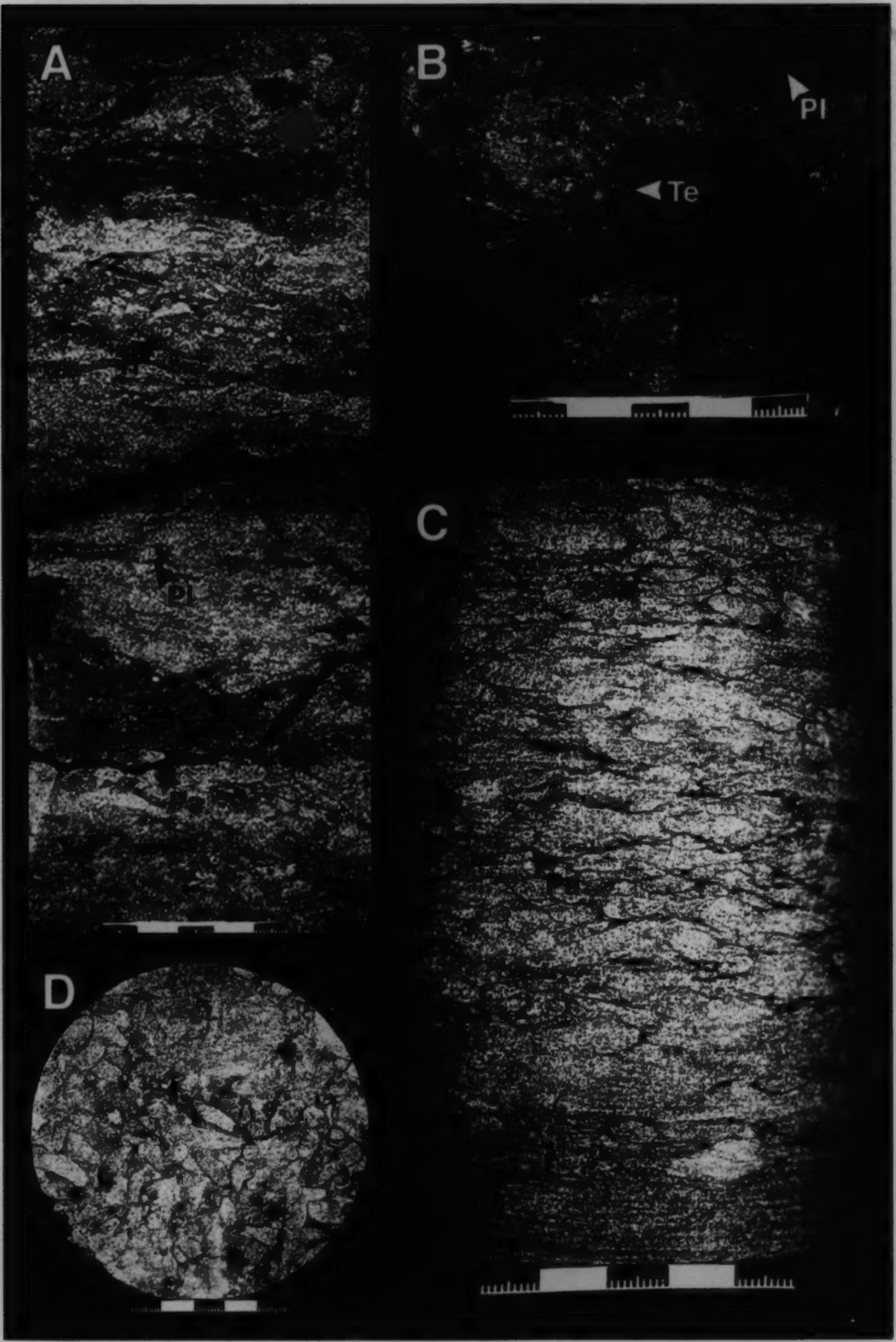
A
B
Pl
Te
C
Pl
D

Plate 7. Commonly developed solitary ichnogenera within very fine-grained sandstone (facies F5): (**A**) *Teichichnus* burrow cross-cutting inclined sub-parallel laminated sandstone. Discrete bed of assymmetric ripple lamination also visible (9-11-67-12W6, 2557.13 m); (**B, C**) Organic-rich lamination deflected downward (*Fugichnia*), by escaping epifauna in response to storm burial (3-17-67-12W6, 2734.20 m; 1-15-67-7W6, 2129.35 m); (**D**) Bedding plane-view of *Ophiomorpha ?irregularae?*. Both circular and cylindrical aspects of boxwork morphology visible (7-24-67-10W6, 2322.10 m).

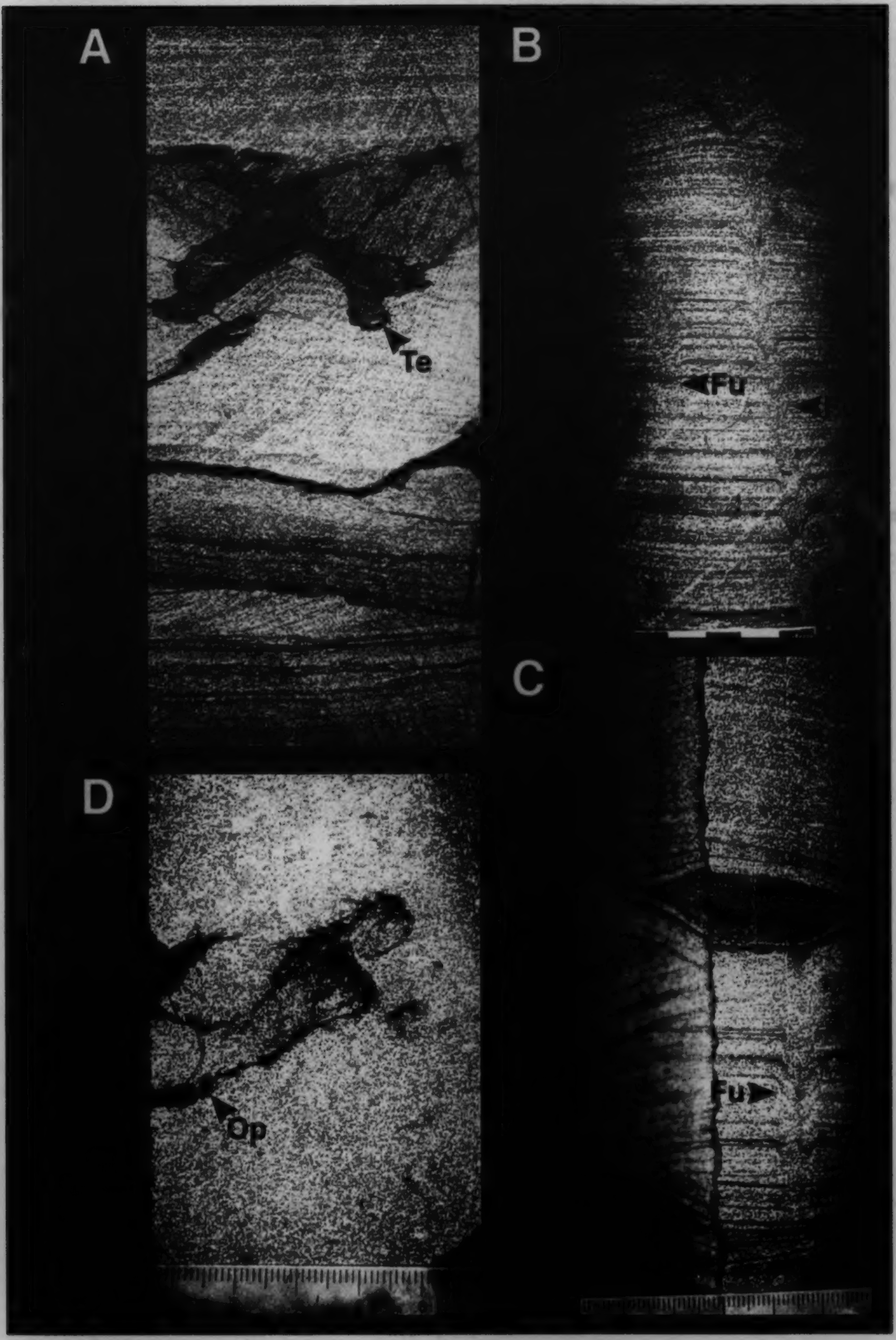
A
Te
B
Fu
C
D
Op
Fu

Plate 8. Composite *Diplocraterion* Burrows: (**A**) *Diplocraterion* and *Teichichnus* burrows originating from a surface detritus feeding depression (top of core). Tear drop-shape of *Diplocraterion* burrow is likely the result of growth of the original tracemaker. Spreiten in these burrows are lined with organic-rich detritus incorporated into burrow walls during surface detritus feeding activities (9-11-67-12W6, 2552.65 m); (**B**, **C**) Bedding plane views showing a horizontal section through *Diplocraterion* ?*parallelum*?. Crescent-shaped spreite converge toward the center of the burrow concave inward creating a "dumbell" appearence (1-11-67-12W6); (**D**) U-shaped *Diplocraterion* traces subtending downward from a surface feeeding depression showing branching morphology (1-11-67-12W6).

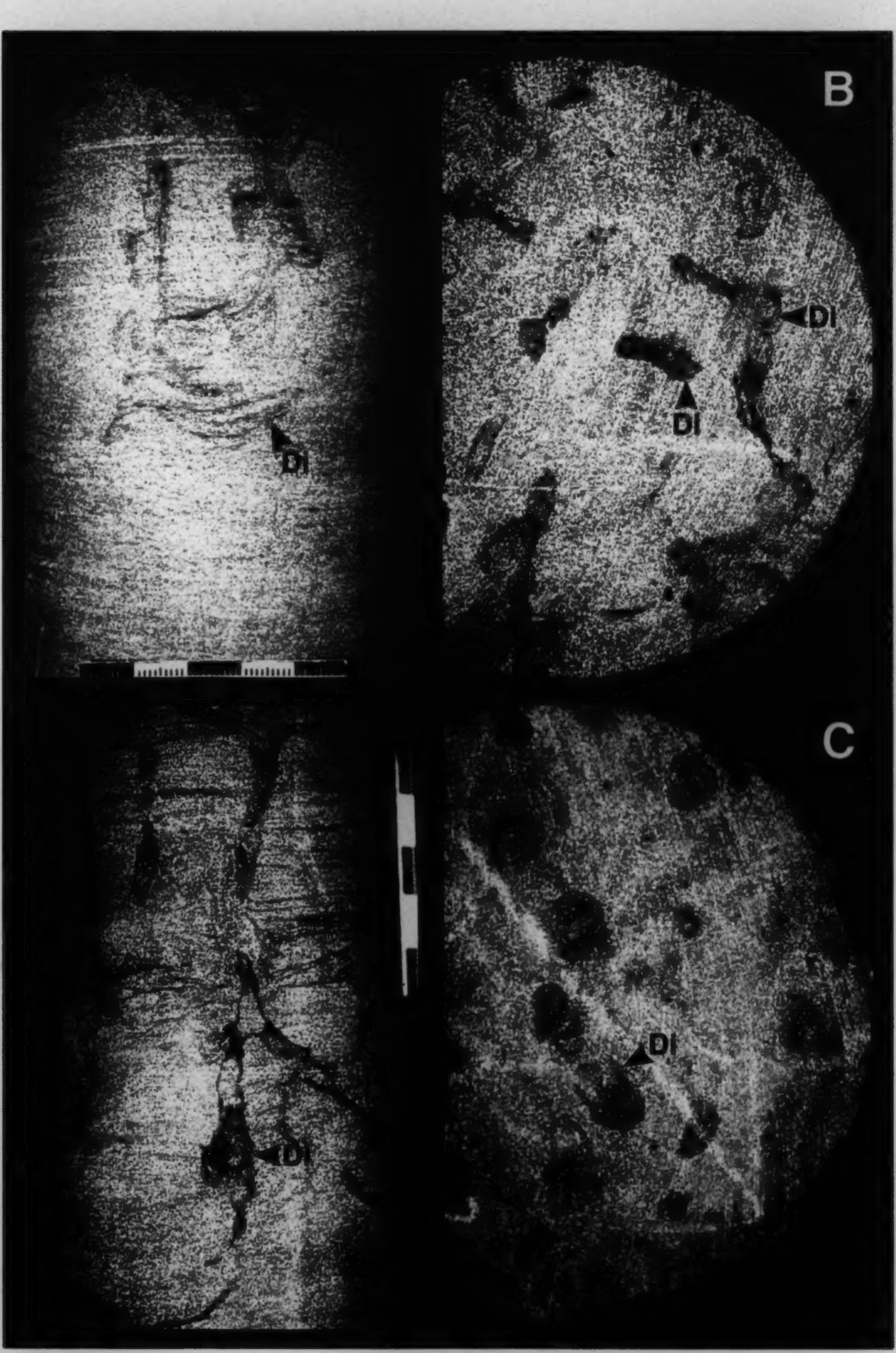
B
DI
DI
DI
C
DI
DI

Plate 9. Vertically oriented ichnogenera: (**A**) *Skolithos* burrow lined with organic matter and infilled with coarser material (fine-grained sandstone) than ambient very fine-grained sandstone. Also present are *Paramacaronichnus* and *Terebellina* traces (10-29-67-10W6, 2396.05 m); Vertically oriented (**B**), and bedding plane (**C**), cross-sectional views of *Arenicolites* burrows cross-cutting organic and mica-rich horizontal laminations (10-9-67-10W6, 2356.40 m); (**D**) Downward deflection of lamination peripheral to *Skolithos* (12-7-67-12W6, 2752.85 m).

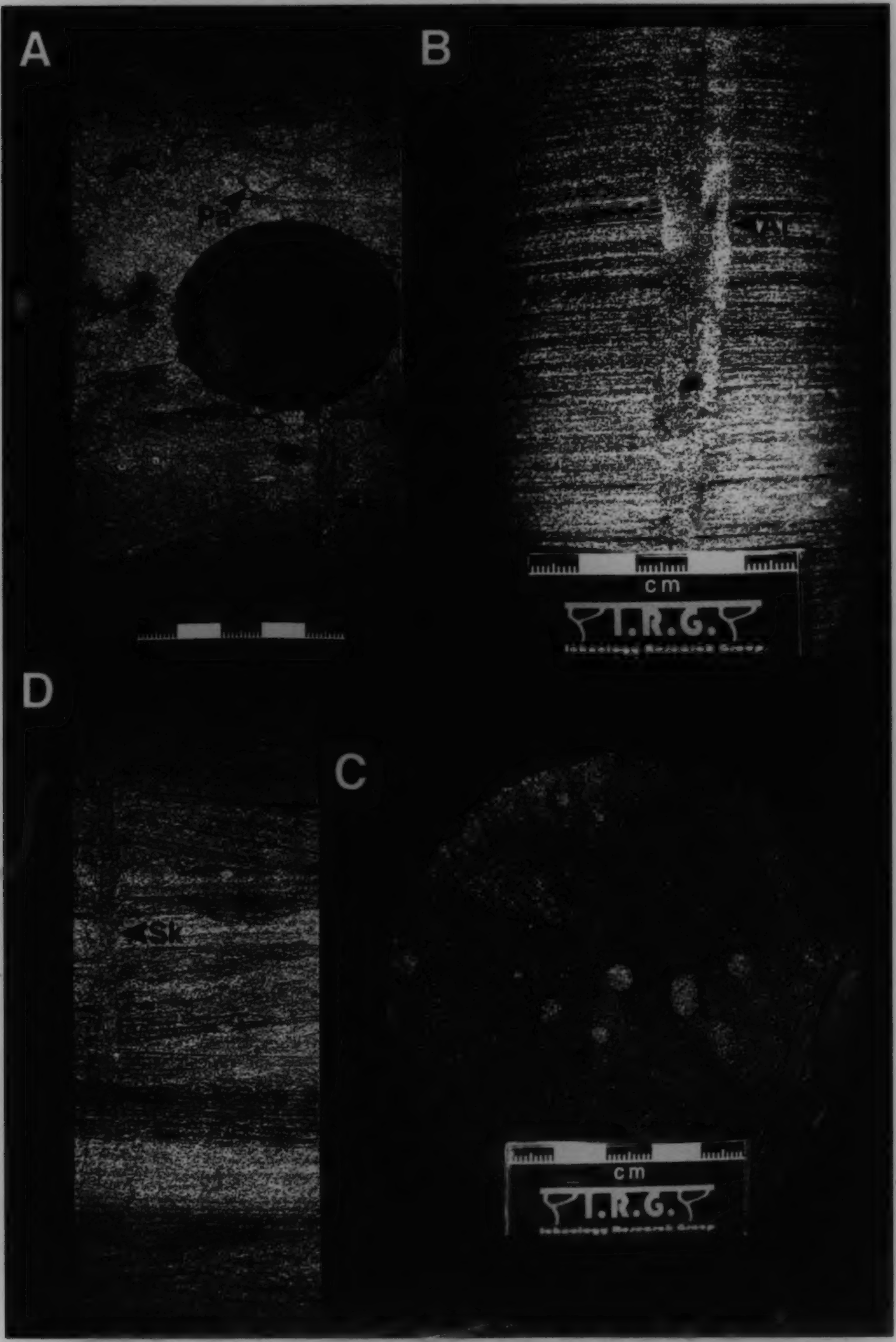
A
Pe
B
AL
cm
I.R.G.
Ichnology Research Group
D
Sk
C
cm
I.R.G.
Ichnology Research Group

Plate 10. Normal and reverse graded bedding: (**A**) 1.5 cm thick fine to very fine-grained beds within facies F6 (12-7-67-12W6, 2747.50 m); (**B**, **C**) Two types of graded bedding. First type (B), there are little or no fines at the base of the bed and grading is expressed as successive increments of finer material upward (11-8-67-11W6, 2507.10 m). The second type shows relatively abundant fine-grained material distributed throughout the bed, grading is produced by fining of the coarsest grain fraction from pebble to fine-grained sand size (12-7-67-12W6, 2749.48 m); (**D**) Reverse graded bedding (12-3-67-12W6, 2616.50-2616.10 m).

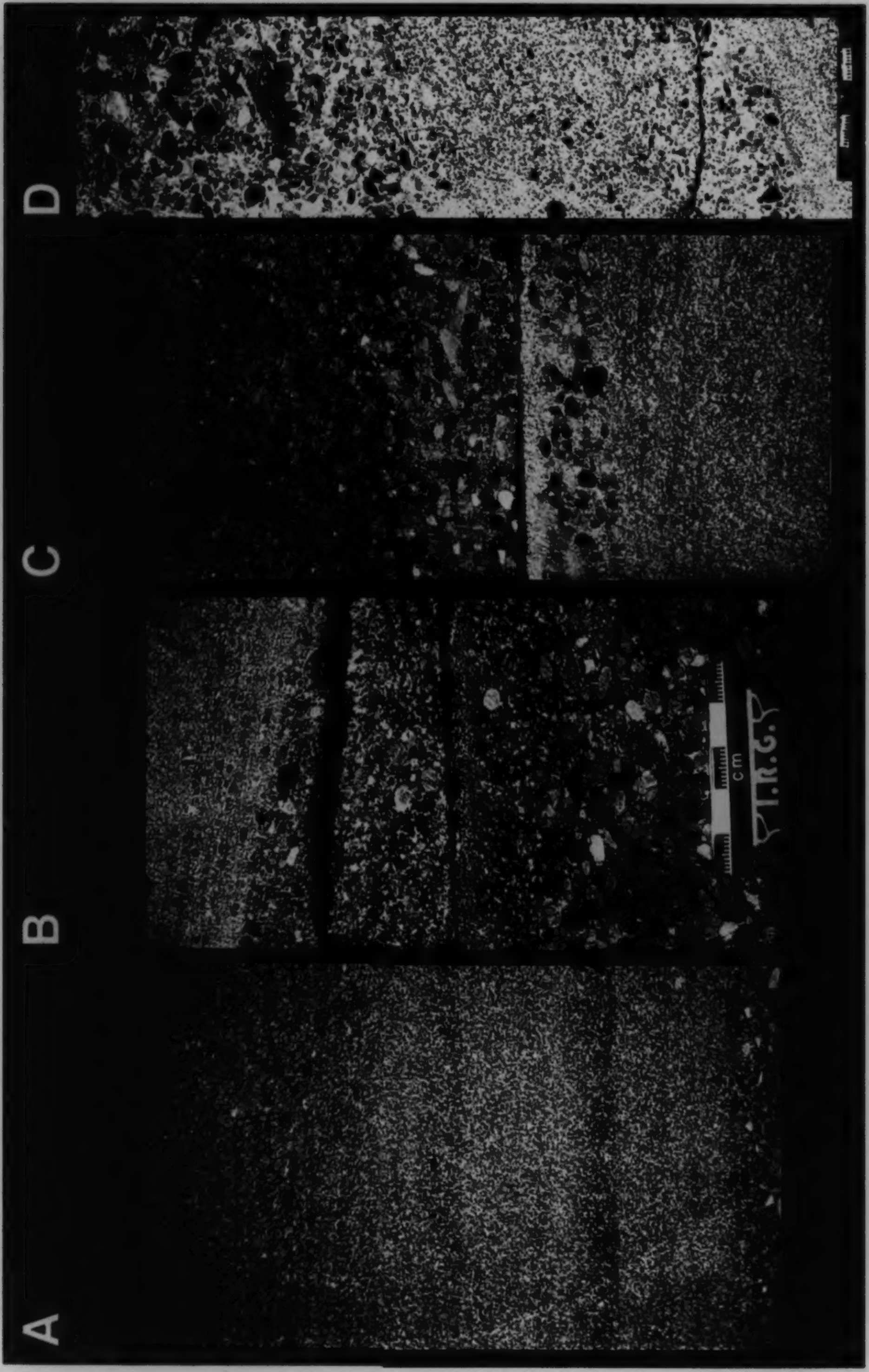
A
B
C
D
cm
I.R.G.

Plate 11. Unimodal conglomerate (facies F10 A): (**A**) Periodic interbeds of very coarse-grained sand define horizontal bedding in unimodal granule conglomerate of great reservoir potential (11-8-67-11W6, 2507.35 m); (**B**) Large pebble-sized clasts presumably aligned parallel with otherwise unrecognizable bedding contacts between unimodal beds (10-12-67-10W6, 2480.7 m); (**C**) Interbedded unimodal and clast-supported conglomerate (faceis F10 B), showing disparity of available pore space as a result of very fine-grained sand matrix within the bimodal conglomerate bed (14-4-67-12W6, 2679.30 m); (**D**) Pebbly unimodal granular chert conglomerate. Horizontal bedding visible where clasts approach very coarse-grained sand size (1-11-67-12W6, 2560.80).

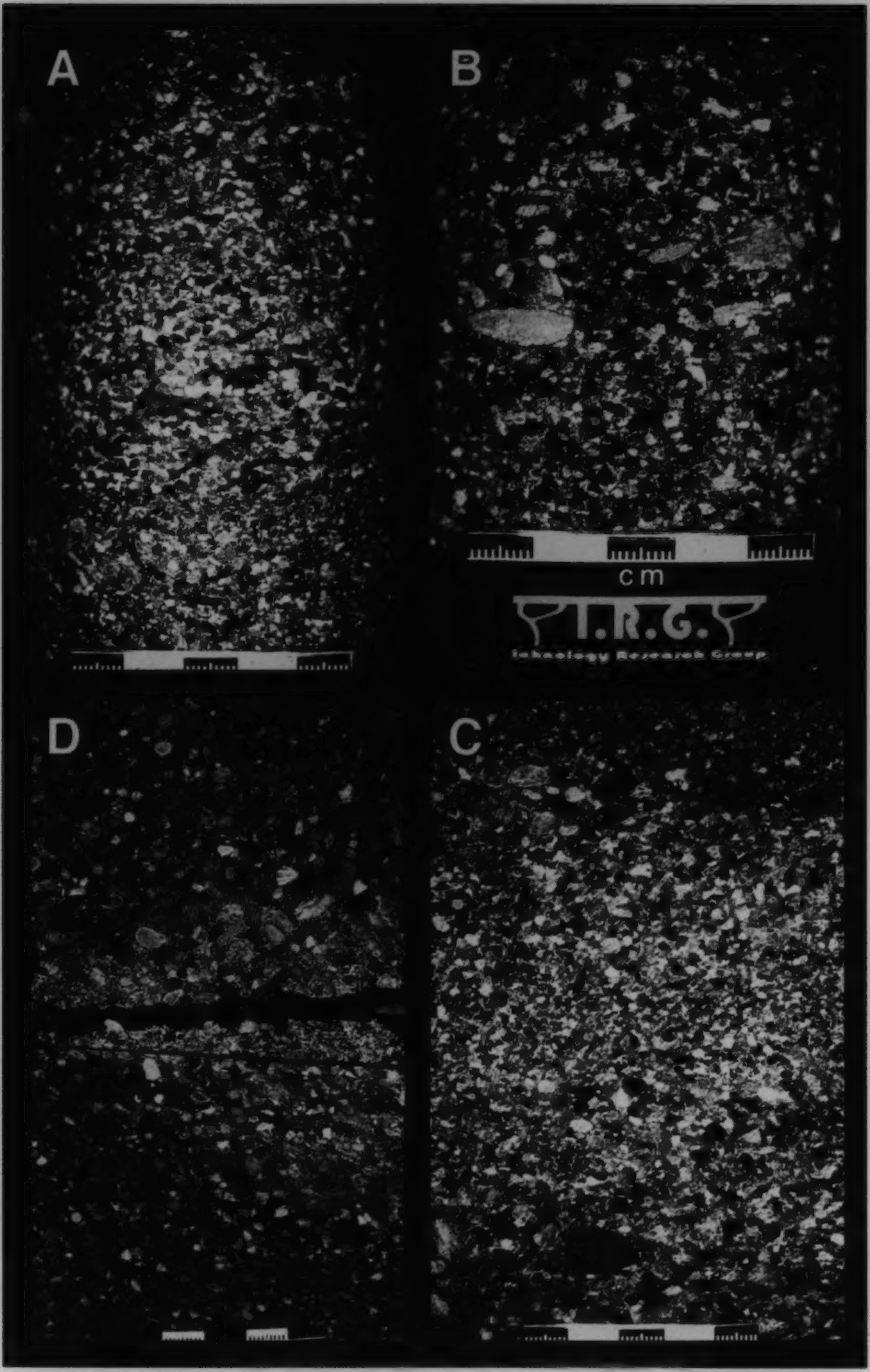
A
B
cm
I.R.G.
Ichnology Research Group
D
C

Plate 12. Interbedded coarse-grained sand (facies F9) and chert conglomerate (facies F10 A, B, C, and D: (**A**) Scoured, erosional contact between coarse-grained sand and underlying bimodal matrix-supported conglomerate (10-9-67-10W6, 2358.20 m); (**B, C**) Interbedded medium-coarse grained sand and polymodal conglomerate (10-9-67-10W6, 2360.20 m; 9-11-67-12W6, 2549.80 m); (**D**) Clast supported bimodal conglomerate (facies F10B), with fine-grained matrix (11-8-67-11W6, 2511.35 m).

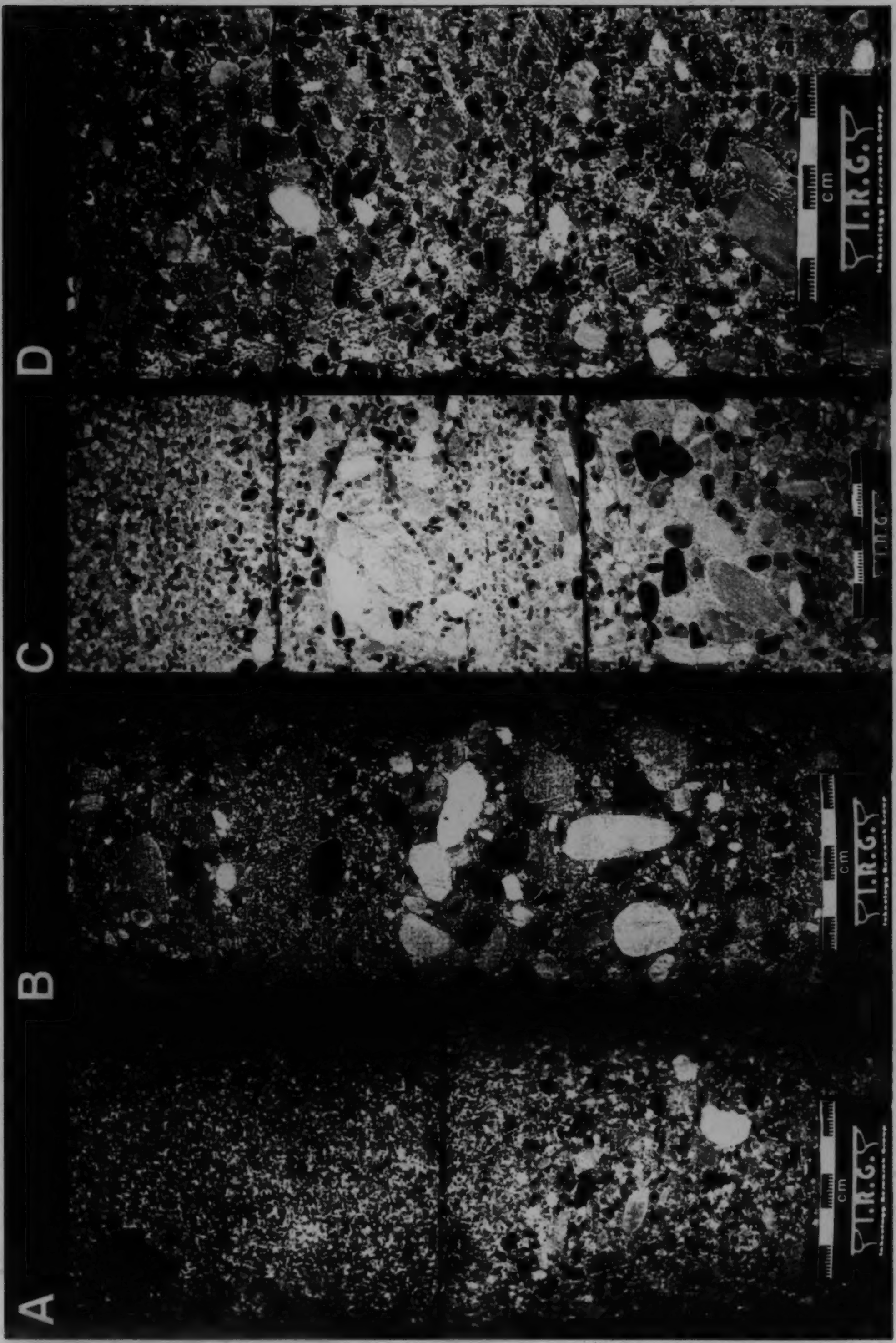
A
B
C
D
cm
I.R.G.

Plate 13. Bedding plane views of several coarse-grained facies within 10-9-67-10W6: (**A**) Randomly oriented carbonaceous wood clasts are typically aligned along bedding contacts (2355.10 m); (**B**) Well sorted coarse-grained chert arenite with patchy distribution of clay minerals between grains (2357.00 m); (**C**) Bimodal clast supported chert conglomerate lacking sandy matrix. Diagenetic clay alteration has produced discontinuous yet enveloping clay mineral concentrations between clasts (2360.30 m); (**D**) Bimodal clast-supported conglomerate with fine-grained sand matrix. Individual clasts show such surface features as pock marks and pits (2358.70 m).

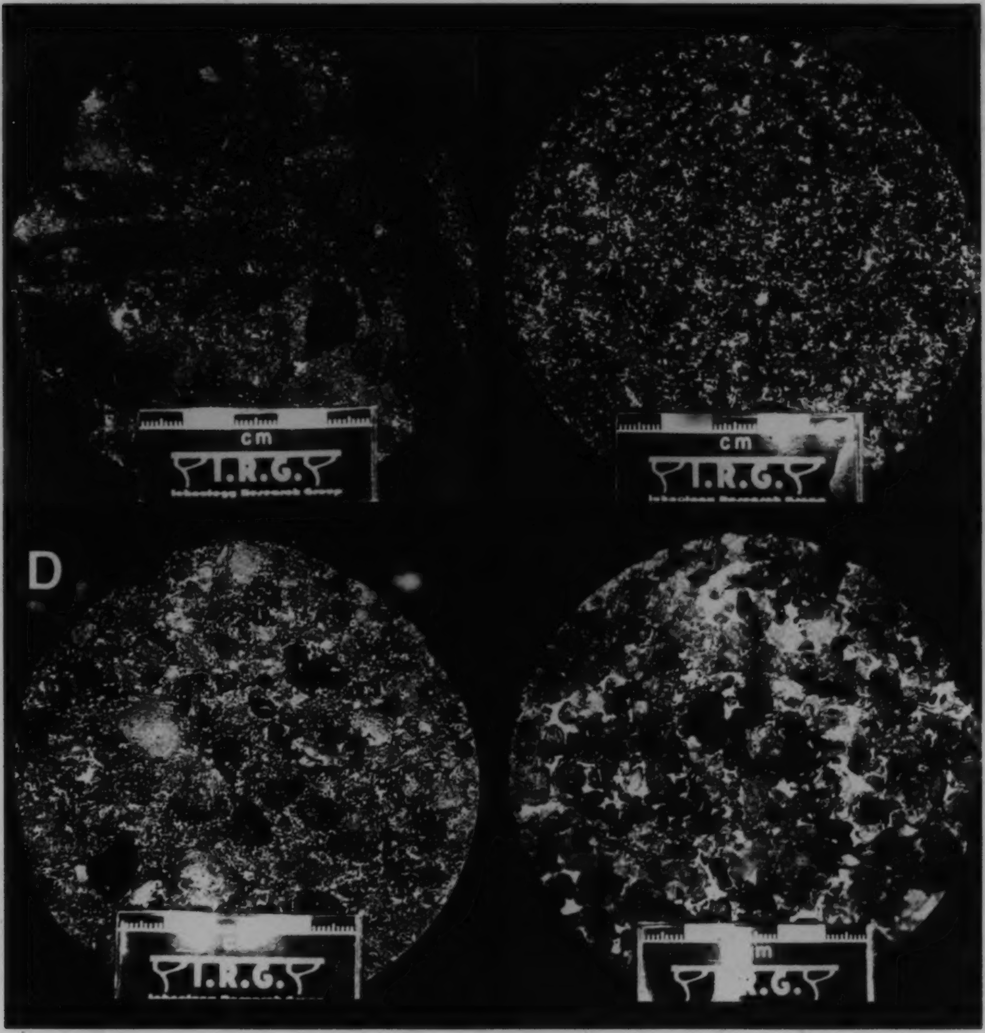
D
cm
I.R.G.
Ichnology Research Group
cm
I.R.G.
I.R.G.
I.R.G.

Plate 14. Variation in matrix composition within polymodal chert conglomerate interval (facies F10 D): (**A**) Sideritized muddy matrix completely impregnates and excludes available intergranular pore space (11-8-67-11W6, 2511.85); (**B**) Polymodal conglomerate with fine-grained sand sized matrix (11-8-67-11W6, 2510.4 m). Greatest permeability likely developed at surface contact between fine sand matrix and chert clasts as suggested by Cant (1984); (**C**) Lack of sandy matrix and original open pore space rendered this polymodal conglomerate most susceptable to the diagenetic effects of deep burial. Pressure soulution along point contacts between chert clasts indicated by visible stylolitization (11-8-67-11W6, 2509.55 m).

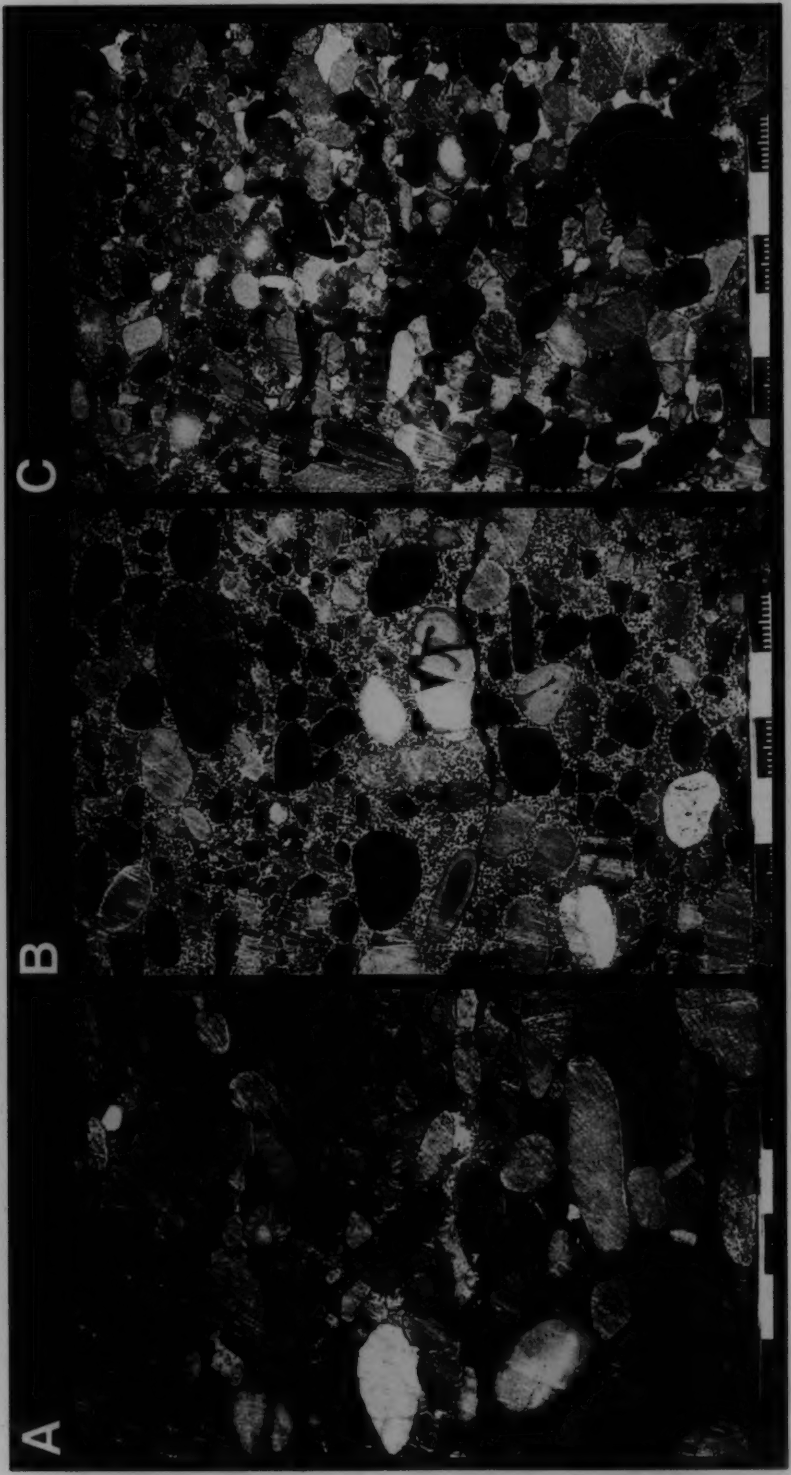
A
B
C

Plate 15. Trough cross-stratification and planar cross-stratification (facies F6 and F7): (**A**, **B**) Graded foreset lamination within trough cross-stratified fine-grained sandstone. Internal lamination size gradations range from fine- to silt-sized (11-8-67-11W6, 2502,30 m; 7-15-67-12W6, 2522.30 m); (**C**) Planar cross-stratified fine-grained sandstone (facies F6), with pebble stringers concentrated along scoured, erosive lower bedding contact (10-9-67-10W6, 2353.00 m); (**D**) Poorly sorted medium-grained planar cross-stratified sandstone (facies F7). Bedding contacts within this facies are typically steeply inclined (>15), relative to those in finer-grained facies (7-18-67-10W6, 2441.31 m).

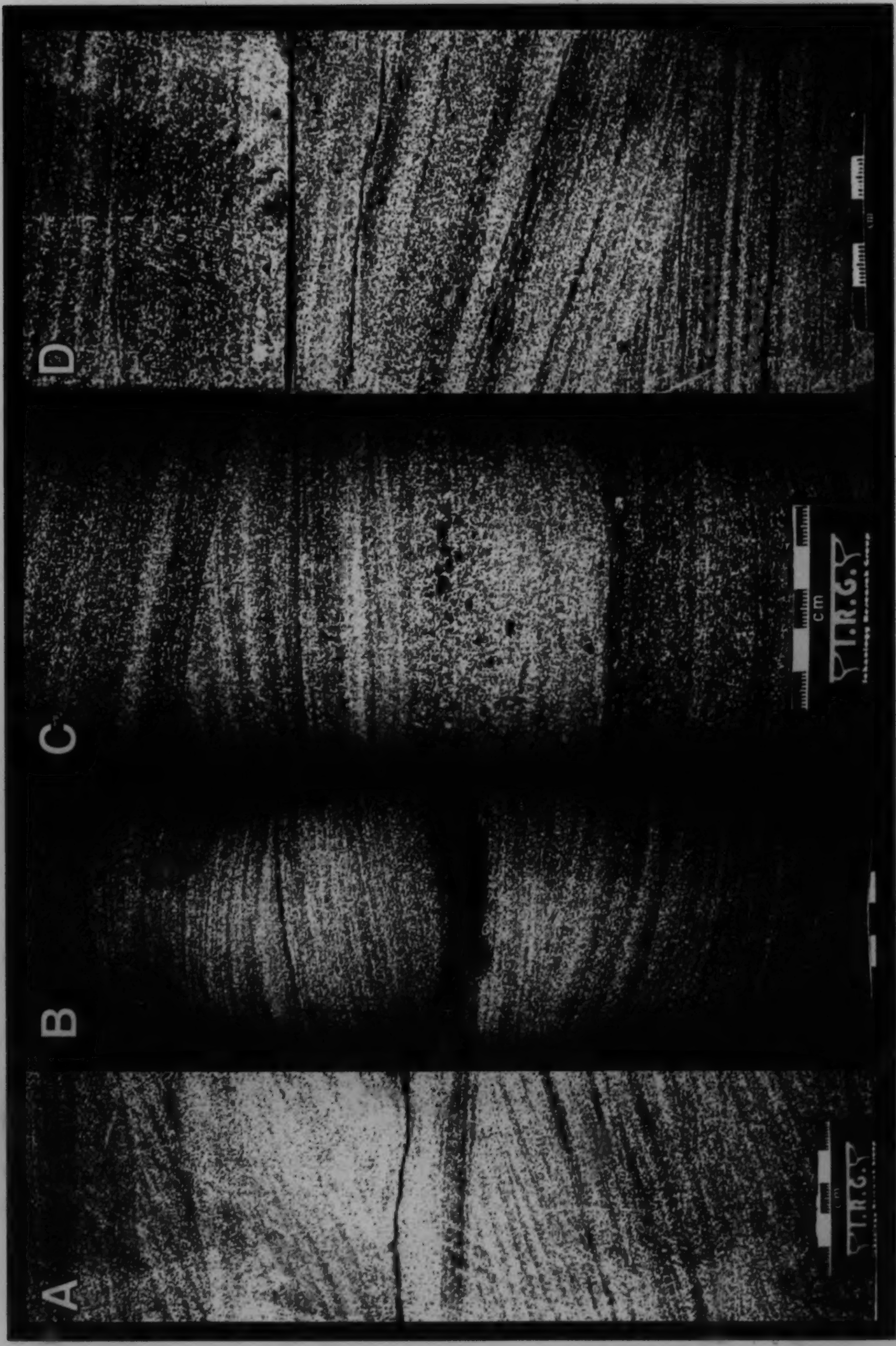
A
B
C
D
cm
T.R.G.
cm
T.R.G.

Plate 16. Cryptically bioturbated sandstone (Facies F5 and F6), produced by interstitial meiofauna: (**A**) "Fuzzy" parallel to sub-parallel laminated very fine-grained sandstone (1-15-67-7W6, 2126.95 m); (**B**) Gently inclined laminated very fine-grained sandstone. Despite 100% bioturbation, vestigial lamination remains clearly visible (12-7-67-12W6, 2750.20); (**C**) Pebbly trough cross-stratified fine-grained sandstone displaying steeply inclined "fuzzy" lamination. Organic flakes concentrated along burrow peripheries highlight *Macaronichnus* burrows and vestigial lamination (6-13-67-11W6, 2473.38 m); (**D**) Flat plane parallel "fuzzy" laminated fine-grained sandstone displaying different size gradations between benthic meiofauna to sediment ingesting macrofauna (11-8-67-11W6, 2501.15 m).

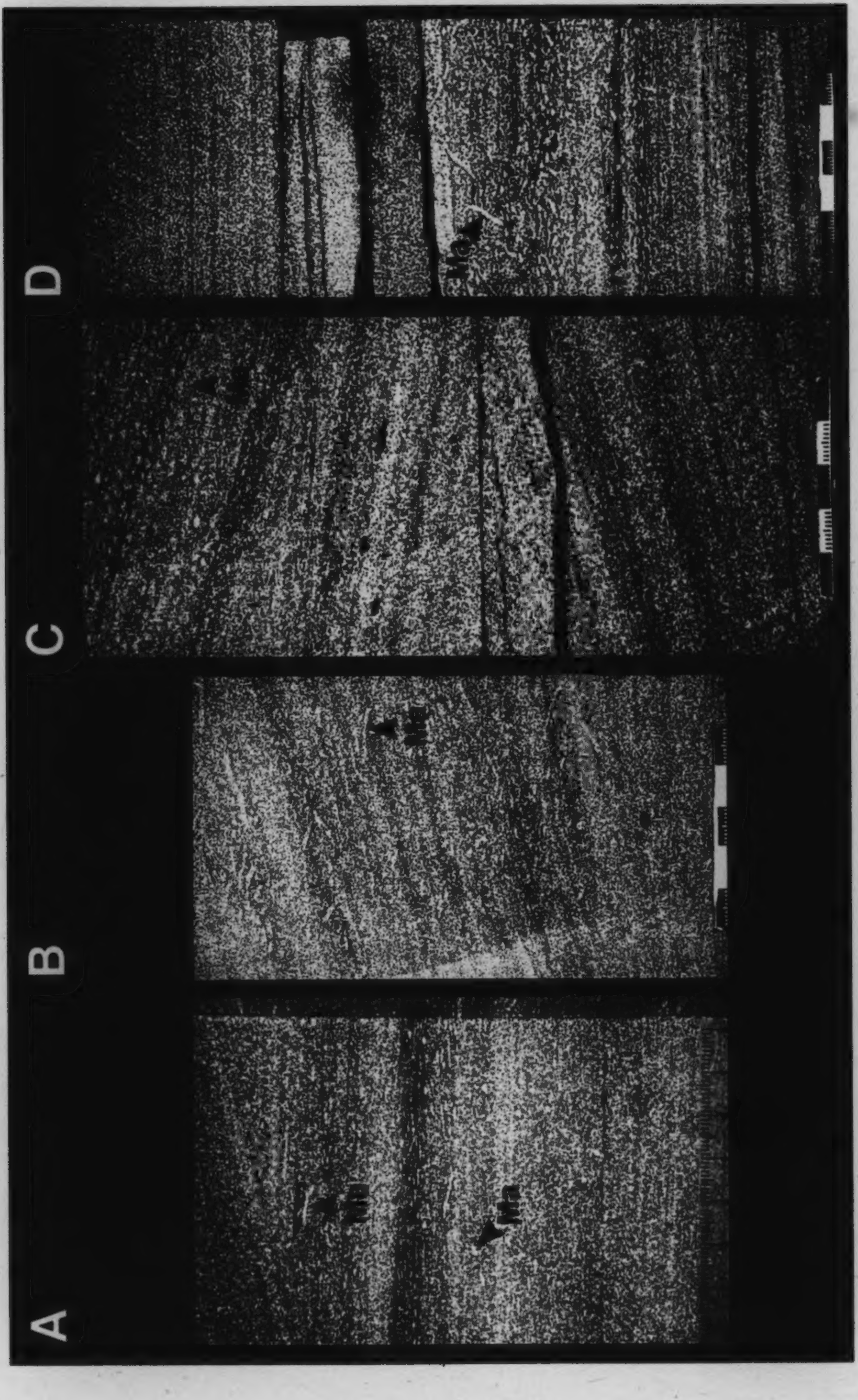
A
B
C
D

Plate 17. *Macaronichnus* assemblage: (**A**) Vestigial lamination preserved -in most cases enhanced- via mica flake and heavy mineral concentration along the periphery of *Macaronichnus segregatis* burrows (11-8-67-11W6, 2501.80 m); (**B**) Rock fabric showing result of generational succession of *Macaronichnus*-producing fauna. Fuzzy lamination represents the smallest life stage where organisms feed interstitially. Grain size-thick burrows represent the initial sediment ingesting phase of juvenile macrofauna while clearly visible *Macaronichnus* burrows represent the adults (6-13-67-11W6, 2472.29 m). (**C**) Three possible originators of *Macaronichnus* as proposed by separate authors. Clockwise from top-left: *Euzonus mucronata* (Kozloff, 1983), *Excirolana chiltoni* (Kikuchi, 1972), and *Ophelidae limicina* (Clifton & Thompson, 1978); (**D**) Bedding plane view of *Macaronichnus simplicatus* displaying random over-crossing behavior as a result of high population densities (10-9-67-10W6, 2353.10 m).

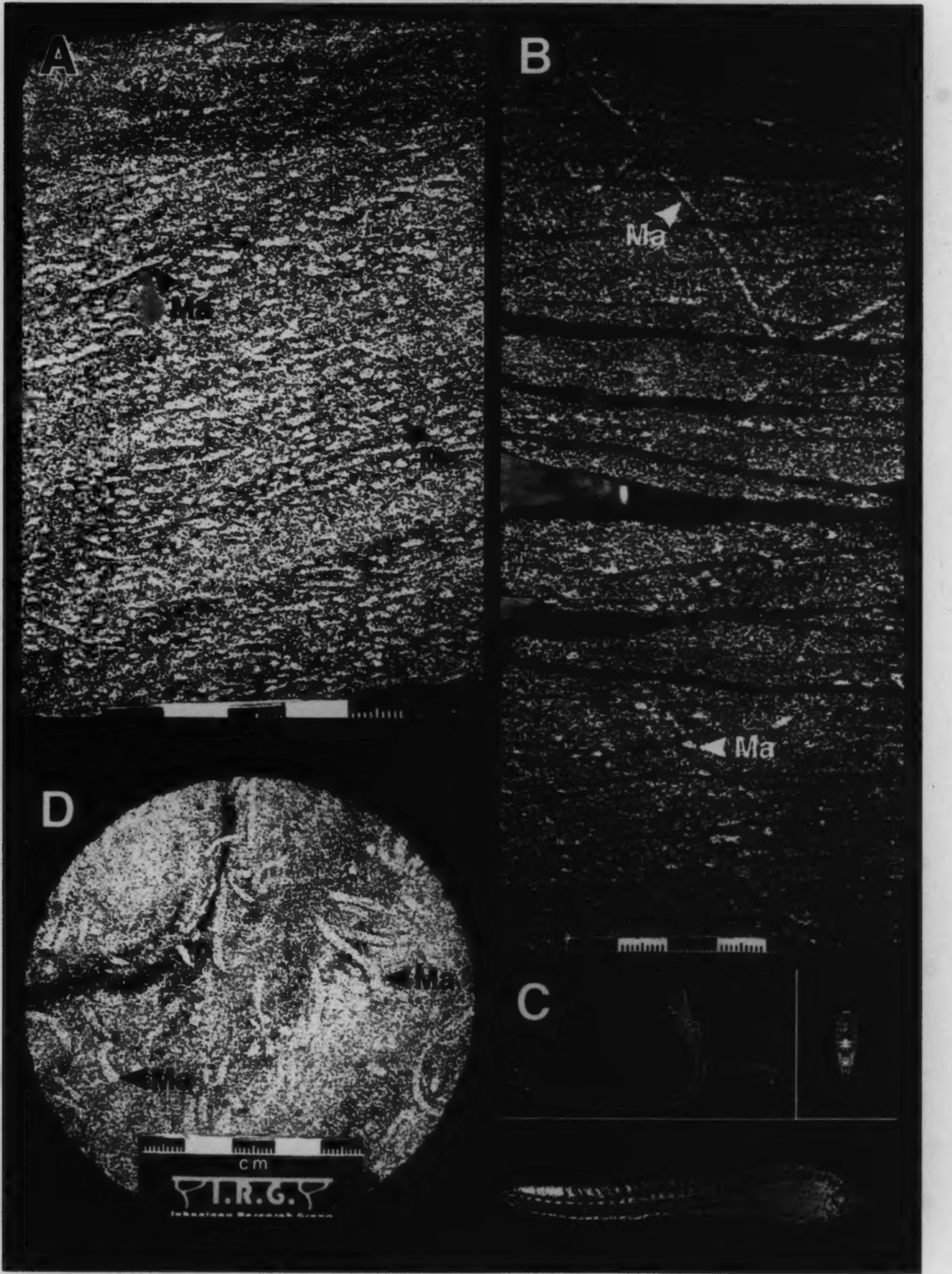
A
Ma
Ma
B
Ma
Ma
D
Ma
Ma
cm
I.R.G.
C

Plate 18. Physically and biologically churned fine-grained facies (facies F2-F4): (**A**) Silty, shaly mudstone (facies F2), showing a diminutive suite of trace fossils (10-29-67-10W6, 2402.95 m); (**B**) Intensely bioturbated sandy, shaly siltstone (facies F4). *Thalassinoides* and *Palaeophycus* are the two dominant biogenic structures present (11-8-67-11W6, 2518.75 m); (**C**) Contorted bedding presumably resulted from sediment slumping shortly after deposition (11-30-68-8W6, 2007.40 m); (**D**) Interbedded silty very fine-grained sandstone and sideritized mudstone (facies F3). Sudden loading and liquefaction of the muddy bed and penecontemporaneous deformation of the fine-grained sand likely accounts for the observed soft-sediment deformation features (10-14-67-9W6, 2296.25 m).

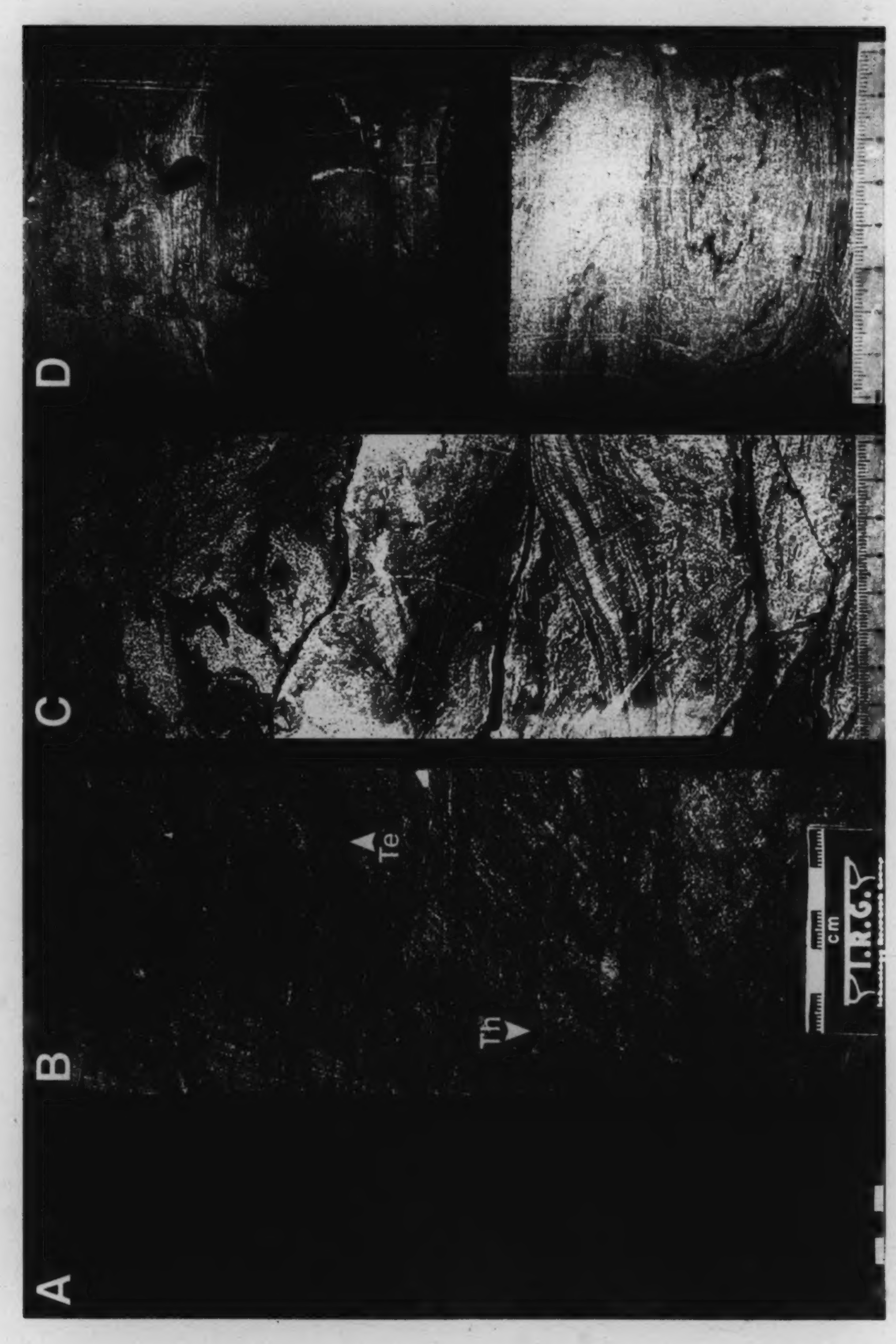
A
B
C
D
Te
Th
cm
I.R.G.

Plate 19. Low-diversity brackish water trace fossil assemblages: (**A**) Monospecific *Teichichnus* assembage within facies F4 (7-20-69-10W6, 2020.95 m); (**B**, **C**) Well developed *Teichichnus* burrows seen in transverse and longitudinal section. Vertical continuity of spreiten burrows interpreted to reflect maintenence of the burrow at the sediment-water interface during relatively continuous deposition (11-30-68-8W6, 2009.15 m and 2012.10 m respectively); (**D**) Bioturbated clean quartzose sands with abundant discontinuous organic laminations. Trace fossil structures include; *Arenicolites*, *Ophiomorpha*, *Skolithos*, *Teichichnus*, *Cylindrichnus*, and *Palaeophycus* (11-30-68-8W6, 2006.00 m).

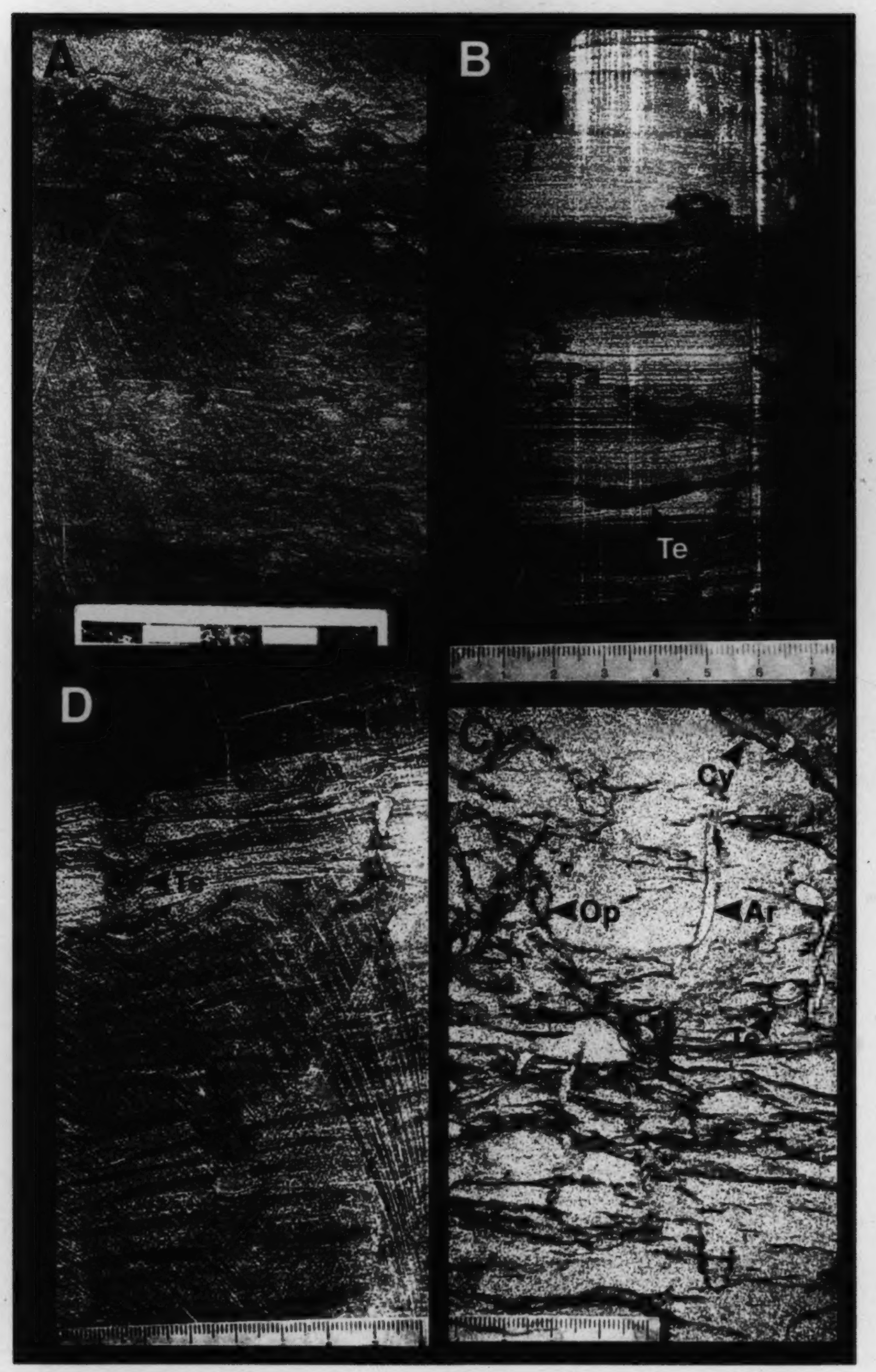
A
B
Te
1
2
3
4
5
6
7
D
Te
C
Cy
Op
Ar
Te

Plate 20. Soft sediment deformation structures and rooted bedding: (**A**) Very fine-grained sandstone 'ball' portion of ball-and-pillow load features (10-1-68-9W6,2215.70 m); (**B**) Tension micro-faulting and flame structure developed in interbedded fine-grained sandstone and mudstone facies (facies F3). Deformation in underlying facies likely resulted from adjacent rapid deposition of thickly bedded fining upward sandstone facies (10-1-68-9W6, 2205.50 m) (**C**) Discontinuous, wavy carbonaceous lamination and stylolitization. Subtending root traces emanate downward from thickly bedded coal beds (facies F11), into underlying fine sandstone (6-13-67-11W6, 2469.18 m); (**D**) Wavy carbonaceous laminae and rooted bedding within sandy siltstone (7-18-67-10W6, 2452.78 m)

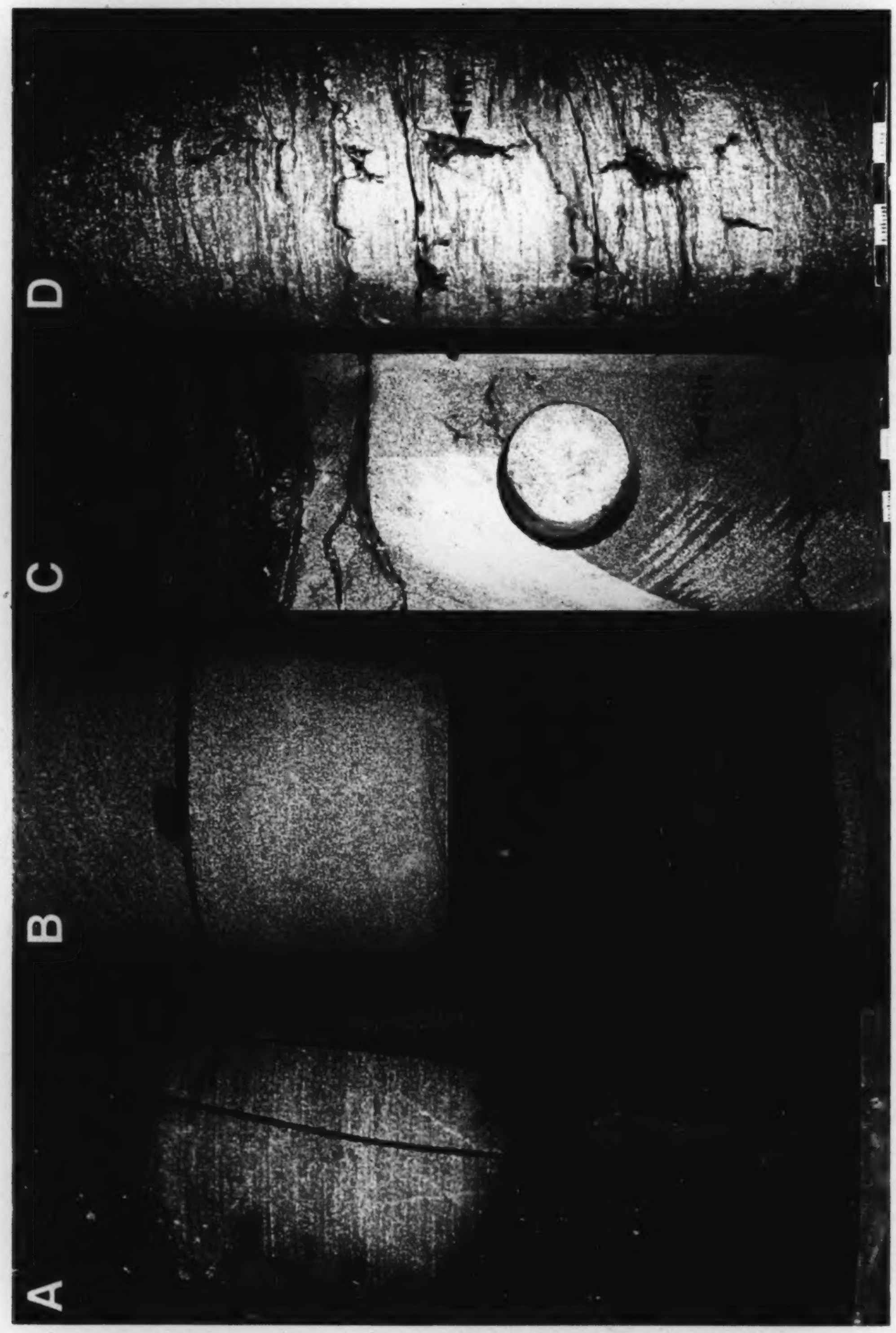
A
B
C
D

Plate 21. Organic-rich mudstone and coal facies (facies F1 and F11): (**A**) Development of load features either as the result of ball-and-pillow structures or load-casted ripples (10-1-68-9W6, 2214.12 m); (**B**) Carbonaceous mudstone showing crudely interlaminated coal and silty mudstone (6-21-67-10W6, 2463.05 m); (**C**) Carbonaceous leaf and stem remains preserved along bedding contacts within facies F1 (10-1-68-9W6, 2200.00 m); (**D**) Sub-bituminous coal (F11), displaying conchoidal fracture (10-1-68-9W6, 2202.55 m).

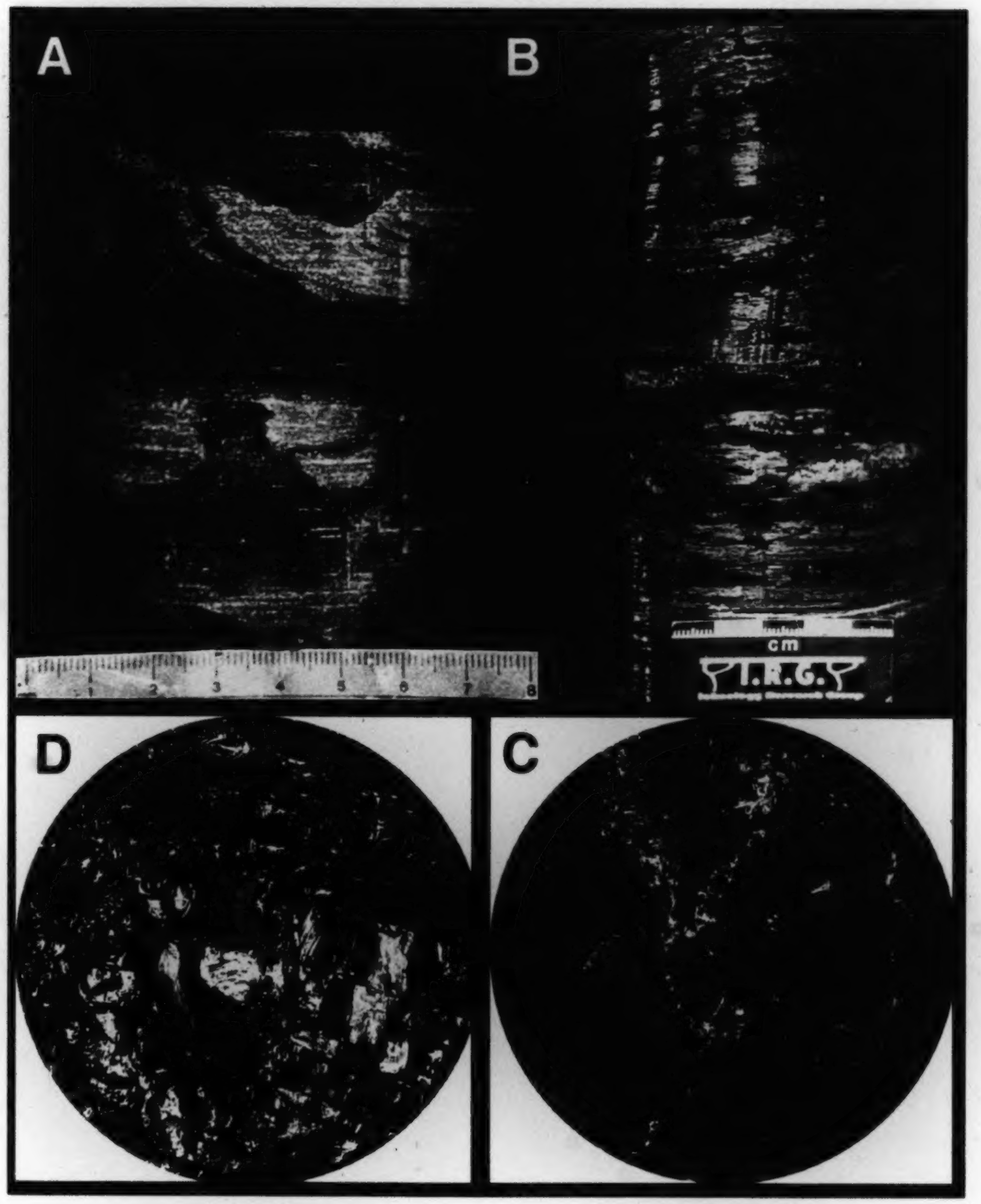
A
B
1
2
3
4
5
6
7
8
cm
I.R.G.
D
C

CHAPTER THREE: Key Surfaces and Stratal Architecture

3.1 Introduction

Four regionally significant stratigraphic surfaces of the Falher "C" sequence are present within the study area. Each surface disconformably bounds allostratigraphic units which are termed the Falher C1, C2, C3 and C4 from oldest to youngest respectively. These surfaces are distinct from facies contacts that define the internal framework of facies associations and inferred environments of deposition. The two types of surfaces are not mutually exclusive and can occupy the same stratigraphic horizon within the Falher "C" sequence. The lowermost and/or uppermost contacts of facies associations described and interpreted within Chapter 2 commonly coincide with regionally significant stratigraphic surfaces. This is because the surfaces separating the allostratigraphic units reflect episodes of relative change in sea level, sediment supply and subsidence rates that initiate basinward or landward shifts of facies. These changes are of regional significance, and can therefore be identified on well logs that have been calibrated to cored intervals of the Falher "C" Member. Correlation of these surfaces between wells containing calibrated log signatures and wells lacking core, but expressing similar log profiles, has yielded seven allostratigraphic cross-sections. These provide the framework for a more detailed analysis of the stratigraphic architecture of the Falher "C" Member. This chapter ultimately explores the relationship between the internal stratigraphic heterogeneity of the four allostratigraphic units and their manifestation within the regional framework.

3.2 Significant Stratigraphic Surfaces and Sub-division of the Falher "C"

Seven allostratigraphic cross-sections have been constructed to demonstrate the distribution of key stratigraphic surfaces and lateral equivalence within the study area of major Falher "C" allostratigraphic units. Six of these sections (A-A' to F-F') trend north-south, parallel to depositional dip (figure 12). Cross-section G-G' trends west-east, parallel to depositional strike (figure 13). Core control is greatest within the strike section because it is constructed using wells from the main producing trend of the Falher "C" Member (Twp. 67). Cored environments extend from brackish marginal marine intervals within the upper Falher "D" through the marine sequences, and upper marginal marine sequence of the Falher "C" Member. The stratigraphic datum used is the second coal horizon at the top of the Falher "C" Member. It is laterally extensive within the study area and readily identifiable on sonic logs. Two dip-oriented cross-sections (figure 12), and the strike-oriented cross-section G-G' (figure 13), are discussed in further detail below. The four dip-sections not addressed in the following discussion can be found in Appendix II.

Dip Sections A-A' and E-E'

Within the study area, the Falher "C" Member is sub-divided into four units termed the C1, C2, C3, and C4 deposited from oldest to youngest respectively. Dip-oriented cross-sections show a thickening of the Falher "C" Member northward or paleobasinward (figure 12). Total stratigraphic thickness of the Falher "C" Member varies from approximately 30 m in proximal areas (Twp. 66) to 40 m in distal areas (Twp. 68). The C1 unit rests disconformably upon a marine flooding surface and transgressive surface of erosion (see Section 3.3). This surface is expressed as a pronounced kick to the left on gamma-ray logs where interbedded shales and coal beds that comprise the uppermost Falher "D" are overlain by relatively "clean" marine sandstones and the base of the C1 unit. Several channelized units within the Falher "C" bottom-out on this surface (figure 12). Channelized deposits are recognized on gamma-ray profiles as blocky interbedded to spiky profiles (6-6-68-9W6M; E-E'), or bell-shaped log profiles (6-27-66-13W6M; A-A'). The C1 unit is well preserved and extensive throughout dip oriented cross-sections. The C1 unit thins significantly in Twp. 67 where it is overlain by C2.

The C2 unit is a lens-shaped stratigraphic interval that reaches a maximum thickness of about 6 m as shown in dip-oriented cross-sections (figure 12). It is confined to Twp. 67 where it lies upon a convex-up and regressive surface of erosion that merges laterally with a transgressive surface of marine erosion (figure 12). Recognition of the basal C2 contact is problematic between occurrences in core vs. geophysical well logs. Within core, the contact is marked by a dramatic and unmistakable superposition of coarse-grained conglomeratic facies (FA2) overlying very fine-grained facies (FA1). Distinction of the same contact using a single log response is difficult. Quite often more than one set of log data has been employed to chose the contact (*e.g.* sonic, gamma-ray, and caliper log). Commonly, there is a subtle kick leftward of the gamma-ray log profiles where the contact is present.

The C3 unit is extensive throughout a large portion of the study area, but unlike the C1 unit, it does not extend landward of the Township 67 (figure 12). Landward expression of the C3 unit is coincident with distribution of the C2 unit. Basinward, the basal contact of the C3 unit merges with the regressive surface of marine erosion. This is accompanied by thickening of the C3 unit, and a corresponding pinching-out of the underlying C2 unit (figure 12). The upper contact between units C3 and C4 is discontinuous across the study area. The contact is marked by a pronounced kick to the right as clean sandstones pass vertically into interbedded organic-rich shales, spiky coal beds and blocky distributary sandstones (figure 12). Cyclical

Figure 12. Dip-oriented Stratigraphic Cross-secti

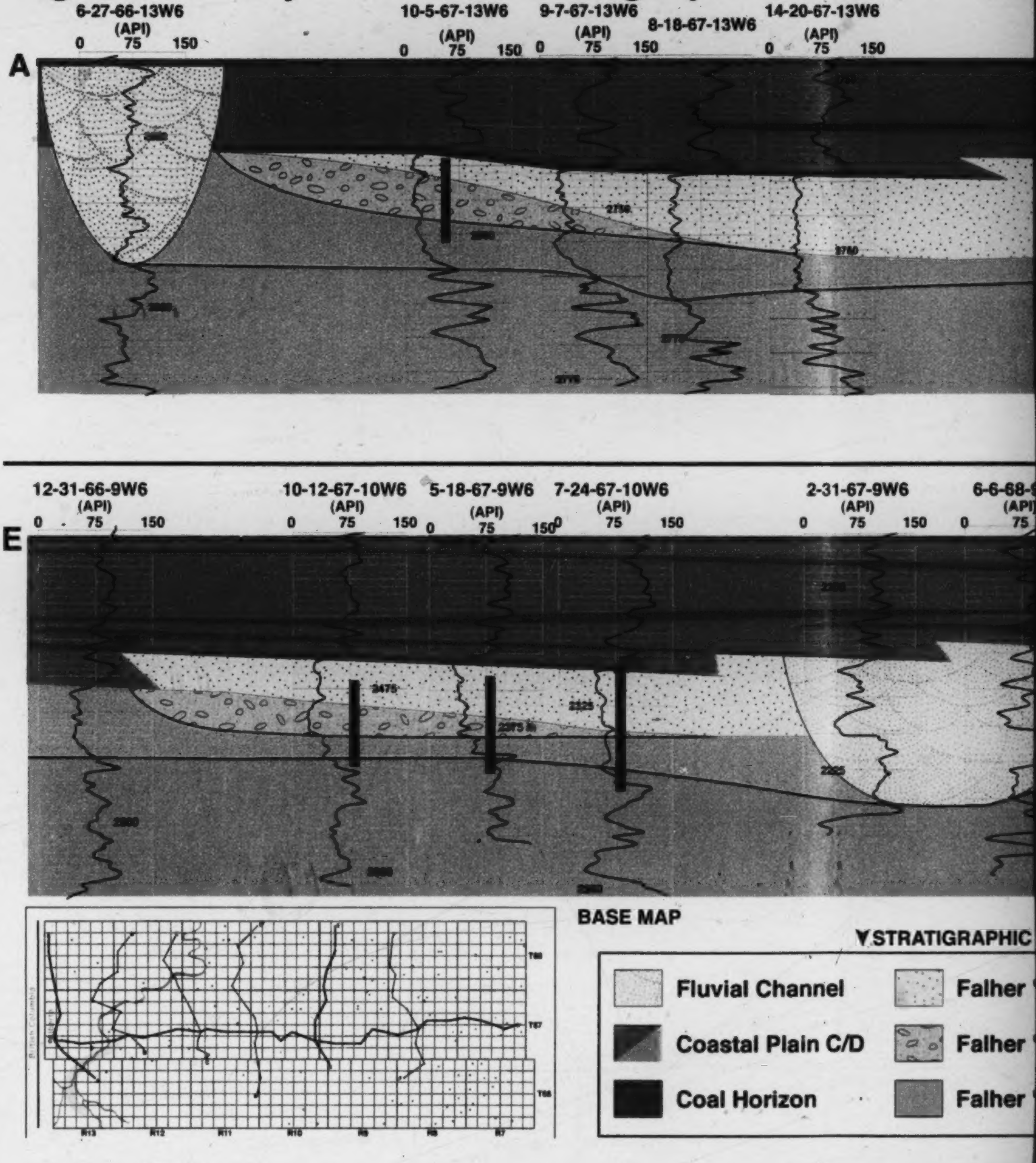

Cross-sections: A-A' and E-E'

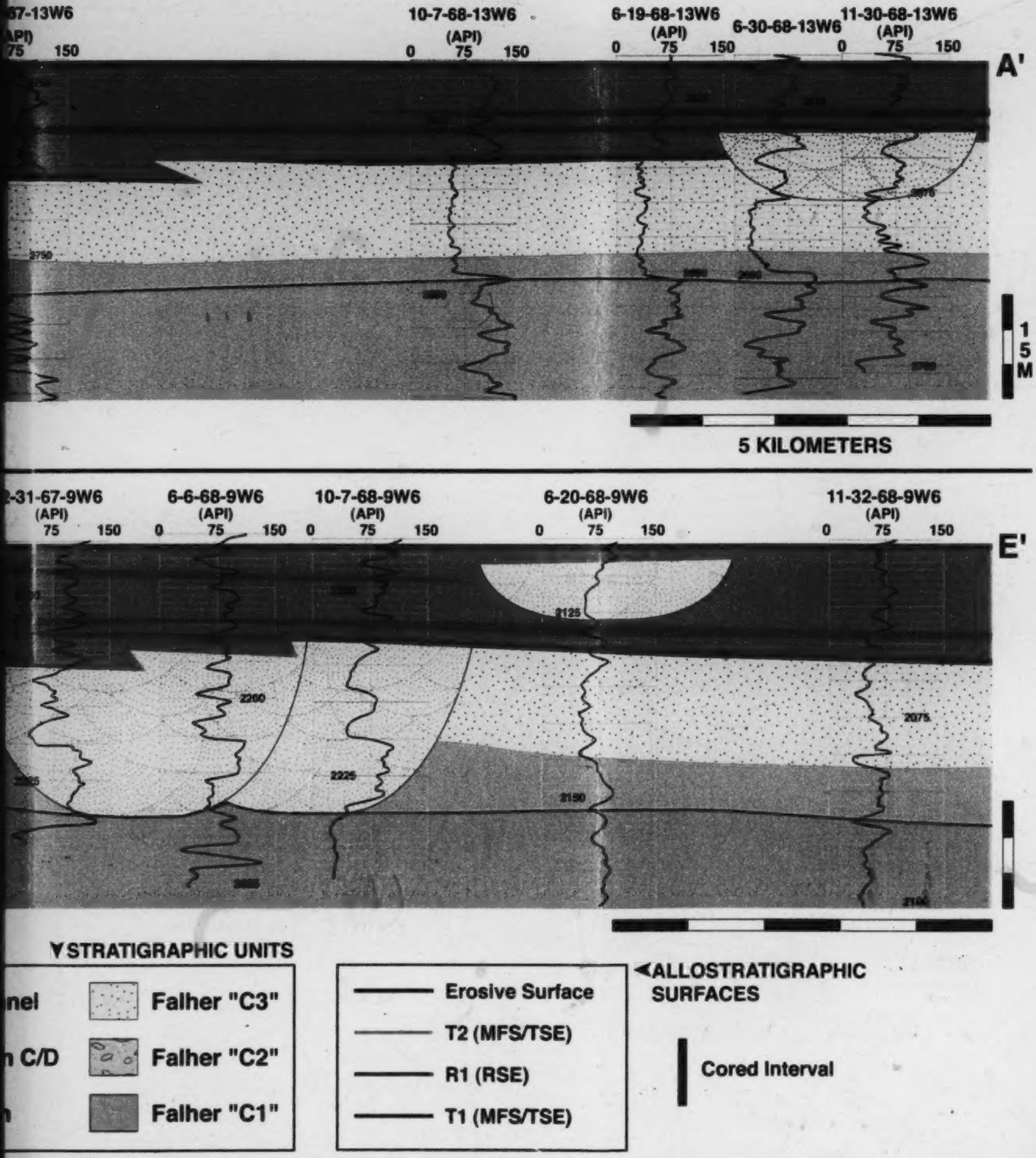

progradation of the C3 unit and capping coal beds produced a stacked succession of laterally discontinuous imbricate coal beds. The lowermost coal bed immediately overlying the C3/C4 contact is indistinguishable from C3 sandstones on gamma-ray logs, but is distinct on sonic logs and in cored intervals (*e.g.* 7-24-67-10W6M). The C4 unit varies between 18 and 15 m thick and is characterized by an erratic gamma-ray log response. Coal horizons that register as spikes on the gamma-ray log are laterally discontinuous where they can be shown to pinch out. Locally, coals are erosionally cross-cut by distributary channel sandstones that register as bell shaped gamma-ray log curves (figure 12).

Strike Section G-G'

Cross-section G-G' lies along the approximate depositional strike of the Falher "C" paleoshoreline and shows the pinching and swelling of all depositional units C1, C2, C3 and C4. The total strike-parallel thickness variation (within Twp. 67), of the Falher "C" Member is 25 m to 35 m. The paleotopographic relief associated with the C1/Falher D contact is therefore as great as 10 m (figure 13). Thickest occurrences of the C1 unit coincide with topographic lows of the Falher "D"/C1 contact, whereas stratigraphically thin intervals of the C1 unit are found over paleotopographic highs (figure 13).

The C2 unit exhibits considerable variability in stratigraphic thickness (3.5-9 m) and stratigraphic position within the Falher "C" sequence. In most instances the C2 interval is sandwiched between the C1 and C3 units. However, the C3 interval is locally absent and in such cases the C2 unit is underlain by C1 overlain by C4. This is particularly important within range 7 (figure 13). Although the C2 trend is interpreted to be present within the length of the study area (Twp. 67), the unit is missing from the western portion of the G-G' section. This is due to the line of section being basinward of the main C2 trend. Where this is the case, superposition of the C3 unit overtop of the C1 unit is shown along an amalgamated surface representing the C3/C1 contact. Where C3 is absent in the easternmost portion of the G-G' section and the C2 unit is shown capping the C1 unit, the section is interpreted to lie landward of the C3 unit. Therefore the presence/absence of depositional units and significant stratigraphic surfaces is viewed as a consequence of the line of section lying along a path oblique to true depositional strike.

In comparison with units C1 and C2, the stratigraphic thickness of unit C3 is more consistent (about 7 m). There is also much less topographic relief associated with the underlying C3/C1 or C3/C2 contact. The overlying coal horizon that marks the C4/C3 contact is more laterally continuous and less imbricated than in dip-section. Where the coal is missing, it has been replaced by channelized deposits that are represented by bell-shaped gamma-ray profiles (figure 13).

Figure 13. Strike Oriented Stratigraphic Cross-sec

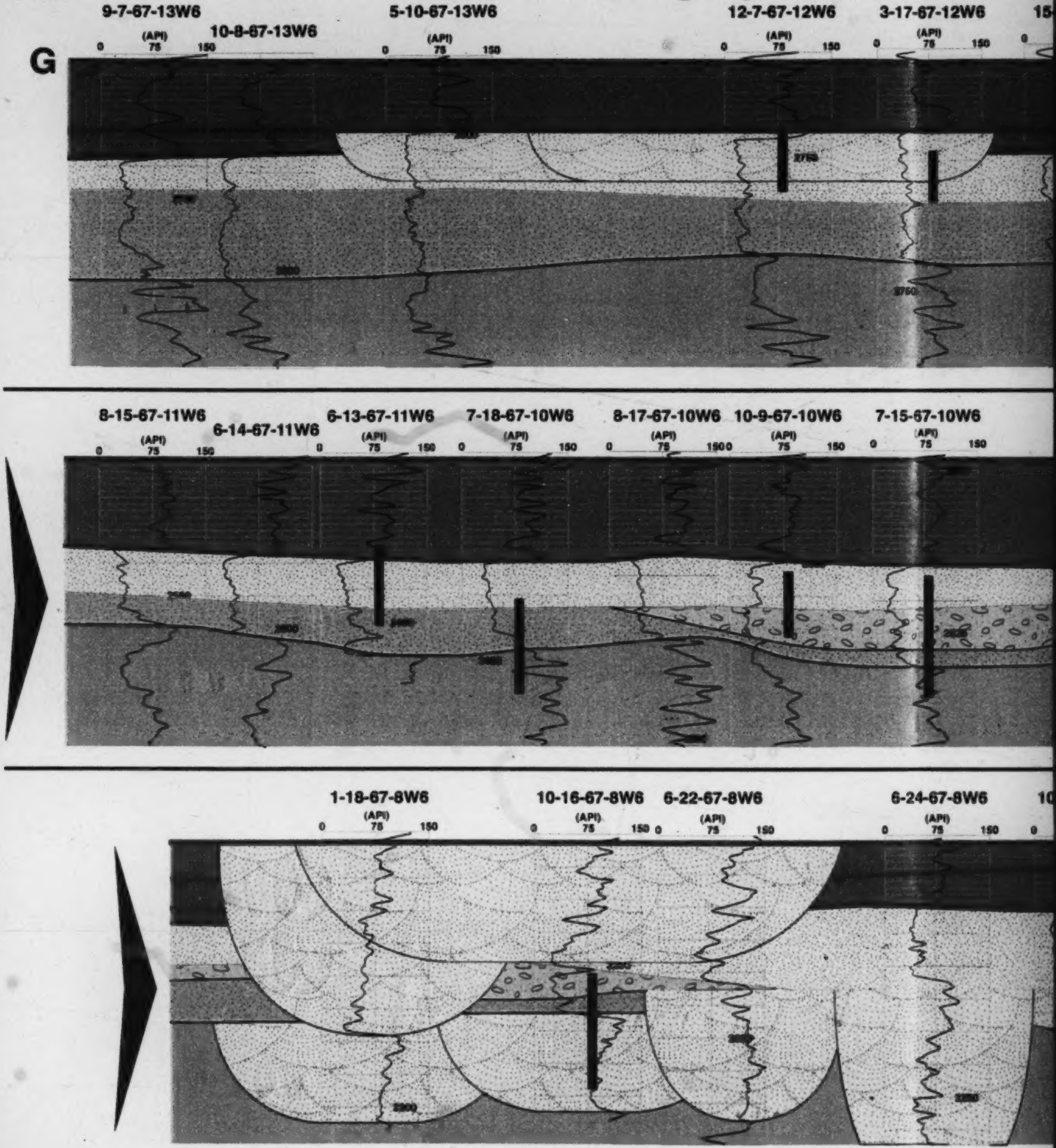

ross-section: G-G’

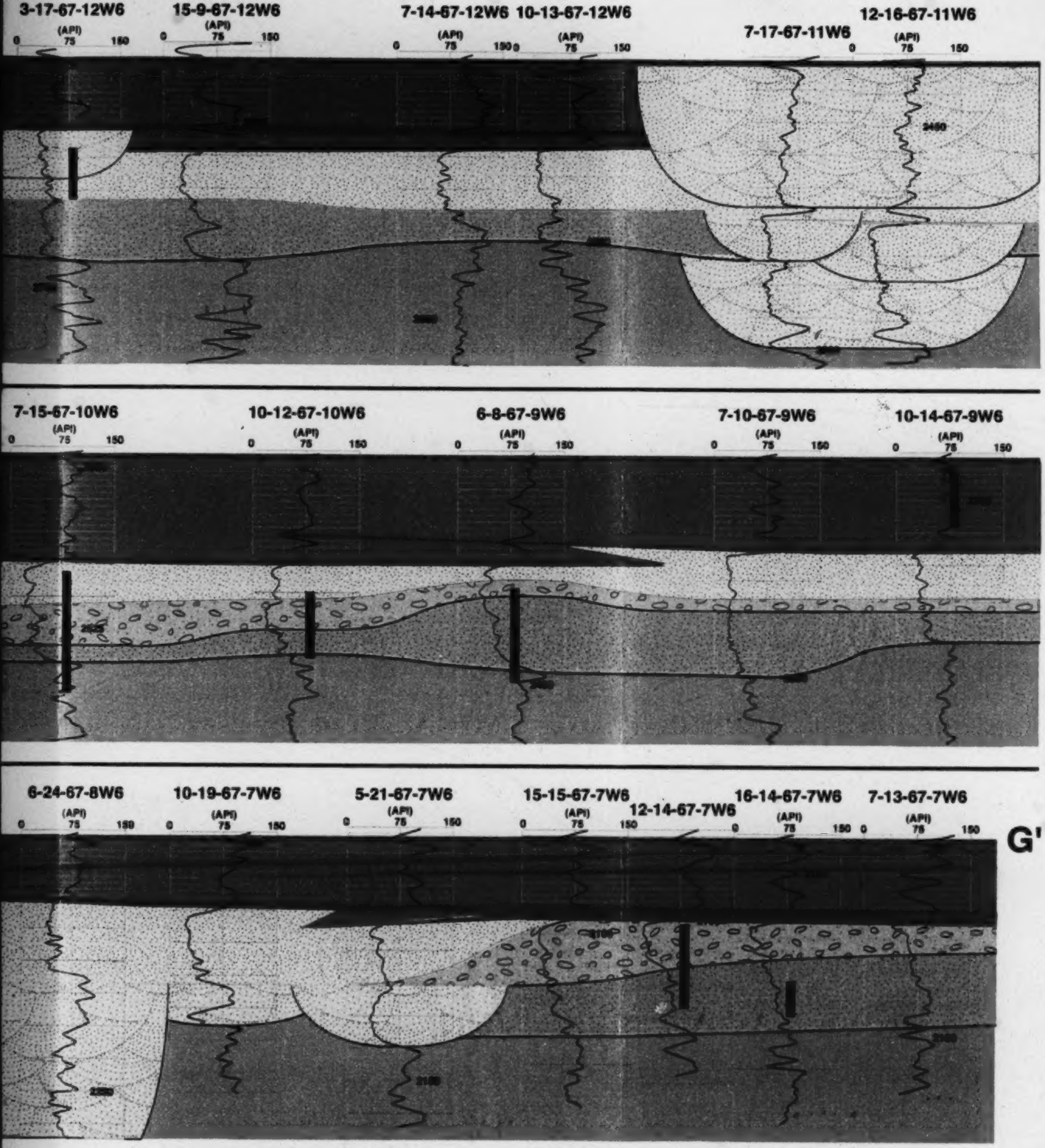

Ranges 11W6M and range 8W6M exhibit conspicuous concentrations of bell-shaped gamma-ray log responses (figure 13). These channelized deposits are interpreted to have aggraded throughout deposition of the Falher "C" interval and continue into underlying and overlying Members "D" and "B" respectively. Wells penetrating these locations show that surfaces separating the individual units of the Falher "C" have been cross-cut by the channels and are not present in these areas. Laterally extensive spiky shales and coals present within unit C4 are also cross-cut and missing within channelized intervals. The channelized units extend to the uppermost second coal used as the stratigraphic datum (figure 13).

3.3 MFS/TSE1: Contact between C1 and Falher D

Description & Occurrence

The basal contact between C1 and the uppermost of Falher "D" Member is sharply overlain by FA1. Facies beneath the C1/Falher D contact belong to either FA4 or FA5. Where FA1 is underlain by FA5 the contact is commonly between very fine-grained sandstone and carbonaceous shale or coal characteristic of FA5 (plate 21, A, B). Thin (<0.10 m), coarse-grained conglomeratic beds sometimes directly overlie facies characteristic of FA5. In such cases a dark, massive shale is sometimes superposed on top of the conglomerate (plate 22, D). FA1 also commonly overlies FA4 above a sharp, and at times, bioturbated contact. One instance of a bioturbated contact between Falher "C1" and "D" is the development of a *Glossifungites* surface within well 1-11-67-12W6M (plate 22, C). This surface is localized as it has not been observed within any other cored intervals of the Falher "C" Member, and cannot be correlated beyond the well location.

Interpretation

It has been shown that the character of the C1/D contact in core is determined by whether the marine-deposited C1 unit is underlain by marginal marine deposits (FA4), or fully terrestrial deposits (FA5). The fact that marginal marine and non-marine facies belonging to the Falher "D" Member are overlain by fully marine deposits (C1), implies that deposition of the Falher "C" began with overall transgression of the shoreline and a consequent landward shift of facies. Relative proximity to the maximum landward extent of the Falher "C1" shoreline can loosely be derived from inferred depositional environment of facies underlying the C1/D contact, and the stratigraphic separation of the initial marine flooding surface (MFS), and the transgressive surface of erosion (TSE1). Amalgamation of interpreted MFS and TSE1 surfaces is observed within wells that coincide with shoreline-proximal portions within the Falher "C1" (*e.g.* 10-4-67-10W6M, 7-18-67-10W6M). In such instances, fully-marine facies immediately overlie terrestrial facies. In more basinward portions of the Falher C1, the C1/D contact coincides with the base of the marine sand (that is equivalent with the base of the Falher "C") and is interpreted as a TSE. In such examples, the MFS lies at the base of the marginal marine interval, within the Falher "D".

The point at which the amalgamated MFS/TSE surface diverges into individual surfaces that border marginal-marine deposits defines the maximum landward extent of base-level. Amalgamation of the MFS and TSE implies net erosion following transgression, however, the preservation of marginal-marine facies above the MFS implies net deposition preceding erosion during transgression. Another important point is that although the onset of Falher "C" transgression is marked by deposition of the MFS, the TSE is correlated as the base of the Falher "C" due to the ease of its identification on gamma-ray logs and correlation within the study area (*i.e.* figure 12).

3.4 RSE: Contact between C2 and C1

Description & Occurrence

Most occurrences of the C2/C1 contact involve the superposition of FA2 on FA1. The contact is invariably sharp and erosive (plate 23. A), and marked by a contrast in sorting and grain-size. The greatest contrast in grain-size is seen where clast-supported chert conglomerate facies F10 (C and D), overlie very-fine to fine-grained arenaceous sandstone (plate 23; B, C, and D). Northward within township 67, the C2 unit becomes transitional between FA2 and FA1, and the C2/C1 contact is recognized at the base of a thin (<0.20 m) conglomeratic lag within FA1 (*e.g.* 6-13-67-11W6M). Within Twp. 68 the C2/C1 contact is equivalent to the second transgressive surface of marine erosion termed TSE2 (see Section 3.5).

There are locations within the study area where the C2/C1 contact is cross-cut by channelized deposits. Wells that have recovered core from these locations, contain a continuous succession of FA4 or FA5. Well 10-30-67-11W6M contains a succession of facies characteristic of FA5. Presumably the C2/C1 contact is equivalent with an erosional contact between two facies within FA5. Core recovered from well 10-30-67-11W6M shows an interval dominated by facies of FA4. Since FA4 represents a more conformable succession, development of the C2/C1 contact in laterally equivalent regions of the study area is probably represented by an interval within FA4 rather than a facies contact. In either case, the C2/C1 contact abruptly terminate against the periphery of these channelized deposits (see figure 13).

Interpretation

Very fine-grained sandstones characteristic of FA1 overlain by conglomerate facies characteristic of FA2 suggests the contact reflects a basinward shift of facies. Disconformable superposition of upper shoreface deposits (C2) on lower shoreface deposits (C1) occurred following overall regression of the C2 shoreline contemporaneous with a relative fall of sea level. Basinward of Twp. 67, the C2/C1 contact merges with TSE2 where facies characteristic of FA1 are found above and below the contact. Coarse-grained deposits lying above the contact were deposited as winnowed storm lags within the lower shoreface, rather than wave-reworked conglomerate in the upper shoreface and foreshore. Within Twp. 68, the C2/C1 contact is therefore less disconformable than occurrences within Twp. 67.

Fluvial incision of the coastline and bypassing of sediments to the C2 shoreline likely accompanied lowering of base level during a relative fall of sea level. Where the C2/C1 contact is missing in core, the facies succession is dominated by FA4 or FA5. It is interpreted that these core are recovered from areas in which fluvial and marginal marine (*i.e.* lagoonal), systems remained active during lowstand progradation of the C2 shoreline. The C2/C1 contact is equivalent with the depositional edge of these channelized systems.

3.5 MFS/TSE2/MxFS: Contact between C3 and C2

Description & Occurrence

In most cases the C3/C2 contact is overlain by a thin (<0.15 m) shale bed. Locally, shale-rich facies are missing, and the contact is overlain by fine to very fine-grained sandstone (*e.g.* 10-12-67-10W6). Where present, the basal shale beds are typically overlain sharply by moderately sorted pebbly sandstone beds (plate 24. B, C). A second shale bed is sometimes present above the first, separated by the pebbly sandstone facies (*e.g.* 10-9-67-10W6M,). The second shale bed contrasts with the first in that it is commonly organic-rich, slightly more massive and thickly bedded. The separation between the two basal shale beds is typically not greater than 1.0 m. Interbedding between shale and pebbly sandstone beds above the C3/C2 contact is generally not observed within core recovered from Twp. 68. Instead cored intervals containing the C3/C2 contact are missing the second shale bed, and the contact can be as subtle as cm-thick shale beds or laminations (plate 24. C).

At the southernmost portion of the C3/C2 contact, there is an abrupt thickening of shale-rich beds that overlie unit C2. Southward of this area, the facies succession within unit C3 is dominated by shale-rich facies included within FA4. The underlying C2 unit is comprised of primarily conglomeratic facies belonging to FA2. Cores recovered from wells that have penetrated the contact at the margin reveal that the contact is gradational between units C2 and C3 (*e.g.* 14-4-67-12W6M, 3-17-67-12W6M). Overall shale thickness reaches up to 5.50 m (14-4-67-12W6M).

Interpretation

Initial flooding of the shoreline during deposition of the C3 unit was marked by a landward shift of facies. Deposition of the basal marine shale bed above the C2 unit took place in offshore settings. Despite its localized absence from cored intervals (*e.g.* 1-15-67-7W6M), the initial marine flooding surface (MFS) was likely present on a regional scale within the study area. Preservation of the MFS was dependant upon the degree of exposure to wave ravinement during frequent storm activity in the lower shoreface. Sediments preserved as interbedded pebbly sandstone beds were derived from the underlying C2 unit during transgressive wave ravinement. The presence or absence of heterogeneous ravinement deposits above the C3/C2 contact is also dependant upon the degree of exposure and topographic relief associated with the underlying surface. Thicker horizons of the heterogeneous pebbly sandstone facies probably reflect infilling of depositional lows associated with the transgressive surface. The contact at the top of the MFS or the base of the ravinement deposit is therefore termed the second transgressive surface of marine erosion (TSE2).

In some regions of the study area, facies overlying the C3/C2 contact have been deposited in prodeltaic settings during progradation of ebb-tidal deltas, as deduced from the organic-rich nature of the second shale and the stratigraphic position. Progradation within ebb-tidal deltaic settings began shortly after maximum transgression of the C3 shoreline. The base of the second shale is therefore termed a maximum flooding surface (MxFS). The second shale designated as a MxFS differs from the traditional conceptualization of the scale and lateral extent of such surfaces. The extent of the MxFs defined in this study is locally present in association with the development of tidal inlets and deposition of ebb-tidal deltas. Such a definition differs sharply with the traditional definition of a MxFS being basin-wide in distribution and capping the transgressive system tract (*sensu stricto*, Van Wagoner *et al.*, 1990).

Thickening of shale-rich facies belonging to FA4 is observed most commonly above conglomeratic facies within the C2 unit. The thickening of the shale is most abrupt above foreshore conglomerates, and probably reflects expansion of brackish back-barrier settings during transgression of the C3 shoreline. The C3/C2 contact does not extend southward of the main C2 trend where progradation of a barrier complex during deposition of the C3 unit initially began.

3.6 Contact between C3 and C4

Description & Occurrence

Most examples of the C4/C3 contact are expressed by sharply superposed coal beds or organic-rich shales belonging to FA5 within unit C4 (plate 21). Coal beds range in thickness from 0.25 m to 0.50 m. Where coal beds are present above the contact, roots extend vertically downward from the contact into the uppermost facies comprising unit C3 (plate 21). Unit C3 typically comprises FA3 within its uppermost interval immediately below the C4/C3 contact. Core from well 11-22-67-7W6M contains a relatively rare occurrence of the C4/C3 contact (at 2086.50 m). Facies belonging to FA3 cap the C3 unit and are sharply overlain by a 0.30 m thick pebbly shale bed containing lenticular beds of very fine-grained sandstone. This shale bed is succeeded by interbedded facies of pebbly very coarse-grained sandstone and medium-grained planar tabular cross-stratified sandstone. Both the shale bed and the heterogeneous sandstone beds are designated as facies from FA4. In this instance, the base of the shale bed represents the C4/C3 contact.

Interpretation

The C4/C3 contact formed by the superposition of back-barrier environments on the preserved C3 sequence concomitant with net progradation of the C3 shoreline. The rooted nature of the contact implies a period of sub-aerial exposure that permitted plants to take root in the backshore. Elsewhere, the contact is overlain by shale and is lacking roots, interpreted to reflect deposition of C4 in subaqueous lagoonal environments.

Lagoonal shales are locally overlain by inclined planar-tabular beds consisting of interbedded heterogenous sandstone facies, representing deposition of storm washover fans. In at least one case (6-25-68-11W6M) the contact between C4 and C3 is apparently erosive, possible due to storm surge channels that scoured portions of the C3 backshore, presumably under peak storm activity.

3.7 Stratigraphic Architecture of the Falher "C" Member

Figure 14 shows the geometry and architectural arrangement of relatively closely spaced cored intervals of the Falher "C" and "D" within a portion of the study area (see base map). The fence diagram is constructed using the same principles applied to cross-sections from Section 3.2. However, this diagram was constructed using the first coal that lies on the C4/C3 contact as a datum. The viewer's perspective is paleolandward, towards the southwest.

As described earlier, the Falher "C" overlies the Falher "D" above the basal MFS/TSE1. Wells that penetrate this contact within the study area show that fully marine facies (FA1), comprising the C1 unit, overlie interbedded organic-rich shales and sandy siltstones (FA4 or FA5), characteristic of the Falher "D" coastal distributary plain. Locally, the basal MFS/TSE1 is missing in wells (*e.g.* 10-30-67-11W6M) where channel incision and aggradation of channelized marginal marine environments has spanned the deposition of the Falher "C" Member within the study area. There are two lines of evidence that support the discrete nature of these channelized units within the Falher "C". The first line of direct evidence is in the form of recovered intervals of core, where the wholly channelized interval has been observed and described. The second line of evidence is derived from production data. Production draw-down curves derived from data available from wells 7-18-67-10W6M and 10-9-67-10W6M show that these two wells are not in communication with each other and are therefore isolated by non-reservoir facies. Presumably a laterally discontinuous, non-reservoir facies association similar to that described from well 10-30-67-11W6M is responsible for isolation of these two wells.

The stratigraphic interval of greatest reservoir potential is that of the C2 unit. The thickest trend of the C2 unit is confined to an east-west striking axis. The orientation of this axis is somewhat oblique to the overall orientation of the fence diagram. As a result, conglomeratic facies within the C2 unit deteriorate in a northwestward direction. Similarly, the C2 unit as a whole pinches-out northwestward as the upper MFS/TSE2 surface merges with the underlying RSE surface. The right-hand side of the fence diagram is therefore missing the C2 unit (figure 14). Portions of the fence diagram that contain the C2 unit (especially the end panel containing 6-8, 5-18-67-9W6M and 7-24-67-10W6M), show a stacking of conglomerate facies that prograde basinward (figure 14).

The C3 unit comprises an upward coarsening interval of progradational parasequences present throughout the study area (figure 14). The transition from marine to non-marine deposition is found between well 6-8-67-9W6M to well 5-18-67-9W6M, representing the landward extent of the Falher "C" shoreline during deposition of the C3 unit. Basinward thickening accompanies progradation of depositional cycles within the C3 unit. The C3 unit thickens to a uniform stratigraphic thickness of approximately 10 m. Internally, parasequences of C3 unit

3-D FENCE DIAGRAM OF THE FALHER “C”: stra

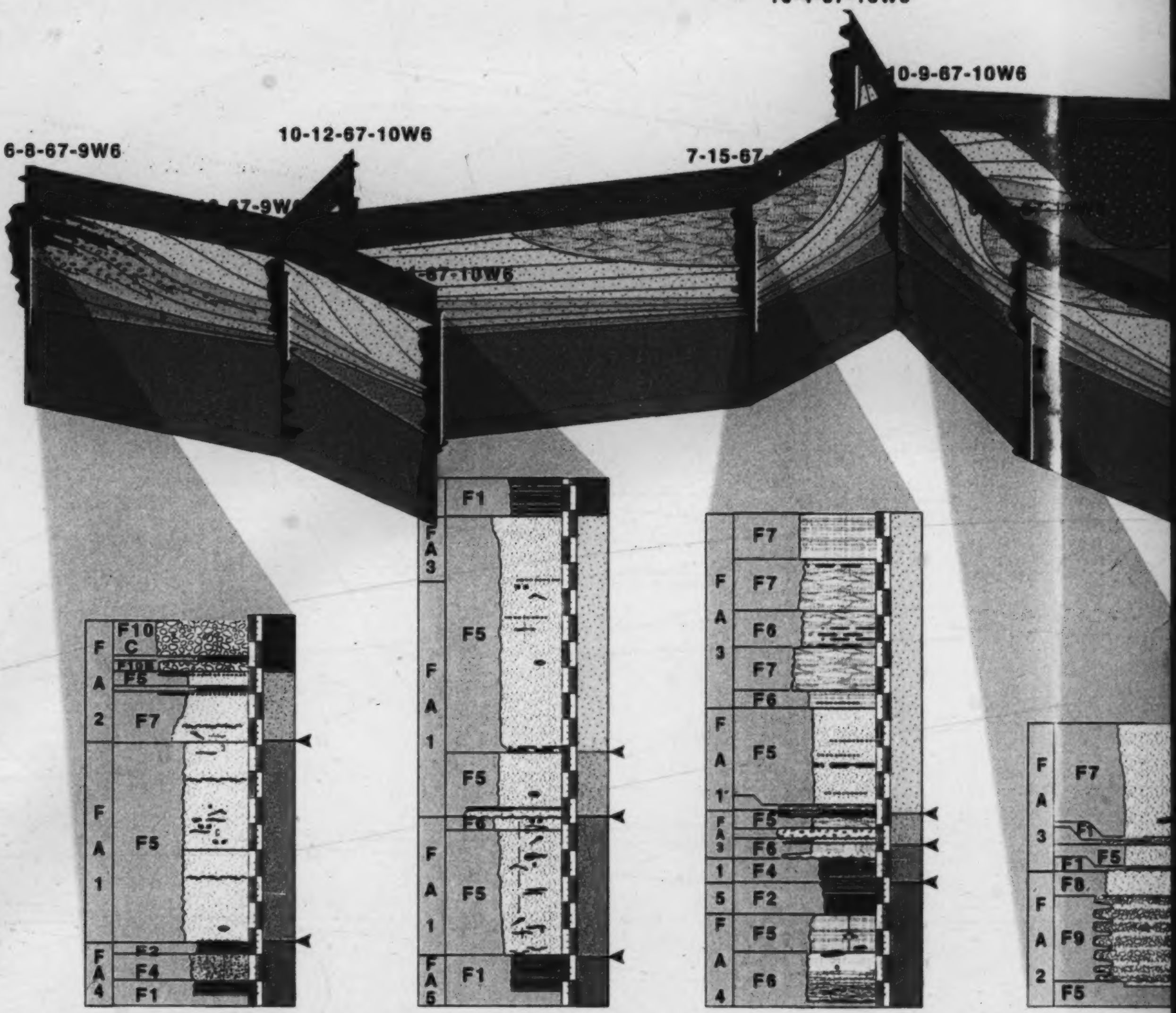

Figure 14. Fence diagram illustrating the stratal geometry of key surfaces and the internal facies architecture of the upperm
Falher “C” Member can be divided into four allomembers termed C1, C2, C3, and C4. The contact at the base of the Falher
Above TSE1, Facies Association One (FA1) is comprised primarily of facies F5 and constitutes the C1 unit. Wells penetrati
a regressive surface of marine erosion (RSE). Basinward of the main trend, the RSE becomes amalgamated with a second tr
body comprised of conglomeratic and interbedded coarse sand facies (FA2), trending ~east-west. The uppermost marine-de
Facies comprising FA3 were deposited within channelized sub-environments of tidal inlet settings and are therefore bounded
as the stratigraphic datum. Above the datum lie successions of facies that were deposited within marginal marine and non-m
representitive of the C4 unit within the study area. Periodically facies characteristic of FA4 lie above an erosional disconfor
marine inundation and subsequent infilling of fluvially incised depositional lows following repeated transgression of the Fal

": stratal geometry and facies architecture

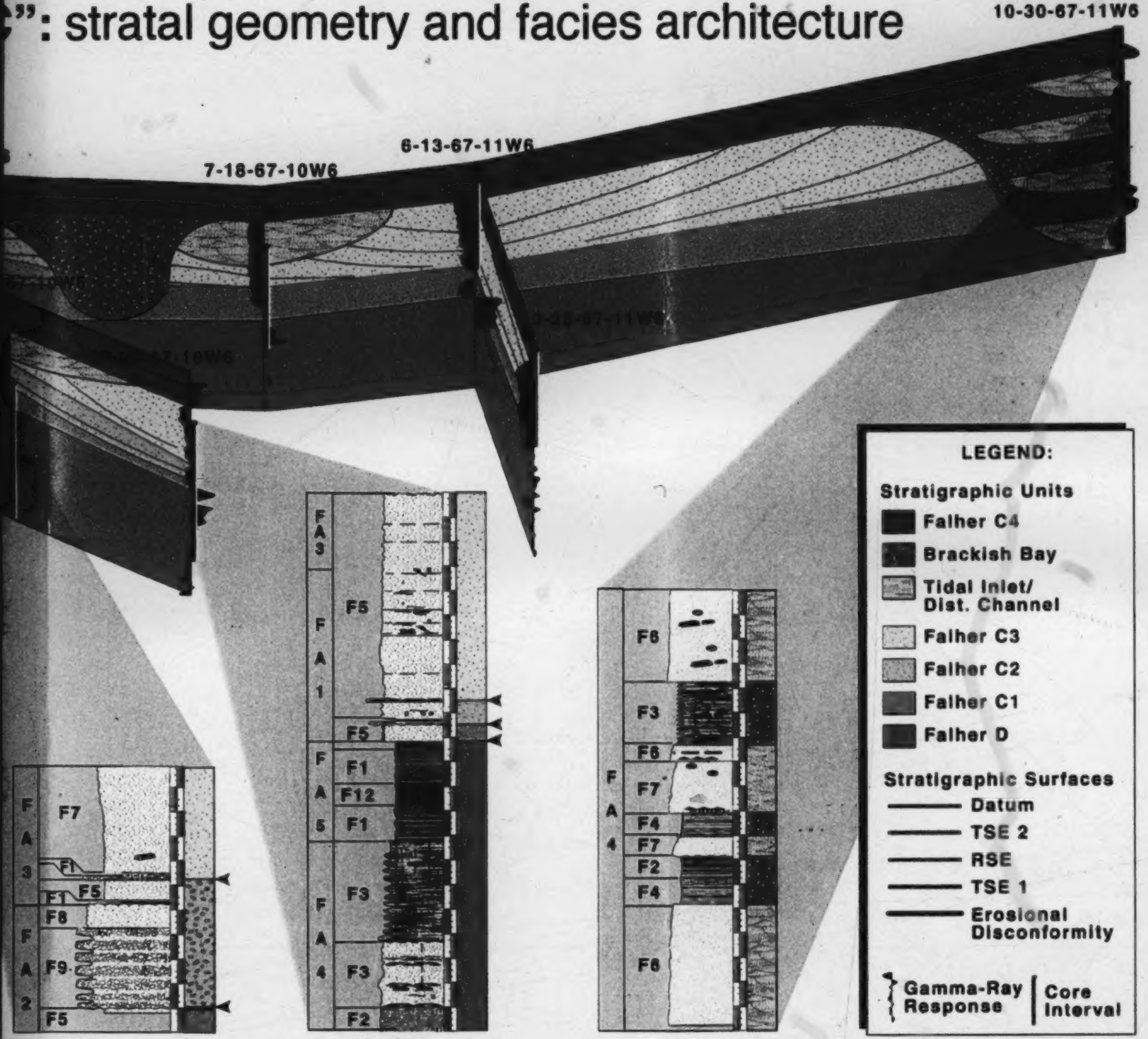

ure of the uppermost Falher "D" Member, and overlying sequence within the Falher "C" Member. Within the study area, the
se of the Falher "C" Member with the underlying Falher "D" Member is a transgressive surface of marine erosion (TSE1).
. Wells penetrating proximal regions of the main trend within township 67 show that the C1 unit is overlain by unit C2 above
with a second transgressive surface of marine erosion termed TSE2. The C2 unit is largely restricted to a lensoid stratigraphic
rmost marine-deposited succession within the Falher "C" Member is comprised of both FA1 and Facies Association Three (FA3).
erefore bounded by a localized erosional disconformity within the C3 unit. The overlying contact above the C3 unit is designated
arine and non-marine environments of deposition. Facies Association Four (FA4), and Facies Association Five (FA5) are
sional disconformity that cross-cuts the regional Falher "C" sequence. These facies are interpreted to have been deposited during
ssion of the Falher "C" shoreline. The long axis of the fence trends ~SE-NW.

are laterally equivalent with tidal inlet channels (*e.g.* 7-15-67-10W6M). These channels are laterally restricted, discrete elements of the overall stratigraphic framework (figure 14). The C4 unit overlies the C3 unit and encompasses marginal marine and coastal disributary plain deposits not unlike those interpreted from the uppermost Falher "D" Member (figure 14).

Internal stratigraphic relationships observed within the C3 Unit.

The C3 Unit represents a stratigraphic sequence that was deposited during long-term progradation of a barrier island complex (see Chapter 4, Section 4.4). Cored intervals recovered from separate portions of the C3 Unit reveal that two distinctive end-member facies successions were deposited contemporaneously with shoreface progradation and tidal inlet migration. These intervals are therefore genetically linked through the internal dynamics governing barrier-island progradation, and stratigraphic equivalence between the two intervals can be demonstrated through consideration of the paleogeographic context in which each succession is interpreted to have been deposited. Figure 15 shows a paleogeographic reconstruction of a migrating tidal inlet and barrier-bar complex (adopted from Saunders, 1989). It has been shown (Chapter 2, Section 2.5), that the C3 Unit contained in core recovered from 7-15-67-11W6M is representative of a fining upward succession of facies deposited during the lateral migration of a tidal inlet and the adjacent spit-platform. A blue star denotes the presumed paleogeographic location of that succession (figure 15).

In contrast, core recovered from 6-13-67-11W6M represents a coarsening upward succession of facies produced by progradation of the upper shoreface and foreshore environments, located on the seaward facing portion of the fore-barrier (red star, figure 15). The stratigraphic framework preserved between the two end-member successions is illustrated by figure 15. Moving laterally away from the inlet environment (blue star) to the main prograding shoreface portion of the barrier-bar (red star) a basinward thinning of fining upward channel facies and corresponding thickening of coarsening upward upper shoreface facies (figure 15) is depicted. An additional element of the stratigraphic framework preserved between the two end-members is interbedded coarse and fine-grained facies interpreted as ebb-tidal delta deposits. Sediments comprising these facies likely originate from the back-barrier and channel bottom. This material was carried basinward by ebb-orriented currents and deposited shortly after emergence from the seaward inlet mouth. There it was subsequently reworked by longshore currents and incident wave activity. Shoreface progradation incorporated material initially deposited by ebb-tidal deltas as finest-grained interval of the coarsening upward succession within 6-13-67-11W6M (figure 15).

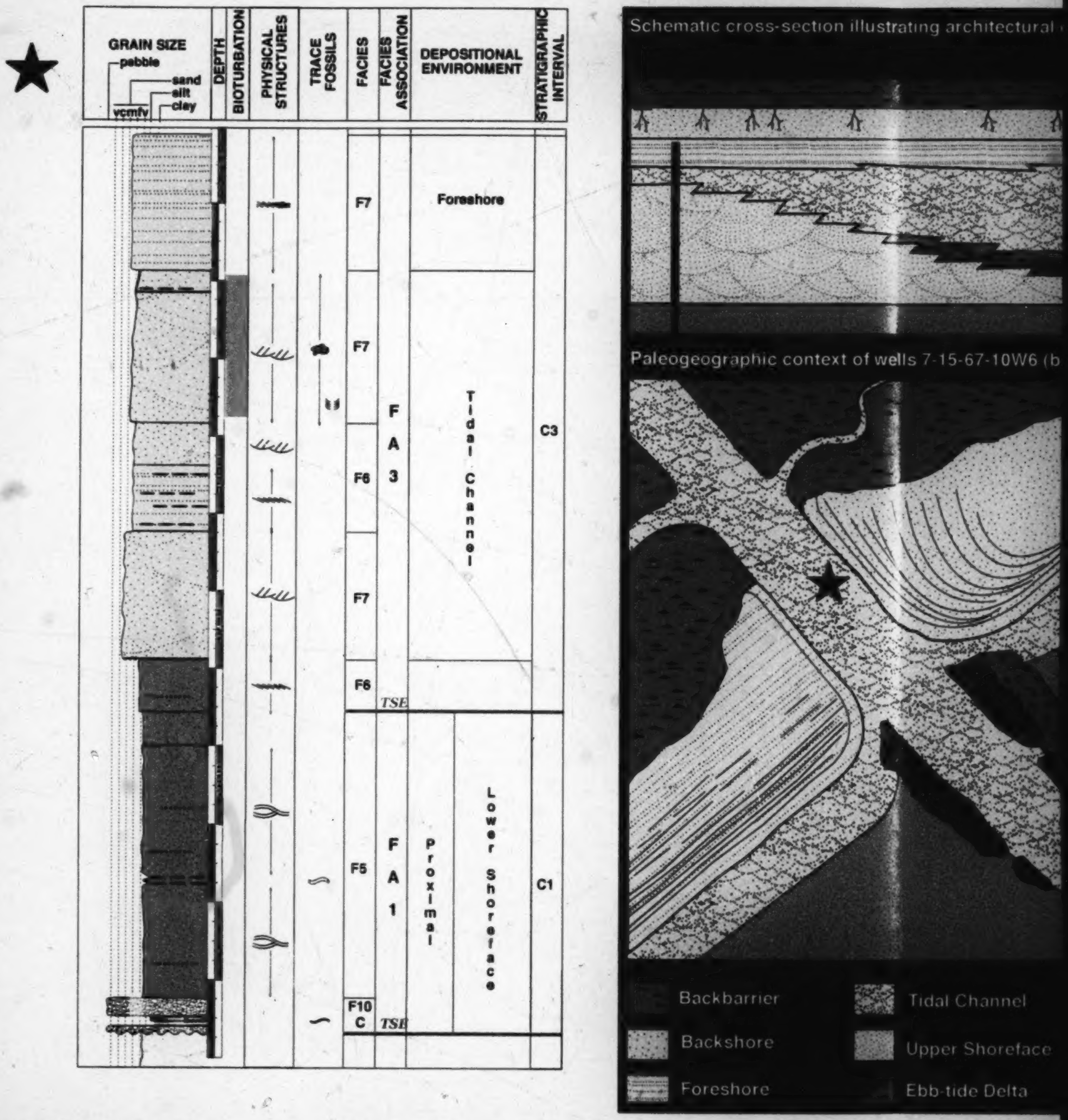

Figure 15. Conceptualization of the paleogeographic context for vertical facies successions observed within the Falher of the barrier complex produces a distinctive cross-sectional framework between two end-member intervals. Core recov deposited within the main tidal channel. Contemporaneous lateral inlet migration and progradation of upper shoreface a 6-13-67-11W6M (red star).

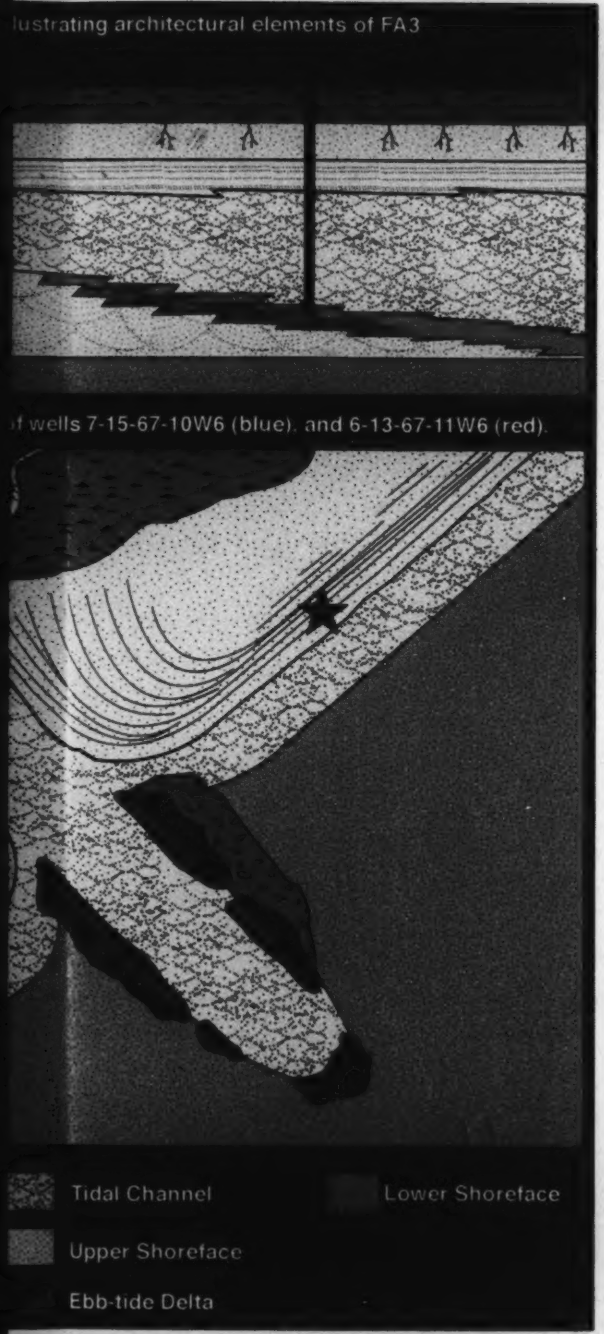
lustrating architectural elements of FA3
f wells 7-15-67-10W6 (blue), and 6-13-67-11W6 (red).
Tidal Channel
Lower Shoreface
Upper Shoreface
Ebb-tide Delta

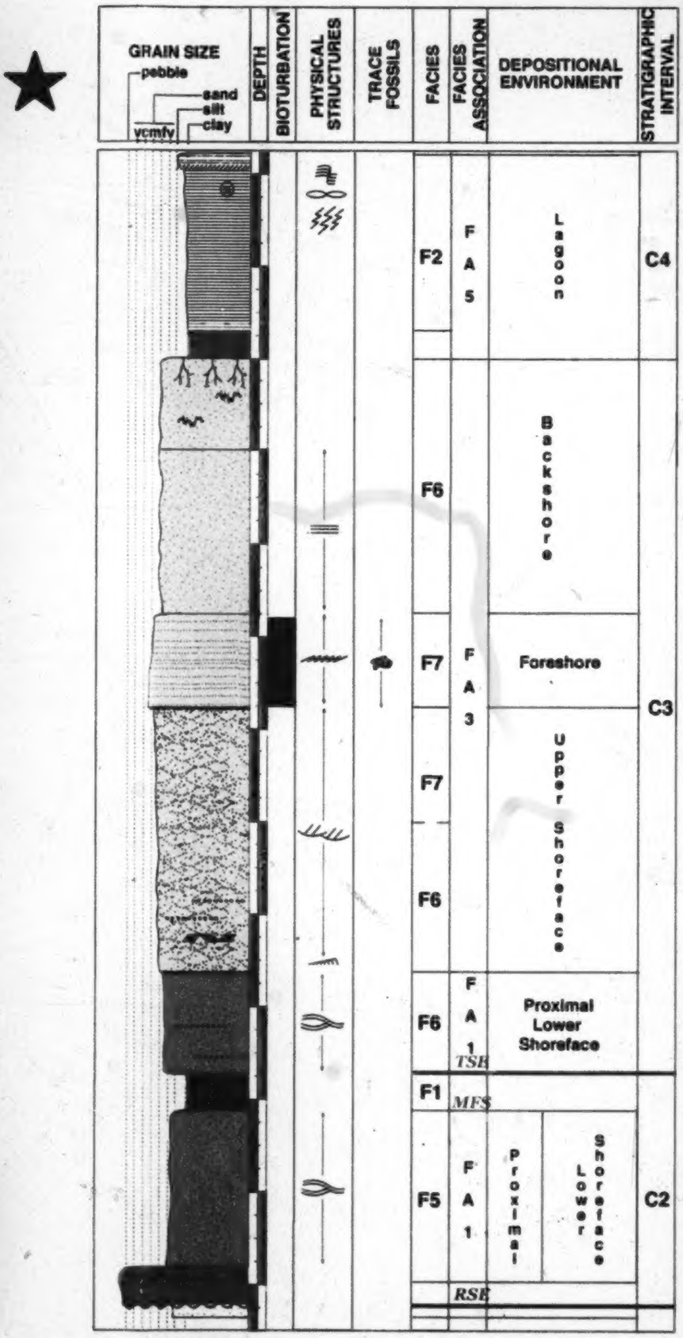

rved within the Falher C3 unit (adapted from Saunders, 1994). Lateral inlet migration coupled with net progradation
intervals. Core recovered from well 7-15-67-11W6M (blue star), contains a fining upward sequence of facies
n of upper shoreface and foreshore fore-barrier environments likely deposited the sequence described from well

Plate 22. Varying expression of basal transgressive surface of erosion (TSE1) separating the Falher "C" from the Underlying Falher "D" Member in core: (**A**) Terrestrial coal successively overlain by a marine flooding shale and very fine-grained planar laminated sandstone. Contact between shale and coal is interpreted as a marine flooding surface (10-16-67-8W6, 2252.35 m); (**B**) Razor-sharp erosional contact between terestrial coal and basal granular lag deposit. Muddy laminations above lag deposit were likely deposited during maximum transgression. Ensuing shoreface progradation deposited very fine-grained hummocky cross-stratified sandstone (6-8-67-9W6, 2399.70 m); (**C**) *Glossifungities* surface demarcated by large *Thalassinoides* burrows infilled with very fine-grained sandstone of the offshore transition. Fine-grained sand infilling burrows contrasts sharply with estuarine mudstone and shaly siltstone (1-11-67-12W6, 2563.15 m); (**D**) Conglomeratic lag deposited during transgressive wave ravinement. Lag is overlain by a maximum transgressive flooding shale (6-21-67-10W6, 2458.75 m).

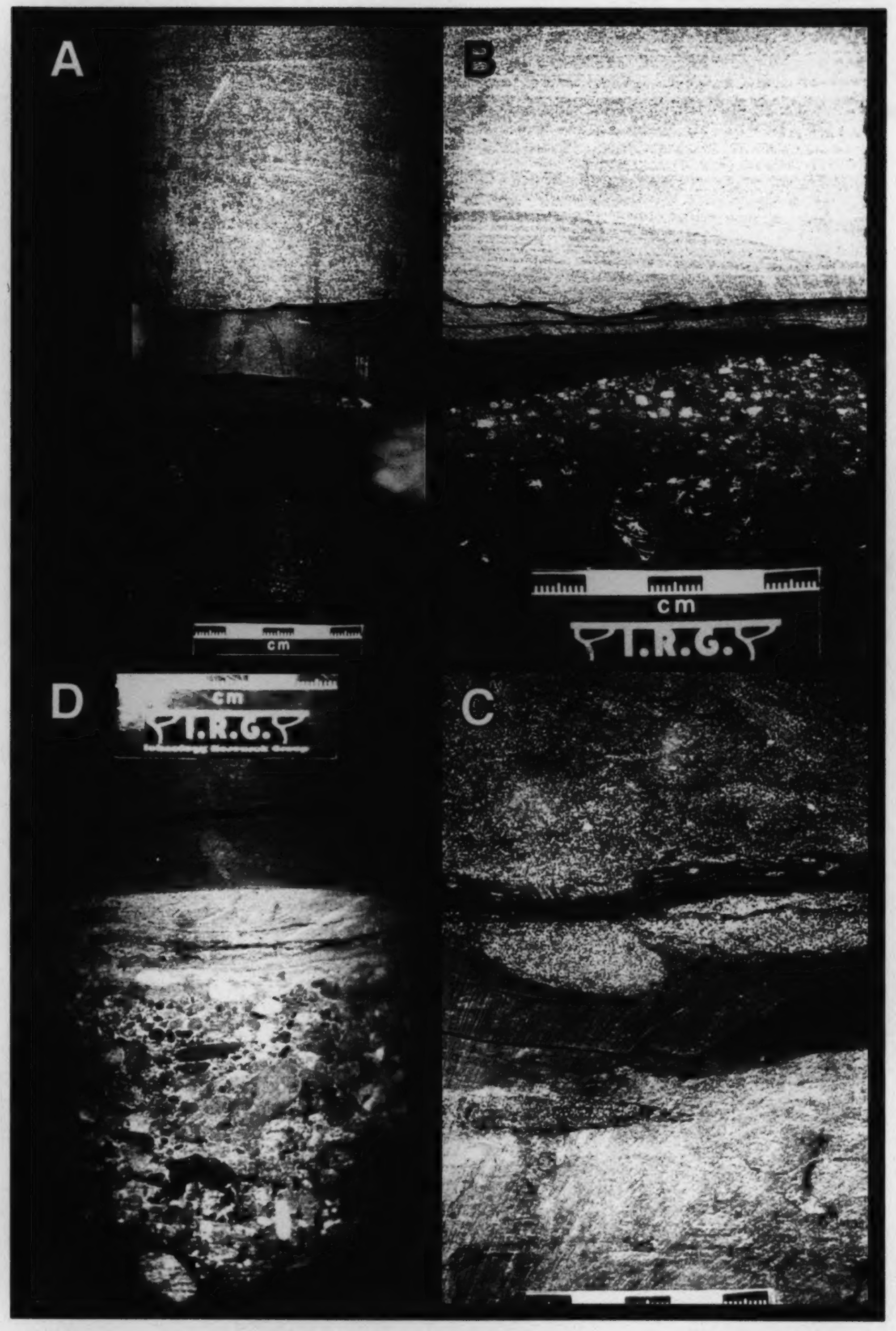
A
B
cm
I.R.G.
cm
D
cm
I.R.G.
C

Plate 23. Sharp, erosive regressive surface of erosion (RSE): (**A**) Pebbly very coarse-grained sandstone disconformably overlying very fine-grained sandstone. Contact is interpreted to have formed during basinward shift of facies associated with forced regression (10-12-67-10W6, 2482.70 m); (**B**, **C**) Polymodal chert conglomerate deposited within the upper shoreface lies disconformably above lower shoreface fine-grained sandstone (6-13-67-11W6, 2451.54 m; 9-11-67-12W6, 2550.20 m); (**D**) Clast supported chert conglomerate overlying horizontal planar laminated very fine grained sandstone. Contact between the two distinct lithologies is interpreted as a regressive surface of marine erosion that formed during a forced regression (12-3-67-12W6, 2617.75 m).

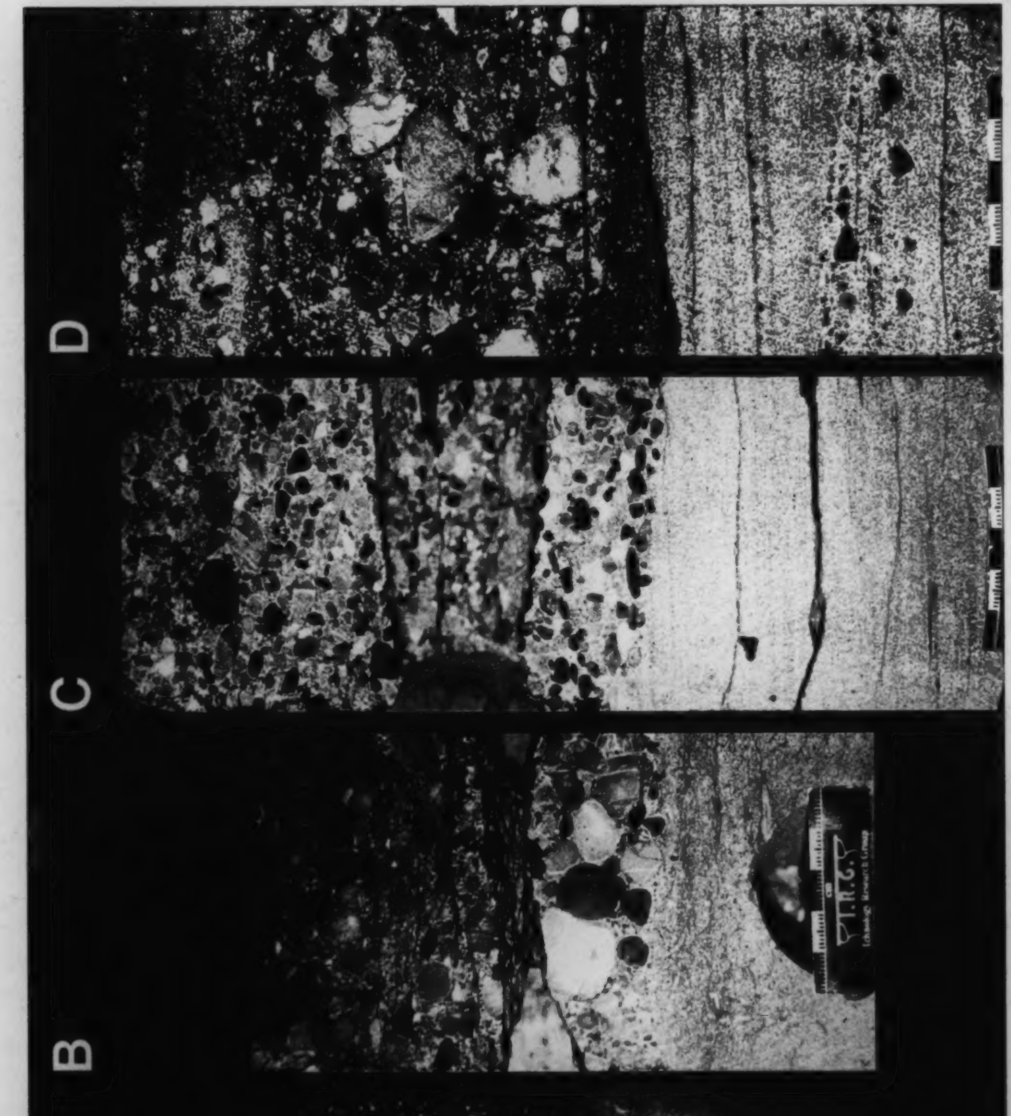
A
B
C
D
cm
T.R.G.
Ichnology Research Group

Plate 24. Second transgressive surface of erosion (TSE2): (**A**) Transgressive fine-grained sandstone lenticles and carbonaceous laminae overlying lagoonal mudstone (11-8-67-11W6, 2505.05 m); (**B**) Marine transgressive flooding shale sandwiched between very coarse-grained foreshore sandstone and planar laminated fine-grained progradational sandstone (10-29-67-10W6, 2396.00 m); (**C**) Granular medium-grained upper shoreface sandstone lying disconformably upon sharply erosive transgressive surface of marine erosion (7-18-67-10W6, 2441.83 m); (**D**) Evidence of marine flooding within the backbarrier environment. Submerged foreshore conglomerate partially reworked during transgression (14-4-67-12W6, 2678.85 m).

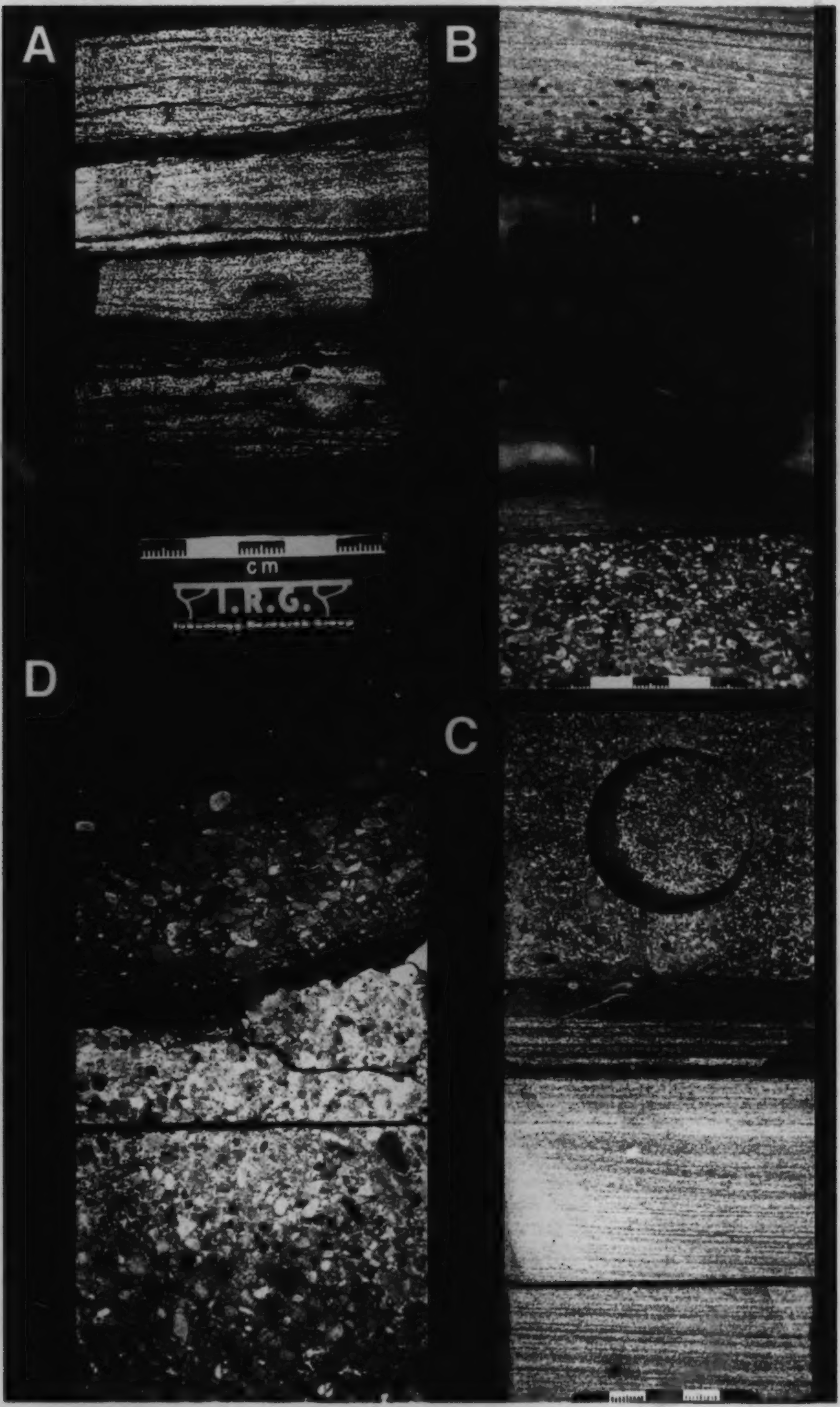
A
B
cm
I.R.G.
D
C

CHAPTER FOUR: Four Stage Depositional Model of the Falher "C" Member

4.1 Introduction

In this Chapter, a four stage depositional model is proposed for the Falher "C" Member sequence. Each stage of the model shows the inferred distribution of facies association and stratigraphic surfaces proposed in the previous two chapters. The relative influence of rate of sea level change, and sediment supply on the evolutionary relationships between marine, marginal marine and non-marine depositional environments is also described. Some other factors driving coastal evolutionary change that are addressed include: incident wave energy, antecedent topography, and the magnitude of the tidal prism.

The four stages of the model coincide with deposition of the previously described depositional units ~~of the~~ Falher "C" Member. In brief, Stage One of the model involves initial transgression of the Falher "D" coastal plain as relative sea level rise outpaced sediment supply to the C1 shoreline. A relative fall of sea level following maximum transgression of the C1 shoreline initiated a forced regression and subsequent deposition of conglomeratic shorefaces in Stage Two. Transgressive recovery from relative lowstand conditions and development of barred brackish embayments was initiated during Stage Three contemporaneous with a rapid rise in sea level. Stage Four is characterized by normal regression of the C4 shoreline during relative stillstand in sea level and abundant fluvial supply to the eastern portion of the study area.

Normal vs. Forced Regression

Basinward movement of any shoreline system can be defined as a normal regression or a forced regression (Posamentier & Allen, 1999). A normal regression occurs as a result of basinward progradation of the shoreline as sediments progressively infill available accommodation space. Therefore a normal regression can only occur if the rate of sediment accumulation exceeds the rate at which new accommodation space is created. A normal regression could conceivably characterize shoreline complexes deposited during a relative rise, fall or stillstand of sea level (figure 16). In contrast to a normal regression, a forced regression only occurs during a relative fall of sea level (figure 16). As well, forced regressions can occur even with minimal sediment supply to the shoreline and are more prone to creating surfaces rather than depositing sedimentary sequences.

First formally proposed by Posamentier *et al.* (1992), the forced regression inevitably involves some degree of subaerial (fluvial), and submarine erosion. Forced regressions occur

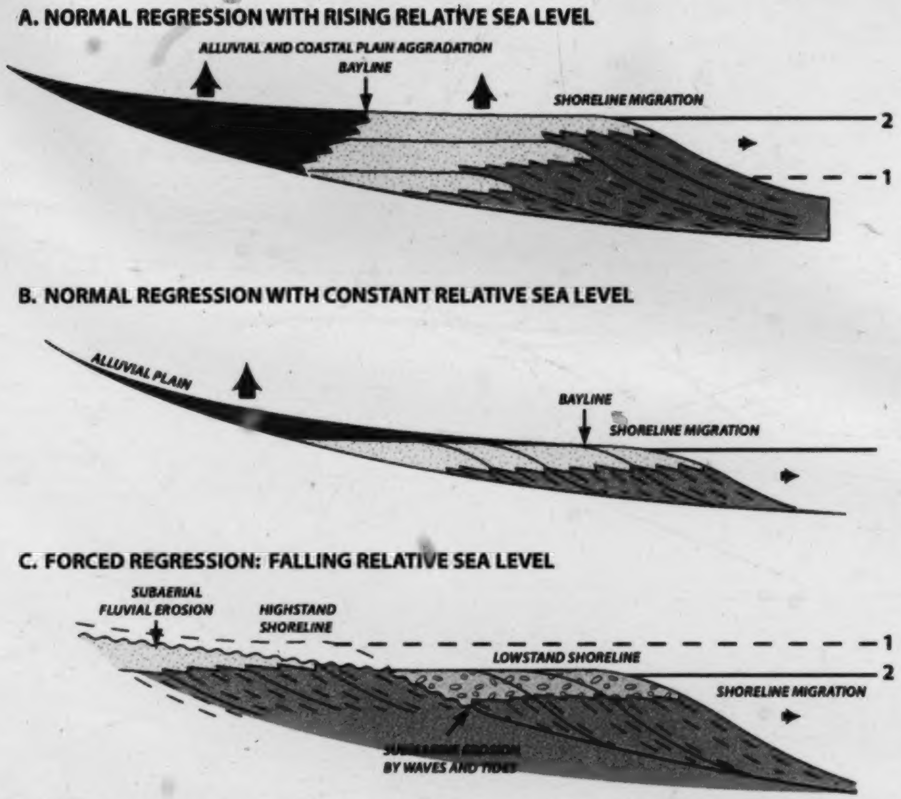

A. NORMAL REGRESSION WITH RISING RELATIVE SEA LEVEL

B. NORMAL REGRESSION WITH CONSTANT RELATIVE SEA LEVEL

C. FORCED REGRESSION: FALLING RELATIVE SEA LEVEL

SUBAERIAL FLUVIAL EROSION
HIGHSTAND SHORELINE
1
LOWSTAND SHORELINE
2
SHORELINE MIGRATION
SUBMARINE EROSION BY WAVES AND TIDES

Figure 16. Normal *vs*. forced regressions (Posamentier *et al.*, 1992). Normal regressions (A, B) occur when the rate of sediment supply exceeds the rate at which accomodation space is created during a rise or constant RSL. Forced regressions occur during a fall of RSL (C). A significant portion of the underlying sequence is removed by subaerial or marine erosion as a result.

during a relative fall in sea level where base level has fallen, and overall accommodation space has diminished. Therefore sediments deposited below base level, subsequent to relative sea level fall are displaced basinward and deposited disconformably over previously deposited sediments in an effort to infill available accommodation space.

Whether a regression occurs in a normal or forced fashion has profound implications on the resultant architecture of the stratal units deposited. Within the Falher "C", an example of the disconformable contact created between sediments deposited before and after a forced regression is the C2/C1 contact. The contact can be traced laterally basinward where it becomes progressively less disconformable. The surface eventually merges with a correlative conformity, presumably within a portion of the study area where the erosional or depositional hiatus has been minimal during deposition of unit C2. One important point to address is that a forced regression is a relatively rapid, surface generating *event* rather than a longer term, progradational *process*. Following a relative sea level fall associated with a forced regression, progradation of shoreline deposits (*i.e.* regression), resumes in a normal fashion once sea level has stabilized at lowstand (figure 16). If there is insufficient sediment supply to the coastline, net erosion would likely occur above base level (wave base), and a greater erosional hiatus would be represented by the resulting unconformity or regressive surface of marine erosion.

4.2 Stage I: Relative rise of sea level and initial transgression of the Falher "C" shoreline

Prior to transgression of the Falher "C" shoreline, the Falher "D" shoreline lay northward of Twp. 73 (Casas, 1997). Within the study area, the depositional setting was characterized by the development of brackish to non-marine conditions (Arnott, 1993; Casas & Walker, 1997). In general, the study area was undergoing fluvial aggradation and expansion of the coastal plain. Well-developed distributary channels were the main agents of sedimentary bypass acting as the main suppliers of sediment to prograding Falher "D" shorelines under overall stillstand conditions of relative sea level (RSL).

A relative rise in sea level initiated southward transgression of the Falher "C" shoreline following maximum progradation of the Falher "D" Member. Inundation of fluvial-dominated localities resulted in expansion of marginal marine brackish bays as shown in figure 17. Maximum landward extent of the shoreline during deposition of the C1 unit was restricted to an east-west trending axis at about the same latitude as the Twp. 66-67 gridline (figure 17). Punctuations of this trend at fluvial point sources is probable, and provided a steady supply of fine-grained material. Sediment was also supplied from basinward areas where coarse-grained shoreface material had been drowned following the relative rise in sea level. Net onshore movement and ravinement of this material is evident basinward of the study area where Casas & Walker (1997) observed "…about 6 m of interbedded sandstones, conglomerates and mudstones". From this description, Casas & Walker (1997) suggest that "…three TSEs can be correlated across Twp. 69-73." Such an interpretation is likely overcomplicated as these deposits may be more parsimoniously interpreted as ravinement deposits associated with reworking and winnowing of coarse grained deposits within the Falher "D" during a single transgression. Within the study area, only one basal surface is equated with initial transgression of the Falher "C" shoreline and has been termed MFS/TSE1 (Chapter 3, Section 3.3).

Maximum transgression likely occurred in concert with stabilization of sea level at a stillstand. Abundant accommodation space created during transgression and a consistent sediment supply resulted in normal regression of the Falher "C" shoreline during deposition of the C1 unit. Progradation of the C1 shoreline complex is evidenced through partial preservation of lower shoreface and offshore transition within Twp. 67 and 68. It is not clear how upper shoreface and foreshore settings responded to continued coastal progradation during deposition of the C1 unit. It is postulated that removal of the upper portion of the C1 unit accompanied subsequent relative fall in sea level during deposition of the C2 unit. The progradational extent of the C1 shoreline complex extended at least as far as the latitude where unit C2 is superposed on the C1 unit (figure 17).

STAGE 1: Initial transgression of the Falher “C” line following a relative rise of sea level

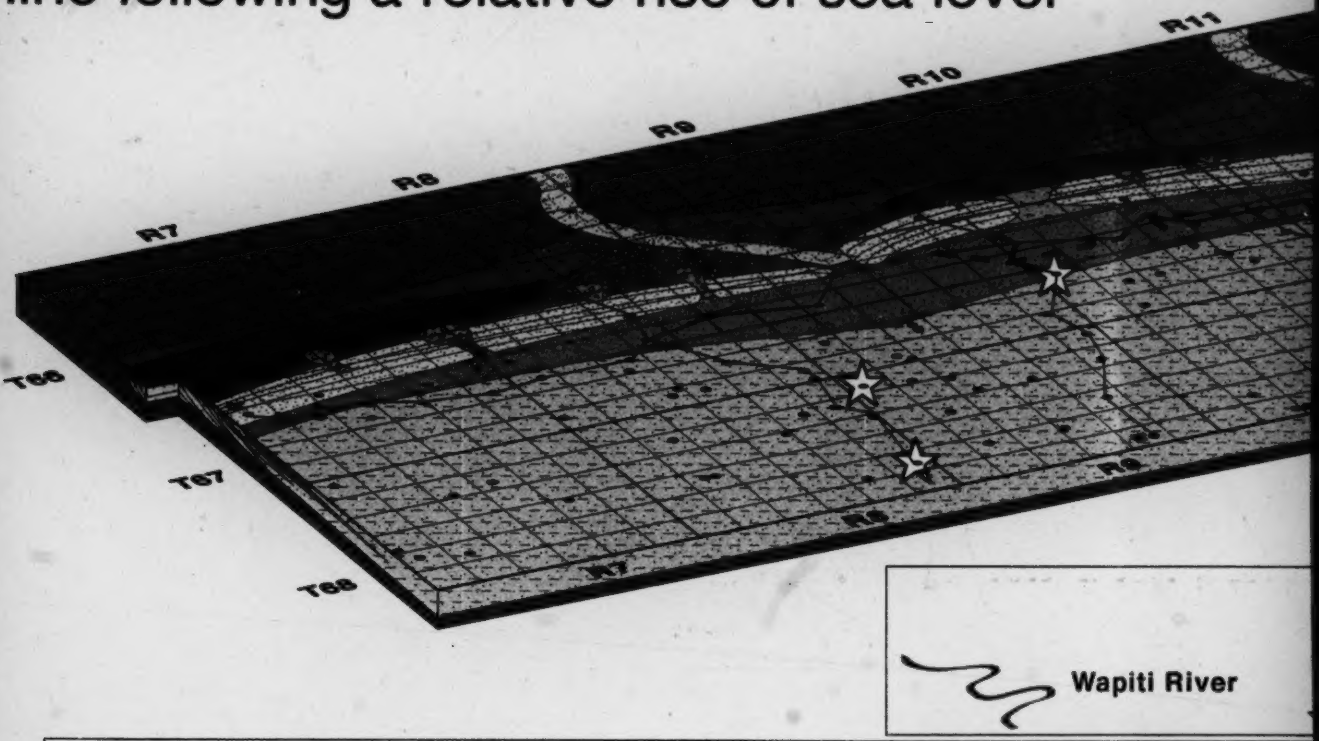

PALEOGEOGRAPHIC LE

TERRESTRIAL

■ **lacustrine deposits**
■ **terrestrial deposits**
■ **upper delta plain**
■ **marsh**
■ **backshore dunes**
▨ **channel sands**

MARGINAL MARIN

■ **lagoonal deposits**
▨ **storm washover sands**
■ **brackish bay**

Figure 17. Paleogeographic reconstruction of the Falher “C” shoreline following initial transgression and subsequer Falher “D” coastal plain coincides with the termination of the basal transgressive surface of marine erosion (TSE1, sh Marine inundation of fluvial valleys and expansion of brackish back-barrier lagoon and estuarine environments occure capping C1 shoreface and lagoonal deposits is speculative, due to subsequent removal of the uppermost portion of the fence diagram featured in Section 3.7 of Chapter 3 (Figure 14, page 101). Line of sight is to the southwest or paleola

ner “C” shore-

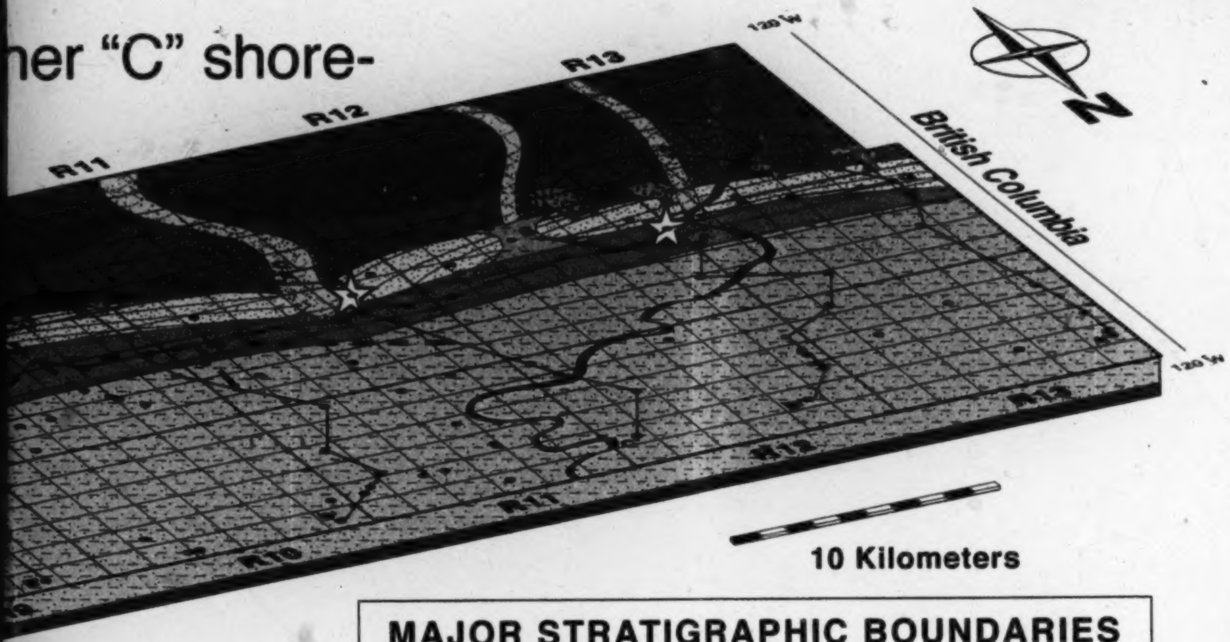

MAJOR STRATIGRAPHIC BOUNDARIES

— T2 surface — RSE — T1 surface

MAP FEATURES

piti River

- No core recovered
- Core recovered
- ☆ Interval Photographed

Z Z' Cross-section Reference

Fence Diagram

RAPHIC LEGEND

RGINAL MARINE

sits

er sands

▨ tidal inlet

▨ channel sands

MARINE

▨ C1 shoreface

▨ transition

▨ C2 shoreface

▨ offshore

▨ C3 shoreface

▨ channel sands

ssion and subsequent progradation of the C1 unit. Maximum landward extent of transgression over the
e erosion (TSE1, shown in red), at the approximate lattitude of the gridline between townships 66 and 67.
nvironments occured in conjunction with initial transgression. The sporadic occurrence of washover sands
rmost portion of the C1 unit during stage 2 (figure 18). Section lines highlight wells contained within the
outhwest or paleolandward.

4.3 Stage II: Increase in sediment supply following a forced regression

Figure 18 shows a reconstruction of the Falher "C" shoreline immediately following a forced regression associated with a relative fall of sea level. The most conspicuous aspect regarding stage two is the rejuvenation and incision of fluvial systems within the marginal marine realm (figure 18) in connection with base level fall. Locations that were previously characterized by brackish conditions and estuarine deposition became areas of sedimentary bypass. The upper portions of the shoreface and foreshore deposited during C1 deposition were subaerially exposed, and subjected to eolian processes and erosion. This lead to the development of an unconformity landward of the Falher "C" shoreline during deposition of unit C2. Continued fluvial aggradation within non-marine areas lead to the ponding of sediments and the development of lacustrine deposits within topographic lows once occupied by lagoonal environments (figure 18).

Relative fall of sea level also impacted fully marine settings during deposition of the Falher C2 unit. The fall of base level and fair-weather wave base initiated a significant basinward shift of facies. Settings once characterized by distal upper shoreface deposition were replaced by wave dominated proximal upper shoreface and foreshore deposition (figure 18). This basinward shift of facies was likely accompanied by erosional bevelling above wave base and emplacement of upper shoreface and foreshore deposits characteristic of C2 unit, disconformably above lower shoreface deposits of the C1 unit. Basinward of Twp. 67 the C2/C1 contact is inferred to be more conformable due to the superposition of comparable facies of the distal lower shoreface. Progradation of the upper shoreface and foreshore settings took place in cyclical manner in response to seasonal variation in hydrodynamic processes controlling net erosion and net deposition. Figure 19 shows the long-term progradational response of the shoreline to seasonal alteration between a non-barred (summer months) and a barred state (winter months) as theorized by Hunter *et al.* (1979). During the summer months, deposits representing the previous winter's bar were reworked and deposited within the upper shoreface and foreshore, resulting in net progradation of the shoreline. The progradational deposit was therefore primarily composed of shoreface and foreshore facies deposited in the summer months, separated by oblique winter erosion surfaces (shown in red) that converge tangentially with a basal disconformity (figure 18).

Longshore variations in sediment characteristics can be attributed to both source area effects and hydraulic factors. The development of fan deltas as a result of the debouching of coarse-grained sediments at point sources along the C2 shoreline produced a more protuberated coastline (figure 18). Localized intensification of geostrophic currents resulted in response to increased angles of wave incidence in and around deltaic systems. Sections of the C2 shoreline laterally adjacent to deltaic systems were characterized by weakened longshore currents because shorelines recurved into an orientation normal to wave approach. Weakening of longshore drift

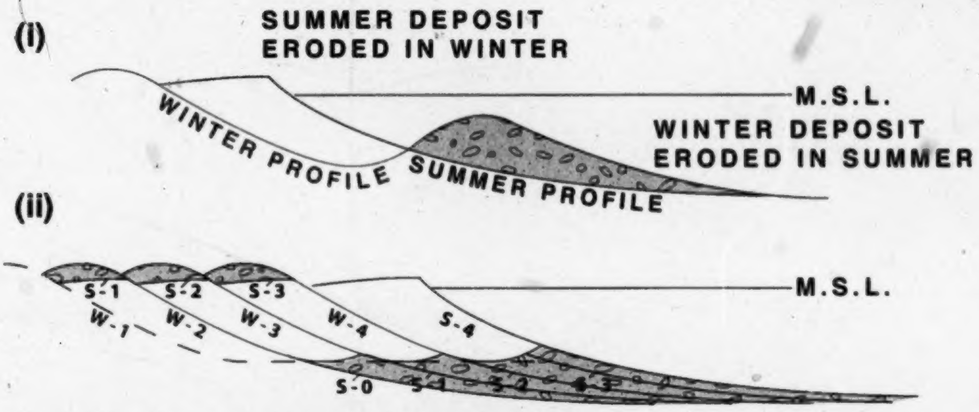

Figure 19. (i) Diagramatic cross-section of the shoreface and nearshore system showing the erosional profile created during the winter season when the system was barred. (ii) Deposit types and erosional disconformities formed over a four season winter(W)/summer(S) cycle as inferred by Hunter *et al.* (1979).

away from fluvial point sources in this manner would also have influenced grain size distributions and sorting characteristics, and hence the shoreline profile. Kirk (1980) demonstrated that zones of greatest grain size coincide with the apices of major fan delta complexes and that there is a corresponding fining of grain size away from major sediment sources (*i.e.* river mouths). With regard to grain-size sorting, McLearen (1979) proposed that sediments become better sorted in the direction of transport. In a subsequent study it was shown that sediments become finer and more negatively skewed at progressively greater distances from their source (McLaren & Bowles, 1985). Based on the above data, it is inferred that during deposition of the C2 unit, regions of the shoreline proximal to major river mouths could be characterized as poorly sorted, coarse-grained reflective shoreface deposits as observed in wells: 10-16-67-8W6M, 11-8-67-11W6M, 10-9-67-10W6M, and 14-4-67-12W6M. In contrast, regions located far from fluvial point sources could be expressed as the finer-grained, better sorted and dissipative shoreface deposits observed within wells: 1-15-67-67-7W6M, 11-22-67-7W6M, 6-13-67-11W6M, and 11-7-68-12W6M.

Along coastlines experiencing rapid depositional regressions, paleowater depth can be inferred from the stratigraphic thickness of a sequence as suggested by Heward (1981). It has been proposed that in coastal settings subject to deltaic progradation immediately subsequent to a regression, the thickness of the nearshore sequence approximates water depth provided several constraints are considered (Klein, 1974; Harms, 1975). These constraints include (among others) clay compaction and rate of subsidence. Accelerated rates of compaction of deposited fines and high rates of subsidence could lead to underestimation of paleowater depth. An assumption of negligible compaction of fines within the depositional sequences of this study is reasonable, because such deposits are absent from the C2 interval. Furthermore, it is unlikely that significant subsidence took place because a large portion of the C1 shoreline had been stripped of its depositional sequence. In other words, subsidence rates within the study area had likely dramatically diminished following erosional unroofing and unweighting of the shoreline before initiation of progradation.

Within the study area, the most accurate estimate of paleowater depths can be obtained from reflective regions of the paleoshoreline, proximal to fluvial point sources where fan-delta progradation is interpreted to have taken place (figure 18). Well 10-9-67-10W6 contains core that has been recovered from such a region. Prior to progradation of the C2 unit, available accommodation space was created by submarine erosion concomitant with the forced regressive stage. Then as sea level reached a relative lowstand, progradation of highly reflective, coarse-grained gilbert-type deltaic deposits likely infilled available accommodation space. Therefore the paleowater depth at the time of C2 progradation is equivalent to the thickness between the RSE (2361.00 m), and the top of the foreshore zone (2356.75 m) within 10-9-67-10W6, or approximately 5 m.

STAGE 2: Increase in sediment supply followi forced regression

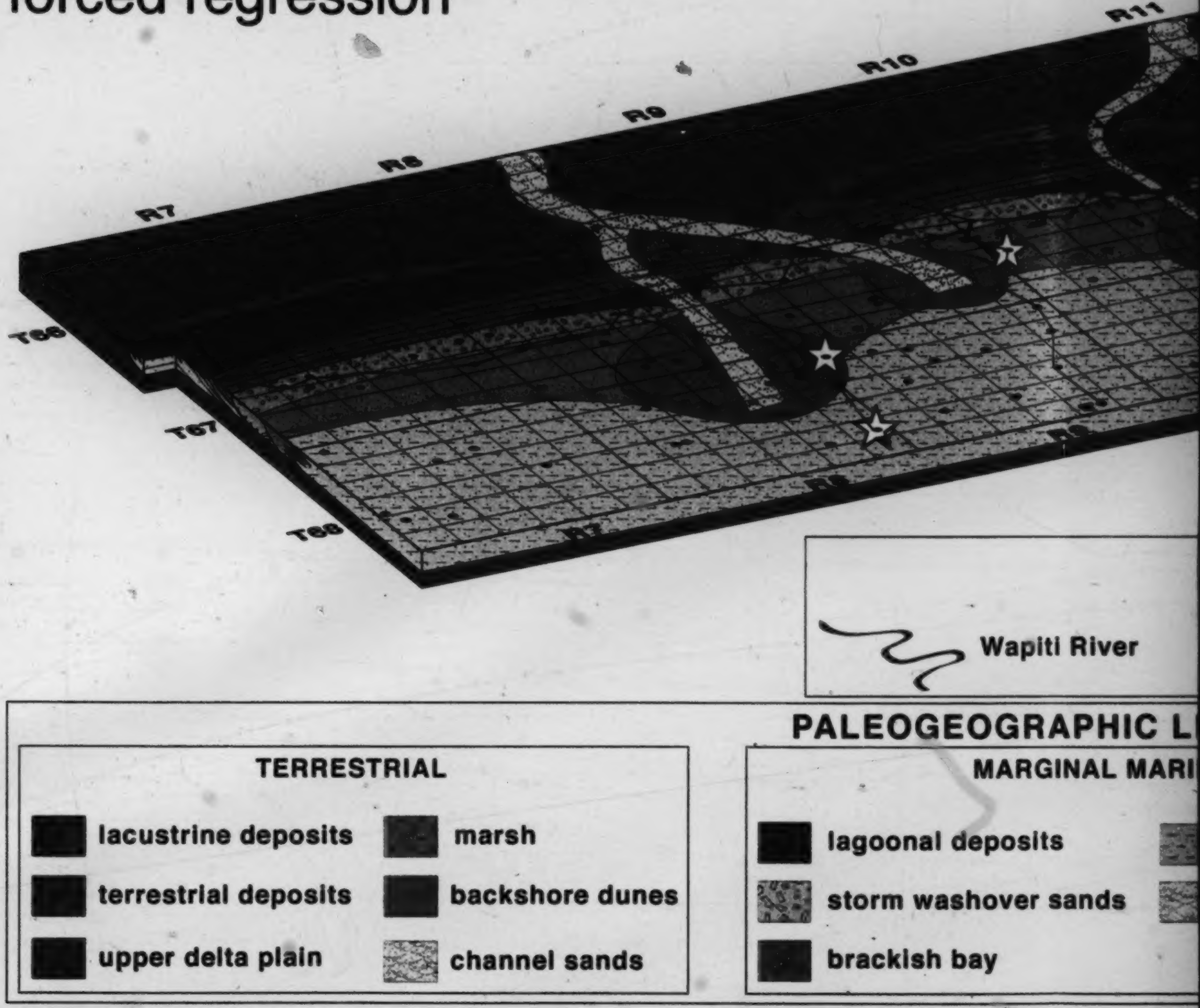

Figure 18. Paleogeographic reconstruction of the Falher “C” shoreline following forced regression and a subseque lowering of base level and fluvial incision of C1 shoreface and marginal marine deposits. Depositional lows within influence, and evolved into lacustrine depo-centres while adjacent C1 barrier crests were partially reworked by subae conglomerate shoreface deposits disconformably above the C1 unit occurred during deposition of the C2 unit. The c purple). Much of the coarse-grained material incorporated into the C2 shoreface deposits were initially sourced from featured in Section 3.7 of Chapter 3 (figure 14, page 101) are also shown. Line of sight is to the southwest or paleol

following a

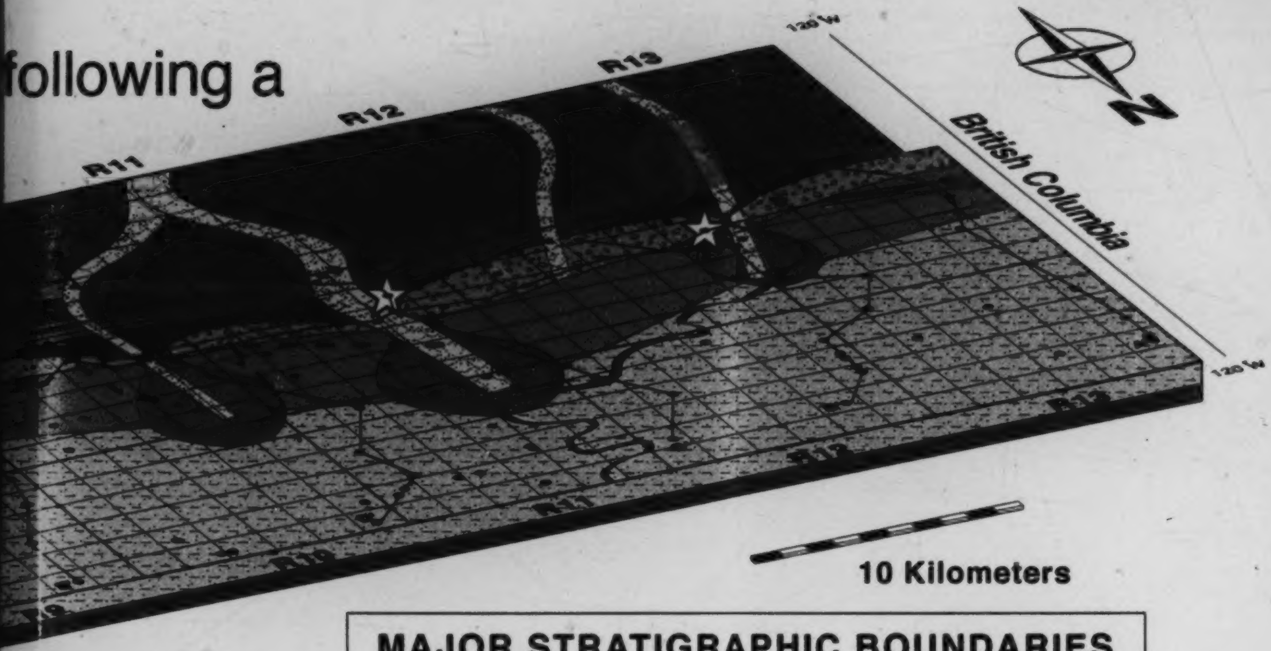

MAJOR STRATIGRAPHIC BOUNDARIES

— T2 surface — RSE — T1 surface

MAP FEATURES

iti River

- No core recovered
- Core recovered
- ☆ Interval Photographed

Z–Z' Cross-section Reference

Fence Diagram

RAPHIC LEGEND

RGINAL MARINE

its

r sands

▨ tidal inlet

▨ channel sands

MARINE

▨	C1 shoreface	■	transition
▨	C2 shoreface	▨	offshore
▨	C3 shoreface	▨	channel sands

and a subsequent subaerial and submarine erosion. Relative fall of sea level was accompanied by a nal lows within back-barrier settings during deposition of the C1 unit became cut-off from any marine worked by subaerial eolian processes. Erosional beveling and emplacement of coarse-grained sand and C2 unit. The contact between C1 and C2 units is a regressive surface of marine erosion (RSE, shown in lly sourced from protruding fan-deltas. Section lines between wells contained within the fence diagram thwest or paleolandward.

4.4 Stage III: Relative rise of sea level and subsequent transgression following lowstand

As sea level began to rise from the relative lowstand conditions outlined in the previous section, erosional wave scouring and reworking of protrusive lowstand deltaic deposits and net landward transport of sediments nurtured the development of barrier island complexes (figure 20). A modern analogue for such coast-perpendicular antecedent topographic control on barrier island initiation and anchoring is present along the Delaware coast (Kraft, 1971; Kraft & John, 1979; Belknap & Kraft, 1985). Erosional beveling of headlands (*i.e.* lowstand deltas) during Stage Two supplied sediments to flanking barriers in much the same manner proposed for barrier island arc development along abandoned Mississippi River deltas (Boyd & Penland, 1984; Penland *et al.*, 1985; Penland *et al.*, 1988). Following erosion, sediments were carried parallel to the coastline by longshore currents and subsequently deposited at the updrift margin of laterally accreting barrier spits. These sediments were then carried landward across the barrier by flood-dominated currents and deposited in the back-barrier as flood tidal deltas. Wells 10-4-67-10W6M, 10-25-67-11W6M and, 14-4-67-12W6M include core that contain flood-tidal deltaic deposits that were deposited along the back-barrier margin (figure 20).

Landward barrier translation occurs primarily through progradation of sediments deposited within flood-tidal deltaic and washover fan settings (Rampino & Saunders, 1980). Lowered rates of shoreface erosion and sediment supply to the flanking barrier would have resulted in a starving of flood-tidal delta progradation, therefore contributing to decreased rates of landward translation of barrier islands during Stage Three. Hoyt & Henry (1967) have proposed that significant erosion on transgressive coasts derives from migration of tidal inlets, where processes involving longshore drift become dominant over net onshore transport of sediments. Cored intervals of the C3 unit recovered from the approximate latitude of the maximum landward extent of barrier translation contain facies successions indicative of tidal inlet migration (*e.g.* 7-15-67-10W6M, 10-12-67-10W6M). Despite reduced rates of landward barrier translation, storm washover sedimentation presumably continued infilling landward-facing portions of the backbarrier, significantly widening the barrier. Widening of the barrier complex would have persisted until washover sedimentation predominantly contributed to vertical aggradation of the barrier rather than infilling of back barrier depocenters. In well 11-22-67-7W6M thickly bedded sands cap foreshore strata and confirm the importance of barrier aggradation through storm washover processes.

Throughout Stage Three, barrier island development occurred contemporaneously with marine inundation of fluvial valleys and costal lowlands that had been reincised and expanded during Stage Two (figure 18). Following transgression and aggradation of the main barrier island chain shown in figure 20, the open water area behind the barrier islands would have been at a maximum. The magnitude of the tidal prism can be approximately equated as the product of both the open water area and tidal range of the embayment. Therefore, regardless of the tidal range of the newly formed brackish embayments, the magnitude of the tidal prism would have also been at a maximum. Because of the magnitude of the tidal prism, the number of tidal inlets, and also their cross-sectional area would have similarly been at a maximum (Fitzgerald, 1988; Oertel, 1988).

Following maximum transgression of the C3 shoreline in Stage Three, the back-barrier settings would have continued to be infilled by sediments of both fluvial and marine origin. Progradation of bay-head deltaic deposits at the fluvial end of the estuary contributed significant volumes of sediment to infilling of available back-barrier accommodation space. Also, encroachment of the margins of the estuary following expansion of tidal flats and abandonment of flood-tidal delta lobes likely accompanied progressive loss of open water area and hence diminished the magnitude of the tidal prism. The erosive potential of tidal channels within inlet settings would have decreased in response to this reduction in the size of the tidal prism. Therefore, sediment accumulation, that would have otherwise been eroded and removed by tidal channel flow at the bayward and seaward margins of tidal inlets, would have effectively lead to choking of the tidal inlets, and eventual inlet closure.

STAGE 3: Relative rise of sea level and subs transgression following lowstand

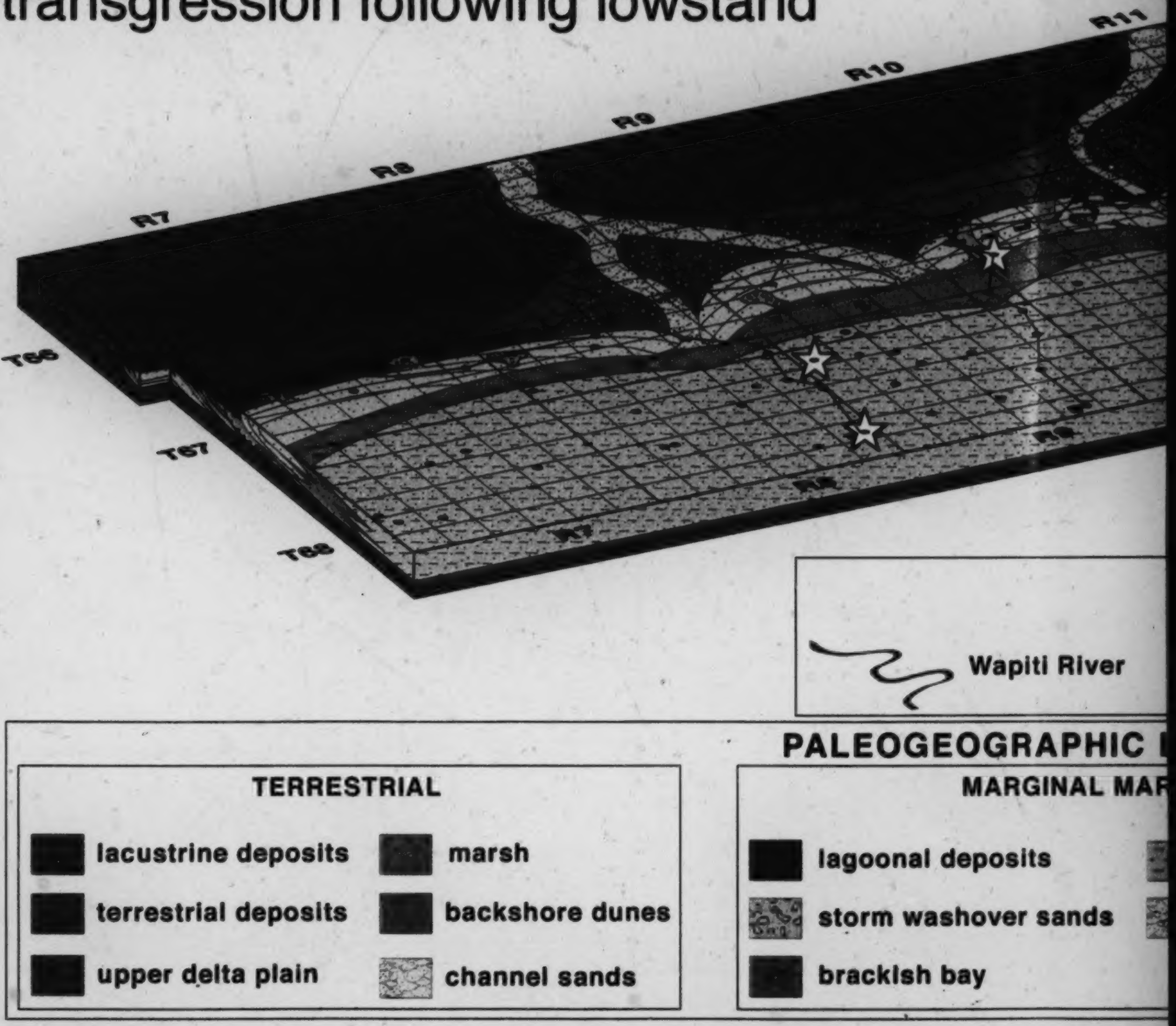

Figure 20. Paleogeographic reconstruction of the Falher "C" shoreline following transgression and barrier island overlying C3 unit is defined as a transgressive surface of marine erosion (TSE2, shown in blue). Fluvial point sour Development of tidal inlets and flanking barrier spits is also interpreted to have occurred during deposition of the C fore-barrier and back-barrier environments. Landward movement of sediment into back barrier environments was f environments were likely more extensive than the initial C1 transgression because of widespread fluvial incision du diagram featured in Section 3.7 of Chapter 3 (figure 14, page 101) are also shown. Model is oriented east-west fron

subsequent

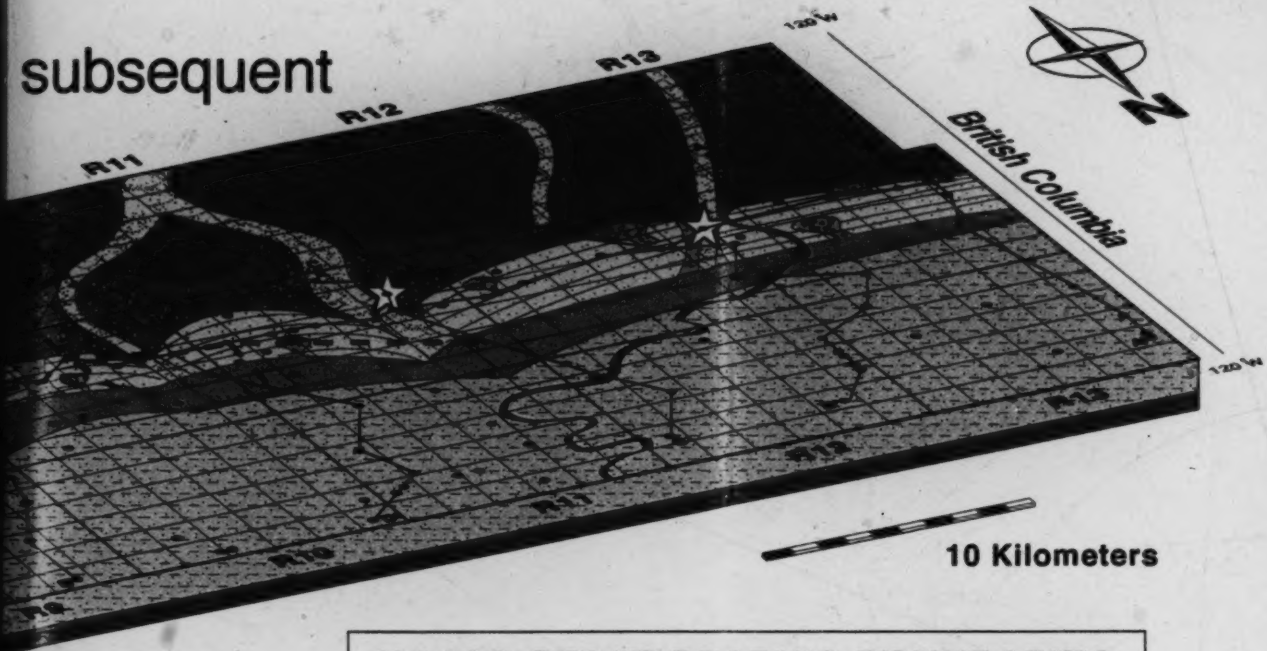

MAJOR STRATIGRAPHIC BOUNDARIES

— T2 surface — RSE — T1 surface

MAP FEATURES

olti River

- No core recovered
- Core recovered
☆ Interval Photographed

Z Z' Cross-section Reference

Fence Diagram

RAPHIC LEGEND

RGINAL MARINE

its ▨ tidal inlet

r sands ▨ channel sands

MARINE

░ C1 shoreface ■ transition

▨ C2 shoreface ▨ offshore

░ C3 shoreface ▨ channel sands

barrier island development. The disconformable contact between the coarse-grained C2 unit and the
vial point sources likely remained active, and supplimented barrier formation through headland erosion.
osition of the C3 unit during Stage 3. Tidal inlets acted as the main agents of sediment bypass between
onments was facilitated by flood-tidal and storm washover deposition. Protected brackish back-barrier
vial incision during the regressive C2 interval. Section lines between wells contained within the fence
l east-west from left to right respectively.

4.5 Stage IV: Normal regression with inconsistent sediment supply

An extended period of RSL stillstand followed the transgression described in Stage Three, and was partially responsible for the distribution of environments shown in Figure 21. Following the closure of tidal inlets as outlined in Section 4.3, progradation of bay head delta complexes continued basinward, progressively infilling accommodation space within the backbarrier realm. Once completely infilled, continued fluvial bypass and supply to the C4 shoreline brought about a normal regression during Stage Four (figure 21). Fluvial-deltaic distributary channels present in the eastern portion of the study area became the principal suppliers of sediment to coastal environments. Delayed supply of sediment to starved portions of the C4 shoreline resulted in relatively slower rates of progradation in the western portion of the study area. As a result, the east-west trend of the coastline likely reoriented along a west southwest-east northeast axis in response to increased rates of shoreline progradation in the eastern portion of the mapsheet (figure 21).

On the coastal plain, ephemeral lake deposits developed within topographic lows that were formerly areas of lagoonal deposition. Lake development was facilitated by ponding of sediment as lagoons became disconnected from marine and marginal marine environments following northward progradation of the shoreline (figure 21). Maximum basinward translation of the Falher "C" shoreline has been established far northward of the study area within Twp. 73 (Cant, 1984; Casas & Walker, 1997).

STAGE 4: Normal regression accompanying progradation of a barrier island arc.

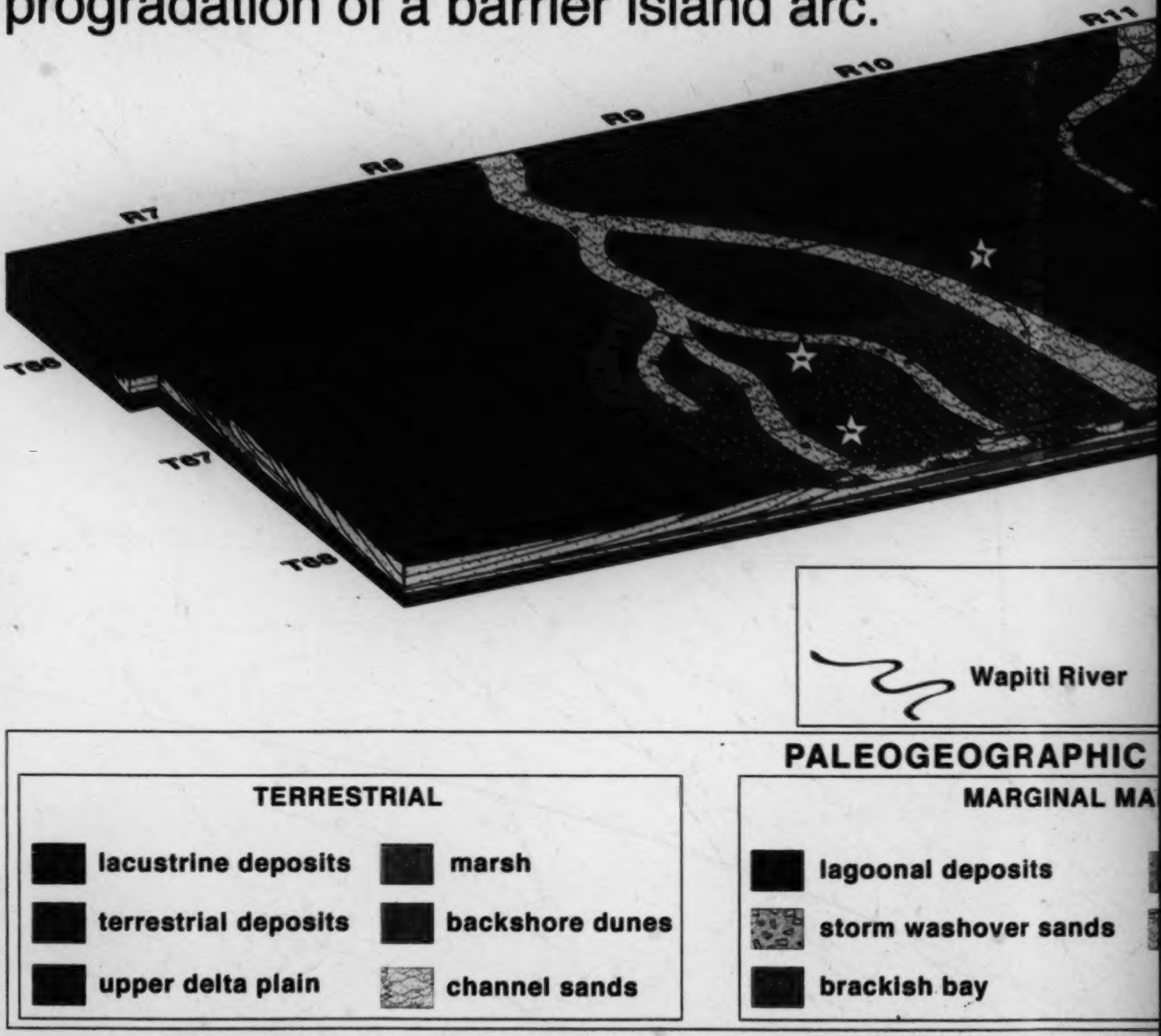

Figure 21. Paleogeographic reconstruction of the Falher "C" shoreline following progradation of the barrier islan marine and fluvial distributary environments of deposition. Relatively rapid infilling of available accommodation s east-west trending axis of the shoreline into a northeast-southwest trend. Observations do not support the develop that the western portion records the youngest progradational events within the C3 unit and that the majority of back aggradation of the coastal plain accounted for deposition of interbedded organic-rich shales and coal beds that cons between wells contained within the fence diagram featured in Section 3.7 of Chapter 3 (Figure 14, page 101) are al

nying

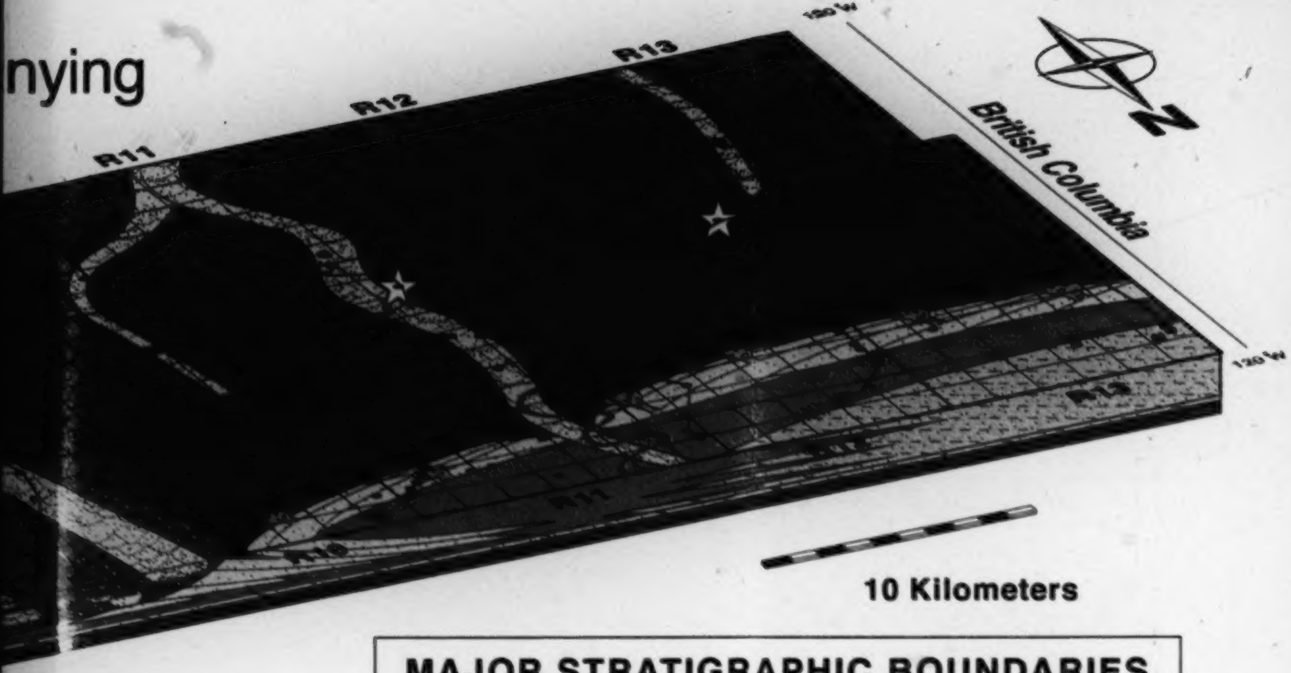

MAJOR STRATIGRAPHIC BOUNDARIES

— T2 surface — RSE — T1 surface

MAP FEATURES

apiti River

- • No core recovered
- • Core recovered
- ☆ Interval Photographed

Z — Z' Cross-section Reference

— — Fence Diagram

GRAPHIC LEGEND

RGINAL MARINE

osits ▨ tidal inlet

ver sands ▨ channel sands

MARINE

▨ C1 shoreface ■ transition

▨ C2 shoreface ▨ offshore

▨ C3 shoreface ▨ channel sands

the barrier island arc and normal regression. The eastern portion of the study area is dominated by marginal ccommodation space in the eastern portion of the study area brought about counterclockwise rotation of the port the development of brackish estuarine systems in the western portion of the study area. It is speculated majority of back-barrier deposition took place in lagoonal environments. Following Stage 4, continued al beds that constitute the C4 unit, thus capping the Falher "C" Member within the study area. Section lines page 101) are also shown. Model is oriented east-west from left to right respectively.

CHAPTER FIVE: Conclusions

5.1 Conclusions

1. Eleven facies (F1 to F11) have been grouped into five facies associations that represent fully-marine (FA1, and FA2), marginal-marine (FA3, and FA4) and non-marine (FA5) environments of deposition.

2. Of the five facies associations, FA2 and FA3 include coarse-grained facies of high reservoir potential. Facies within FA2 were deposited within wave-dominated upper shoreface and foreshore environments. The facies succession within FA3 was deposited contemporaneously with tidal inlet migration and lateral accretion of the adjacent spit platform.

3. Four units that contain an architectural arrangement of one or more of the five facies associations constitute the Falher "C" Member within the study area. From oldest to youngest these are: C1, C2, C3 and C4. Three stratigraphic surfaces termed TSE1, RSE, and TSE2 disconformably bound each of the units.

4. A depositional model demonstrates the geomorphological influence of changes in the rate of sediment supply and sea level rise/fall on the distribution of facies associations and significant stratigraphic surfaces at four progressive stages in deposition of the Falher "C" Member.

5. Paleogeographic and isopach mapping of the Falher "C" Member has demonstrated an intimate link between fluvial, tidal, and marine controls on the distribution of potential reservoir quality facies within the Falher "C" Member.

REFERENCES

Alberta Study Group. 1954. *Lower Cretaceous of the Peace River Region; Western Canada Sedimentary Basin.* Rutherford Memorial Volume, American Association of Petroleum Geologists, Tulsa, Oklahoma: p. 268-278.

Allen, J.R.L. 1965. *A review of the origin and characteristics of recent alluvial sediments.* Sedimentology, Vol. 5: p. 89-191.

Arnott, R.W.C. 1993. *Sedimentological and sequence stratigraphic model of the Falher "D" pool, Lower Cretaceous, northwestern Alberta.* Bulletin of Canadian Petroleum Geology, Vol. 41, No. 4: p. 453-463.

Badgley, P.C. 1952. *Notes on the subsurface stratigraphy and oil and gas geology of the Lower Cretaceous Series in central Alberta.* Geological Survey of Canada, Paper 52-11.

Belknap, D.F., and J.C. Kraft. 1985. *Influence of antecedent geology on the stratigraphic preservation potential and evolution of Delaware's barrier systems.* Marine Geology, Vol. 63: p. 235-262.

Benyon, B.M., S.G. Pemberton, D.A. Bell, and C.A. Logan. 1988. *Environmental implications of ichnofossils from the Lower Cretaceous Grand Rapids Formation, Cold Lake oil sands deposit. In:* D.P. James, and D.A. :Leckie (eds.), Sequences, Stratigraphy, Sedimentology: surface and subsurface. Canadian Society of Petroleum Geologists, Memoir 15: p. 275-290.

Berelson, W.M., and S.D. Heron. 1985. *Correlations between Holocene flood tidal and barrier inlet fill sequences: Back Sound-Shackleford Banks, North Carolina.* Sedimentology, Vol. 32: p. 215-222.

Bergman, K.M., and R.G. Walker. 1987. *The importance of sea level fluctuation in the formation of linear conglomerate bodies: Carrot Creek Member of the Cardium Formation, Cretaceous Western Interior Seaway, Alberta, Canada.* Journal of Sedimentary Petrology, Vol. 57, No. 4: p. 651-665.

Bernard, H.A., and C.F. Major, Jr. 1963. *Recent meander belt deposits of the Brazos River: an alluvial "sand" model.* American Association of Petroleum Geologists Bulletin, Vol. 47: 350-351.

Bluck, B.J. 1967. *Sedimentation of Beach gravels- examples from South Wales.* Journal of Sedimentary Petrology, Vol. 37: p. 128-157.

Bluck, B.J. 1969. *Particle rounding in beach gravels.* Geological Magazine, Vol. 106: p. 1-14.

Boersma, J.R. 1991. *A large flood-tidal delta and its successive spill-over apron: detailed proximal-distal facies relationships (Miocene Lignite Suite, Lower Rhine, Germany). In*: D.G. Smith, G.E. Reinson, B.A. Zaitlin and R.A. Rahmani (eds.), Tidal Sedimentology, Canadian Society of Petroleum Geologists Memoir 16: p. 227-254.

Bourgeois, J., and E.L. Leithold. 1984. *Wave-worked conglomerates: depositional processes and criteria for recognition. In:* E.H. Koster, and R.J. Steel (eds.), Sedimentology of Gravels and Conglomerates. Canadian Society of Petroleum Geologists, Memoir 10: p. 1-31.

Boyd, R., and S. Penland. 1984. *Shoreface translation and the Holocene stratigraphic record: examples from Nova Scotia, the Mississippi delta and eastern Australia.* Marine Geology, Vol. 60: p. 391-412.

Bromley, R.G. 1995. *Trace fossils: biology, taphonomy and applications.* Chapman and Hall, London: 361 p.

Burst, J.F. 1965. *Subaqueously formed shrinkage cracks in clay.* Journal of Sedimentary Petrology, Vol. 35: p. 348-353.

Caddel, E.M. 1999. *The Sedimentology and Stratigraphy of the Falher C Member, Spirit River Formation, Northeastern British Columbia.* Unpublished M.Sc. thesis, University of Calgary.

Caldwell, W.G.E., B.R. North, C.R. Stelck, and J.H. Wall. 1978. *A foramineferal zonal scheme for the Cretaceous system in the Interior Plains of Canada. In*: C.R. Stelck and B.D.E. Chatterton (eds.), Western and Canadian Biostratigraphy, Geological Association of Canada Special Paper 18: p. 495-575.

Cant, D.J.. 1983. *Spirit River Formation – A stratigraphic-diagenetic gas trap in the Deep Basin of Alberta.* American Association of Petroleum Geologists Bulletin, 67: p. 577-587.

Cant, D.J. 1984. *Development of shoreline-shelf sand bodies in a Cretaceous epeiric sea deposit.* Journal of Sedimentary Petrology, Vol. 54: p. 0541-0556.

Cant, D.J. 1988. *Regional structure and development of the Peace River Arch, Alberta: a Paleozoic failed-rift system?* Bulletin of Canadian Petroleum Geology, Vol. 36: p. 284-295.

Cant, D.J., and V.G. Ethier. 1984. *Lithology-dependant diagenetic control of reservoir properties of conglomerates, Falher Member, Elmworth Field, Alberta.* American Association of Petroleum Geologists Bulletin, Vol. 68, No. 8: p. 1044-1054.

Casas, J.E., and R.G Walker. 1997. *Sedimentology and depositional history of units C and D of the Falher Member, Spirit River Formation, west-central Alberta.* Bulletin of Canadian Petroleum Geology, Vol. 45: p. 218-238.

Clifton, H.E. 1973. *Pebble segregation and bed lenticularity in wave-worked versus alluvial gravel.* Sedimentology, Vol. 20: p. 173-187.

Clifton, H.E., and Thompson. 1978. Macaronichnus segregatis: *a feeding structure of shallow marine polychaetes.* Journal of Sedimentary Petrology, Vol. 48: p. 1293-1302.

Dalrymple, R.W., B.A. Zaitlin, and R. Boyd. 1992. *Estuarine facies models; conceptual basis and stratigraphic implications.* Journal of Sedimentary Petrology, Vol. 62: p. 1130-1146.

Davidson-Arnott, R.G.D., and B. Greenwood. 1974. *Bedforms and structures associated with bar topography in the shallow-water wave environment, Kouchibouguac Bay, New Brunswick, Canada.* Journal of Sedimentary Petrology, Vol. 44: p. 698-704.

Dawson, G.M. 1881. *Report on an exploration from Port Simpson on the Pacific Coast to Edmonton on the Saskatchewan, embracing a portion of the northern part of British Columbia and the Peace River Country.* Geological Survey of Canada, Report of Progress 1879-1880, part B: 177 p.

Dott, R.H. 1983. *1982 SEPM presidential address: episodic sedimentation- how normal is average? How rare is rare? Does it matter?* Journal of Sedimentary Petrology. Vol. 53, No. 1: p. 0005-0023.

Dott, R.H., and J. Bourgeois. 1982. *Hummocky stratification: significance of its variable bedding sequences.* Geological Society of America Bulletin, Vol. 93: p.663-680.

Duke, W.L. 1985. *Hummocky cross-stratification, tropical hurricanes, and intense winter storms.* Sedimentology, Vol. 32: 167-194 p.

Duke, W.L., R.W.C. Arnott, and R.J. Cheel. 1991. *Shelf sandstones and hummocky cross-stratification: new insights on a stormy debate.* Geology, Vol. 19: p. 625-628.

Fitzgerald, D.M. 1988. *Shoreline erosional-depositional processes associated with tidal inlets.* Lecture Notes on Coastal and Estuarine Studies, Vol. 29: p. 186-225.

Frey, R.W., 1990, Trace fossils and hummocky cross-stratification, Upper Cretaceous of Utah: Palaios, Vol. 5, p. 203-218.

Frey, R.W., and R. Goldring. 1992. *Marine event beds and recolonization surfaces as revealed by trace fossil analysis.* Geology Magazine, 129: p. 325-335.

Gingras, M.K., S.G. Pemberton, T. Saunders, and H.E. Clifton. 1999. *The ichnology of modern and Pleistocene brackish water deposits at Willapa Bay, Washington: variability in estuarine settings.* Palaios, Vol. 14: p. 352-374.

Greenwood, B., and P.R. Mittler. 1985. *Vertical sequence and lateral trasitions in the facies of a barred nearshore environment.* Journal of Sedimentary Petrology, Vol. 55: p. 366-375.

Harms, J.C., J.B. Southard, D.R. Spearing, and R.G. Walker. 1975. *Depositional environments as interpreted from primary sedimentary structures and stratification sequences.* Society of Economic Paleontologist and Mineralogists Short Course No. 2, Lecture Notes: 161 p.

Hart, B.S., and A.G. Plint. 1989. *Gravelly shoreface deposits: a comparison of modern and ancient facies sequences*: Sedimentology, Vol. 36: p. 551-557.

Hayes, M.O. 1980. *General morphology and sediment patterns in tidal inlets.* Sedimentary Geology, Vol. 26: p. 139-156.

Hennessy, J.T., and G.A. Zarillo. 1987. *The interrelation and distinction between flood-tidal delta and washover deposits in a transgressive barrier island.* Marine Geology, Vol. 78: p. 35-56.

Heron, S.D., T.F. Moslow, W.M. Berelson, J.R. Herbert, G.A. Steel, and K.R. Susman. 1984. *Holocene sedimentation of a wave-dominated barrier island shoreline: Cape Lookout, North Carolina.* Marine Geology, Vol. 60: p. 413-434.

Heward, A.P. 1981. *A review of wave-dominated clastic shoreline deposits.* Earth Science Reviews, Vol. 17: p. 223-276.

Howard, J.D., and R.W. Frey. 1975. *Estuaries of the Georgia coast, U.S.A.; sedimentology and biology.* Senckenbergiana Maritima, Vol. 7: p. 1-31.

Hoyt, J.H., and V.J. Henry. 1967. *Influence of inlet migration on barrier island sedimentation.* Geological Society of America Bulletin, Vol. 78: p. 77-86.

Hunter, R.E. 1980. *Depositional environments of some Pleistocene coastal terrace deposits, southwestern Oregon- case history of a progradational beach and dune sequence.* Sedimentary Geology, Vol. 27: p. 241-262.

Hunter, R.E., H.E. Clifton, and R.L. Phillips. 1979. *Depositional processes, sedimentary structures and predicted vertical sequences in barred nearshore systems, southern Oregon coast.* Journal of Sedimentary Petrology, Vol. 49: p.411-726.

Hunter, R.E., and H.E. Clifton. 1982. *Cyclic deposits and hummocky cross-stratification of probable storm origin in the Upper Cretaceous of Cape Sebastian area, southwestern Oregon.* Journal of Sedimentary Petrology, Vol. 52: p. 127-144.

Jeletsky, J.A. 1964. *Illustrations of Canadian fossils, Lower Cretaceous marine index fossils of western and arctic Canada.* Geological Survey of Canada Special Paper 64-11: 100 p.

Jeletzky, J.A. 1968. *Macrofossil zones of the marine Cretaceous of the western interior of Canada and their correlation with the zones of and stages of Europe and the western interior of the United States.* Geological Survey of Canada, Paper 67-72: 66 p.

Jeletzky, J.A. 1971. *Marine Cretaceous biotic provinces and paleogeography of western and arctic Canada: illustrated by a detailed study of ammonites.* Geological Survey of Canada, Paper 70-22, 92 p.

Kalkreuth, W., and D.A. Leckie. 1989. *Sedimentological and petrographical characteristics of Cretaceous strandplain coals: a model for coal accumulation from the North American Western Interior Seaway.* International Journal of Coal Geology, Vol. 12: p. 381-424.

Kamola, D.L. 1984. *Trace fossils from marginal-marine facies of the Spring Canyon Member, Blackhawk Formation (Upper Cretaceous), east-central Utah.* Journal of Paleontology, Vol. 58: p. 529-541.

Kikuchi, T. 1972. *A characteristic trace fossil in the Narita Formation and its paleogeographical significance.* Journal of the Geological Society of Japan, 78: p. 137-144.

Kirk, R.M. 1980. *Mixed sand and gravel beaches: morphology, processes and sediments.* Progress in Physical Geography, Vol. 4: p. 189-210.

Klein, G.deV. 1974. *Estimating water depths from analysis of barrier island and deltaic sedimentary sequences.* Geology, Vol. 2, 409-412.

Kozloff, E.N. 1983. *Seashore life of the northern Pacific Coast; an illustrated guide to northern California, Oregon, Washington, and British Coloumbia.* Douglas and McIntyre: 370 p.

Kraft, J.C. 1971. *Sedimentary facies patterns and geologic history of a Holocene transgression.* Geological Society of America Bulletin, Vol. 82: p. 2131-2158.

Kraft, J.C., and C.J. John. 1979. Lateral and vertical facies relationships of a transgressive barrier. American Association of Petroleum Geologists Bulletin, Vol. 63: p. 2145-2163.

Kumar, N., and J.E. Sanders. 1974. Inlet Sequence: a vertical succession of sedimentary structures and textures created by the lateral migration of tidal inlets: Sedimentology, Vol. 21, 491-532.

Leckie, D.A., and R.G. Walker. 1982. *Storm and tide dominated shorelines in the Cretaceous Moosebar-Lower Gates interval- outcrop equivalents of the Deep Basin gas trap in western Canada.* American Association of Petroleum Geologists Bulletin, Vol. 66, No. 2: p. 138-157.

Leckie, D.A. 1986. *Rates, controls, and sand-body geometry of transgressive-regressive cycles: Cretaceous Moosebar and Gate Formations, British Columbia.* American Association of Petroleum Geologists Bulletin, Vol. 70, No. 5: p. 516-535.

Leithold, E.L., and J. Bourgeois. 1984. *Characteristics of coarse-grained sequences deposited in nearshore, wave-dominated environments-examples from the Miocene of south-west Oregon.* Sedimentology, 31: p. 749-775.

MacEachern, J.A., D.J. Bechtel, and S.G. Pemberton. 1992. *Ichnology and sedimentology of transgressive deposits, transgressively-related deposits and trangressive systems tracts in the Viking Formation, central Alberta. In*: S.G. Pemberton (ed.), Applications of Ichnology to Petroleum Exploration: A Core Workshop. SEPM Core Workshop No. 17: p. 251-290.

MacEachern, J.A. and S.G. Pemberton. 1994. *Ichnological aspects of incised-valley fill systems from the Viking Formation of the Western Canada Sedimentary Basin, Alberta, Canada. In*: R.W. Dalrymple, R. Boyd, and B.A. Zaitlin (eds.), Incised Valley Systems: origin and sedimentary sequences. Society for Sedimentary Geology, Special Publication No. 51: p. 129-157.

Massari, F., and G.C. Parea. 1988. *Progradational gravel beach sequences in a moderate- to high-energy, microtidal marine environment.* Sedimentology, Vol. 35: p. 881-913.

McCabe, P.J. 1984. *Depositional environments of coal and coal bearing strata. International Association of Sedimentologists*. Special Publication 7: p. 1-30.

McLachlan, A., I.G. Eliot and D.J. Clarke. 1985. *Water filtration through reflective microtidal beaches and shallow sublittoral sands and its implications for an inshore ecosystem in Western Australia.* Estuarine, Coastal and Shelf Science 21: 91-104.

McLaren, P., and D. Bowles. 1985. *The effects of sediment transport on sediment grain-size distributions.* Journal of Sedimentary Petrology, Vol. 55, No. 4: p. 0457-0470.

McLean, J.R. 1979. *Regional considerations of the Elmworth Field and the Deep Basin.* Bulletin of Canadian Petroleum Geology, Vol. 27, No. 1: p. 53-62.

McLearn, F.H.. 1918. *Peace River section, Alberta.* Geological Survey of Canada, Summary Report 1917, pt. C: p. 14-21.

McLearn, F.H.. 1923. *Peace River canyon coal area, British Columbia.* Geological Survey of Canada, Summary Report 1922, pt. C: p. 1-46.

McLearn, F. H. 1944. *Revision of the Paleogeography of the Lower Cretaceous of the Western Interior of Canada.* Geological Survey of Canada, paper 44-32: 11 p.

McLearn, F.H., and E.D. Kindle. 1950. *Geology of northeastern British Columbia.* Geological Survey of Canada Memoir 259. 236 p.

McLearn, J.R. 1979. *Regional considerations of the Elmworth Field and the Deep Basin.* Bulletin of Canadian Petroleum Geology, Vol. 27: p. 53-62.

Moslow T.F., and S.D. Heron Jr. 1978. *Relict inlets: preservation and occurrence in the Holocene stratigraphy of southern Core Banks, North Carolina.* Journal of Sedimentary Petrology, Vol. 48: 1275-1286.

Moslow, T.F., and R.S. Tye. 1985. *Recognition and characterization of Holocene tidal inlet sequences*. Marine Geology. Vol. 63: p. 129-151.

Murakoshi, N., and F. Masuda. 1991. *A depositional model for a flood-tidal delta and washover sands in the late Pleistocene, Paleo-Tokyo Bay, Japan. In*: D.G. Smith, G.E. Reinson, B.A. Zaitlin and R.A. Rahmani (eds.), Tidal Sedimentology, Canadian Society of Petroleum Geologists Memoir 16: p. 219-226.

Nemec, W., and R.J. Steel. 1984. *Alluvial and coastal conglomerates: their significant features and some comments on gravelly mass-flow deposits. In:* E.H. Koster, and R.J. Steel (eds.), Sedimentology of Gravels and Conglomerates. Canadian Society of Petroleum Geologists, Memoir 10: p. 1-31.

Nottvedt, A., and R.D. Kreisa, 1987, Model for the combined-flow origin of hummocky cross-stratification: Geology, Vol. 15, p. 357-361.

Oertel, G.F. 1988. *Processes of sediment exchange between tidal inlets, ebb deltas and barrier islands.* Lecture Notes on Coastal and Estuarine Studies, Vol. 29: p. 297-317.

Orford, J.D. 1975. *Discrimination of particle zonation on a pebble beach.* Sedimentology, 22: p. 441-463.

Orford, J.D., and R.W.G. Carter. 1982. *Crestal overtop and washover sedimentation on a fringing sandy gravel barrier coast, Carnsore Point, southeast Ireland.* Journal of Sedimentary Petrology, Vol. 52, No. 1: p. 265-278.

Pemberton, S.G., P.D. Flach, G.D. Mossop. 1982. *Trace fossils from the Athabasca oil sands, Alberta, Canada.* Science, Vol. 217: p. 825-827.

Pemberton, S.G., and R.W. Frey. 1984. *Ichnology of storm-influenced shallow marine sequence: Cardium Formation (Upper Cretaceous) at Seebe, Alberta. In:* D.F. Stott and D.J. Glass (eds.), The Mesozoic of North America. Canadian Society of Petroleum Geologists, Memoir 9: p. 281-304.

Pemberton, G.G., J.A. MacEachern, M.J. Ranger. 1992. *Ichnology and event stratigraphy: the use of trace fossils in recognizing tempestites. In*: Pemberton, S.G. (ed.), Applications of ichnology to petroleum exploration - a core workshop. Society of Economic Paleontologists and Mineralogists, Core Workshop No. 17: 85-118.

Pemberton, S.G, J.C. Van Wagoner, and G.D. Wach. 1992. *Ichnofacies of a wave-dominated shoreline. In*: Pemberton, S.G. (ed.), Applications of ichnology to petroleum exploration - a core workshop. Society of Economic Paleontologists and Mineralogists, Core Workshop No. 17: 339-382.

Pemberton, S.G., and D.M. Wrightman. 1992. *Ichnological characteristics of brackish water deposits. In*: Pemberton, S.G. (ed.), Applications of ichnology to petroleum exploration - a core workshop. Society of Economic Paleontologists and Mineralogists, Core Workshop No. 17: 141-168.

Pemberton, S.G., and J.A. MacEachern. 1997. *The ichnological signature of storm deposits: the use of trace fossils in event stratigraphy.* In: C.E. Brett, and G.C. Baird (eds.), Paleontological events. Columbia University Press, New York: p. 74-109.

Pemberton, S.G., M. Spila, A.J. Pulham, T. Saunders, J. MacEachern, D. Robbins, and I. Sinclair. 2001. *Ichnology and sedimentology of shallow to marginal marine systems- Ben Nevis and Avalon reservoir, Jeanne d'Arc Basin.* Geological Association of Canada, Short Course Notes 15: 353 p.

Penland, S., J.R. Sutter, and R. Boyd. 1985. *Barrier island arcs along abandoned Mississippi river deltas.* Marine Geology, Vol. 63: p. 197-233.

Penland, S., R. Boyd, and J.R. Sutter. 1988. *Transgressive depositional settings of the Mississippi delta plain: a model for barrier island and shelf sand development.* Journal of Sedimentary Petrology, Vol. 58, No. 6: p. 932-949.

Posamentier, H.W., G.P. Allen, D.P. James, and M. Tesson. 1992. *Forced regressions in a sequence stratigraphic framework: concepts, examples and exploration significance.* American Association of Petroleum Geologists Bulletin, Vol. 76: p. 1687-1709.

Posamentier, H.W., and G.P. Allen, (eds.). 1999. *Siliclastic Sequence Stratigraphy- Concepts and Applications.* SEPM Concepts in Sedimentology and Paleontology #7, Tulsa, Oklahoma: 210 p.

Rahmani, R.A. 1984. *Facies control of gas trapping, Lower cretaceous Falher A cycle, Elmworth area, northwestern Alberta. In*: J.A. Masters (ed.), Elmworth: case study of a deep basin gas field. American Association of Petroleum Geologists Memoir 38, Tulsa, Oklahoma: p. 141-152.

Rampino, M.R., and J.E. Sanders. 1980. *Holocene transgression in south-central Long Island, New York.* Journal of Sedimentary Petrology, Vol. 50, No. 4: p. 1063-1080.

Reddering, J.S.V. 1983. *An inlet sequence produced by migration of a small microtidal inlet against longshore drift: the Keurbooms Inlet, South Africa.* Sedimentology, Vol. 30: p. 201-218.

Reinson, G.E. 1992. *Transgressive barrier island and estuarine systems. In:* Walker, R.G., and James, N.P. (eds.), Facies Models: response to sea level change. Geological Association of Canada: p. 179-194.

Rouble, R., and R.G. Walker. 1997. *Sedimentology, high-resolution allostratigraphy, and key stratigraphic surfaces in Falher Members A and B, Spirit River Formation, west-central Alberta. In*: S.G. Pemberton, and D.P. James (eds.), Petroleum geology of the Cretaceous Mannville Group, western Canada. Canadian Society of Petroleum Geologists Memoir 18: p. 1-28.

Saunders, T. 1989. *Trace fossils and sedimentology of a late Cretaceous progradational barrier island sequence: Bearpaw-Horeseshoe Canyon Formation transition, Dorothy, Alberta.* Unpublished M.Sc. thesis, University of Alberta: 187 p.

Saunders, T., J.A. MacEachern, and S.G. Pemberton. 1994. *Cadotte Member sandstone: progradation in a boreal basin prone to winter storms.* C.S.P.G. Manville Core Conference, Canadian Society of Petroleum Geologists, Exploration Update: p. 331-349.

Selwyn, A.R.C. 1877. *Report on exploration in British Columbia in 1875.* Geological Survey of Canada, Report of Progress 1875-1876: 432 p.

Short, A.D. 1984. *Beach and nearshore facies: southwest Australia.* Marine Geology, Vol. 60: p. 261-282.

Stelck, C. R., J.H. Wall and W.G. Bahan, and L.J. Martin. 1956. *Middle Albian Foraminifera from Athabasca and Peace River drainage areas of Western Canada.* Research Council of Alberta, Report 75: 60 p.

Stott, D.F. 1968. *Lower Cretaceous Bullhead and Fort St. John Groups, between Smokey and Peace Rivers, Rocky Mountain Foothills, Alberta and British Columbia.* Geological Survey of Canada Bulletin 152: 279 p.

Stott, D.F. 1984. *Cretaceous sequences of the foothills of the Canadian Rocky Mountains; In The Mesozoic of North America. In:* D.F. Stott and D.J. Glass (eds.), Canadian Society of Petroleum Geologists, Memoir 9: p. 85-107.

Swift, D.J.P., A.G. Figueiredo, G.L. Freeland, and G.F. Oertel. 1983. *Hummocky cross-stratification and megaripples: a geological double standard?* Journal of Sedimentary Petrology, Vol. 53: p. 1259-1317.

Van Wagoner, J.C., R.M. Mitchum, K.M. Campion, and V.D. Rahmanion. 1990. *Siliclastic sequence stratigraphy in well logs, cores and outcrops.* American Association of Petroleum Geologists, Methods in Exploration Series No. 7: 55 p.

Vos, R.G., and D.K. Hobday. 1977. *Storm beach deposits in the Late Palaeozoic Ecca Group of South Africa.* Sedimentary Geology, Vol. 19: p. 217-232.

Vossler, S.M., and S.G. Pemberton. 1988. *Ichnology of the Cardium Formation (Pembina oilfield): implications for depositional and sequence stratigraphic interpretations. In:* D.P. James, and D.A. Leckie (eds.), Sequences, Stratigraphy, Sedimentology: Surface and Subsurface. Canadian Society of Petroleum Geologists, Memoir 15, p. 237-254.

Wescott, W.A., and F.G. Ethridge. 1980. *Fan-delta sedimentology and tectonic setting- Yallahs fan delta, southeast Jamaica.* American Association of Petroleum Geologists Bulletin, Vol. 64: p. 374-399.

Whiteaves, J.F. 1885. *Description of a new species of ammonite from the Cretaceous rocks of Fort Saint John on the Peace River.* Royal Society of Canada, Proceedings and Transactions, Vol. 2, Sec. 4: p. 239-240.

Whiteaves, J.F. 1893. *Notes on the ammonites of the Cretaceous rocks of the district of Athabaska, with descriptions of four new species.* Royal Society of Canada, Proceedings and Transactions, Vol. 10, Sec. 4: p. 111-121.

Wickenden R.T.D., and G. Shaw. 1943. *Stratigraphy and structure in Mount Hulcross-Commotion Creek map-area, British Columbia.* Geological Survey of Canada, Paper 43: 13 p.

Wightman, D.M., S.G. Pemberton, and C. Singh. 1987. *Depositional Modelling of the Upper Mannville (Lower Cretaceous), central Alberta: implication for the recognition of brackish-water deposits. In:* R.W. Tillman, and K.J. Weber (eds.), Reservoir Sedimentology, Society of Economic Paleontologists and Mineralogists, Special Publication 40: p. 189-220.

Williams, G.D., and C.R. Stelck. 1975. *Speculations on the Cretaceous paleogeography of North America. In:* W.G.E. Caldwell (ed.), The Cretaceous System in the Western Interior of North America, , The Geological Association of Canada, Special Paper Number 13: p. 1-20.

Wright, L.D., and A.D. Short. 1984. *Morphodynamic variability of surf zones and beaches: a synthesis.* Marine Geology, Vol. 56: p. 93-118.

APPENDIX I: Core Logs

List of Core Included in Appendix I

Well Location				Core interval (m)			
l.s.d.	Section	Township	Range (W6)	Top	Bottom	Total Length (m)	Cross-Section Reference
11	7	68	12	2473	2490.25	17.25	B-B'
6	25		11	2112.25	2187	14.75	D-D'
6	36			2251.5	2266.25	14.75	
6	16			2277.25	2294.75	17.5	
10	1		9	2198.25	2217.75	19.5	
11	30		8	2001	2019.75	18.75	F-F'
10	5	67	13	2958.25	2967	8.75	
10	5			2792.25	2805.25	13	A-A'
3	17		12	2728.5	2736.25	7.75	B-B', G-G'
9	11			2549	2555.25	6.25	
1	11			2548	2568	20	
12	7			2746.25	2755.25	9	G-G'
14	4			2681	2695.75	14.75	E-E'
12	3			2613	2621.5	8.5	
10	20		11	2421	2438.25	17.25	C-C', F.D.
10	25			2406	2420	14	D-D', F.D.
6	13			2437.75	2450.25	12.5	G-G', F.D.
11	8			2500	2519.25	19.25	C-C'
10	19		10	2388	2408	20	F.D.
7	24			2317.75	2337.5	19.75	E-E'
6	21			2452	2472	20	F.D.
7	18			2438.75	2455.75	17	D-D'/G-G', F.D.
7	15			2516	2534.75	18.75	G-G', F.D.
10	12			2475	2485	10	E-E'/G-G', F.D.
10	9			2331.25	2361.25	30	G-G', F.D.
10	4			2477	2489.25	12.25	F.D.
5	18		9	2340	2351	11	E-E', F.D.
10	14			2295	2304	9	G-G'
6	8			2385.25	2399.75	14.5	G-G', F.D.
10	16		8	2250.75	2269.25	18.5	G-G'
11	22		7	2083.75	2103	19.25	
10	17			2160.25	2174	13.75	
1	15			2121.75	2135	13.25	
16	14			2499.5	2504.5	5	G-G'
12	14			2102.25	2115	12.75	G-G'

List of Symbols used in Core Logs

Physical Sedimentary Structures

- Synaeresis cracks
- Soft sediment faulting
- Soft sediment deformation
- Convolute lamination
- Load casts
- Flaser Bedding
- ∞ Lenticular Bedding
- Wavy bedding (heterolithic)
- Wavy bedding (homogeneous)
- ∧∧ Ripple Laminations (wave)
- Ripple Laminations (current)
- Climbing Ripples
- Low angle cross-stratification
- Hummocky cross-strat.
- Planar cross-stratification
- Trough cross-stratification
- Over steepened cross-strat.
- ≡ Planar bedding
- Scour and Fill

Fossil Symbols

- Gastropod
- Bivalved pelecypod
- Wood and leaves

Ichnofossil Symbols

- U *Arenicolites (Ar)*
- *Chondrites (Ch)*
- ▽ *Conichnus/Bergaueria (Co)*
- *Cylindrichnus (Cy)*
- *Diplocraterion (Di)*
- *Fugichnia (Fu)*
- *Gyrolithes (Gy)*
- *Helminthopsis (He)*
- *Macaraonichnus (Ma)*
- *Ophiomorpha (Op)*
- *Palaeophycus (Pa)*
- *Planolites (Pl)*
- *Rhizocorallium (Rh)*
- Root Traces/Casts
- *Roselia*
- *Skolithos (Sk)*
- *Teichichnus (Te)*
- *Terebelina (Ter)*
- *Thalassinoides (Th)*
- Undifferentiated Bioturb.
- *Zoophycos (Zo)*

Extras

- Rip-up clasts
- ▲▲▲ Mud clasts
- ·········· Pebble lag
- Carbonaceous matter
- Carbonaceous laminae
- - - - - Shale laminae
- Graded Bedding
- Glauconite
- Stylolite
- Pyrite
- Ⓟ Phosphate
- Ⓢ Siderite
- Photo Available
- ✕ Sample collected
- *Glossifungites* surface

Contacts

- Unconformity
- Erosional/Disconformity
- Scoured/Storm event
- ——— Sharp
- Gradational

11-7-68-12W6

2473.00-2490.10 m

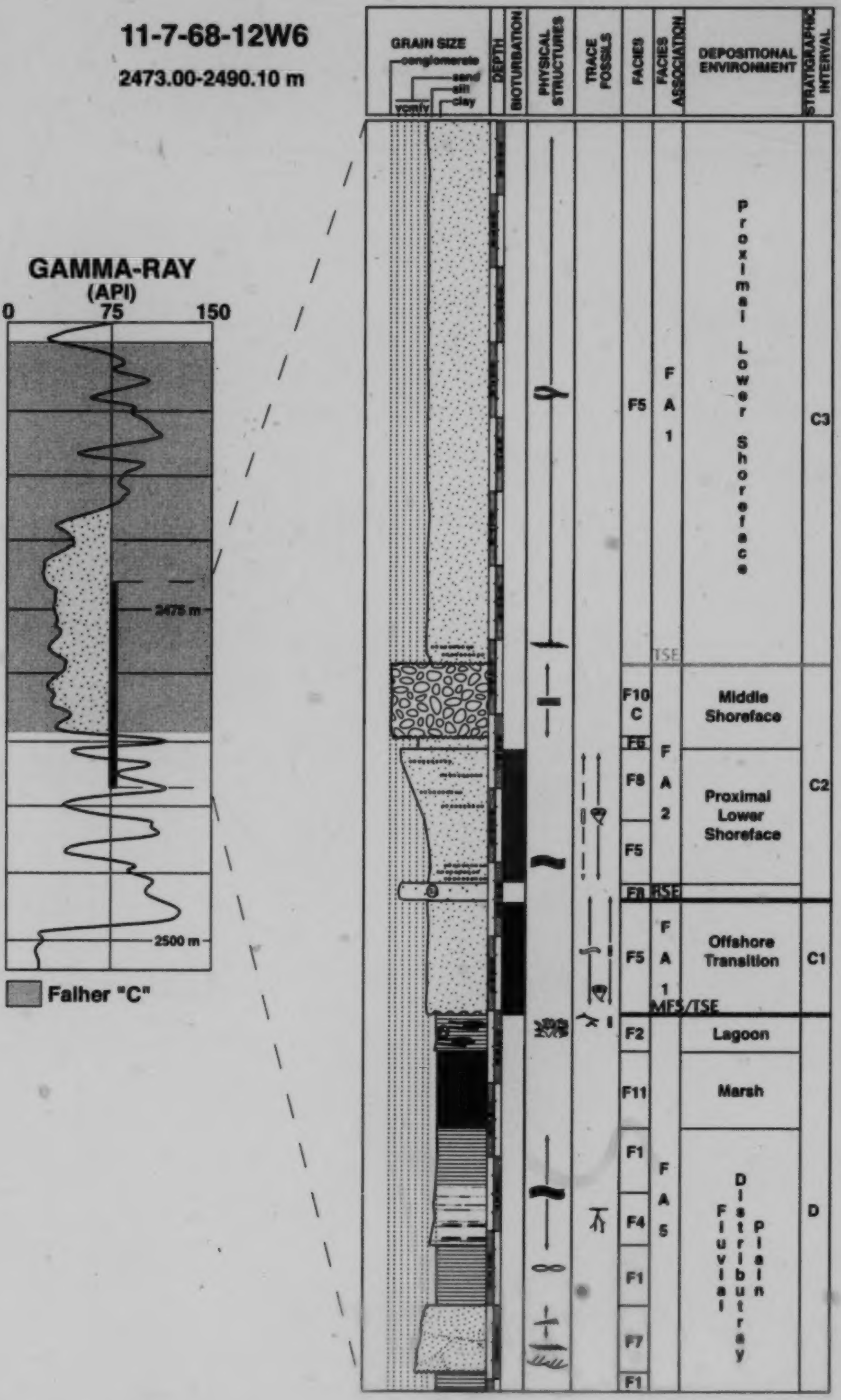

6-25-68-11W6

2172.25-2187.00 m

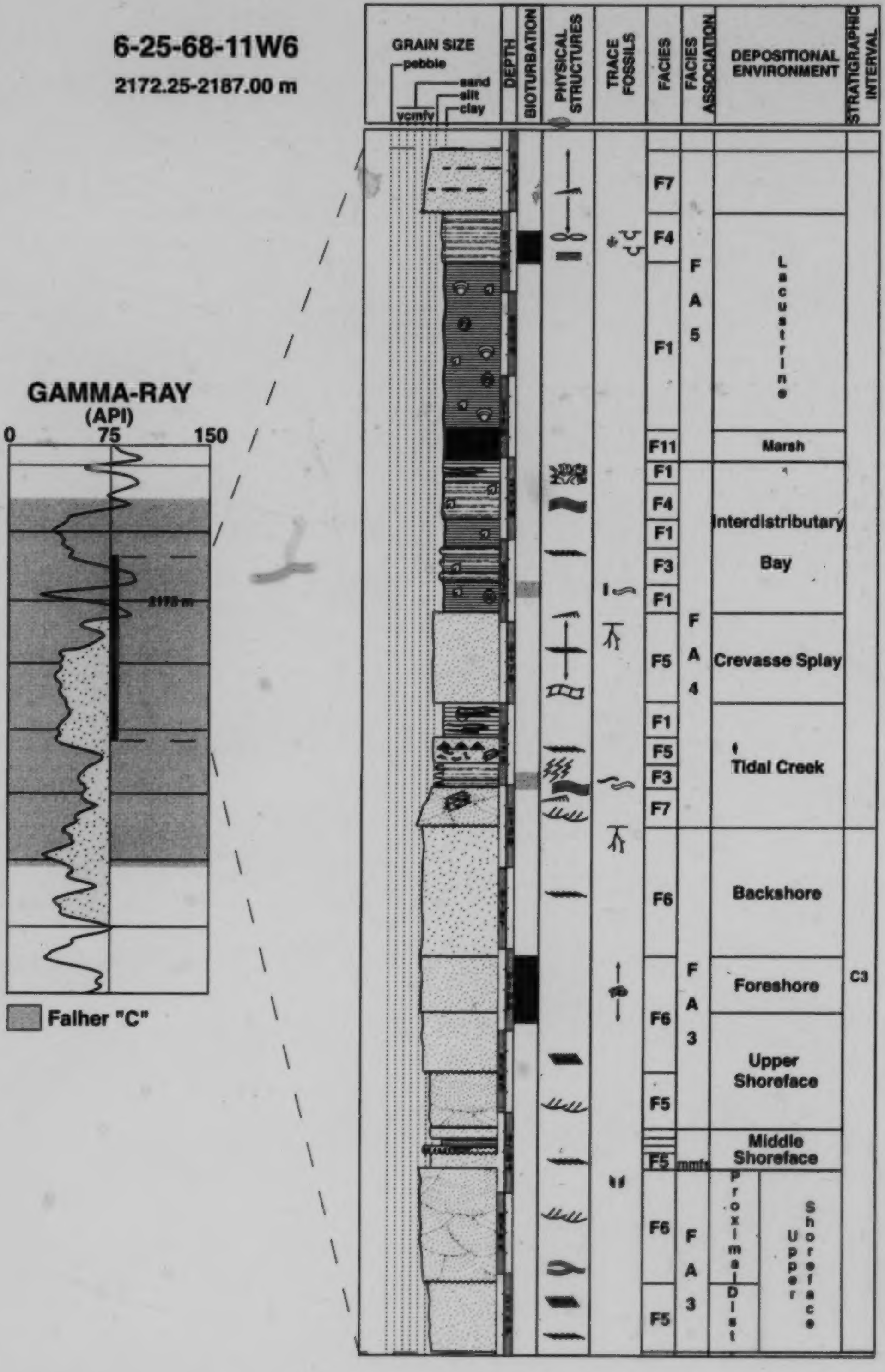

6-16-68-11W6

2253.20-2268.25 m

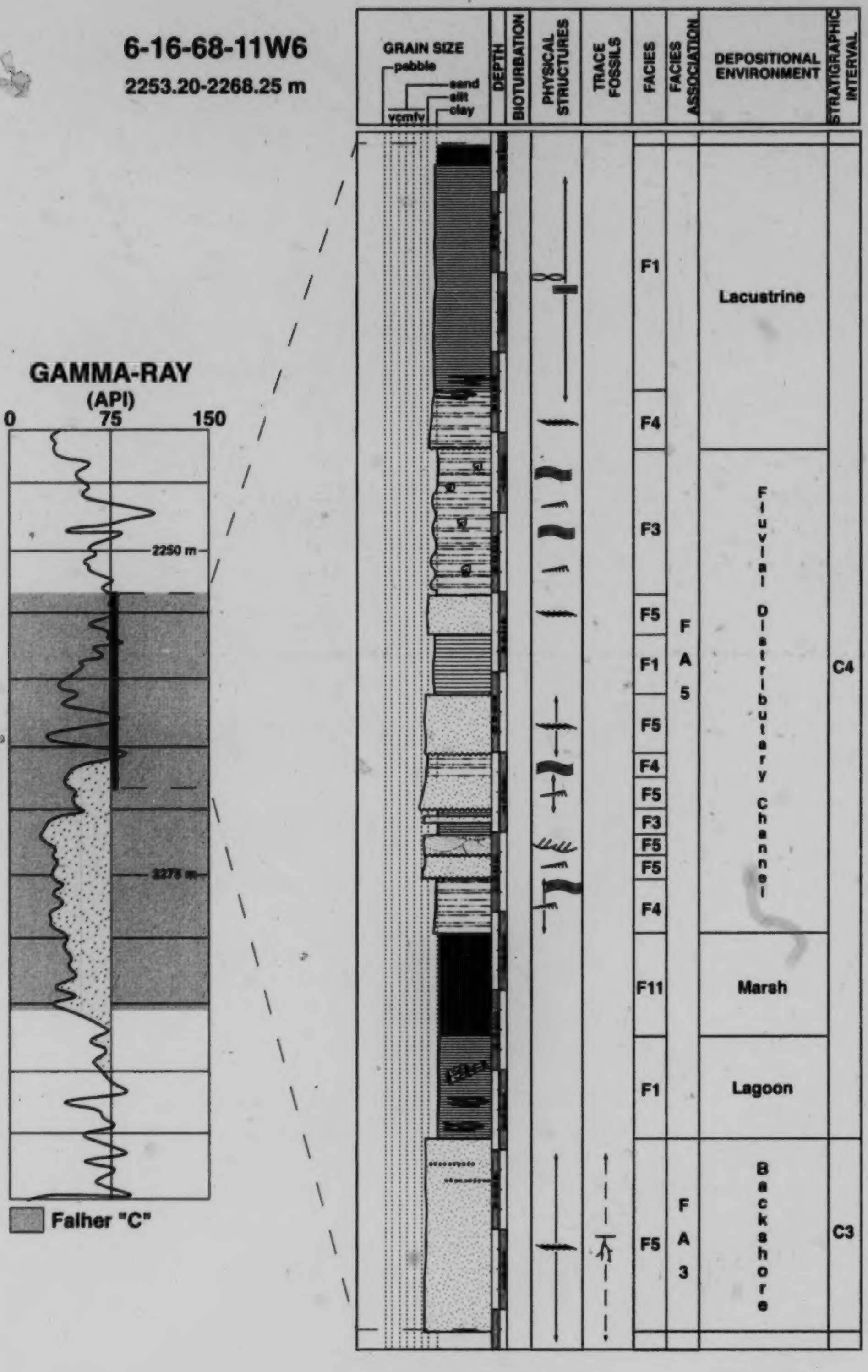

6-16-68-11W6

2277.25-2294.75 m

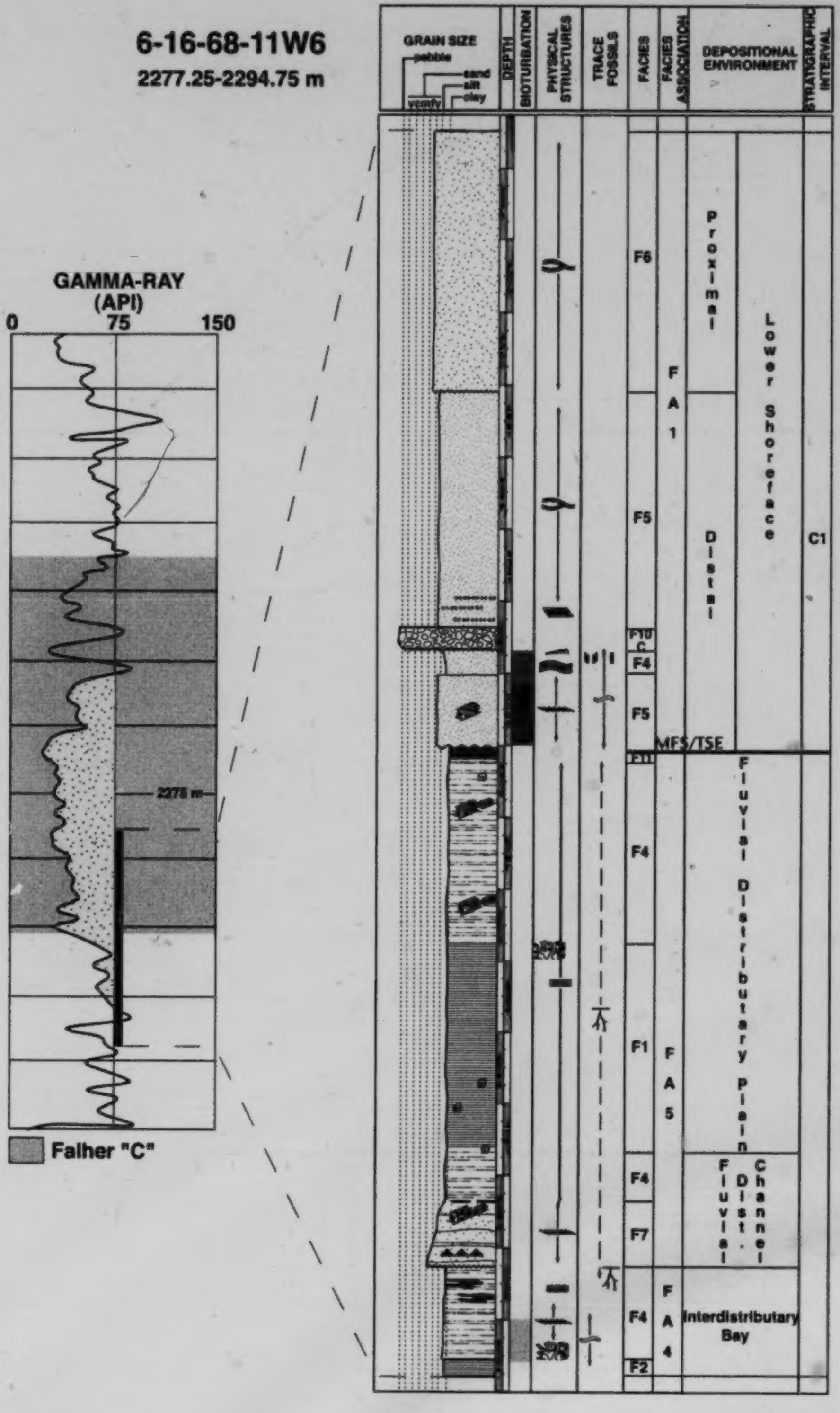

10-1-68-9W6

2199.00-2216.00 m

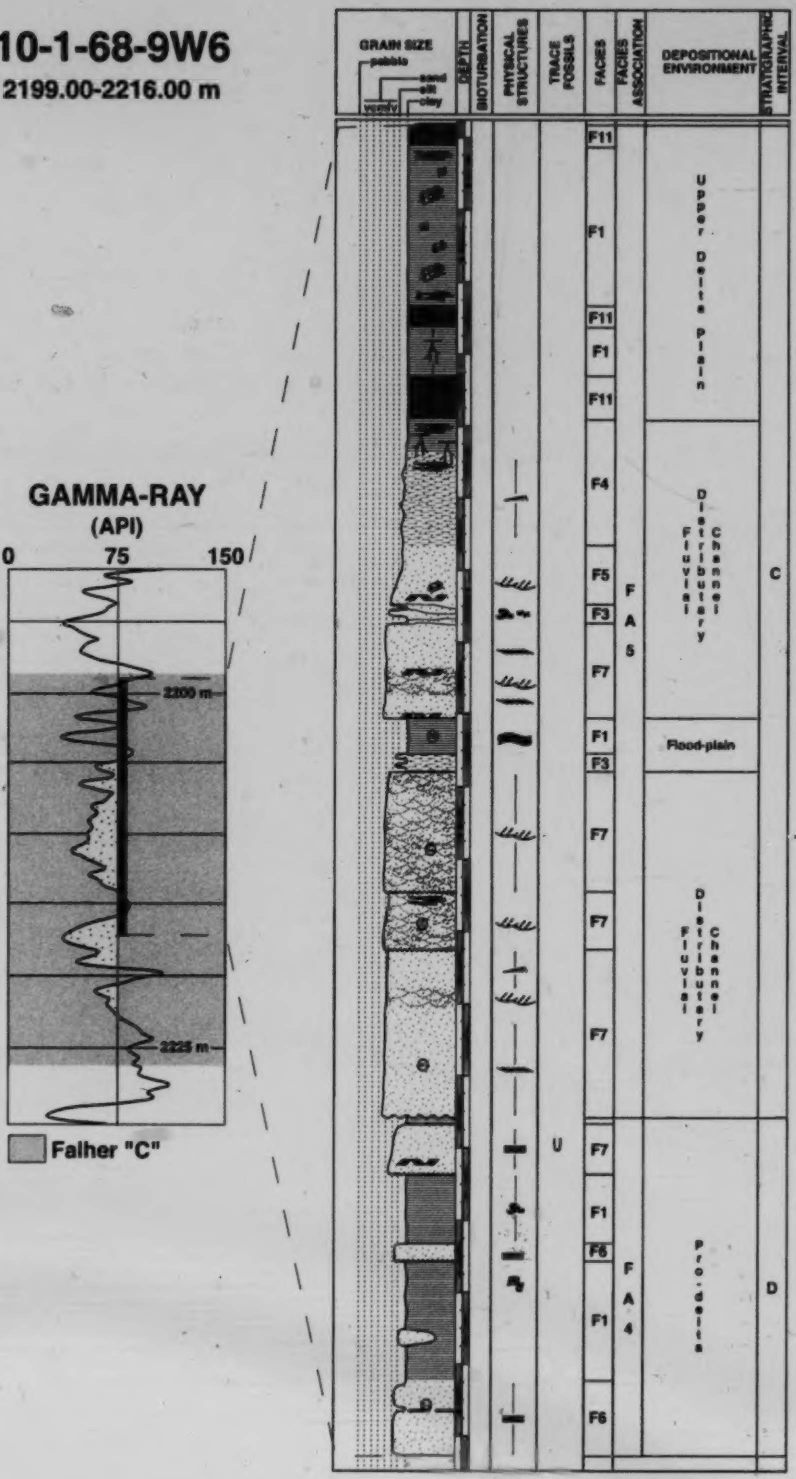

11-30-68-8W6

2199.00-2216.00 m

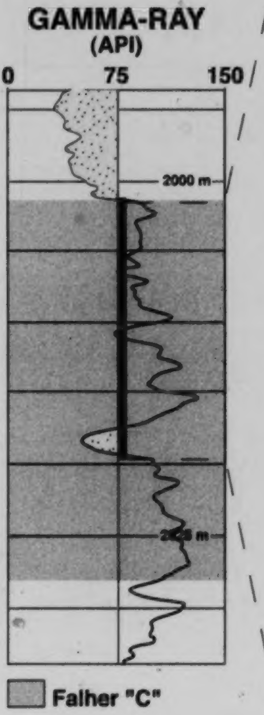

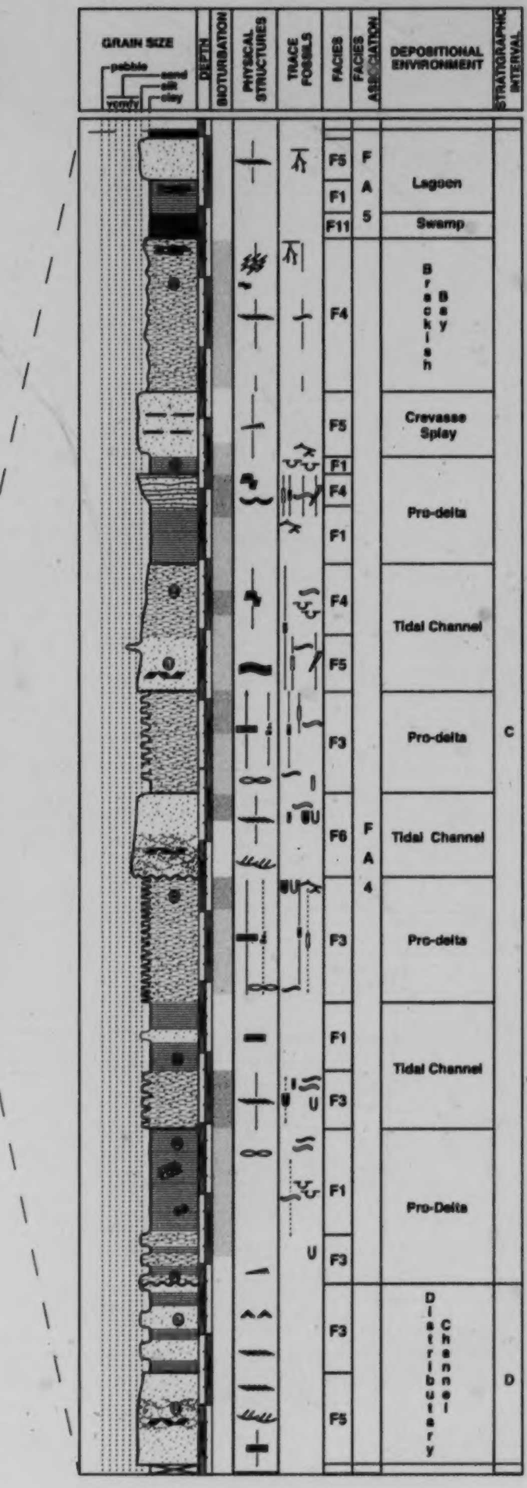

10-5-67-13W6

2792.26-2805.00 m

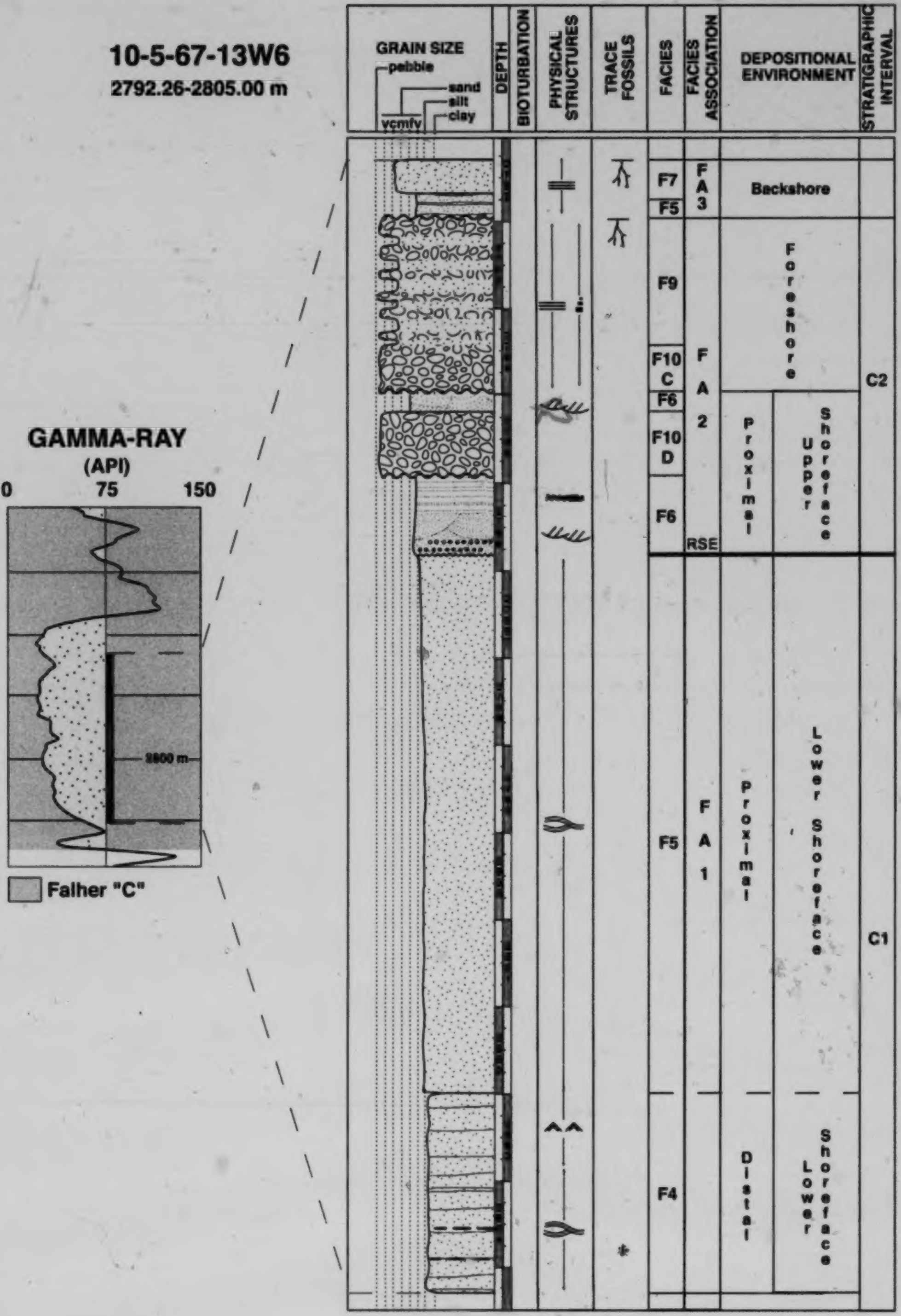

10-5-67-13W6

2958.25-2967.00 m

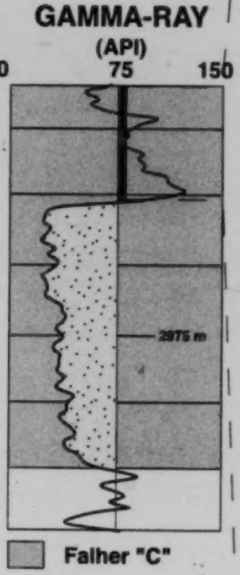

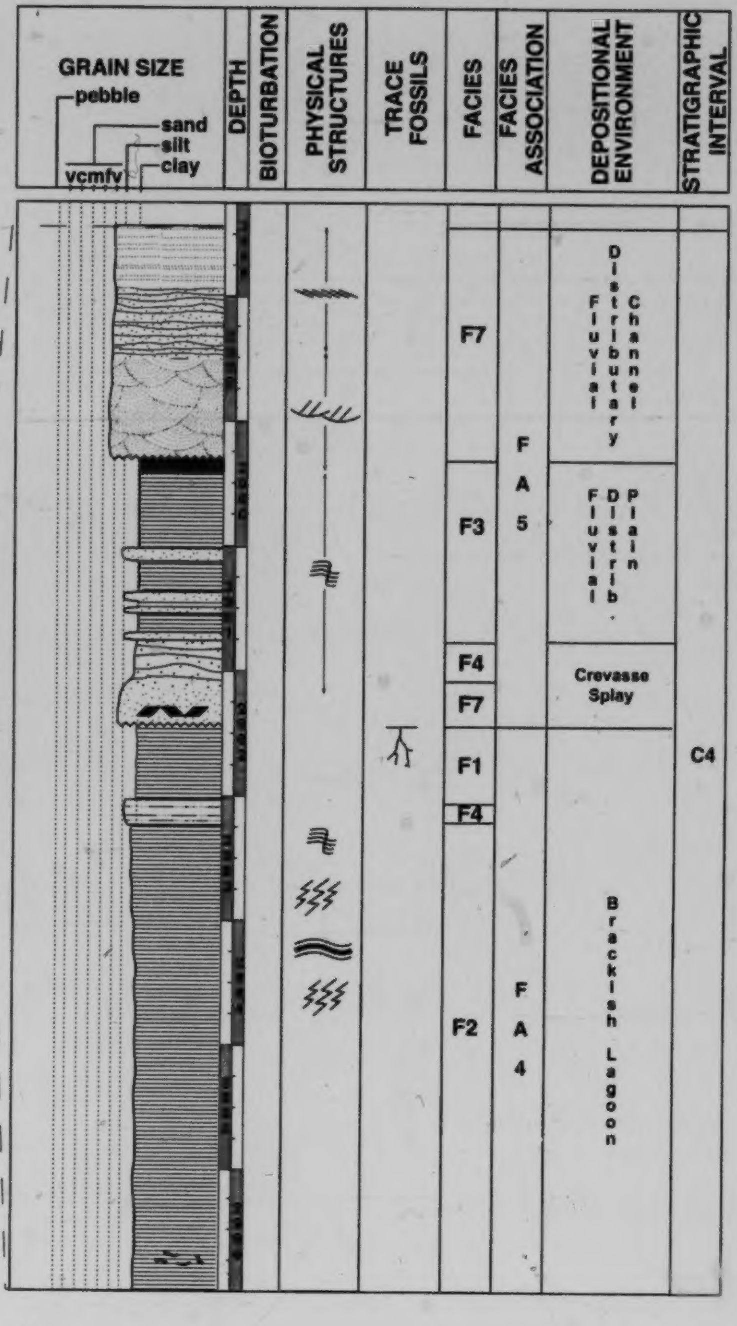

3-17-67-12W6
2728.50-2736.00 m

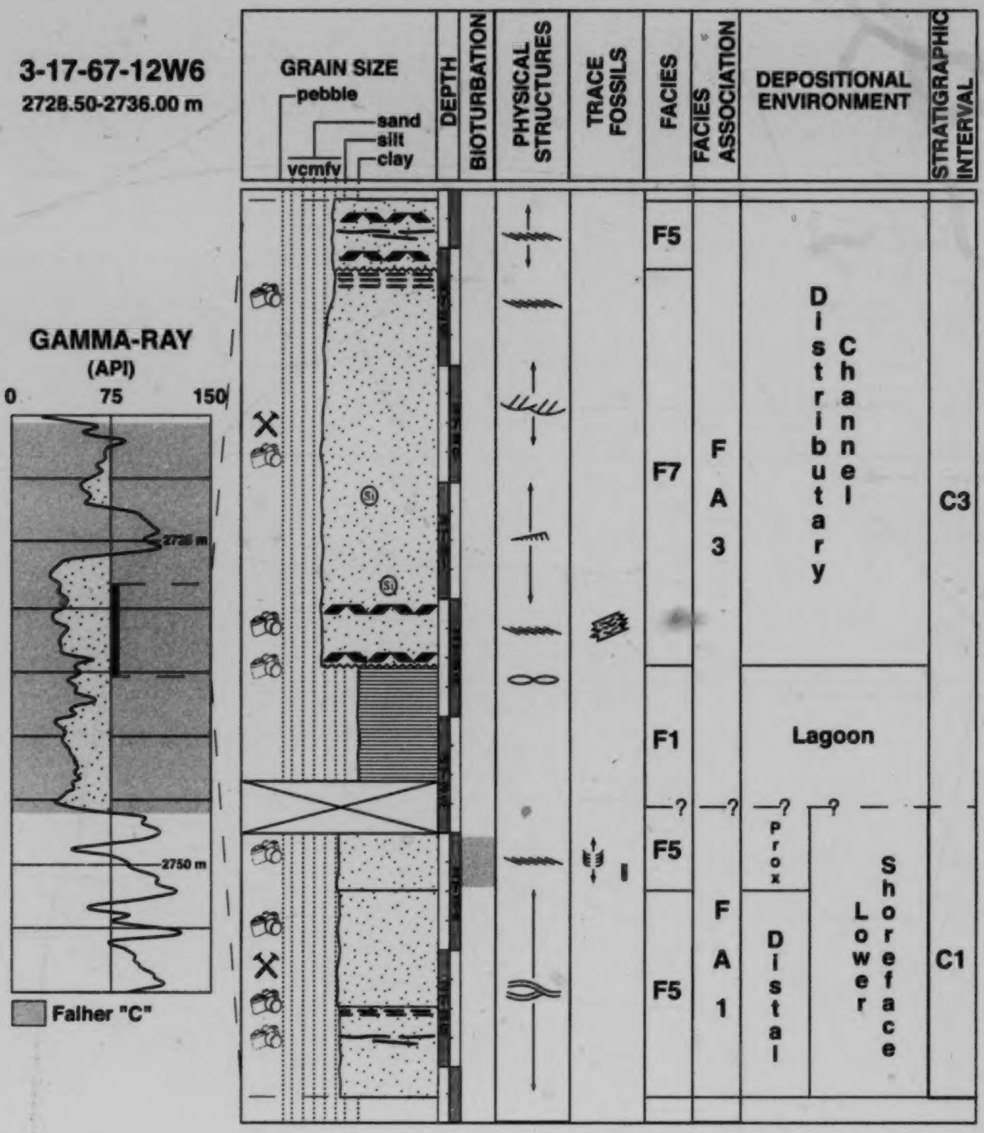

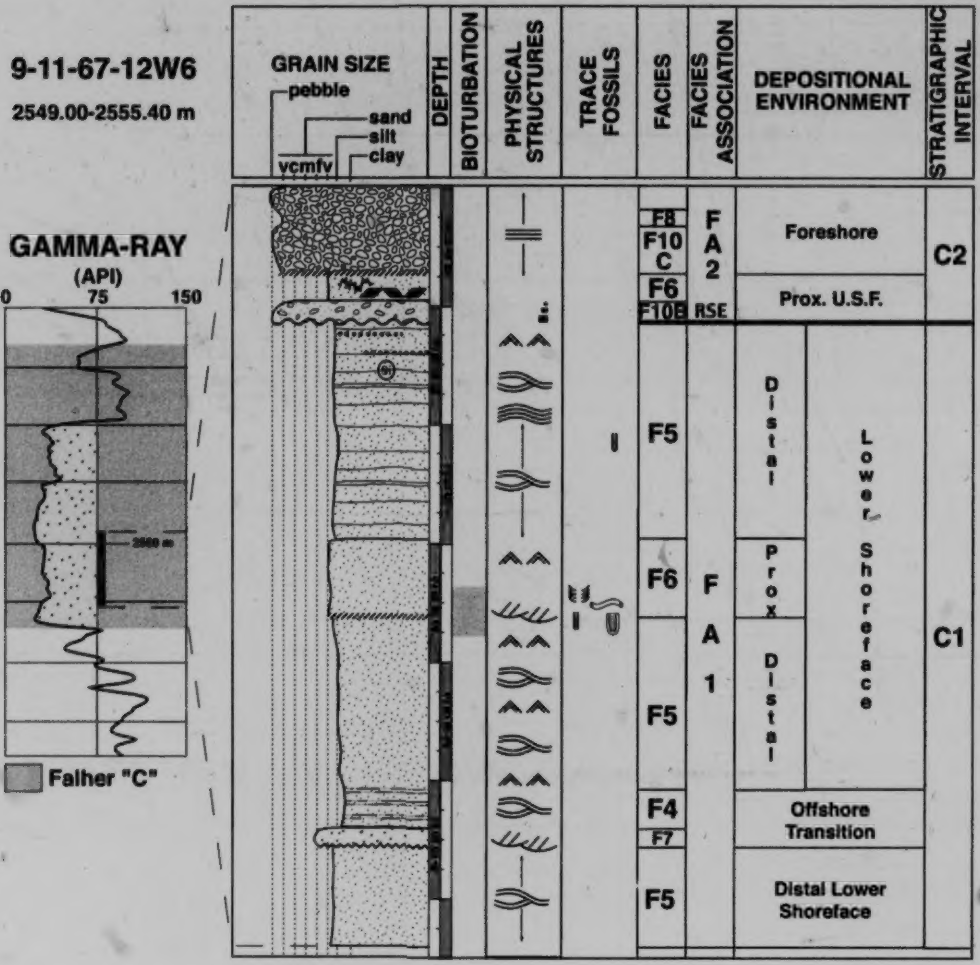
9-11-67-12W6
2549.00-2555.40 m
GAMMA-RAY
(API)
0
75
150
2550 m
Falher "C"
GRAIN SIZE
pebble
sand
silt
clay
vcmfv
DEPTH
BIOTURBATION
PHYSICAL STRUCTURES
TRACE FOSSILS
FACIES
FACIES ASSOCIATION
DEPOSITIONAL ENVIRONMENT
STRATIGRAPHIC INTERVAL
Si
F8
F10 C
F6
F10B
F5
F6
F5
F4
F7
F5
FA 2
RSE
FA 1
Foreshore
Prox. U.S.F.
Distal
Prox
Distal
Lower Shoreface
Offshore Transition
Distal Lower Shoreface
C2
C1

1-11-67-12W6

2548.00-2568 m

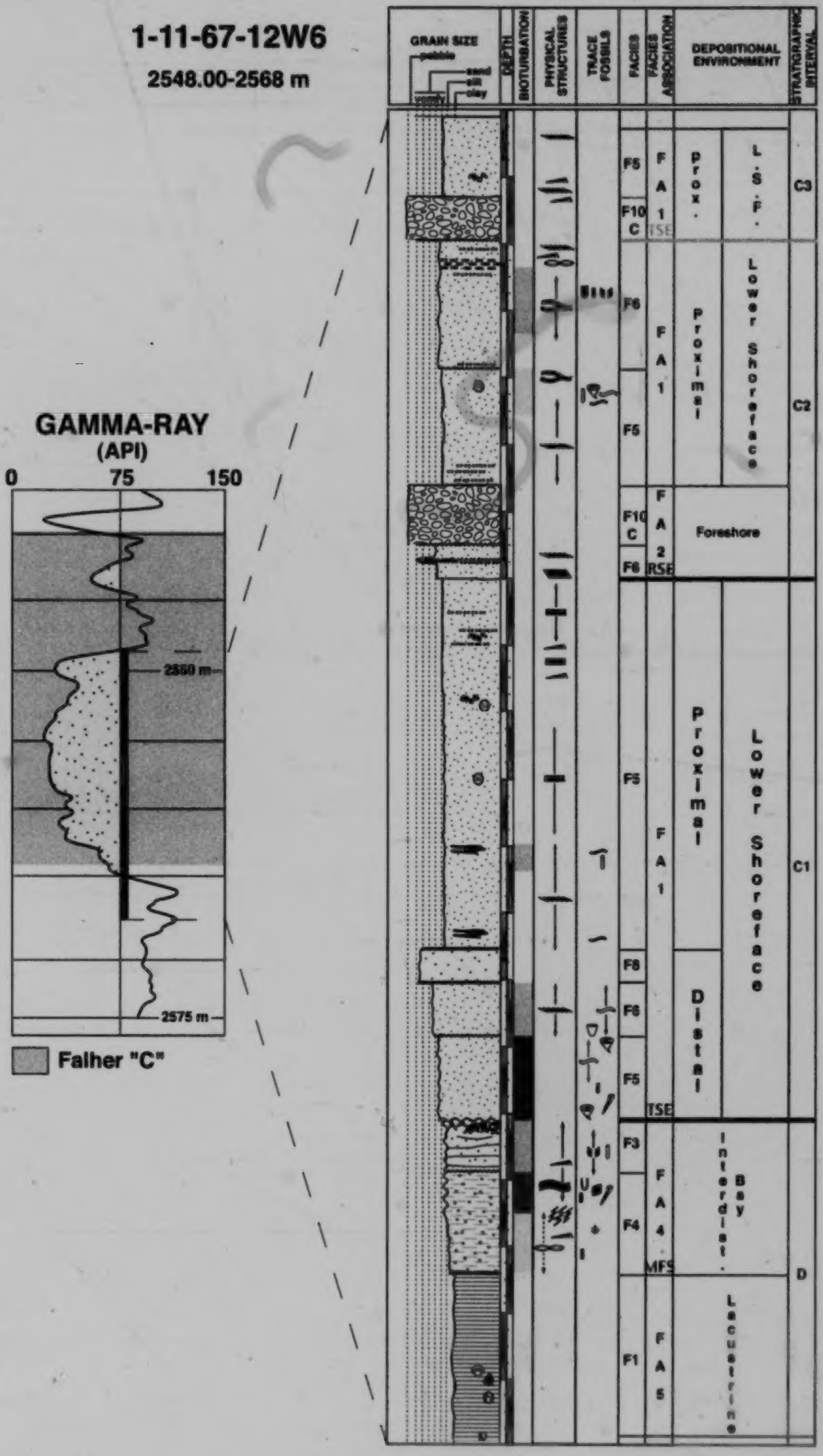

12-7-67-12W6

2746.25-2755.25 m

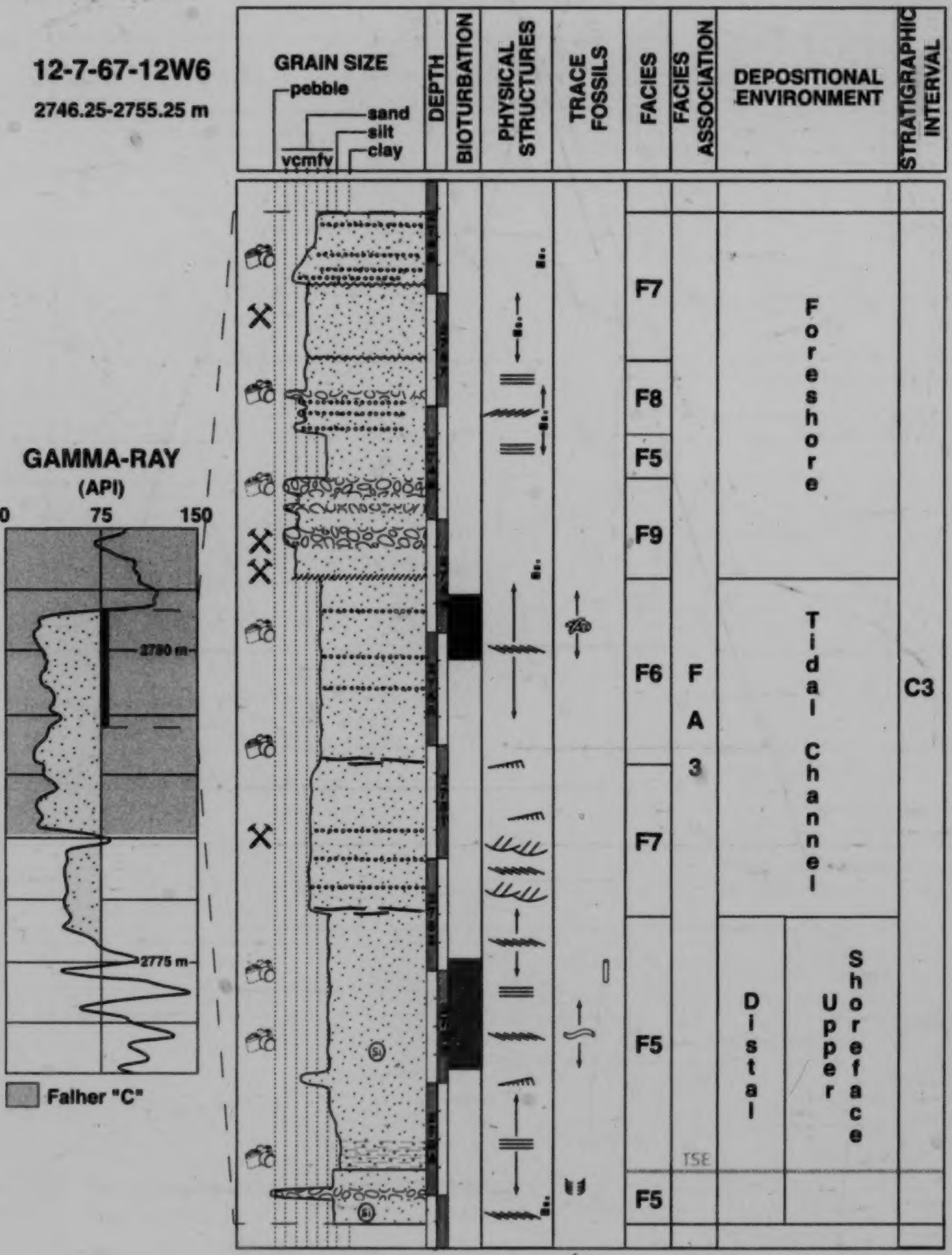

14-4-67-12W6

2680.75.00-2695.10 m

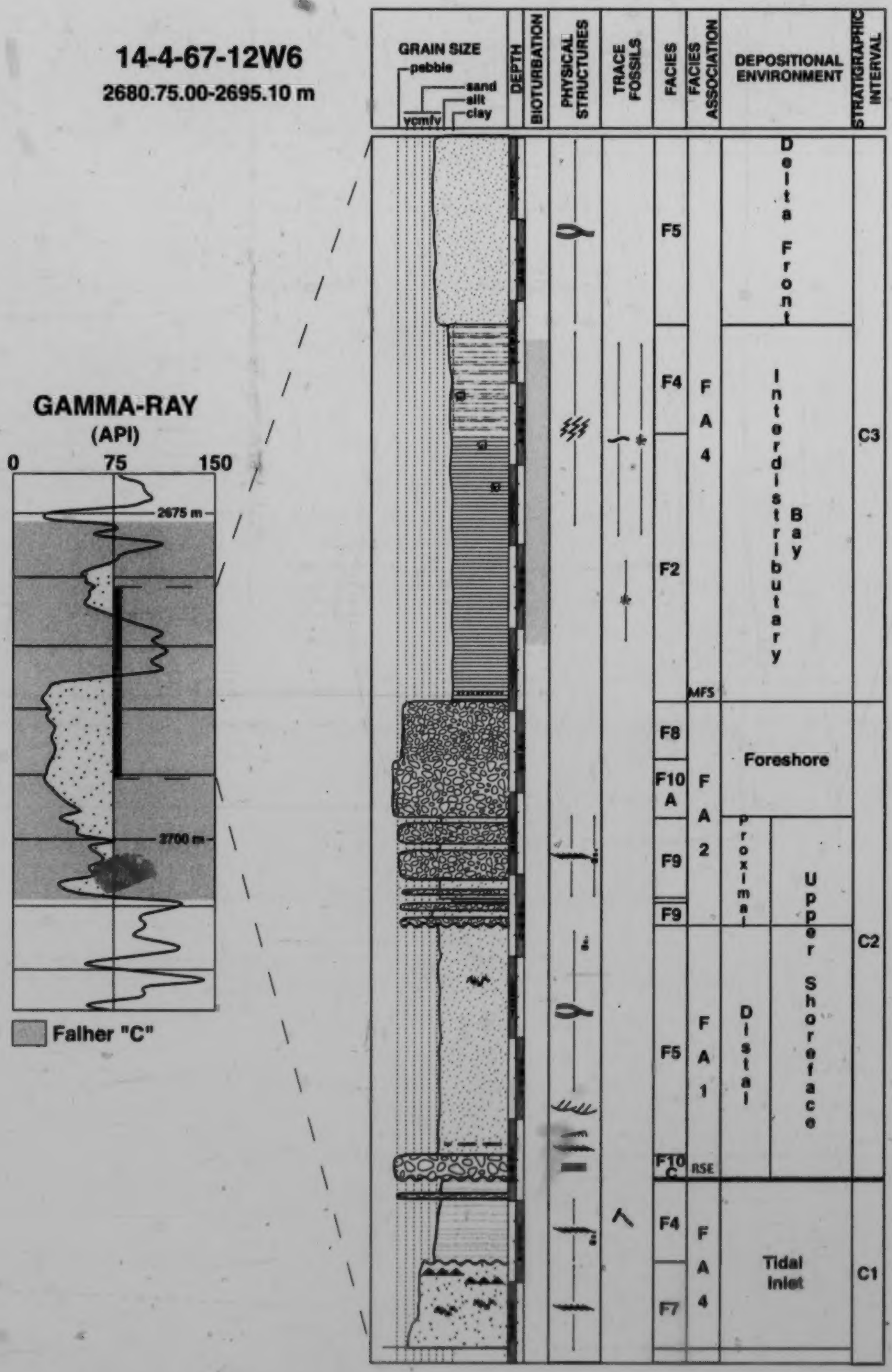

12-3-67-12W6

2613.00-2621.70 m

No Gamma-ray Log Available

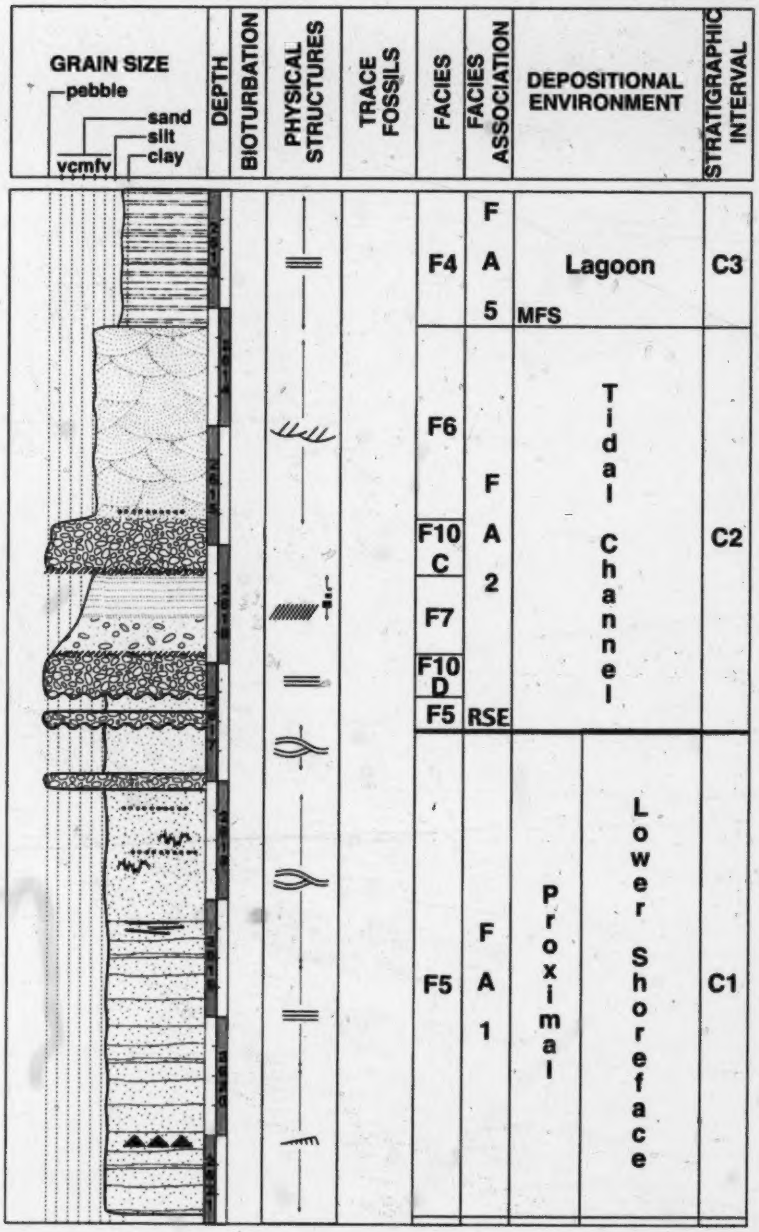

10-30-67-11W6

2421.00-2438.75 m

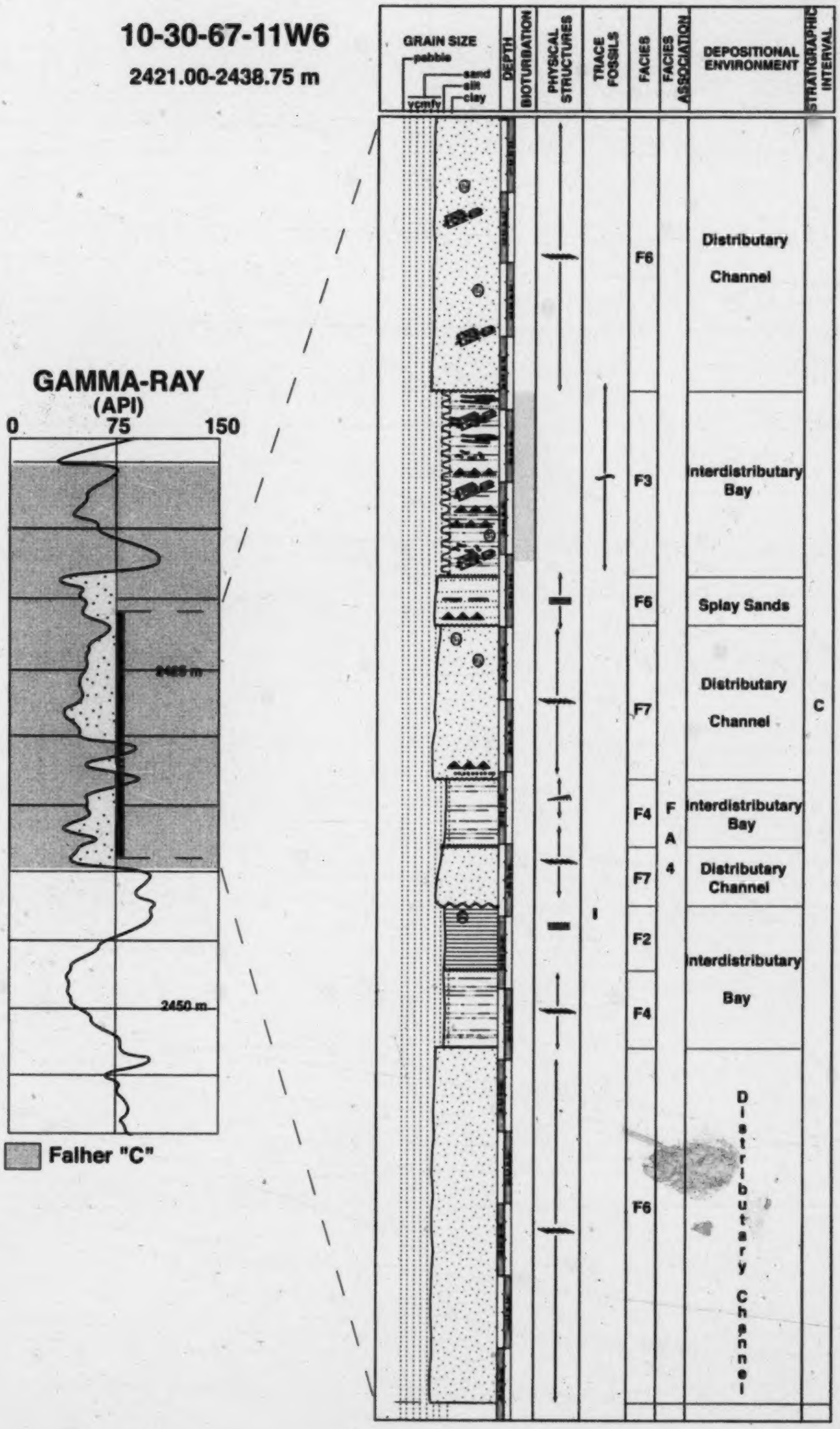

10-25-67-11W6

2406.00-2419.90 m

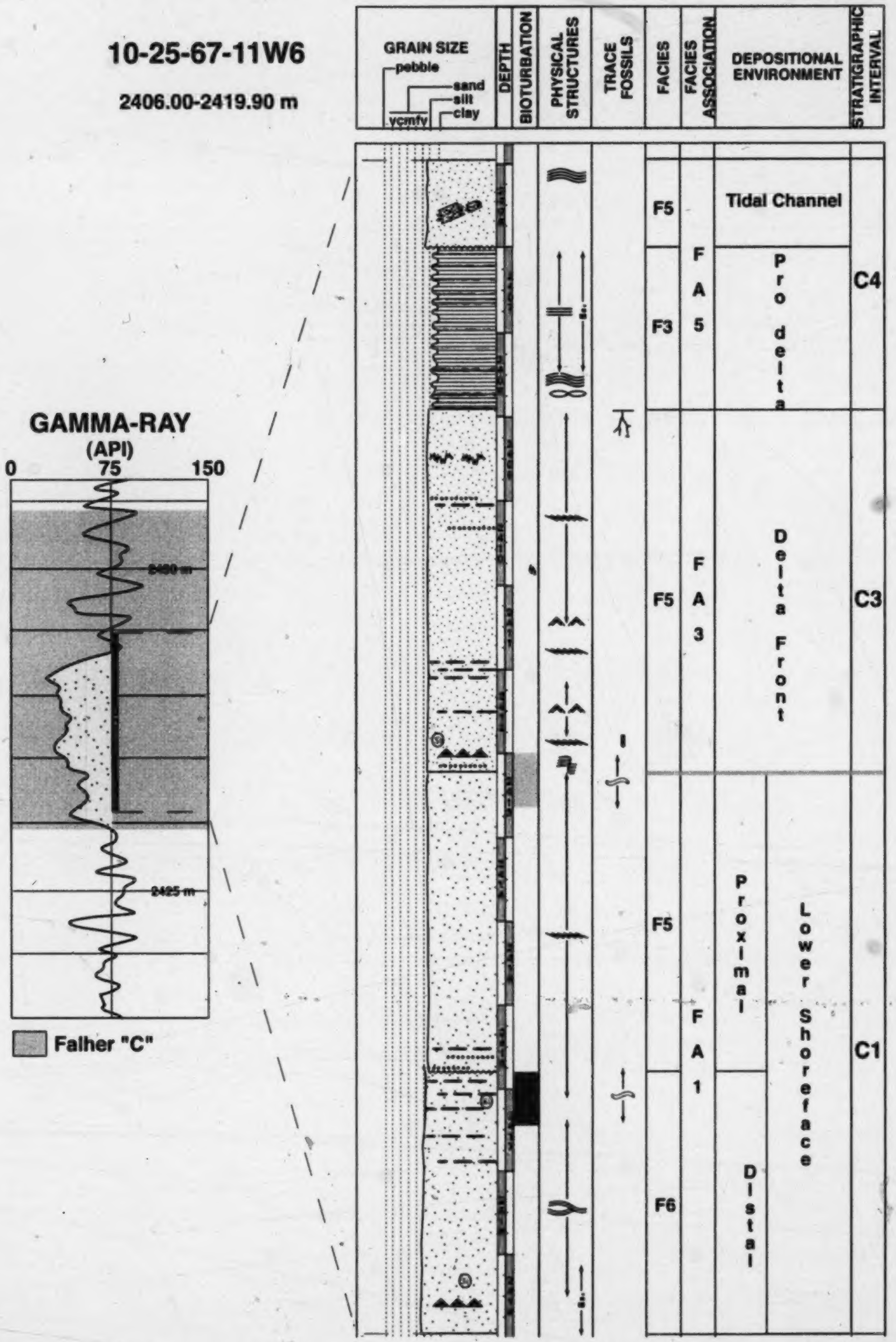

6-13-67-11W6

2438.00-2445.25 m

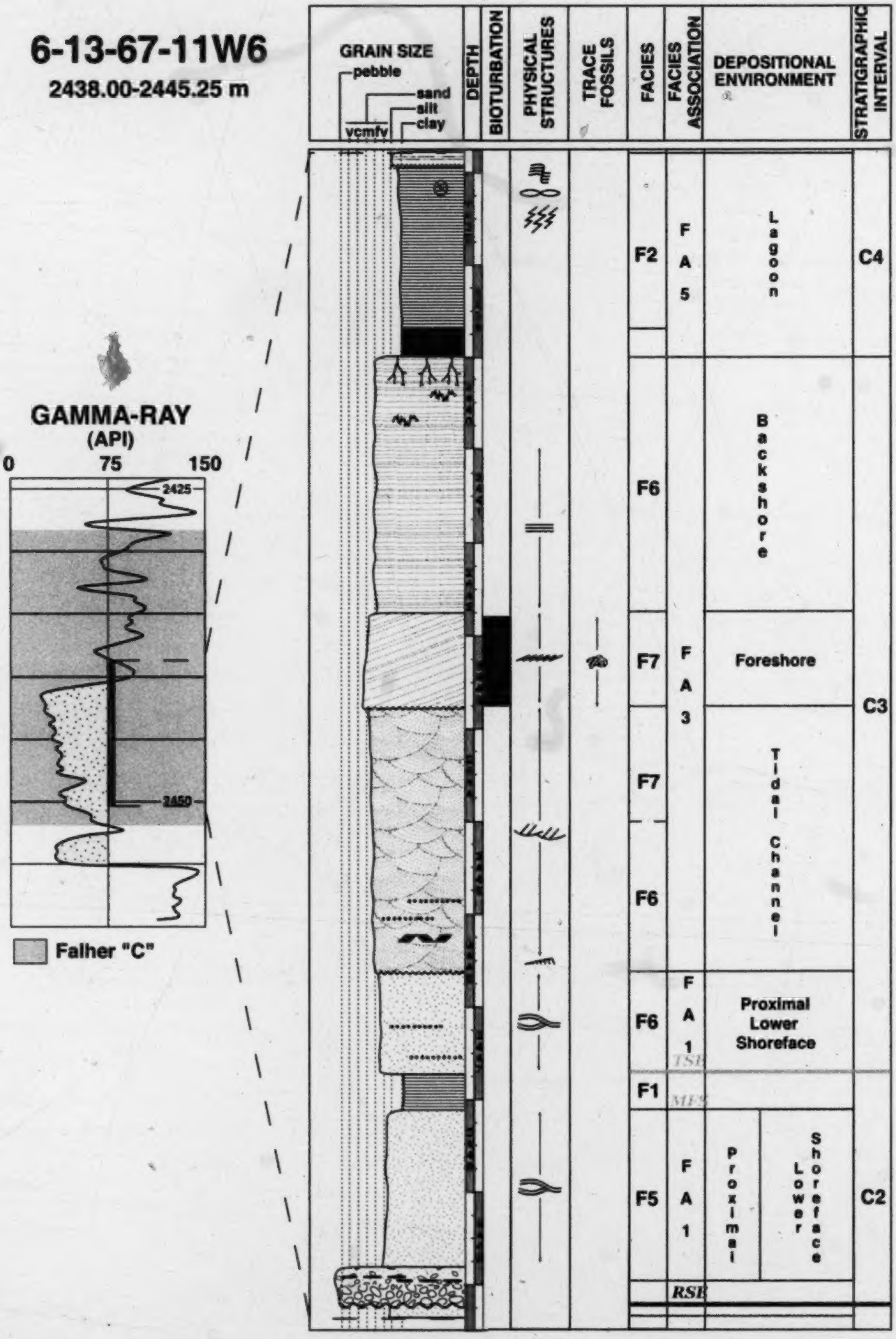

11-8-67-11W6

2500.00-2519.25 m

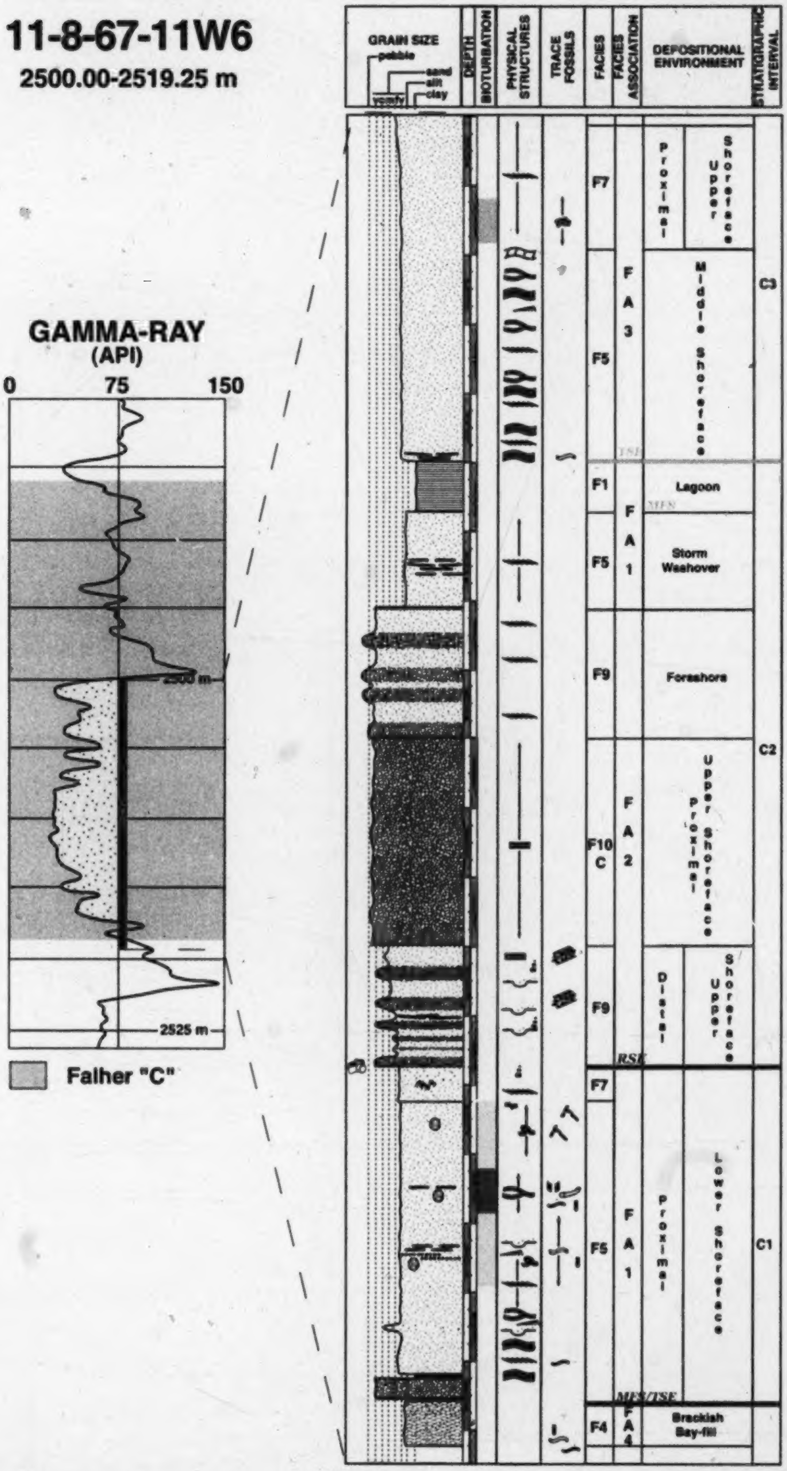

10-29-67-10W6

2386.00 - 2397.00 m

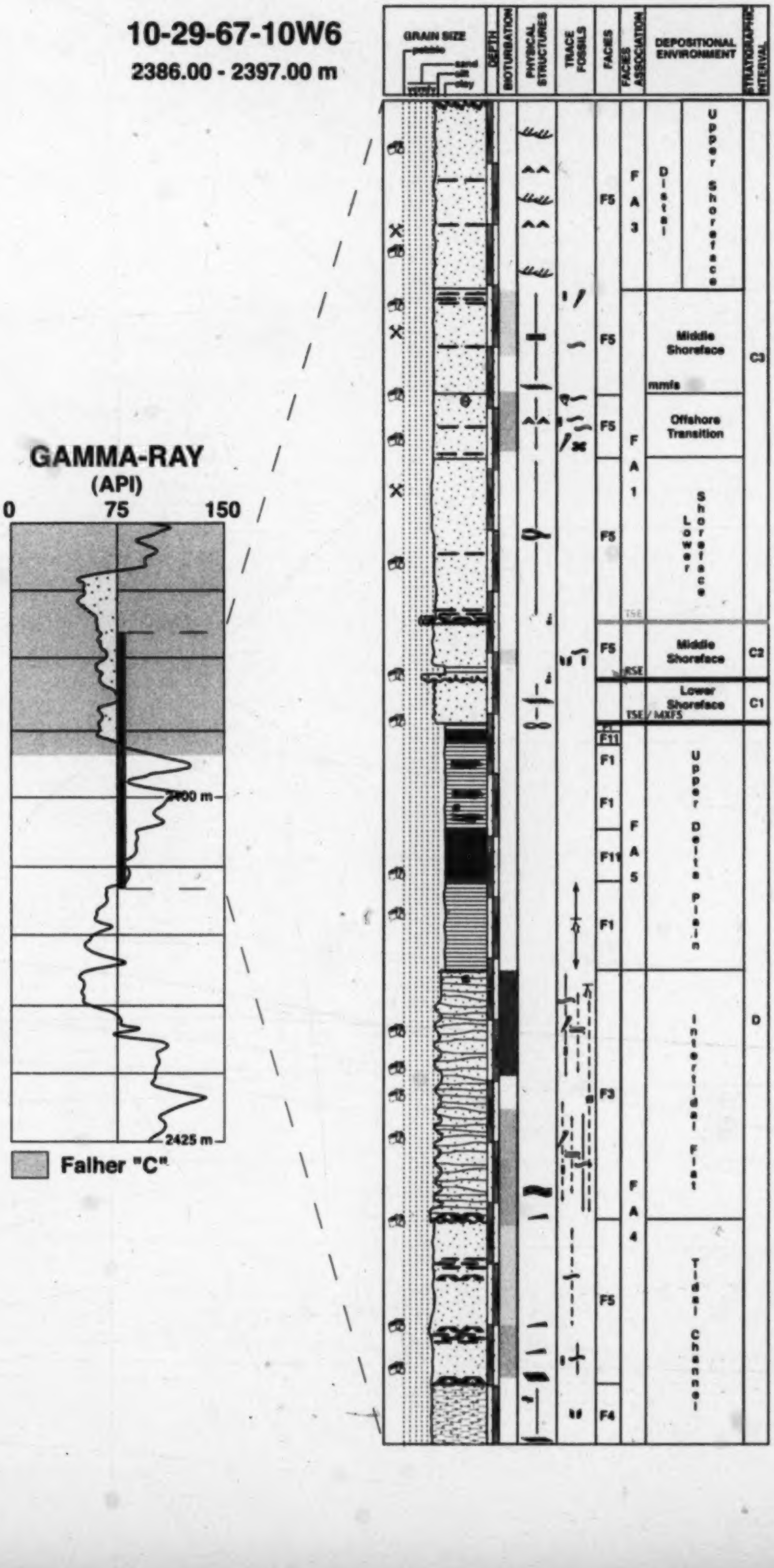

7-24-67-10W6

2318.00-2337.50 m

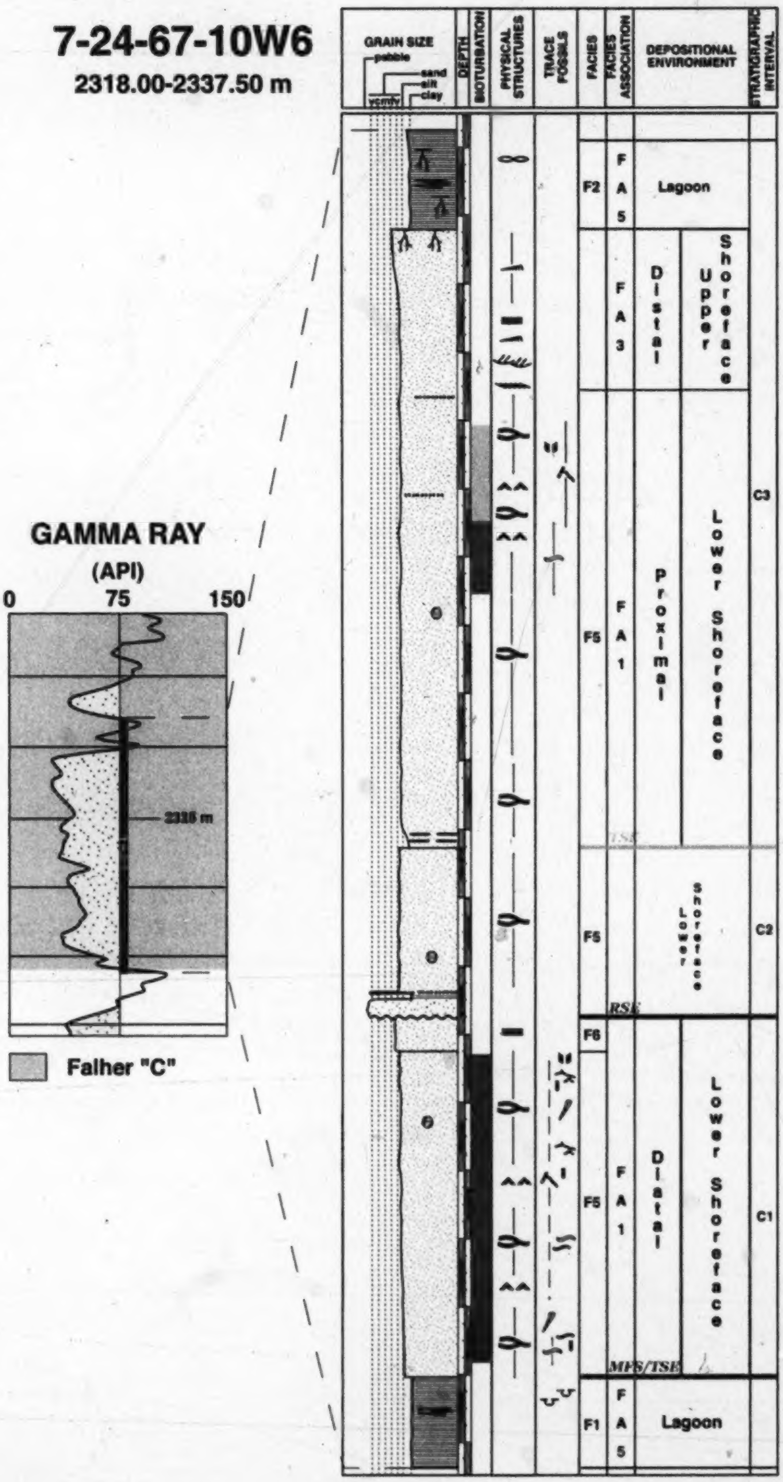

6-21-67-10W6

2453.10 - 2473.00 m

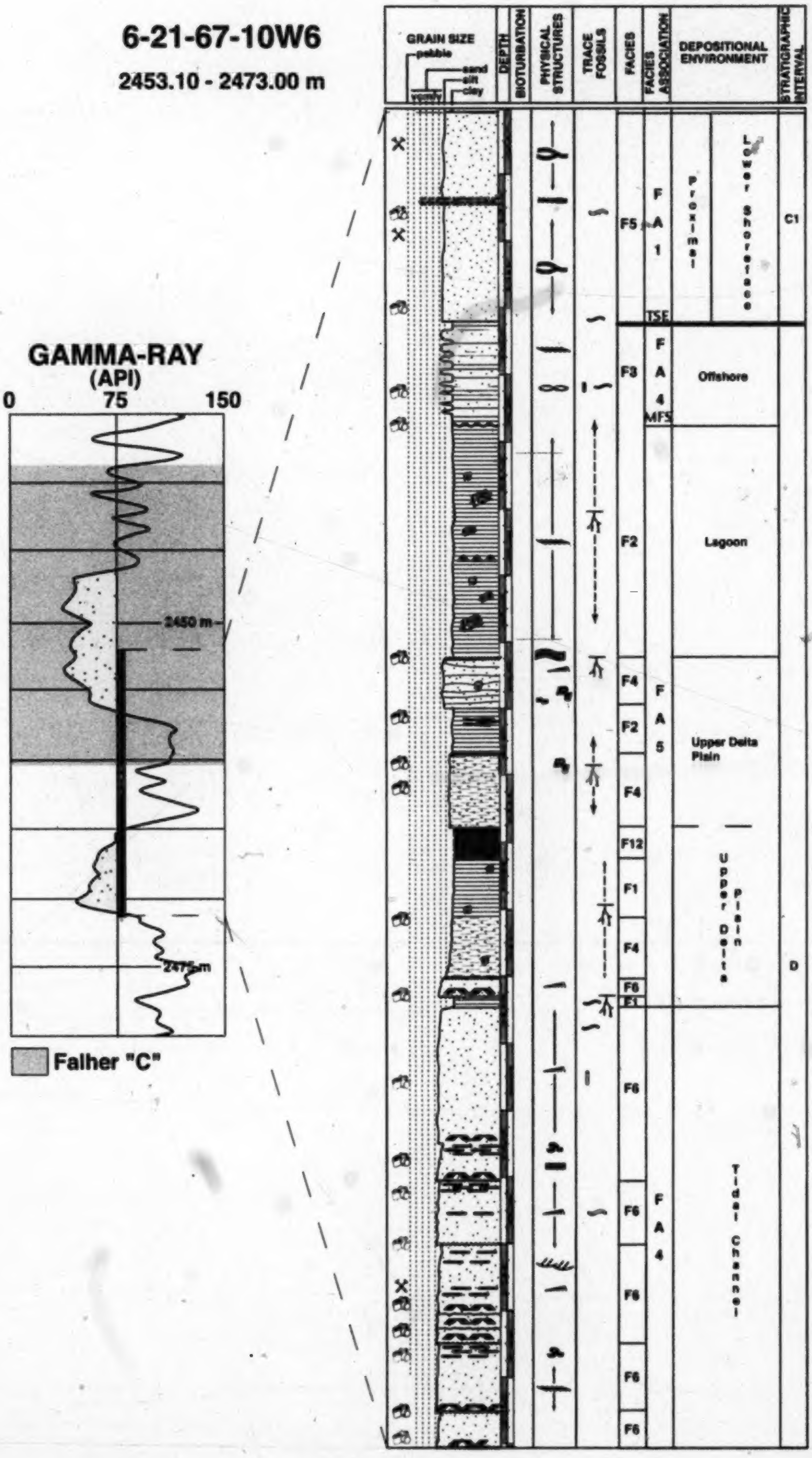

7-18-67-10W6
2438.80-2455.75 m

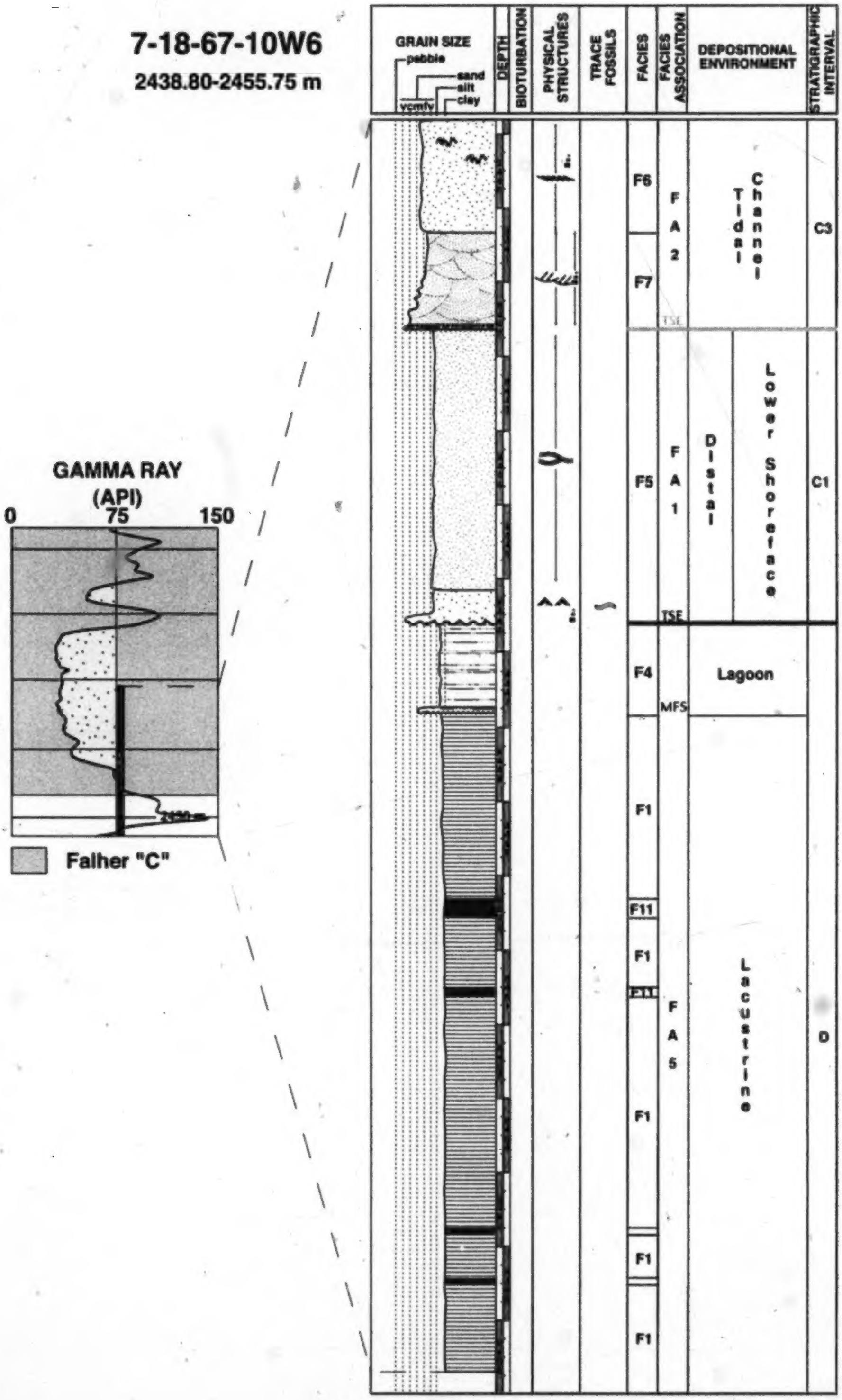

7-15-67-10W6

2516.00-2534.00 m

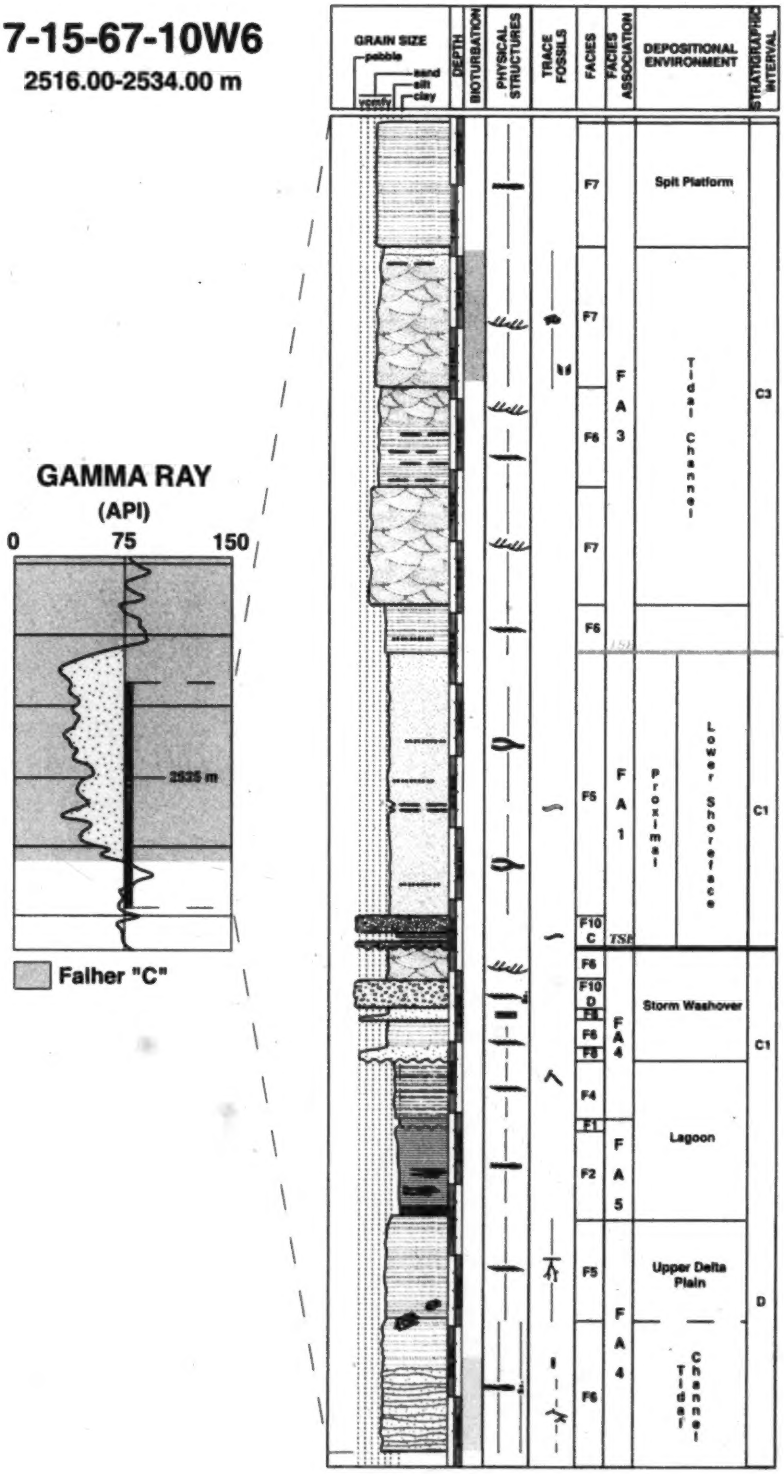

10-12-67-10W6
2475.00 - 2485.00 m

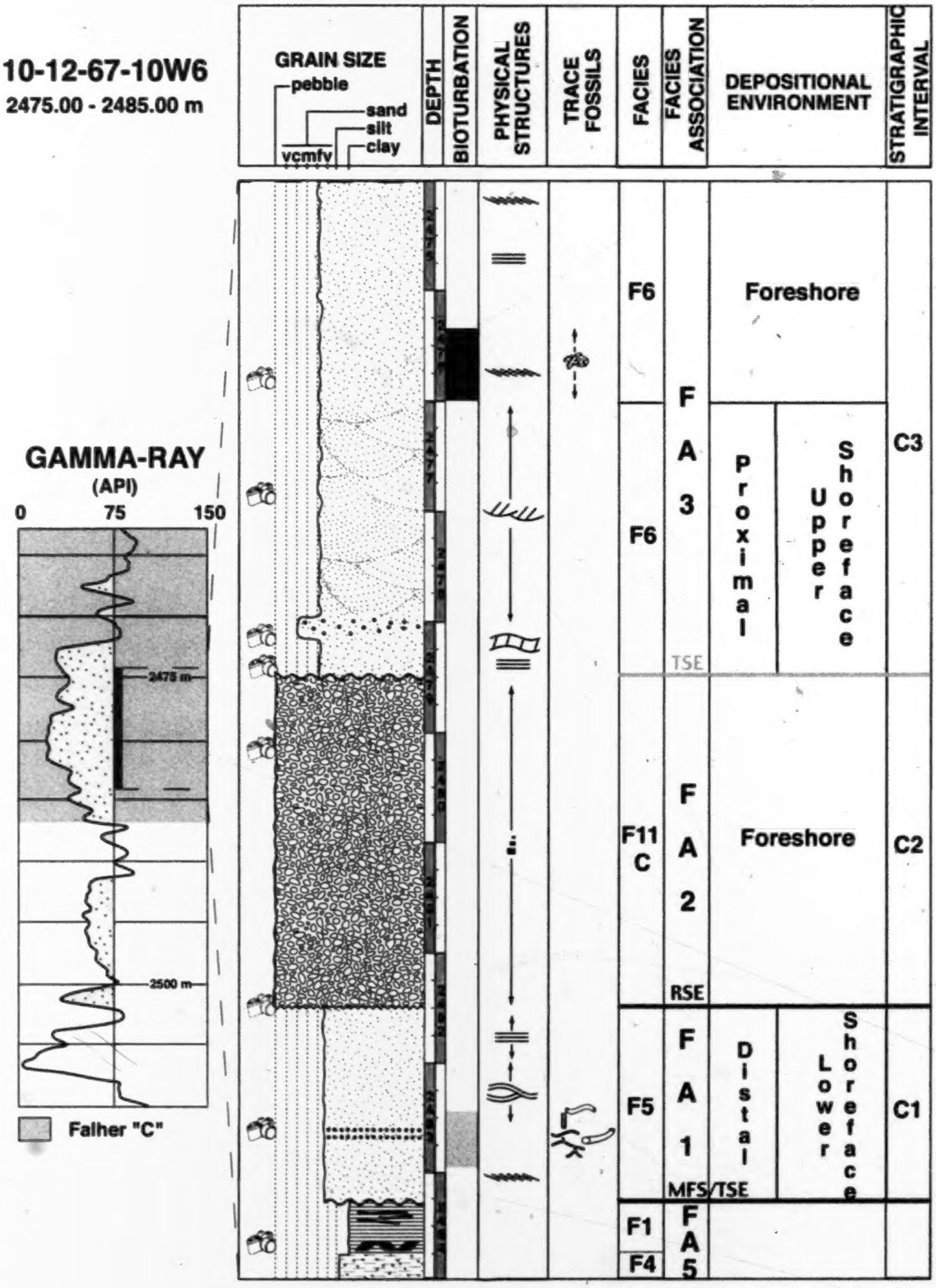

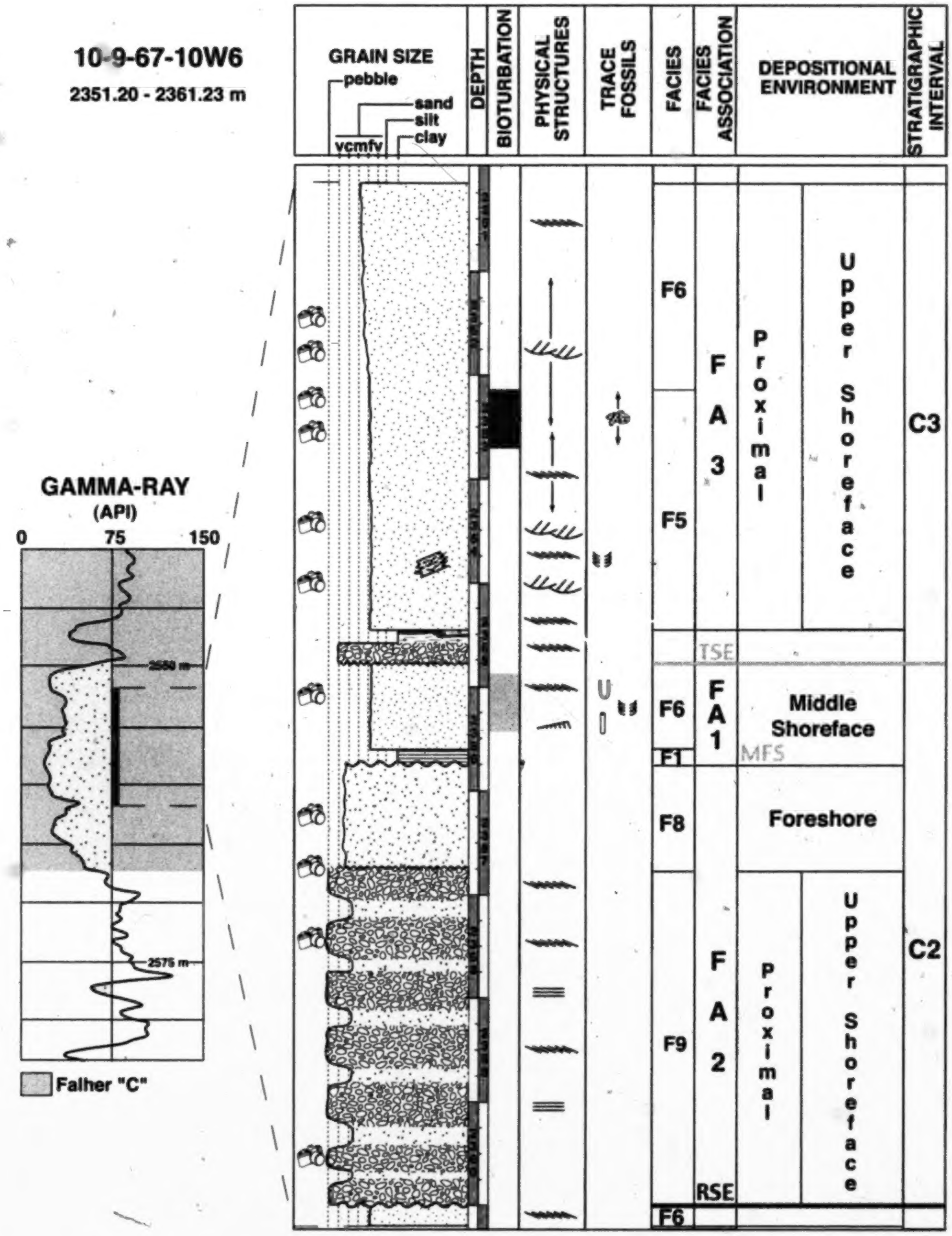
10-9-67-10W6
2351.20 - 2361.23 m
GAMMA-RAY
(API)
0
75
150
2550 m
2575 m
Falher "C"
GRAIN SIZE
pebble
sand
silt
clay
vcmfv
DEPTH
BIOTURBATION
PHYSICAL STRUCTURES
TRACE FOSSILS
FACIES
FACIES ASSOCIATION
DEPOSITIONAL ENVIRONMENT
STRATIGRAPHIC INTERVAL
F6
F5
FA3
Proximal
Upper Shoreface
C3
TSE
F6
FA1
Middle Shoreface
F1
MFS
F8
Foreshore
F9
FA2
Proximal
Upper Shoreface
C2
RSE
F6

10-4-67-10W6

2477.00-2479.00 m

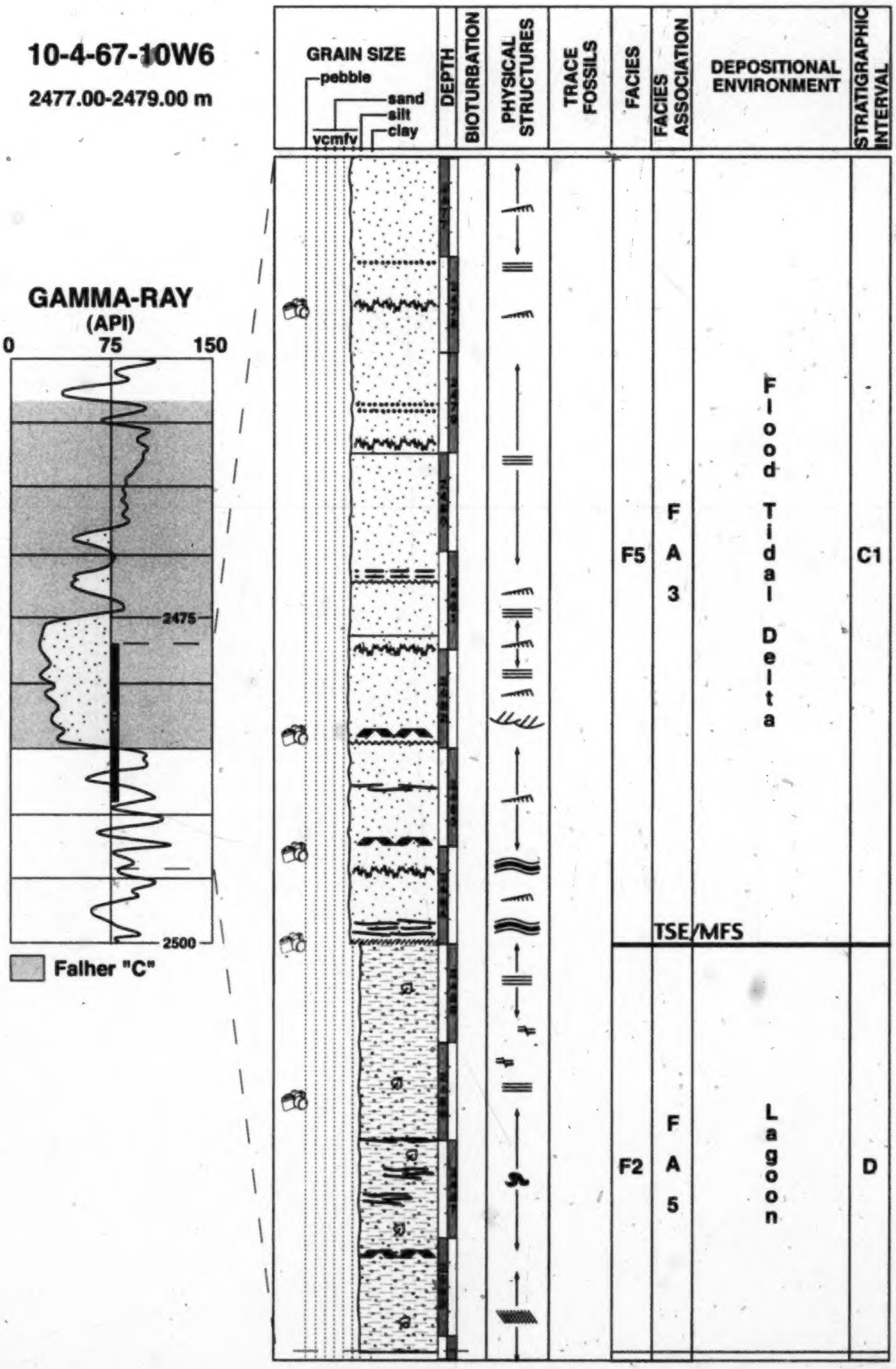

5-18-67-9W6
2368.00-2381.00 m

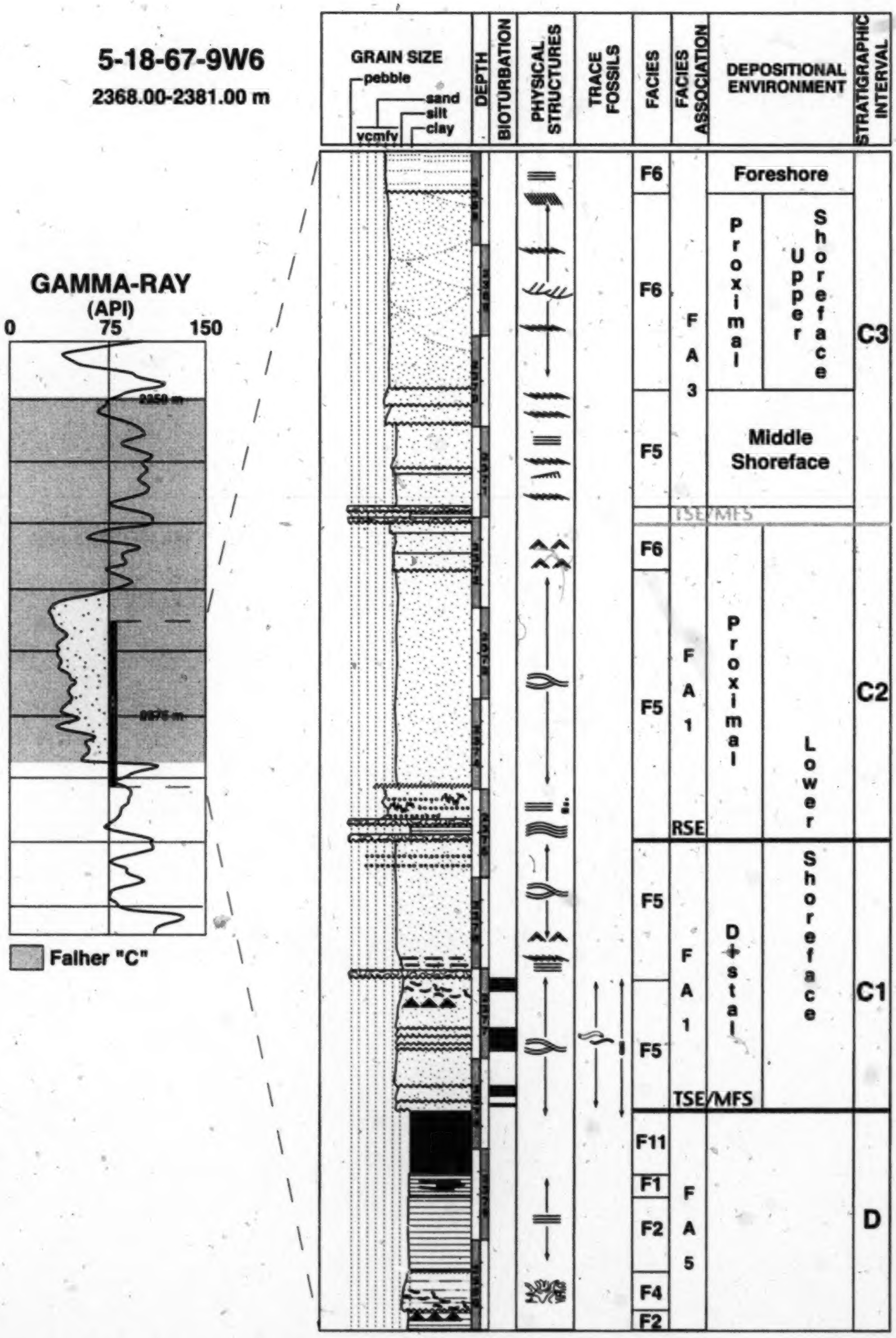

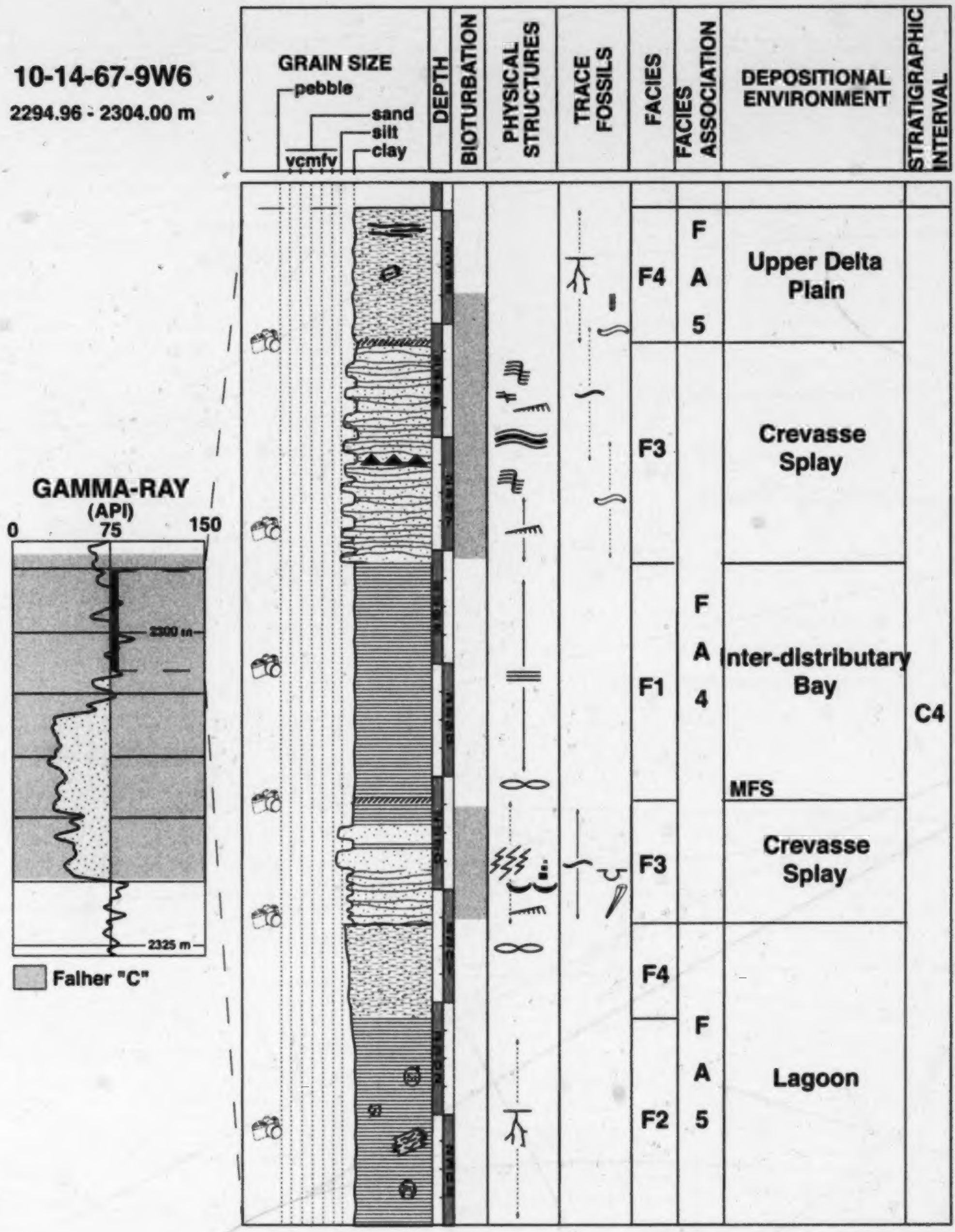
10-14-67-9W6
2294.96 - 2304.00 m
GRAIN SIZE
pebble
sand
silt
clay
vcmfv
DEPTH
BIOTURBATION
PHYSICAL STRUCTURES
TRACE FOSSILS
FACIES
FACIES ASSOCIATION
DEPOSITIONAL ENVIRONMENT
STRATIGRAPHIC INTERVAL
F4
FA5
Upper Delta Plain
F3
Crevasse Splay
F1
FA4
Inter-distributary Bay
C4
MFS
F3
Crevasse Splay
F4
F2
FA5
Lagoon
GAMMA-RAY
(API)
0
75
150
2300 m
2325 m
Falher "C"

6-8-67-9W6
2385.25-2339.75 m

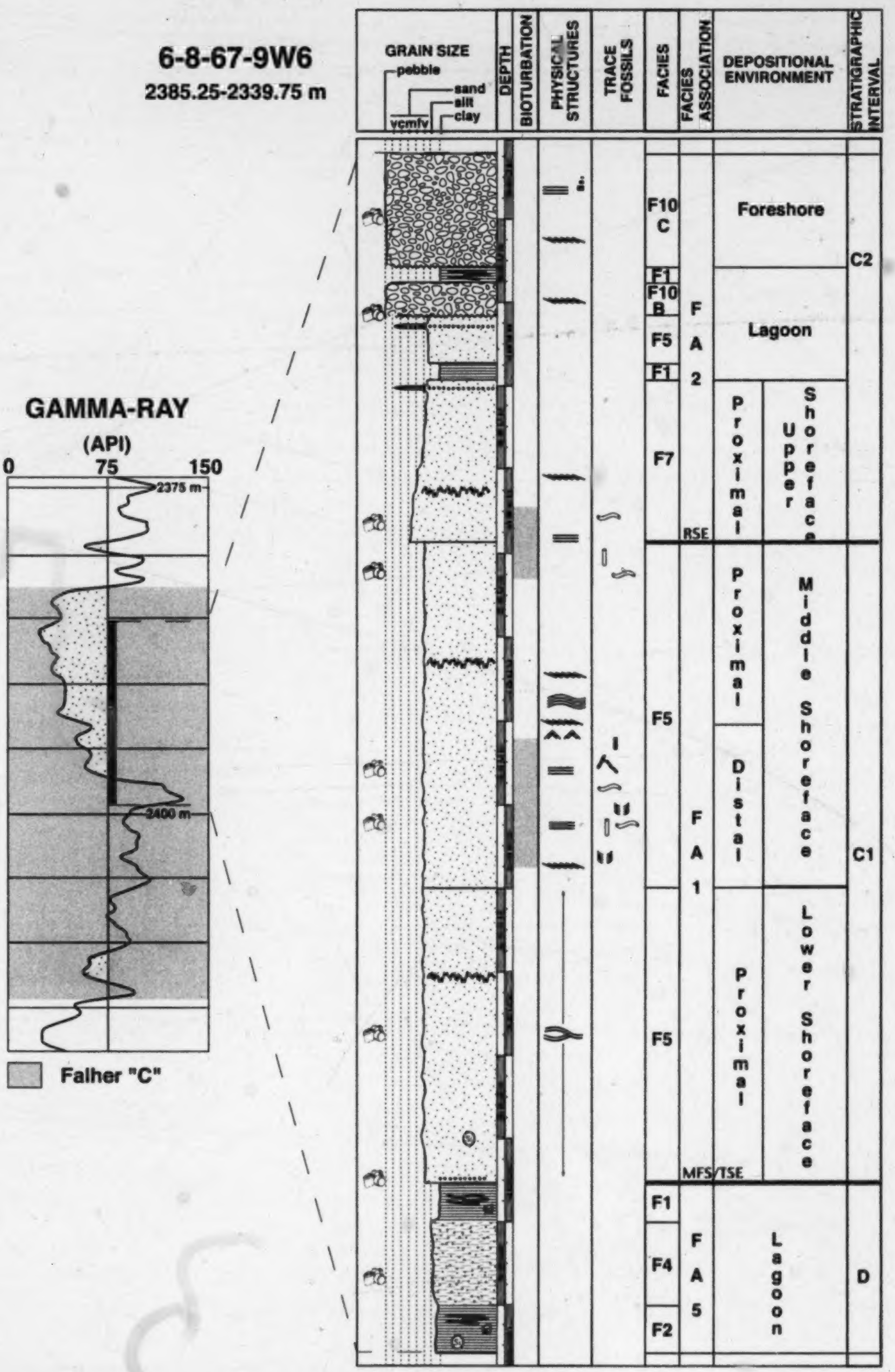

10-16-67-8W6

2250.75-2268.00 m

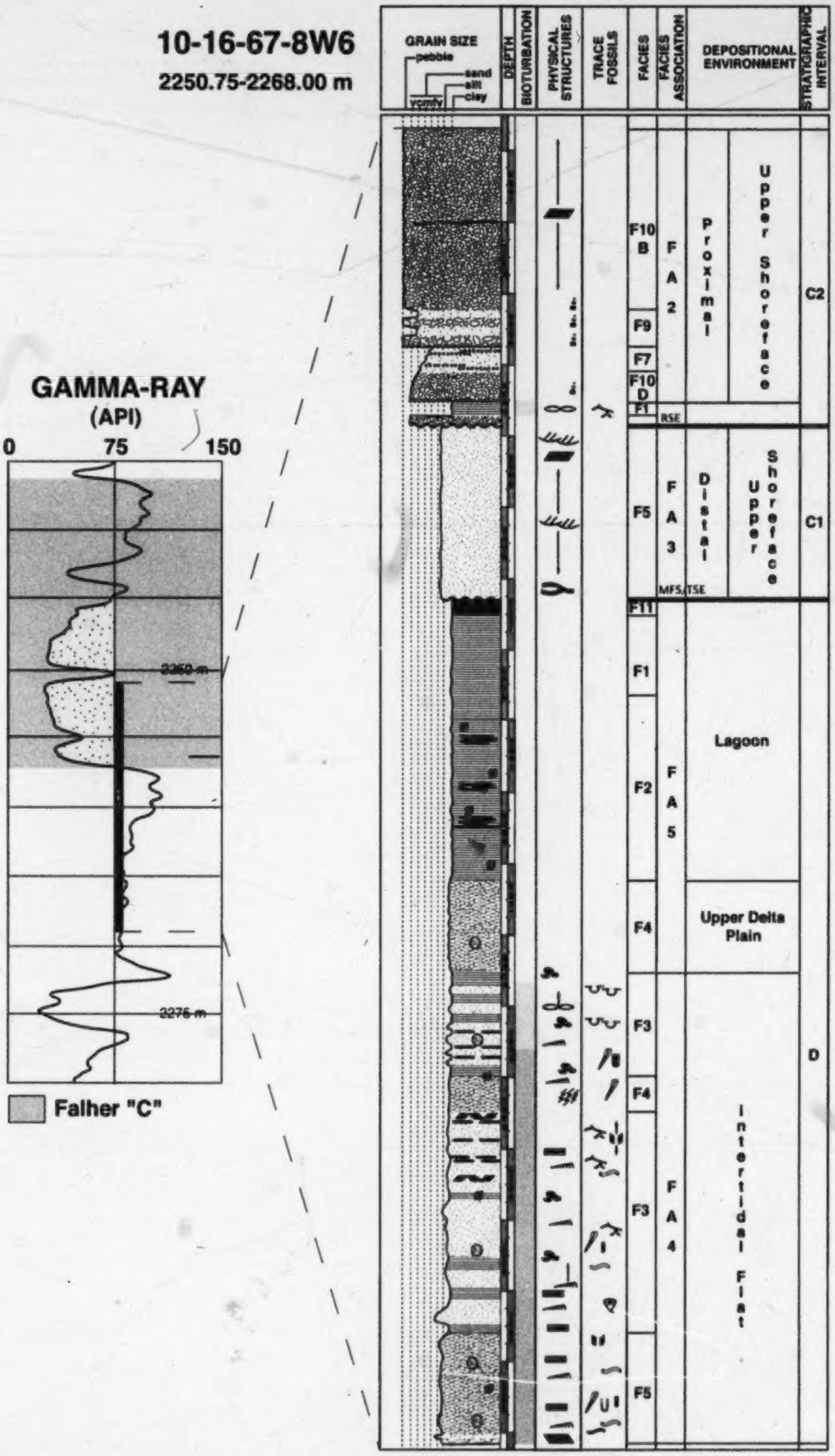

11-22-67-7W6
2083.75-2103.00 m

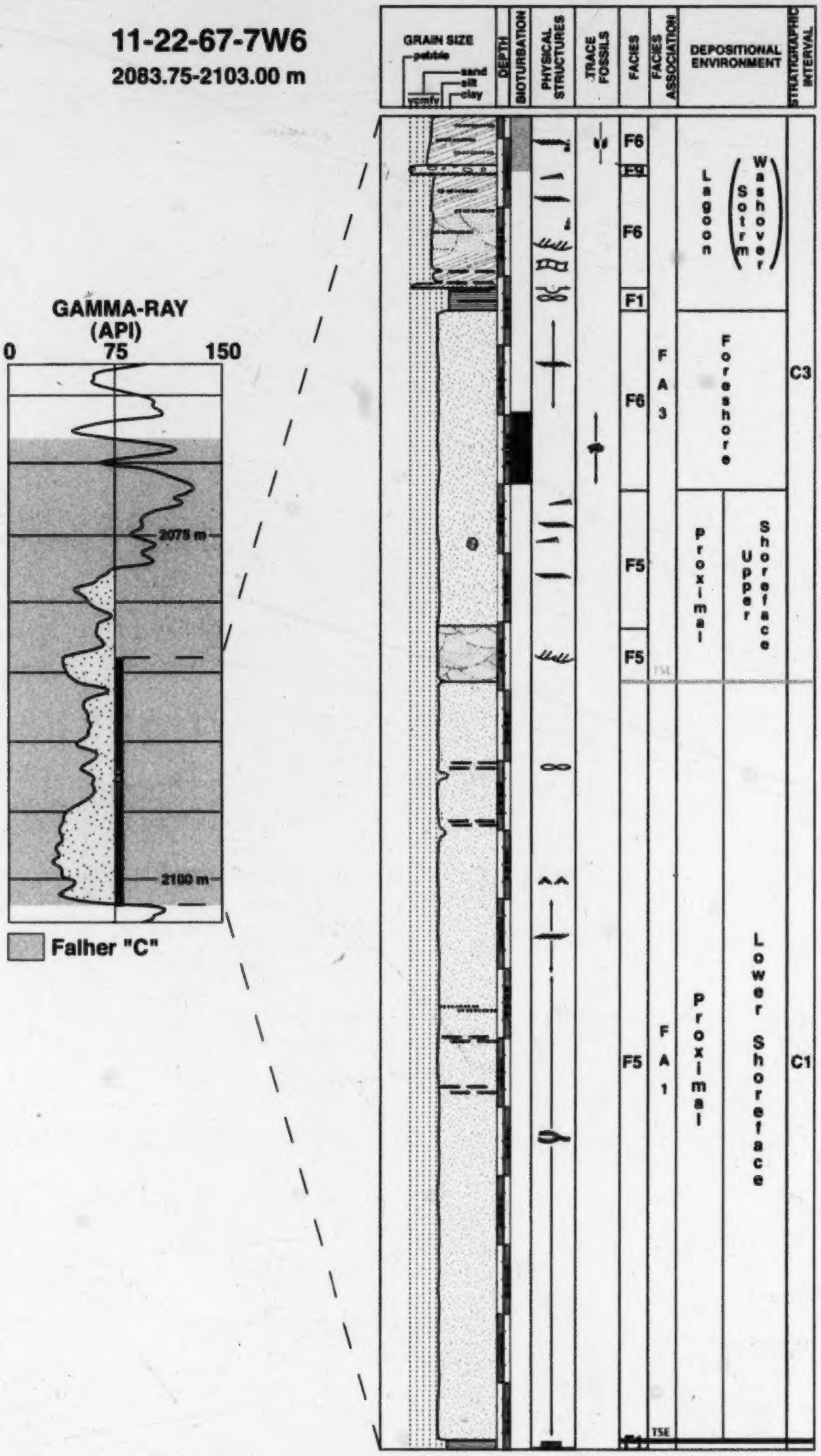

10-17-67-7W6

2160.25-2174.00 m

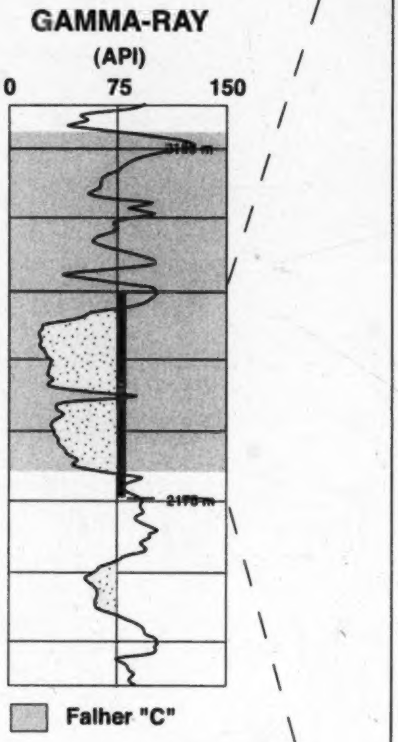

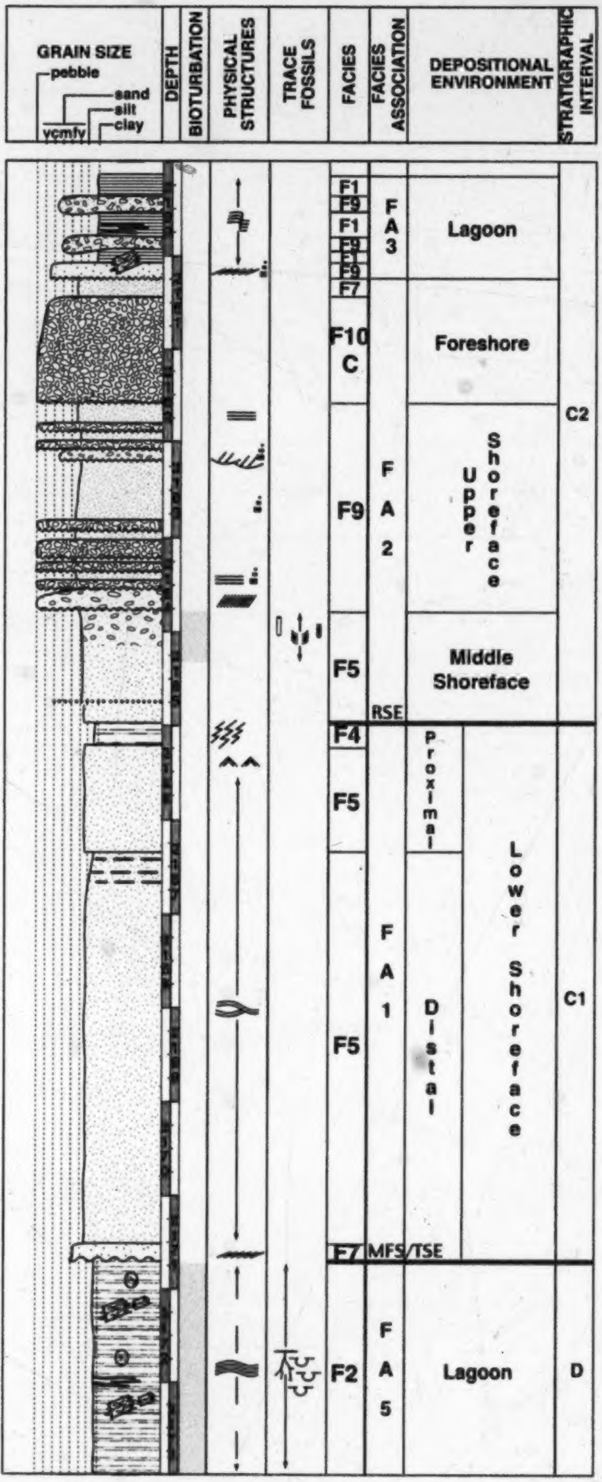

1-15-67-7W6

2121.90-2135.00 m

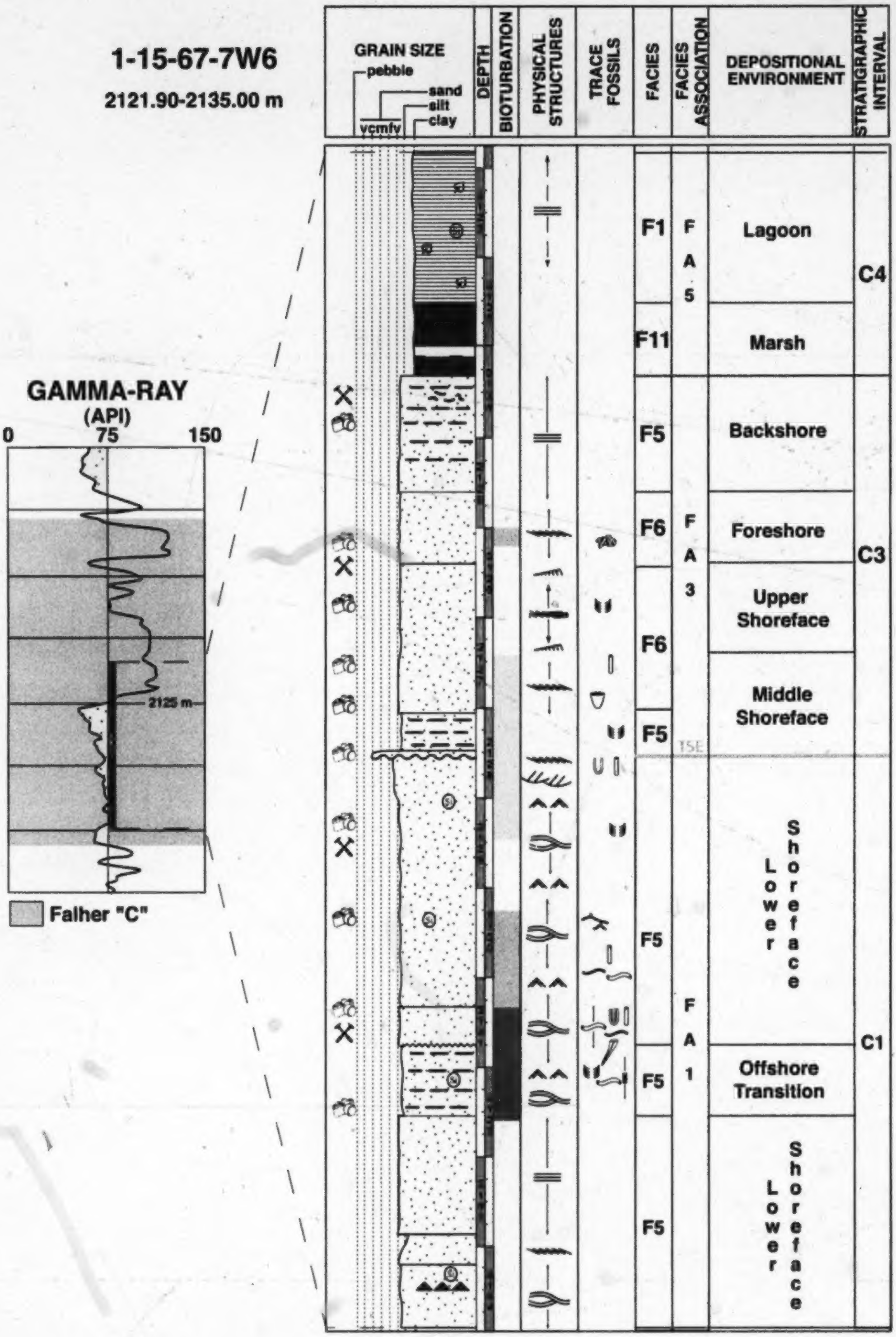

12-14-67-7W6

2102.00-2115.00 m

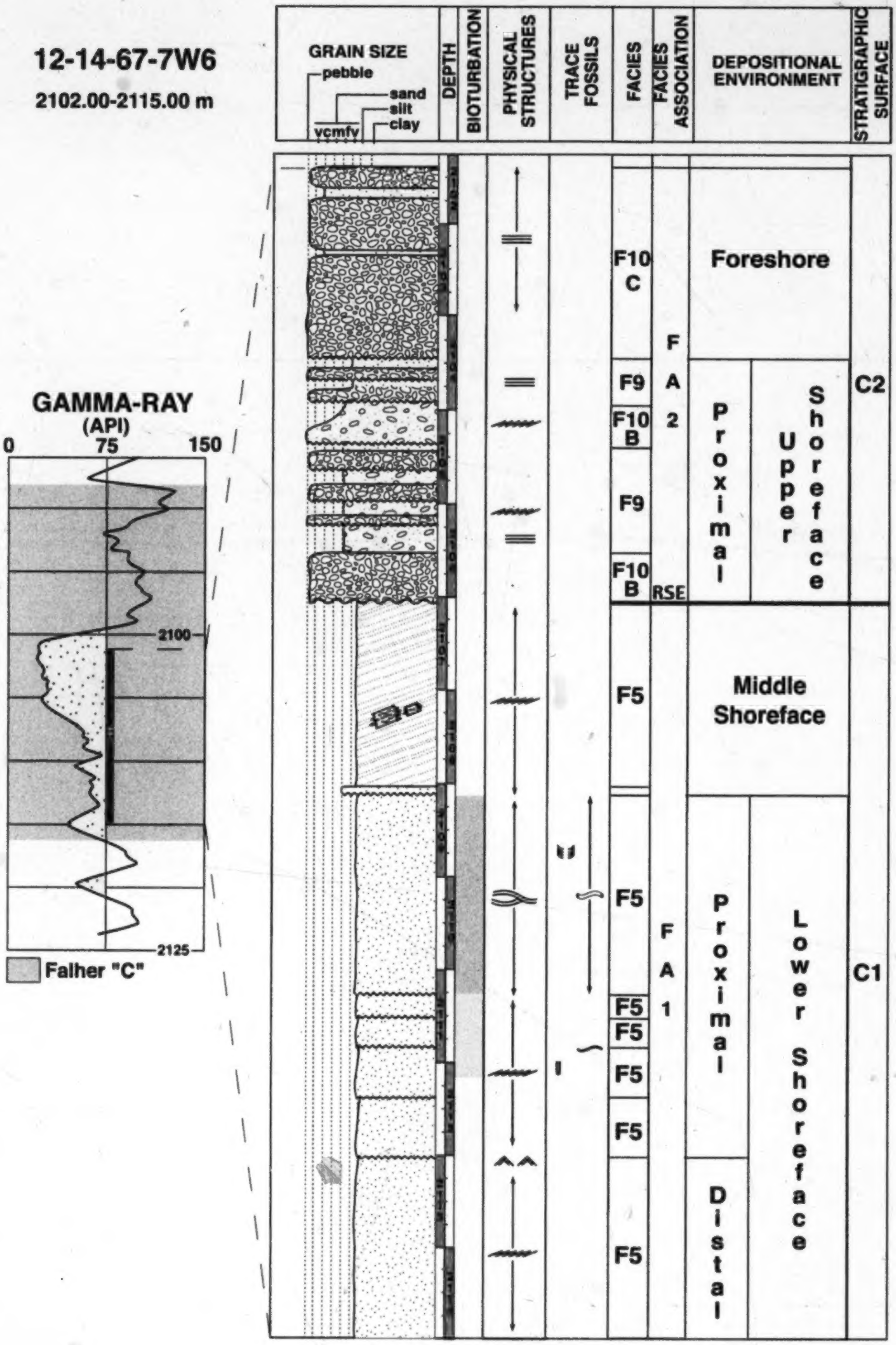

APPENDIX II: Cross Sections

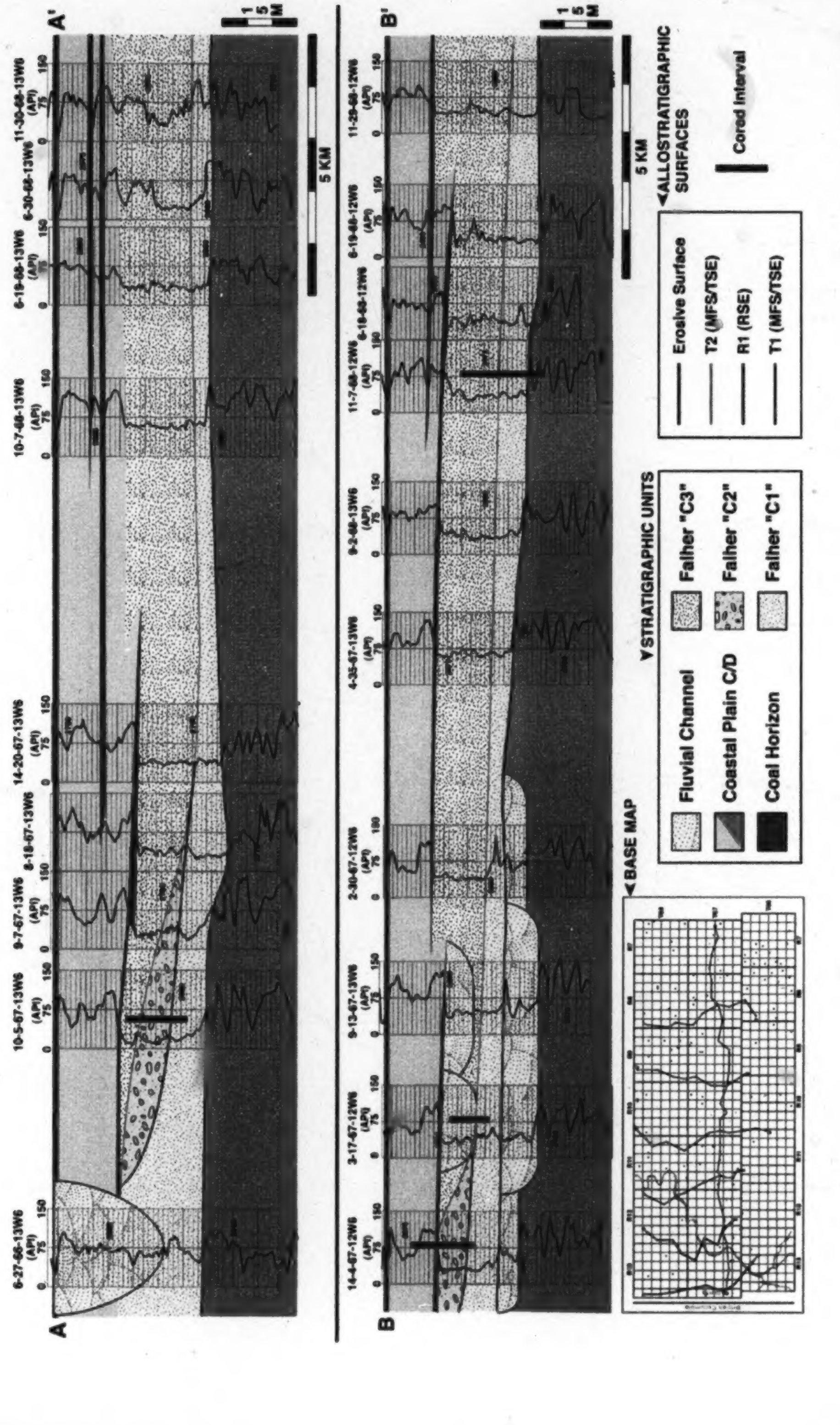
A
A'
6-27-66-13W6
10-5-67-13W6
9-7-67-13W6
8-18-67-13W6
14-20-67-13W6
10-7-68-13W6
6-19-68-13W6
6-30-68-13W6
11-30-68-13W6
(API)
0
75
150
1
5
M
5 KM
B
B'
14-4-67-12W6
3-17-67-12W6
9-13-67-13W6
2-30-67-12W6
4-35-67-13W6
9-2-68-13W6
11-7-68-12W6
6-18-68-12W6
6-19-68-12W6
11-29-68-12W6
BASE MAP
STRATIGRAPHIC UNITS
Fluvial Channel
Coastal Plain C/D
Coal Horizon
Falher "C3"
Falher "C2"
Falher "C1"
ALLOSTRATIGRAPHIC SURFACES
Erosive Surface
T2 (MFS/TSE)
R1 (RSE)
T1 (MFS/TSE)
Cored Interval

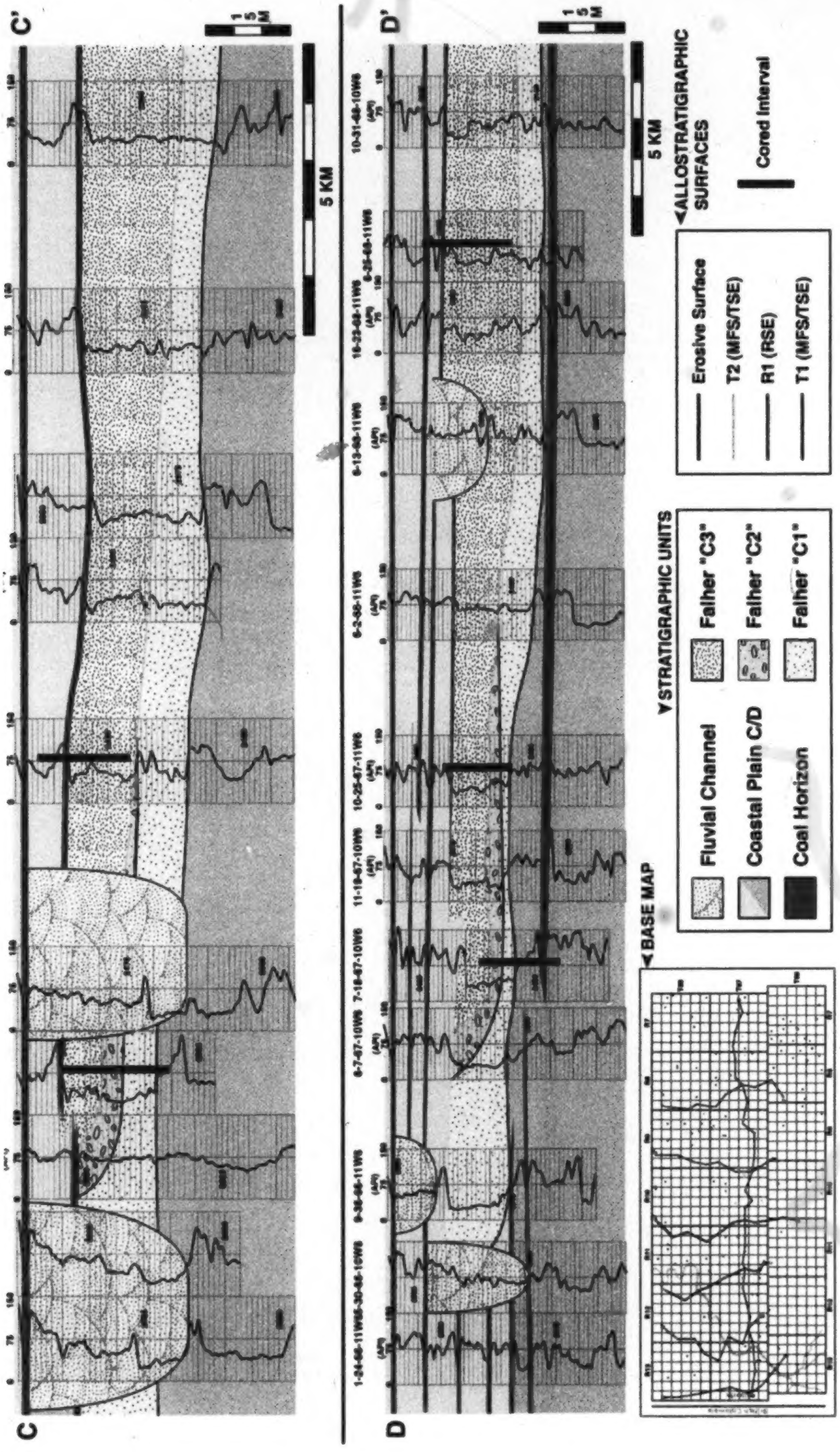
C
C'
D
D'
1
5
M
5 KM
(API)
0
75
150
1-24-66-11W6
6-30-66-10W6
9-36-66-11W6
6-7-67-10W6
7-18-67-10W6
11-19-67-10W6
10-25-67-11W6
6-2-68-11W6
6-13-68-11W6
16-23-68-11W6
6-25-68-11W6
10-31-68-10W6
BASE MAP
STRATIGRAPHIC UNITS
Fluvial Channel
Coastal Plain C/D
Coal Horizon
Falher "C3"
Falher "C2"
Falher "C1"
ALLOSTRATIGRAPHIC SURFACES
Erosive Surface
T2 (MFS/TSE)
R1 (RSE)
T1 (MFS/TSE)
Cored Interval

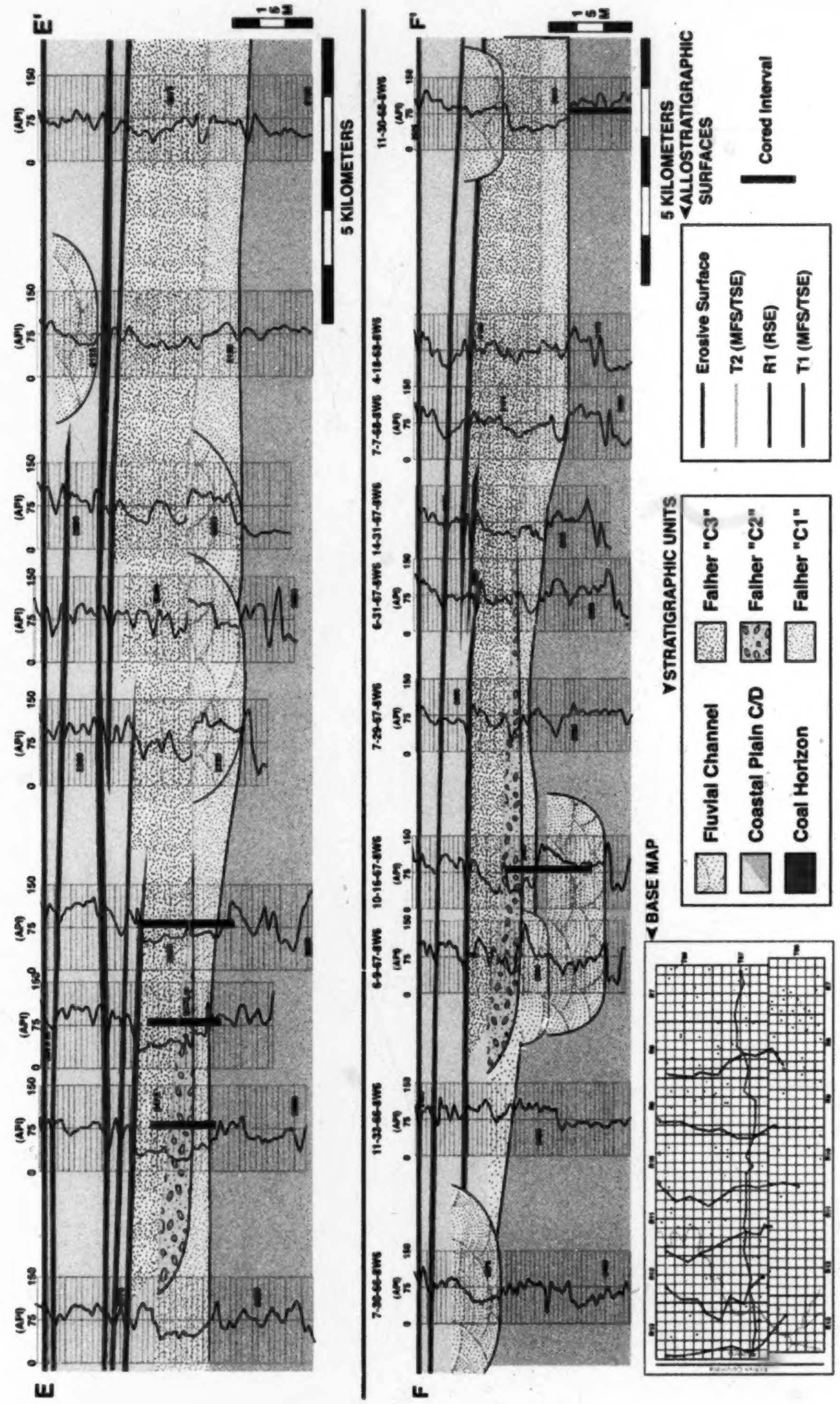
E
E'
F
F'
(API)
0
75
150
5 KILOMETERS
1
5
M
7-30-66-8W6
11-33-66-8W6
6-9-67-8W6
10-16-67-8W6
7-29-67-8W6
6-31-67-8W6
14-31-67-8W6
7-7-68-8W6
4-18-68-8W6
11-30-68-8W6
BASE MAP
STRATIGRAPHIC UNITS
Fluvial Channel
Coastal Plain C/D
Coal Horizon
Falher "C3"
Falher "C2"
Falher "C1"
ALLOSTRATIGRAPHIC SURFACES
Erosive Surface
T2 (MFS/TSE)
R1 (RSE)
T1 (MFS/TSE)
Cored Interval

APPENDIX III: Maps

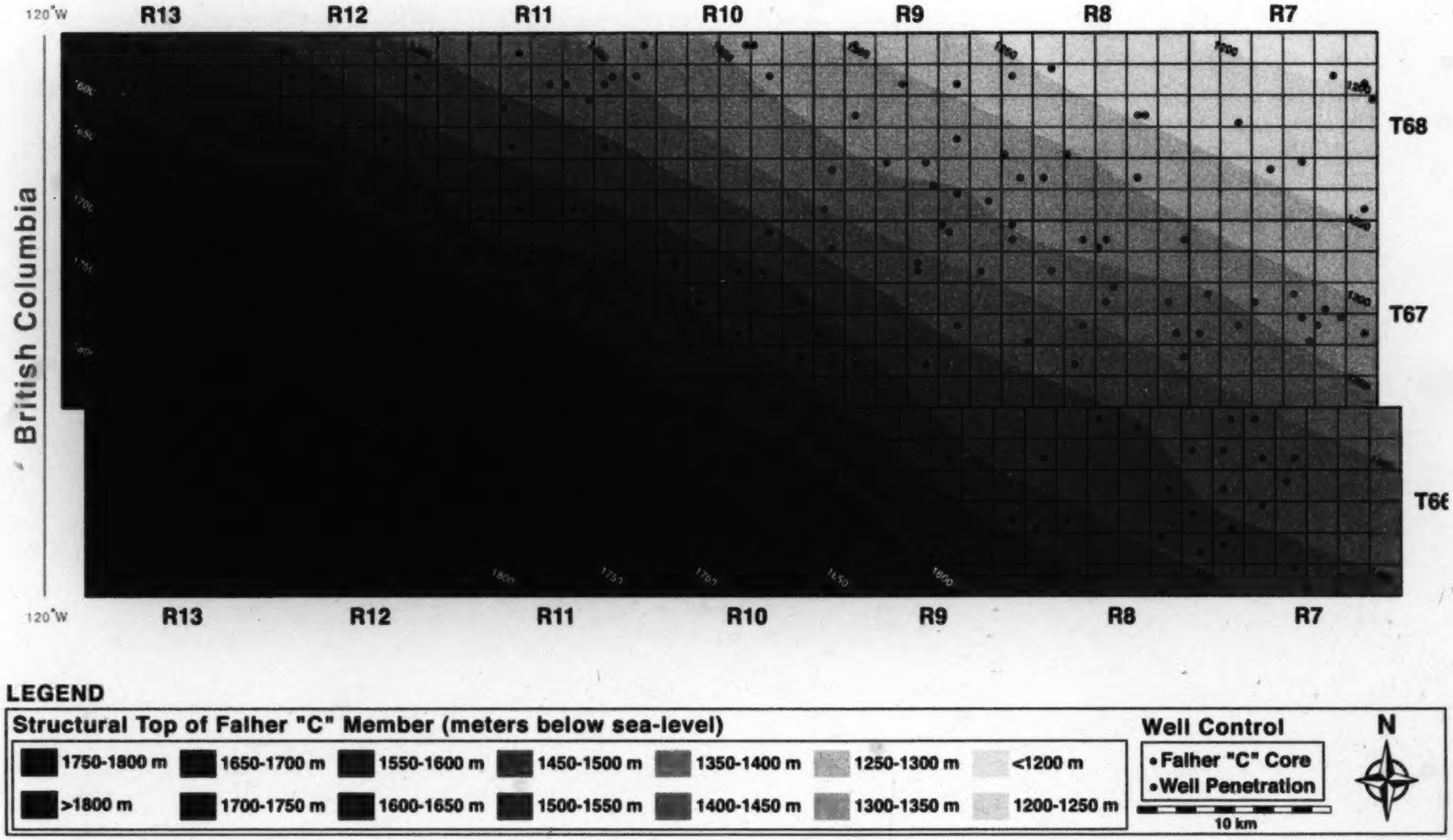
120°W
R13
R12
R11
R10
R9
R8
R7
T68
T67
T66
British Columbia
1200
1250
1300
1350
1400
1600
1650
1700
1750
1800
LEGEND
Structural Top of Falher "C" Member (meters below sea-level)
1750-1800 m
>1800 m
1650-1700 m
1700-1750 m
1550-1600 m
1600-1650 m
1450-1500 m
1500-1550 m
1350-1400 m
1400-1450 m
1250-1300 m
1300-1350 m
<1200 m
1200-1250 m
Well Control
• Falher "C" Core
• Well Penetration
10 km
N

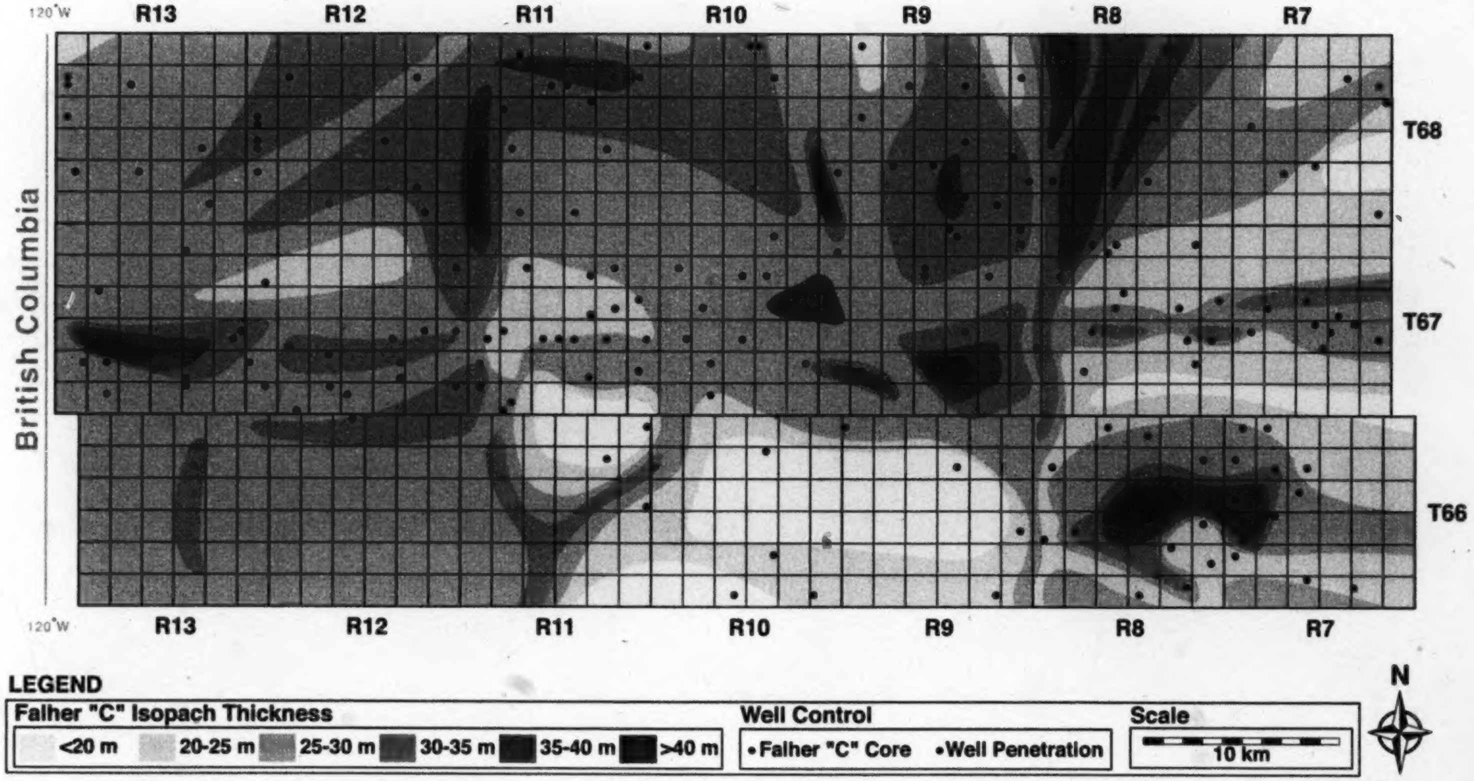
120°W
R13
R12
R11
R10
R9
R8
R7
T68
T67
T66
British Columbia
120°W
R13
R12
R11
R10
R9
R8
R7
N
LEGEND
Falher "C" Isopach Thickness
<20 m
20-25 m
25-30 m
30-35 m
35-40 m
>40 m
Well Control
• Falher "C" Core
• Well Penetration
Scale
10 km